Characterizing the Drought Stress Response of Vitis vinifera Varieties

Mark Gowdy

Doctoral Thesis

Characterizing the Drought Stress Response of *Vitis vinifera* Varieties

Mark Gowdy

20 July 2022

Université de Bordeaux
Ecole Doctorale: Sciences de la Vie et de la Santé

Institut National de Recherche pour l'Agriculture, l'Alimentation et l'Environment (INRAE)

Institut des Sciences de la Vigne et du Vin (ISVV)
UMR – 1287: Ecophysiologie et Génomique Fonctionnelle de la Vigne

Jury Members:

M. Cornelis VAN LEEUWEN Full professor, Bordeaux Sciences Agro	Directeur de thèse
M. Thierry SIMONNEAU Full professor, INRAE	Président du jury
Mme Josefina BOTA Associate Professor, Universitat de les Illes Balears, Departament de Biologia	Rapporteur
M. Andrea PITACCO Full professor, University of Padua, Institute of Pomology	Rapporteur
Mme Anne PELLEGRINO Associate Professor, Institut Agro Montpellier	Examinateur

Acknowledgements

I want to start by thanking Kees van Leeuwen for entrusting me with the opportunity to do this PhD, and for his support and guidance throughout. I also want to thank the folks at Hennessy for their financial support and interest in my studies, including Xavier Poitou, Mathilde Boisseau, and Sandrine Weingartner.

The work of this thesis was not possible without the support of everyone at the UMR Ecophysiologie et Génomique Fonctionnelle de la Vigne at ISVV. I'm particularly grateful for the *travail d'équipe*, both in the vineyard and the laboratory with Agnes Destrac Irvine, the invaluable technical collaboration with Greg Gambetta, Bruno Suter, Philippe Pieri, and Elisa Marguerit, and the ever-important administrative support from Cathy Thioulouse and Catherine Chabirand. And of course, Nathalie Ollat for her excellent management of a diverse group of researchers, particularly during the trying times of the COVID pandemic.

I also want to thank the numerous interns that I worked with over the five years of both my masters and doctoral studies at ISVV, in particular Martina Haines (2017), Wenxin Li (2018), Stephan Lamy (2019), Guillermo Gutiérrez, Eylul Kadaifci, and Alfonso Domínguez Zamudio (2020), and Marc Plantevin (2021). They all contributed so much to my studies and it was a real pleasure working with all of them.

I also want to acknowledge the many work colleagues that contributed to my professional development over the years. In particular Chris Foe and Les Grober from the California State Water Resources Control Board who mentored me in the ways of good scientific method and writing and presentation skills.

I also very much appreciate the support of my family and friends. In particular my mother, Betty Gowdy Stice and my late father, Hank Gowdy for instilling in me the importance of academics, and to my step-father James Stice for his initial encouragement and commiseration throughout my PhD.

And last, but not least… my wife Lynn for all her love and support through the many difficult times during my studies. I look forward to our next chapter together.

"It is a capital mistake to theorize before one has data."
— Sherlock Holmes

"All models are wrong, but some are useful."
— Jay Lund (UC Davis)

"Perfection is the enemy of progress."
— Winston Churchill

Abstract

Climate change has the potential to affect wine producing regions around the world. As the availability of water to vineyards potentially decreases, whether by decreased precipitation or irrigation water supplies, and/or their use of water increases due to increasing temperatures and atmospheric demand, the drought stress they experience will become greater. Grapevine (*Vitis vinifera*) varieties can modify their physiology in various ways in response to drought stress, with some better able to maintain their water status in response to decreasing soil water availability, and/or to increasing atmospheric demand than others. The severity and timing of drought stress can affect the quality potential and yield of grapes produced by a vineyard and is manageable to some degree by growers in meeting their objectives. Understanding the drought stress response of different varieties will help growers anticipate and react accordingly.

The objectives of the studies presented in this thesis were to characterize drought stress response in terms of how grapevines modify their water use, doing so on different time scales. This was achieved using different approaches including: i) measurement of carbon isotope discrimination ($\delta^{13}C$) in berry juice to characterize water use efficiency and drought stress responses during the berry ripening period; and ii) high frequency determination of vine canopy conductance over a season using heat balance sap flow sensors and other measurements to characterize how transpiration is regulated diurnally and seasonally in response to changes in vine water status and atmospheric variables. In both cases, leaf water potential was also measured to corroborate and further inform findings.

Measurements of these indicators were then used to develop empirical characterizations and classifications of drought stress response across several varieties. Being performed in the VitAdapt common-garden vineyard, with randomly distributed replicate plantings, the effects of variable soil conditions, even within the same vineyard, can be properly accounted for. Also, being performed in the vineyard, these studies produced findings more likely to be relevant to the design and management of working vineyards compared to those obtained in the greenhouse.

Abstract (continued)

The well documented use of $\delta^{13}C$ as an indication of drought stress during the berry ripening period was confirmed by corresponding measurements of predawn water potential over four years. A classification of drought responses for 48 varieties was then made using a hierarchical cluster analysis based on certain $\delta^{13}C$ metrics and giving consideration to vine phenology. The development of hydroscapes for five different varieties from measurements of predawn and leaf water potential measurements also found relationships between the level of stomatal control in response to increasing drought stress and the innate water use efficiency as estimated by $\delta^{13}C$ measurements taken in years with less severe soil water deficits during berry ripening. The $\delta^{13}C$ of wine brandy (*eau de vie*) was also studied and found to be conserved during the double distillation process involved in the production of Cognac. This suggests that it could be used for studies of the effect of drought stress during the berry ripening period on sensory attributes of eau de vie.

A simplified method is also presented for determining vine canopy conductance in a vineyard based on an established crop canopy energy flux model using measurements of individual vine sap flow, temperature and humidity within the vine canopy, and estimates of net radiation absorbed by the vine canopy. This field method was then used to characterize variety-specific regulation of vine canopy conductance, and hence transpiration, in response to changes in soil water deficits and atmospheric demand. Multiple linear regression analysis was then used to quantify these relationships and will help to improve modeling of vine canopy transpiration in vineyard water balance models.

The topic of varietal responses to water deficits is complex, with many physiological responses and time frames to consider, and numerous means of measurement available. The studies presented in this thesis characterized the drought stress response of several different varieties both in terms of changes in water use efficiency over the berry ripening period and changes in vine conductance both diurnally and seasonally, while using and comparing a number of different approaches to determining these responses.

Résumé en français

Caractérisation de la réponse au stress de la sécheresse des variétés de Vitis vinifera

Introduction

Le changement climatique est susceptible d'affecter les régions viticoles du monde entier, avec des changements incertains et différents selon les régions en matière de précipitations et des températures généralement plus élevées. Comme la disponibilité de l'eau pour les vignobles diminue potentiellement et que leur utilisation de l'eau augmente en raison de l'augmentation des températures et de la demande atmosphérique, le déficit hydrique qu'ils subissent deviendra plus important. Les variétés de vigne (*Vitis vinifera*) peuvent modifier leur physiologie de différentes manières en réponse à la sécheresse, certaines étant plus aptes que d'autres à maintenir leur statut hydrique en réponse à la diminution de la disponibilité en eau du sol et/ou à l'augmentation de la demande atmosphérique.

La sévérité et le moment de la contrainte hydrique peuvent affecter le potentiel qualitatif et le rendement des raisins produits par un vignoble. L'état hydrique peut affecter la croissance végétative de la vigne, qui à son tour peut affecter le microclimat des grappes de raisin, la dynamique de maturation et les rendements. Il peut également augmenter l'accumulation de composés flavonoïdes tels que les anthocyanines et les flavanols dans les baies, ce qui peut affecter la qualité de la production de vin rouge en particulier. L'état hydrique de la vigne peut être géré dans une certaine mesure par les producteurs pour atteindre leurs objectifs. Comprendre comment l'état hydrique de la vigne répond aux changements de la disponibilité en eau du sol et des températures aidera les producteurs à anticiper et à mettre en place des adaptations nécessaires.

Les objectifs des études présentées dans cette thèse étaient de caractériser la réponse à la sécheresse en termes de modification de l'utilisation de l'eau par la vigne, et ce à différentes échelles de temps. Pour ce faire, différentes approches ont été utilisées, notamment : i) mesure de la discrimination isotopique du carbone ($\delta^{13}C$) dans le jus de raisin à maturité pour caractériser l'efficience de l'utilisation de l'eau et les réponses à la contrainte hydrique pendant la période de maturation des baies; et ii) détermination de la conductance de la

canopée de la vigne sur des intervalles de 15 minutes pendant une saison, en utilisant des capteurs de flux de sève à bilan thermique pour caractériser comment elle répond aux changements de l'état hydrique de la vigne et des variables atmosphériques. Dans les deux cas, le potentiel hydrique des feuilles a également été mesuré pour corroborer les résultats. Les mesures de tous ces indicateurs ont ensuite été utilisées pour élaborer des caractérisations et des classifications empiriques de la réponse à la contrainte hydrique pour plusieurs variétés. Réalisées au vignoble, avec des vignes soumises à des conditions proches de celles de la production, ces études devraient produire des résultats plus pertinents pour la conception et la gestion des vignobles en activité que des études réalisées en serre.

Réponse à la contrainte hydrique pendant la maturation des baies

La mesure de la discrimination isotopique du carbone dans le jus de raisin à maturité ($\delta^{13}C$) et les mesures du potentiel hydrique pendant la période de maturation des baies sur quatre saisons, ont confirmé les résultats d'études antérieures qui suggèrent que le $\delta^{13}C$ fournit une évaluation intégrative de l'état hydrique de la vigne pendant la période de maturation des baies. Cela peut être un outil utile pour les producteurs, les acheteurs de raisins et les coopératives pour estimer rétrospectivement l'état hydrique de la vigne qui existait dans le vignoble au cours de la saison de production.

Diverses mesures de $\delta^{13}C$ et de la phénologie de la vigne réalisées sur 48 variétés différentes, dans des conditions de sol et de climat similaires, pendant sept années, ont ensuite été utilisées pour créer une classification de la tolérance à la sécheresse qui correspondait bien aux connaissances empiriques de la tolérance relative à la sécheresse des variétés étudiées. La classification a été réalisée à l'aide d'une analyse hiérarchique en grappes (HCA) basée sur les traits observés suivants pour chaque variété : le jour de l'année (DOY) de la véraison ; le $\delta^{13}C$ de l'année la plus humide ; et la fourchette des valeurs du $\delta^{13}C$ entre celle de l'années la plus sèche et la plus humide. Pour chaque variété, ces mesures tiennent compte respectivement de l'effet du moment de la maturation des baies sur les conditions de sécheresse subies, de l'efficacité innée de l'utilisation de l'eau et de la sensibilité à la contrainte hydrique sur plusieurs saisons. La classification HCA obtenue de cette manière sera utile pour la sélection du matériel végétal basée sur les réponses potentielles au stress dans les futures conditions climatiques.

Par ailleurs, en utilisant des mesures du potentiel hydrique foliaire de base et de potentiel hydrique foliaire de mi-journée (Ψ_{PD} et Ψ_L respectivement) sur un sous-ensemble de six variétés, des *hydroscapes* ont été créés et une série de paramètres indiquant la sensibilité de la régulation stomatique du statut hydrique de la vigne au stress hydrique a été produite. De tels *hydroscapes* sont indicatifs de la gamme de Ψ_L sur laquelle la vigne peut fonctionner, avec des *hydroscapes* plus petits associés à des variétés plus isohydriques et des *hydroscapes* plus grands indiquant des variétés anisohydriques. Il a été observé que la taille de l'*hydroscape* d'une variété dépend fortement du niveau le plus bas de Ψ_L dans des conditions non limitantes et du niveau le plus bas de Ψ_L à des niveaux élevés de stress hydrique. On a ensuite constaté que ces paramètres clés de l'*hydroscape* étaient bien corrélés avec le $\delta^{13}C$ obtenu au cours des années où les conditions hydriques étaient peu limitantes. Cela suggère que le comportement anisohydrique d'un *hydroscape* plus grand est associé à un niveau inférieur d'efficience d'utilisation de l'eau dans des conditions bien arrosées, comme l'indique un $\delta^{13}C$ plus négatif. Une utilisation accrue de l'eau dans des conditions non limitantes, comme le suggère un *hydroscape* plus grand, peut entraîner des déficits hydriques plus importants plus tard dans la saison et donc une augmentation du *δ13*C (vers des valeurs plus faiblement négatifs). La relation entre ces paramètres d'*hydroscape* et de $\delta^{13}C$ permet d'interpréter et de valider l'importance du paramètre $\delta^{13}C$ obtenu au cours d'une année avec peu de contrainte hydrique, ce dernier étant relativement facile à obtenir dans le vignoble sur plusieurs saisons et sur une large gamme de variétés.

Discrimination isotopique du carbone dans l'eau-de-vie en comparaison avec celle obtenue dans le vin

Il a été démontré que le $\delta^{13}C$ du sucre du moût de raisin est fortement corrélé au $\delta^{13}C$ de l'éthanol qui résulte de sa fermentation au cours de la transformation du moût de raisin en vin. Cela fournit alors un moyen d'estimer à partir d'un échantillon de vin l'état hydrique de la vigne qui existait pendant la période de maturation des baies qui ont produit ce vin, et peut être utilisé pour établir des relations entre l'état hydrique de la vigne et des attributs sensoriels spécifiques du vin. au cours de cette thèse nous avons examiné comment le $\delta^{13}C$ dans l'eau-de-vie de vin produite par un processus de double distillation, tel que celui utilisé dans la région de Cognac en France, est potentiellement affecté lorsqu'il est comparé

au vin source et au moût de raisin correspondant. Si le signal $\delta^{13}C$ dans le moût de raisin, le vin et l'eau de vie est conservé, alors le $\delta^{13}C$ dans l'eau de vie peut être utilisé pour estimer l'état hydrique de la vigne qui existait pendant la période de maturation des baies. À son tour, cela pourrait être utile pour explorer comment les attributs sensoriels de l'eau de vie sont liés au statut hydrique de la vigne, comme cela a été fait précédemment pour le vin.

Les mesures de $\delta^{13}C$ dans l'eau de vie produite à partir d'un processus de double distillation ont été comparées au $\delta^{13}C$ du vin source et du moût de raisin correspondant. Une forte relation linéaire a été trouvée entre le $\delta^{13}C$ du moût de raisin, du vin et de l'eau de vie, suggérant que ce dernier pourrait être utilisé pour estimer l'état hydrique de la vigne qui existait pendant la période de maturation des baies correspondante. Cela permet une estimation rétrospective de l'état hydrique de la vigne qui existait pendant la maturation des raisins utilisés pour produire le vin et l'eau de vie.

La conductance stomatique de la canopée de la vigne

En réponse aux changements de son statut hydrique, la vigne régule la transpiration en utilisant divers mécanismes physiologiques qui modifient la conductance de l'eau à travers le continuum sol-plante-atmosphère. Une méthode simplifiée est présentée dans cette thèse pour déterminer la conductance de la canopée de la vigne dans un vignoble, basée sur un modèle établi de flux d'énergie de la canopée de la culture, utilisant des mesures du flux de sève de la vigne, de la température et de l'humidité dans la canopée de la vigne, et des estimations du rayonnement net absorbé par la canopée de la vigne. Cette méthode respecte la dynamique particulière des flux d'énergie des vignobles à couvert ouvert, tout en évitant les mesures complexes du flux de chaleur du sol et de la conductance de la couche limite nécessaires à d'autres méthodes, qui peuvent interférer avec les opérations courantes de la conduite du vignoble. Cette méthode fournit un moyen plus simple et plus robuste de calculer la conductance de la canopée de la vigne, nécessaire à l'étude de sa réponse au changement climatique.

Une analyse de sensibilité utilisant une analyse de régression non paramétrique a révélé que le flux de transpiration et le déficit de pression de vapeur sont les variables d'entrée les plus importantes pour le calcul de la conductance stomatique de la canopée, ce qui justifie

l'attention portée à leur mesure sur le terrain. D'autre part, le rayonnement net absorbé et la résistance de la couche limite globale se sont avérés beaucoup moins importants, ce qui suggère des possibilités de simplification de la méthode qui n'auraient pas d'impact significatif sur la qualité des résultats. Il a été observé que les estimations du rayonnement net à grandes longueurs d'onde absorbé par la canopée de la vigne étaient très faibles par rapport au rayonnement net à longueurs d'onde courte absorbé, ce qui suggère qu'il pourrait être éliminé de cette méthodologie sans impact significatif sur le calcul de la conductance stomatique de la canopée. L'avantage de simplifier la méthode et de la rendre plus facile à mettre en œuvre peut l'emporter sur cette perte de précision, bien que la vérification de cette constatation reste nécessaire dans des vignobles dont la taille du couvert, l'espacement des rangs et l'orientation sont différents. Une méthode simplifiée sur le terrain augmente la possibilité de recueillir davantage de données sur différentes variétés, climats et conditions de conduite.

Réponse de la conductance de la canopée de la vigne à un environnement changeant

La capacité de caractériser la régulation spécifique à la variété de la conductance de la canopée de la vigne, et donc de la transpiration, en réponse aux changements du déficit en eau du sol et de la demande atmosphérique, aiderait à améliorer la modélisation de la composante de la transpiration de la canopée de la vigne dans les modèles de bilan hydrique du vignoble. À cette fin, la méthodologie simplifiée ci-dessus a été utilisée pour estimer la conductance stomatique de la canopée à des intervalles de 15 minutes sur plusieurs vignes de Cabernet-Sauvignon, Merlot, Tempranillo, Ugni blanc et Sémillon dans un vignoble non irrigué, et sa réponse a été comparée à un certain nombre de paramètres biotiques et abiotiques. Après un processus d'itérations pour prendre en considération la colinéarité et la non-linéarité des données pour les différentes variables, une analyse de régression linéaire multiple a été utilisée pour développer un modèle facilement interprétable de la conductance stomatique de la canopée en fonction de l'état hydrique de la vigne, du déficit de pression de vapeur et du rayonnement net, les coefficients de régression pour les différentes variables prédictives étant physiquement significatifs et comparables entre eux et entre les différentes variétés.

Résumé en français (suite)

Pour toutes les variétés, la variabilité du déficit de pression de vapeur dans le couvert végétal de la vigne au cours de la journée et le potentiel hydrique de base au cours de la saison expliquent une grande partie de la variabilité de la conductance stomatique de la canopée, la variabilité du rayonnement net absorbé par le couvert végétal expliquant beaucoup moins. L'effet de l'état hydrique de la vigne sur la conductance était plus différencié entre les cinq variétés que l'effet du déficit de pression de vapeur. Et bien qu'il y ait une différence dans l'effet du rayonnement net entre les variétés, son effet global était beaucoup plus faible que celui de l'état hydrique de la vigne et du déficit de pression de vapeur. On a également observé que la réponse de la conductance modélisée, calculée à l'aide des coefficients de régression pour les différentes variables, était de plus grande ampleur (qu'elle soit positive ou négative), aux changements des variables prédicteurs lorsque la conductance dans des conditions non limitantes était plus grande. Il a également été observé que Tempranillo met davantage l'accent sur la réduction de sa conductance en réponse à la diminution de l'état hydrique de la vigne qu'en réponse à l'augmentation des déficits de pression de vapeur, par rapport aux autres variétés.

Les simulations de transpiration basées sur les équations de régression utilisant les données d'entrée de la même saison ont révélé des différences similaires entre les variétés en termes de transpiration quotidienne et saisonnière. Ces simulations se sont également bien comparées à celles d'un modèle reconnu de bilan hydrique du vignoble, bien qu'il semble y avoir des différences entre les deux approches en ce qui concerne le taux de réduction de la conductance, et donc de la transpiration, en fonction de la diminution de la teneur en eau du sol.

Bien que les modèles actuels de bilan hydrique constituent un outil précieux pour aider les viticulteurs à concevoir et à gérer leurs vignobles, ils sont génériques et ne permettent pas de prendre en compte les différences de comportement entre variétés. Bien que davantage de données collectées à l'aide de l'approche décrite soient probablement nécessaires pour caractériser de manière plus définitive le comportement des différentes variétés, elles pourraient permettre de développer un paramétrage spécifique à la variété de la composante transpiration de la vigne dans les futurs modèles de bilan hydrique. En caractérisant mieux la réponse de la conductance stomatique de la canopée aux conditions environnementales, la dynamique de la transpiration de la vigne peut être mieux

paramétrée dans la modélisation de l'utilisation de l'eau dans les vignobles pour des scénarios climatiques actuels et futurs.

Un autre défi majeur dans la modélisation du bilan hydrique des vignobles est la nécessité de développer une estimation pertinente de l'eau totale transpirable du sol (*TTSW*). Après la réalisation de l'étude ci-dessus, une relation universelle entre le potentiel matriciel du sol et les déficits en eau du sol a été trouvée, qui pourrait fournir une base à l'avenir pour une méthode d'estimation du *TTSW* à partir des mesures du potentiel hydrique de base sur la saison. Les estimations réalisées par cette approche pourraient valider les hypothèses de *TTSW* faites dans cette étude et fournir un moyen raisonnable pour l'estimation de *TTSW* dans des études futures, bien que l'estimation correcte de la profondeur d'enracinement dans un contexte de vignoble reste un défi majeur.

The studies presented in this thesis were carried out with financial support from Jas. Hennessy & Co. (16100 Cognac, France) and the French National Research Agency (ANR) in the frame of the Investments for the future Programme, within the Cluster of Excellence COTE (ANR-10-LABX-45).

The VitAdapt vineyard is supported by the Conseil Interprofessionnel des Vins de Bordeaux (CIVB), the Conseil Régional d'Aquitaine, Bordeaux University through LabEx, and the Institut National de Recherche pour l'Agriculture, l'Alimentation et l'Environnement (INRAE). The vineyard is maintained by the UE 1442 Vigne & Vin Bordeaux Grande Ferrade.

The final version of this document includes clarification regarding the overall thesis objectives and thoughts regarding potential future studies, which came up during the jury discussions.

Table of Contents

Table of Contents (continued)

1 Introduction

Climate change has the potential to affect wine producing regions around the world with uncertain and regionally differing changes in precipitation, all of which have the potential to significantly alter soil and plant water relations (Schultz, 2016). Higher temperatures will increase atmospheric demand for both plant transpiration and soil evaporation, with a tendency towards lower relative humidity in near-surface air already observed over the last 20 years in the mid-latitudes and Mediterranean (Willett et al., 2014). Even changes in global radiation, which provide the energy needed for evapotranspiration, can be affected by changes in cloud cover associated with climate change (Mendoza et al., 2021) and by human-induced pollution and its interaction with the climate (Wild, 2009).

As the availability of water to plants decreases (e.g., increasing soil water deficits, or drought), and/or the use of water increases (e.g., increased atmospheric demand), the water status of the plant will decrease. As the plant water status and associated water potential decreases, drought stress becomes greater (Turner, 1981) and plants can adapt their physiology differently whether in the short-term or long-term (Tardieu et al., 2018). This is true also for the different varieties of *Vitis vinifera*, which can modify their physiology in various ways in response to drought stress (Lovisolo et al., 2010), with some better able to maintain water status in response to decreasing soil water availability, and/or to increasing atmospheric demand than others (Chaves et al., 2010; Costa et al., 2012; Domec and Johnson, 2012; Bota et al., 2016; Levin et al., 2020).

The severity and timing of drought stress can affect the quality potential and yield of grapes produced by a vineyard, with the optimal levels depending on grower objectives. Water status can affect the vegetative growth of the vine, which in turn can affect grape cluster microclimate, ripening dynamics, and yields (Smart and Robinson, 1991). Water status during the berry ripening period can also increase the accumulation of flavonoid compounds such as anthocyanins and flavanols in the berries (Castellarin et al., 2007), which can affect the quality of red wine production in particular (van Leeuwen et al., 2009). Vine water status is manageable to some degree by growers and understanding how

vine water status responds to changes in soil water availability and temperatures will help growers anticipate and react accordingly (Pellegrino et al., 2004).

Because vine physiology is altered by vine water status, measurements of physiological indicators such as transpiration, leaf water potential, changes in stem diameter, leaf and air temperature differences, carbon isotope discrimination, and growth parameters, can be used to assess vine water status (van Leeuwen et al., 2010). For the studies presented in this thesis it was chosen to characterize water status in terms of changes in grapevine water use on different time scales, as achieved by: i) measurement of $\delta^{13}C$ in berry juice as an indication of water use efficiency during the berry ripening period; and ii) high-frequency measurements of changes in transpiration by heat balance sap flow sensors over a growing season in order to estimate vine canopy conductance. In both cases, leaf water potential is also measured to corroborate and further inform findings. These indicators are then used to develop empirical characterizations and classifications of drought stress response across several varieties. And performed in the vineyard, with the vines experiencing realistic growing conditions, these studies should produce findings more relevant to the design and management of working vineyards than those obtained from greenhouse studies.

Much has been published on how plants regulate their water use efficiency and water status in response to drought using measurements of carbon isotope discrimination ($\delta^{13}C$) in berry juice (Chaves et al., 2010; Costa et al., 2012; Gaudillère et al., 2002; Tomás et al., 2012; Bchir et al., 2016; Bota et al., 2016). The study presented in Chapter 3 of this thesis expands on that work and evaluates a range of 48 Mediterranean varieties planted in replicate in the same vineyard, with the intent of classifying their drought response based on varying drought conditions experienced over seven growing seasons. Measurements of $\delta^{13}C$ were also compared against hydroscapes created from measurements of midday and predawn leaf water potential to look for additional relationships. The resulting variety classification should help growers select plant material well adapted for their objectives under future climate scenarios.

The $\delta^{13}C$ of the sugar in grape must has been shown to be strongly correlated to the $\delta^{13}C$ of the ethanol that results when it is fermented to wine (Guyon et al., 2015). This then provides a means of estimating from a sample of wine the vine water status that existed

during the corresponding berry ripening period, and can be used to establish relations between vine water status and specific sensory attributes of wine quality (Picard et al., 2017). The study presented in Chapter 4 of this thesis examines how the $\delta^{13}C$ in wine spirit (*eau de vie*) produced by a double distillation process, such as that used in the Cognac region of France, is potentially affected when compared to the source wine and parent grape must. If the $\delta^{13}C$ signal in grape must and wine and eau de vie is conserved, then the $\delta^{13}C$ in eau de vie can be used to estimate the vine water status that existed during the berry ripening period. In turn, this could be useful for exploring how sensory attributes of eau de vie are linked to vine water status, such as has been done previously for wine.

In response to changes in vine water status, grapevines regulate transpiration using various physiological mechanisms that alter conductance of water through the soil-plant-atmosphere continuum (McElrone et al., 2013). A simplified method is presented in Chapter 5 of this thesis for determining vine canopy conductance in a vineyard based on an established crop canopy energy flux model (Shuttleworth and Wallace, 1985) using measurements of individual vine sap flow, temperature and humidity within the vine canopy, and estimates of net radiation absorbed by the vine canopy. This methodology respects the particular energy flux dynamics of vineyards with open canopies, while avoiding problematic measurements of soil heat flux and boundary layer conductance needed by other methods, which can otherwise interfere with ongoing vineyard management practices. This method provides a more straightforward and robust means of calculating vine canopy conductance as needed to study its response to climate change.

Being able to characterize variety-specific regulation of vine canopy conductance, and hence transpiration, in response to changes in soil water deficits and atmospheric conditions would help improve modeling of the vine canopy transpiration component in vineyard water balance models. The purpose of the study presented in Chapter 6 of this thesis is to quantify and differentiate the response of bulk stomatal conductance (g_{bs}) of different grapevine varieties to changes in vine water status, vapor pressure deficit in the vine canopy, and net radiation absorbed by the vine canopy. Using coefficients from a readily interpretable multiple linear regression model, simulations of transpiration are then compared to those from an existing vineyard water balance model to understand how well variety specific behavior might be distinguished. Current water balance models are not

parameterized to distinguish differences in conductance regulation between varieties, which might otherwise be useful for modeling adaptations to future climate change.

A general review of literature in presented in Chapter 2, followed by the four chapters described above, each centered around a journal article, including additional background and discussion. Chapter 7 concludes with a summary of study results and their implications.

2 Literature Review

The following is a review of literature relevant to concepts that apply generally across all chapters of this thesis. In each subsequent chapter, further topic-specific literature is presented in the background and discussion sections and in the associated journal articles.

2.1 Stomatal regulation

A key physiological reaction of grapevines, as in most plants, in response to drought is to modulate their stomatal aperture and thereby regulate transpiration and the associated hydraulic gradients in its vasculature. The resistance to water vapor diffusion through open stomata is much greater than the resistance of water through the vasculature, with that through the stomata becoming the controlling factor in overall transpiration (Sack and Holbrook, 2006; Krounbi and Lazarovitch, 2011).

Stomatal openings are created between two so-called guard cells that are regulated through a process of osmotic (turgor pressure) adjustment, which changes the size of the aperture between them. Stomata regulate both the diffusion of CO_2 into the intercellular space as needed for photosynthesis and the diffusion of water vapor out of the intercellular space (Roelfsema and Hedrich, 2005; Meinzer et al., 2016). As the plant experiences water deficits, the plant adjusts its stomata to conserve water (Roelfsema and Hedrich 2005). Stomata also act to control minimum leaf water potential (Meinzer et al., 2014) and protect plant vasculature (Sperry et al., 2002). Stomatal opening can also respond to other environmental factors such as light levels, rooting and rootstock, fruit load, temperature, and nutrient status (Keller, 2015). The closure of stomata in response to water stress is influenced by: i) decreases in water potential and hydraulic conductivity in response to decreasing soil water potential; ii) decreases in leaf water potential in response to increasing vapor pressure deficit; and/or iii) abscisic acid hormones (ABA) generated in roots in response to drying soil, which is then transported to leaves via xylem (Franks et al., 2007; Lovisolo et al., 2010; Domec and Johnson, 2012).

Water Potential / Conductivity - Stomata regulation is affected by changes in water potential, although the mechanisms linking the two are not clearly understood (Oren et al., 1999; Roelfsema and Hedrich, 2005). Changes in water potential, and hence stomatal

regulation, can be associated with decreasing hydraulic conductivity in the plant vasculature by: i) formation of xylem embolisms (Sperry et al., 2003; Chouzouri and Schultz, 2005); ii) changes in xylem characteristics (Lovisolo and Schubert, 1998); iii) changes to functioning of aquaporins (Lovisolo et al. 2010); and iv) hormonal (ABA) signalling (Stoll et al., 2000).

Vapor pressure deficit - Water potential in the leaves can also decrease if there is an increase in vapor pressure deficit (i.e., atmospheric demand). Vapor pressure deficit (VPD) is the difference in the partial pressure of water measured in the ambient air versus that of saturated air at the same temperature (Kramer and Boyer, 1995). At high levels of VPD, the stomata will begin to close to protect the vasculature of the leaf and the rest of the plant (Sperry et al., 2002). For example, a study of five *Vitis vinifera* varieties found that stomatal conductance remained at maximum levels, depending on variety, up to a threshold level of VPD ranging between 1.36 kPa to 1.91 kPa. However, once VPD increased beyond this threshold, stomatal aperture and gas exchange both decreased, with varieties demonstrating differences in how much their gas exchange rates changed per unit increase in VPD (Prieto et al., 2010). Similarly at the whole vine level, in a combined modeling and field study with the variety Sultana, vine canopy conductance, as measured by sap flow, decreased exponentially as VPD increased (Lu et al., 2003). The VPD experienced by vine itself can also be affected by stomatal regulation, as the effects of evaporative cooling and temperature around the leaf changes, thereby changing VPD (Tardieu and Simonneau, 1998). As described further below, plant water potential and ABA triggers can further affect stomatal closure sensitivity to changes in VPD.

Abscisic acid (ABA) - Plants modify their stomatal response to changes in vapor pressure deficits as soil water deficits change (Domec & Johnson 2012). ABA is a stress hormone produced in the roots, which is transported in sap via the xylem to the leaves where it increases the sensitivity of stomata to changes in VPD (Lovisolo et al. 2010). Stomatal closure is triggered by ABA as part of a chemical reaction that reduces the osmotic/turgor pressure of the guard cells (Roelfsema and Hedrich 2005). While the molecular mechanisms of how ABA affects guard cells are fairly well known, the mechanisms by which water potential and VPD directly, or indirectly affect guard cells are less well known (Roelfsema and Hedrich 2005). The production of ABA in drying leaves has also

been identified as a driver of stomatal response to VPD (Lovisolo et al. 2010). It has been hypothesized that osmotic regulation of guard cells may be connected by a feedback mechanism involving the water status of cells near the stomata (Buckley, 2005).

Light levels & photosynthesis - Light conditions, and hence photosynthesis and stomatal conductance can vary greatly within the vine canopy (Smart, 1974). As photosynthesis rate changes in association with changing light conditions or darkness, the plant will adjust its stomata to help conserve water (Roelfsema and Hedrich 2005). The presence of photosynthetic-active radiation triggers light perception pathways in the guard cells that cause them to open. The guard cells also sense a decrease in CO_2 concentration in the intercellular leaf space as it is depleted by photosynthesis (Shimazaki et al., 2007). The size of stomatal openings are affected by the variable intensity of PAR during the day or as a result of cloudiness (Shimazaki et al., 2007). To the extent it affects stomatal opening, the rate at which photosynthesis responses to changes in light, and the maximum rate of this photosynthesis, can also be affected by nitrogen availability (Meinzer et al., 2017).

Temperature - Increased temperature was found to both increase stomatal opening and stimulate photosynthesis in Shiraz, with the associated evaporative cooling helping leaves adapt (Montoro and Sadras, 2014). Leaves can also adapt their orientation to avoid heat stress (Gamon and Pearcy, 1989). However, as leaf temperatures approach 35^{o}C, photosynthesis becomes inhibited, at the same time increased vapor pressure deficit tends to increase transpiration, which can lead to excessive water loss from the vine canopy (Keller 2015). Eventually, increasing heat and inhibition of photosynthesis will lead to stomatal closure, which will reduce transpiration and evaporative cooling, leading to heat damage in the leaves (Keller 2015).

Rooting and rootstock - When vine roots sense low soil water status, a series of biochemical and genetic responses are triggered that favor selective root growth over leaf and shoot growth in an effort to locate water and nutrients for continued growth (Lovisolo et al. 2010). The type of rootstock can also affect the ability of the plant to find water, (Lavoie-Lamoureux et al., 2017), with this ability also affected by the duration and intensity of soil water deficit conditions (Marguerit et al., 2012). Roots may also

preferentially access water from areas of higher water content within the root zone (Krounbi and Lazarovitch, 2011).

Fruit load - Numerous studies have found an increase in gas exchange (i.e., transpiration) and carbon assimilation rates (i.e., photosynthesis) in association with increased fruit load. This was observed in a study of Sauvignon blanc (Naor et al., 1997) and a study of Pinot noir found that increased fruit load relative to leaf area also increased the rate of photosynthesis as the leaves tried to satisfy demand for photosynthates in ripening berries (Petrie et al., 2000). Conversely, cluster thinning can reduce demand from ripening berries, leading to a surplus of carbohydrates from photosynthesis, leading to inhibition of photosynthesis in a feedback loop (Keller 2015).

2.2 Carbon isotope discrimination ($\delta^{13}C$)

The source of carbon for the photosynthesis of carbohydrates in the chloroplasts of the mesophyll of leaves comes from the CO_2 that diffuses into the intercellular space of the mesophyll through the stomata. During this process there is a discrimination in favor of CO_2 containing ^{12}C isotopes due to its higher reactivity with the Rubisco enzyme in the photosynthesis reaction. In addition, the rate of diffusion of $^{13}CO_2$ through the stomata and leaf boundary layer is also less than for $^{12}CO_2$. Both of these processes contribute to lower $^{13}C/^{12}C$ isotope ratios in carbohydrates generated by photo-synthesis when compared to atmospheric CO_2 (Farquhar, 1989; Santesteban et al., 2015).

These $^{13}C/^{12}C$ isotope ratios, however, are modified when stomata close and cut off diffusion of CO_2 into the intercellular space of the leaves, causing the relative concentration of $^{13}CO_2$ to $^{12}CO_2$ to rise in the intercellular space (due to ^{12}C discrimination). In the range of moderate water deficit, photosynthesis has been shown to decrease at more negative water potentials than that which induces the onset of stomatal closure. In the range of moderate water stress, photosynthesis continues as stomata begin to close, thereby increasing water use efficiency (Chaves et al. 2010). At the leaf level, water use efficiency (WUE) is the mass of carbon assimilated by photosynthesis per mass of water transpired. As it is also related to the relative rates of carbon assimilation and

stomatal aperture, $\delta^{13}C$ has been demonstrated to be a useful proxy for WUE, with less negative $\delta^{13}C$ corresponding to less stomatal opening and higher WUE (Bchir et al. 2016).

As stomata close, the sugars formed by the continuing photosynthesis process will contain a modified ratio of carbon isotopes (Bchir et al., 2016). Of particular interest in viticulture are the relative isotope concentrations of the sugars accumulated in the berries, as this provides an integrative measure of extent of water stress (i.e., stomata closure) that existed during the berry ripening period when those sugars were synthesized and accumulated (Gaudillère et al., 2002; van Leeuwen et al., 2010; Santesteban et al., 2015). Water deficit during the time of berry-ripening is also important from a canopy management perspective, as it helps control vine vigor and improves berry cluster microclimate (Smart and Robinson 1991). This makes $\delta^{13}C$ of berry juice sugar a particularly useful measure of vine water status (Gaudillère et al., 2002). A comparative study of $\delta^{13}C$ measurements taken on different plant tissues and at different times of the growing season also concluded berry juice sugar measurements to be most appropriate for characterizing drought stress and WUE (Bchir et al. 2016).

As stomata close in response to water deficit, $\delta^{13}C$ becomes less negative usually in a linear relationship with plant water potential, with some varieties showing a significantly different response. A linear relationship between stem water potential and $\delta^{13}C$ was found, with small differences in response observved between Cabernet-Sauvignon, Merlot, and Cabernet franc (van Leeuwen et al., 2010). For Chardonnay, the minimum predawn water potential measured during berry ripening also demonstrated a linear relationship with $\delta^{13}C$, with a slope of about 1‰ $\delta^{13}C$ per change of −0.2 MPa in water potential. This was similar to observations for Cabernet-Sauvignon, Merlot, Cabernet franc, and Shiraz in two other studies, although the intercepts of the linear relationships were significantly different, suggesting genetic differences between varieties (Brillante et al., 2017). A study of Moscatel and Castelão also found a linear relationship between $\delta^{13}C$ and predawn water potential measurements integrated over the growing season, however, Moscatel was found to keep stomata open over a larger range of water potentials, while Castelão was more sensitive (Souza et al., 2005). A study of six *Vitis vinifera* varieties also found a strong positive correlation between $\delta^{13}C$ and leaf-level WUE (Tomás et al., 2012).

With $\delta^{13}C$ being related to WUE, studies of WUE in response to water stress are also useful in understanding stomatal regulation, and have been performed on numerous varieties (Tomás et al., 2012), with an extensive review of leaf level WUE studies also provided by Medrano et al. (2015). As an example, a potted-plant study of 20 different Spanish varieties, plus Cabernet-Sauvignon, and Chardonnay for comparison, found strong differences between WUE in well-watered treatments. In water stressed treatments, however, stomatal conductance and WUE, and to a lesser degree chlorophyll fluorescence, were affected differently across varieties, with a change in the type of response in some cases when compared to well-watered conditions (Bota et al., 2001).

Another study of both WUE and $\delta^{13}C$ characteristics of 23 Spanish and other varieties in field conditions over three years found differences between varieties in WUE under well-water conditions, but with differences not being as great as observed in the potted-plant studies performed by Bota et al. (2001), thereby highlighting the importance of performing such studies in the vineyard (Bota et al., 2016). The WUE differences between varieties were observed to be driven more by differences in water vapor gas exchange than carbon assimilation, perhaps due to differences in mesophyll conductance or the efficiency of certain photosynthesis reactions (Bota et al. 2016). Under water stress conditions, there were differences in stomata response to water stress observed between varieties, but also changes in the nature of the response for some varieties when compared to well water conditions (Bota et al. 2016).

2.3 Water potential and hydroscapes

Water potential is the potential energy per unit volume of water relative to that of pure water at the same temperature and pressure and is defined with units of pressure such as MPa (megapascals) or bars, with 1 MPa = 10 bars (Koide et al., 2000). The components of water potential most important to plants are those related to pressure (i.e. turgor) potential, osmotic potential, and gravity potential, although the latter tends to be negligible except in tall trees (Taiz and Zeiger, 2002, Ch. 3), while the turgor and osmotic pressure components tend to be most physiologically relevant (Hsiao et al., 1976; Turner, 1981)

The pressure chamber method is the most common technique for measuring water potential in plants, with many references existing on the underlying theory and its application (Koide et al. 2000). The technique involves cutting individual leaves from the plant and inserting them into the chamber with the petiole visible through a hole with an adjustable gasket. Gas is applied to the chamber with increasing pressure until sap just begins to exude from the petiole (Ritchie and Hinckley, 1975). Generally there are three types of water potential measurements: i) mid-day leaf (ψ_l); ii) mid-day stem (ψ_s); and iii) predawn leaf (ψ_{pd}) (Williams and Araujo, 2002).

Midday leaf water potential (ψ_l) is measured by standard pressure chamber procedure (Scholander et al., 1965) using an sun-exposed mature leaf from a primary shoot. The leaf water potential is a measure of the immediate negative water potential in the leaf in response to factors such as vapor pressure deficit, stomatal closure, soil water status, and plant hydraulic conductivity (Choné et al. 2001). Midday stem water potential is measured by enclosing the leaf while still on the vine in a plastic bag wrapped in aluminum foil at least 45 minutes prior to measurement of its water potential by standard pressure chamber procedure. With the leaf enclosed on the plant, the stomata will close and the leaf will reach equilibrium with the water potential of the adjacent shoot xylem, providing an indication of the whole plant water status based on its transpiration and current soil and root conductivity conditions (Choné et al. 2001). These measurements should be performed on fully developed leaves from primary shoots, and if being compared, should be taken from the same shoot if possible (Choné et al. 2001; Williams and Araujo 2002).

While leaf water potential measurements have been used extensively for studies of grapevine physiology and water relations (Williams & Araujo 2002), various other studies have concluded that stem water potential may be a more reliable indicator of plant water status, as it relates to changes in transpiration and soil water status (McCutchan and Shackel, 1992; Naor et al., 1995, 1997; Choné et al., 2001), particularly when the plant is experiencing moderate to severe soil water deficit (Choné et al. 2001). Because the leaf is bagged and the stomata are closed at the time of measurement, there is less variance in the stem water potential measurement when compared to the variable light conditions experienced by the un-bagged leaf water potential measurements (McCutchan and Shackel 1992; Choné et al. 2001).

Predawn leaf measurements give water potential of the plant when, in theory, the stomata are closed, there is no transpiration, and the plant is in equilibrium with the root zone water potential (Choné et al. 2001). Although this method is widely accepted for evaluation of water potential across the soil and roots, some studies suggest the equilibrium may be with the wettest portion of the root zone (Pellegrino et al., 2004; Williams and Trout, 2005). Nighttime transpiration can also potentially affect these measurements (Rogiers et al., 2009), although such transpiration decreases as plant water stress increases (Escalona et al., 2013). It also has been observed that predawn measurements can equilibrate with even a small portion of the root zone that contains moisture (Améglio et al., 1999), therefore consideration might need to be given to recent rainfall, or access by a portion of the roots to a water source, as can be the case in irrigated vineyard with variable soil water content.

Alternative frameworks for characterizing stomatal response to water stress have been proposed based on metrics derived from the relationships between midday leaf water potential (ψ_l) and predawn leaf water potential (ψ_{pd}), or $\Delta\psi$ (i.e. $\psi_l - \psi_{pd}$) (Martínez-Vilalta et al. 2014; Meinzer et al. 2016). One such metric is called the "hydroscape", which is developed from the area covered by a plot of ψ_l versus ψ_{pd} data. The larger the area covered by the hydroscape (MPa^2), the less stomata regulate leaf water potential, indicating a more anisohydric behavior. Conversely a small hydroscape indicates more stringent stomatal regulation, and hence isohydric behavior (Meinzer et al. 2016). Another metric is the slope of the regression line through a plot of $\log(\Delta\psi)$ vs. ψ_{pd}, which shows the relationship between diurnal fluctuation of plant water potential (i.e. degree of stomatal regulation) as a function of predawn measurements (Meinzer et al. 2016). In addition, pressure-volume curves, as developed from water potential measurements at the turgor loss point (ψ_{TLP}) and cell osmotic potential at full turgor ($\psi_{\Pi\,100}$), have been found to correlate well with the two methods described above, and other stomatal and photosynthetic responses. Such curves may provide a simpler proxy for characterizing drought tolerance of different species and varieties (Bartlett et al., 2012; Meinzer et al., 2017).

2.4 Transpiration and conductivity/conductance

Around 95% of the water taken up by the plant is not actually consumed, but rather passes through to satisfy the evaporative demand from transpiration. But plants also use water as a solvent to transport nutrients from the soil up into the plant and later to distribute the products of photosynthesis back for development of various plant tissues and organs (Keller 2015). Water is also used to maintaining plant cell turgor pressure as needed to give the plant structure, and to perform other physiological functions such as opening/closing of stomata. Evaporative cooling from the surface of the leaves is also important in maintaining an acceptable temperature for the leaves (Keller 2015).

At the leaf level, transpiration is measured as the stomatal conductance (g_s) of water vapor from the leaf surface (mmol m^{-2} sec^{-1}) and is a function of diffusion rates through the stomatal opening, stomatal density, and the size and degree of opening of the stomata at any particular time (Keller 2015). The water vapor diffusion rate through the stomatal opening is affected by: i) solar radiation, which adds energy to the diffusion; ii) vapor pressure deficit, which is the driving force for diffusion; and iii) wind, which affects the boundary layer resistance to diffusion at the leaf surface (Keller 2015). Due to variable conditions within the canopy, the stomatal conductance of leaves in the canopy can be highly variable (Smart and Robinson, 1991).

Two of the main ways to measure stomatal conductance at the leaf level are by: i) porometer; and ii) infra-red gas analyzer, with a recent review of multiple studies finding the former giving readings about 2.1 times higher than the latter, and the use of infra-red gas analyzers gradually replacing use of porometers due to better precision and accuracy (Lavoie-Lamoureux et al. 2017). At the whole plant, or canopy level a bulk stomatal conductance can be measured using sap flow measurements such as described in Chapter 5 of this thesis. Bulk stomatal conductance is effectively the parallel combination of the leaf-level stomatal conductance of every leaf in the crop canopy (Kelliher et al., 1995).

Across the *soil-plant-atmosphere continuum*, as depicted in Figure 1, transpiration, as driven by atmospheric demand in the gas phase, must create a more negative water potential than in the liquid phase, including that in the water supply in the soil and the

resistances to water transport through the plant (Choné et al., 2001; Krounbi and Lazarovitch, 2011; McElrone et al., 2013). The continuity of this negative pressure from the leaves to the roots is maintained by the cohesion between bi-polar water molecules, and adhesion between these molecules and the xylem walls by capillary action. Referred to as "cohesion-tension theory" this explanation of water movement through plants is generally accepted in the literature (Kirkham, 2005).

The relationship between a change in transpiration and the associated water potential gradient across either the whole plant, or a portion of the plant in the soil-plant-atmosphere continuum is governed by the associated hydraulic conductance (Krounbi and Lazarovitch 2011). Using an analogy with Ohms law for electricity, while neglecting osmotic and elevation water potential and capacitance, this relationship is represented by Equation 1:

$$E = K_p \, x \, \Delta\psi \qquad \text{(Eqn. 1)}$$

where E is the average transpiration flux per unit leaf area (mmol m^{-2} s^{-1}), $\Delta\psi$ is the change in water potential (MPa) across the whole plant, and K_p is the hydraulic conductance of the whole plant (mmol m^{-2} s^{-1} MPa^{-1}), which when expressed in terms of flux is referred to as *leaf-specific hydraulic conductance* (Tyree and Ewers, 1991; Domec et al., 2009; Krounbi and Lazarovitch, 2011).

Regarding terminology, *conductance* refers to the relationship between flow through the plant, as driven by transpiration, and the water potential gradients along the entire pathway being considered, for example from the roots to the leaves. This is different from *conductivity*, which describes the flow and water potential relationships across a unit length of flow, for example along a segment of stem, or *specific conductivity,* which applies on a cross-sectional area basis for structures like xylem (Keller 2015).

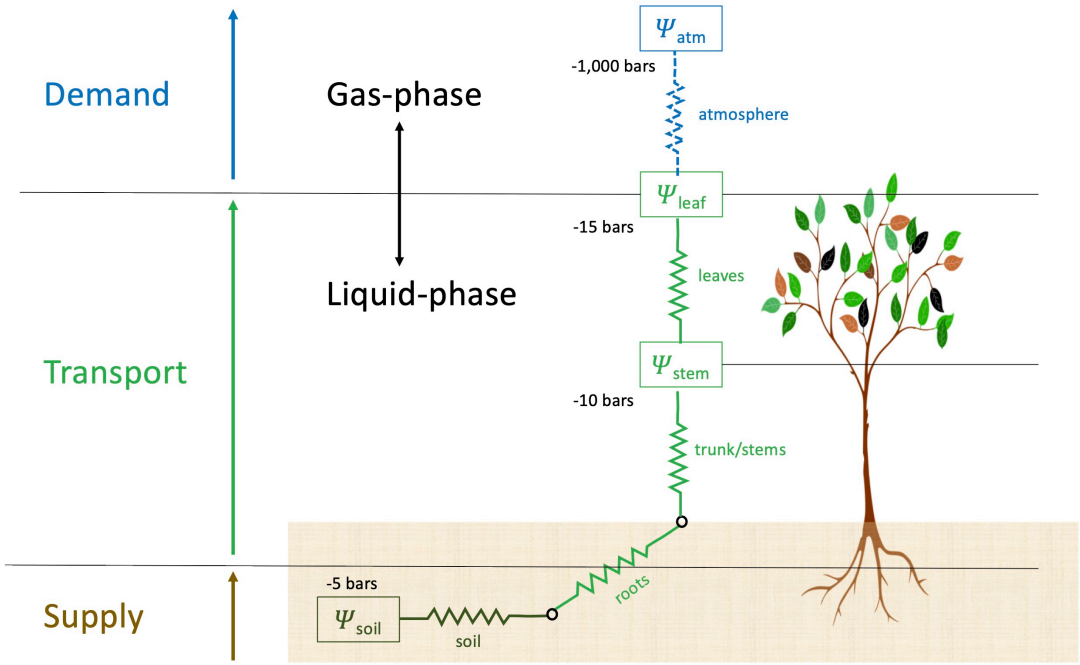

Figure 1. Schematic depiction of the soil-plant-atmosphere continuum, showing gradients of water potential across different elements of the supply, transport and atmospheric demand for water, and the boundary between gas and liquid phases.

The Ohm's law analogy assumes that flow in the soil-plant-atmosphere continuum is steady state, meaning there is no flow to or from storage elsewhere in the plant (i.e. capacitance). In reality, however, there can be some capacitance. For example, over the growing season plant tissues or organs such as leaves or berries can be a sink for water as associated cells are expanding (Koide et al., 2000). On a diurnal basis water can be released from storage in the trunks, cordons, stems, and fruits in the morning when transpiration begins and stored back again in the afternoon (Steppe and Lemeur, 2004). While not addressed in the above equation, or in discussions below, capacitance may need to be considered in short duration studies of plant hydraulics (Martínez-Vilalta et al. 2014).

When considered across the individual elements along the flow pathway, including the roots, stems, leaves, stomata, and boundary layer, the associated individual conductance of each element is summed in series to give the whole plant conductance (Tyree and Ewers 1991; Choné et al. 2001; Krounbi and Lazarovitch 2011). Changes in the conductance of such elements in response to drought tend to happen in the short-term, while in the long-term plant water use is more affected by changes in phenology, yield loss, root architecture, and photosynthetic and water use efficiency (Tardieu et al., 2018). In the

short-term, changes in vapor pressure deficit elicit a decrease in conductance by the regulation of stomata within minutes to hours over the course of the day (Buckley, 2016; Tardieu et al., 2018). Plants can also respond to rapid changes in water potential by adjusting the hydraulic conductance of water in roots and shoots as facilitated by aquaporins. Plant can also modify hydraulic conductivity by adjusting cell osmotic water potential and turgor (Lovisolo et al., 2010; Tardieu et al., 2018). Together, these mechanisms inhibit shoot growth and control transpiration by modifying water use over the season (Tardieu et al., 2018), with these responses potentially varying depending on rootstock (Lovisolo et al., 2010). Hydraulic conductance can also be affected by the ratio of the sapwood cross-sectional area to leaf area being supplied. If there is greater sapwood cross-sectional area supplying a given leaf area, there will be less resistance to flow and less decrease in water potential across the associated vasculature (Zhang et al. 2012).

Resistance to flow in leaves represents an important part of the overall resistance to flow in the whole plant and can vary depending on the light conditions of the shoots and leaves (Schultz and Matthews, 1993). As long as embolisms do not occur, the vascular structure, and hence conductivity of mature leaves is considered to be fairly constant, and therefore, the difference between ψ_s and ψ_l, as measured simultaneously on two leaves from the same shoot, is considered to be a good indicator of transpiration across a range of soil water and vapor pressure deficits, with an increase in the difference indicating an increase in transpiration (Choné et al. 2001).

The hydraulic conductance through the plant tends to be controlled by the resistance to flow through plant tissues in the roots and leaves rather than through the xylem. The xylem generally has higher conductance, except in the case of embolisms (Tardieu et al., 2018). As water potential becomes more negative in response to increasing water deficit, this can result is embolism formation in the xylem, whereby air enters at certain vulnerable points in the xylem structure and breaks the adhesion of the water column leading to a drastic decrease in conductance (Sperry et al. 2003; Chouzouri and Schultz 2005). Stomata have been shown to fully close several days before embolisms appear in the leaves, with basal leaves being more vulnerable to embolism than apical leaves. Once embolisms form, these basal leaves drop, which helps protect the stem and younger leaves and prevents further water loss. (Hochberg et al., 2017b). Also, when vine roots sense low soil water status,

biochemical and genetic responses are triggered that lead to reduction of xylem vessel size, which decreases hydraulic conductivity helping moderate transpiration and prevent embolism formation in stems and leaves (Lovisolo and Schubert 1998).

As vines acclimate to water deficits over the course of the season, there also appear to be physiological changes in the hydraulics of their vasculature and leaf area that allows for increased gas exchange in later drought events when compared to well water vines (Hochberg et al., 2017a). It was also demonstrated that grapevines can increasingly maintain stomatal conductance and adjust their turgor loss in the face of increasingly negative stem water potential over the season, suggesting it is important to account for such seasonal changes when characterizing drought response (Herrera et al., 2021).

The ability of the soil to deliver water through its pore spaces to the roots is also a key component in the soil-plant-atmosphere continuum. As the soil dries, more negative pressure is needed by the plant to overcome increasingly negative soil matric potential, particularly once the fraction of transpirable soil water drops below about 0.4, depending on the texture of the soil. This leads to a corresponding reduction in the hydraulic conductivity within the soil matrix supplying water to the roots (Krounbi and Lazarovitch 2011). Studies suggest the greatest resistance to flow between the soil and the plant occurs at the soil/root interface rather than within the soil matrix, particularly at higher soil water contents. At very low soil water content the resistances from the interface and the soil matrix become similar (Krounbi and Lazarovitch 2011). Studies suggest, however, the resistance to flow at the soil/root interface is due more to a decrease in soil water conductivity as soil dries rather than the associated decrease in soil water potential. It has been hypothesized this is due mostly to root shrinkage, which reduces the contact between the root and the surrounding soil (Krounbi and Lazarovitch 2011). The extent of the rooting system for a given plant can also affect overall plant conductance, with a more extensive root system better able to locate water. Grapevines also adjust relative root to shoot growth, reducing root growth less than aboveground growth in response to increasing soil water deficit (Krounbi and Lazarovitch 2011; Lovisolo et al. 2010).

2.5 Varietal differences in stress response

Plants tend to modify their stomatal response to changes in vapor pressure deficits as soil water deficits increase, with different plant species, as well as *Vitis vinifera* varieties, regulating their stomata differently in response to changes in these variables (Chaves et al., 2010; Costa et al., 2012; Domec and Johnson, 2012; Bota et al., 2016; Levin et al., 2020). Plant species that readily close their stomata to maintain constant leaf water potential when faced with increasing VPD, and/or decreasing soil water status are classified as *isohydric*. Plant species that keep their stomata open (continuing with gas exchange and transpiration) and allow leaf water potential to decrease when faced with increasing VPD and/or decreasing soil water status are classified as *anisohydric* (Tardieu and Simonneau 1998). Stomatal regulation, however, does not always fit neatly into these categories (Martínez-Vilalta et al. 2014), with some species demonstrating responses that vary with water stress, or a hybrid response such as *isohydrodynamic*, whereby stomata are regulated to maintain a roughly constant difference between leaf and soil water potential (Franks et al. 2007; Zhang et al. 2012; Domec & Johnson 2012).

Within the species *Vitis vinifera*, different varieties also demonstrate a range of response dynamics, which are difficult to categorize, or they display inconsistent dynamics across numerous different studies (Chaves et al. 2010; Lavoie-Lamoureux et al. 2017). For example, Syrah has often been found in studies to demonstrate anisohydric response (Schultz, 2003; Prieto et al., 2010), but in others has demonstrated near-isohydric response (Pou et al., 2012). And whether isohydric or anisohydric varieties are more “drought tolerant” is subject to interpretation and circumstances. For example, in non-irrigated vineyards an anisohydric variety under conditions of water stress could be more at risk during a drought (Domec and Johnson 2012; Lovisolo et al. 2010). On the other hand, under moderate water deficit, as in an irrigated vineyard, an anisohydric variety might maintain stomata open longer and assimilate more carbon and have potentially higher yields (Pou et al. 2012).

Regardless of how they are characterized, the differing varietal responses to drought stress appear to result from the varying interplay of the different mechanisms controlling stomata. For example, studies on typically anisohydric varieties Merlot (Zhang et al., 2012)

and Semillon (Rogiers et al., 2012) observed anisohydric response at higher soil water status, but more isohydric response for both varieties at lower soil water status. For both varieties, the isohydric response tended towards greater changes in leaf/canopy gas exchange rates in response to changes in vapor pressure deficit, with this behavior being well correlated with reference gas exchange rates as expected from empirical and theoretical modeling (Oren et al., 1999; Domec and Johnson, 2012). The reference gas exchange rate is the gas exchange rate (mmol m^{-2} sec^{-1}) at under conditions of no water stress and full solar radiation. In the Merlot study, it was suggested the transition from anisohydric to isohydric response was due to a decrease in whole-plant, leaf-specific conductance associated with decreased soil water status (Zhang et al. 2012). The Semillon study suggested the shift to isohydric behavior was attributable to increased ABA generated at lower soil water status, which further increases stomatal sensitivity to vapor pressure deficits (Rogiers et al. 2012; Domec and Johnson 2012). Similarly, the typically anisohydric variety Shiraz demonstrated a more isohydric response when subjected to partial root zone drying than when receiving the same level of water over the whole root zone. This was attributed to higher ABA levels being generated in the dried portion of the root during the treatment (Collins et al., 2010).

Studies in other species may also provide insights on stomatal response. In a study on *Pinus taeda* (loblolly pine) by Domec (2009) it was found as soil dried, the canopy reference gas exchange (at VPD = 0) decreased as expected based on the findings of Oren et al. (1999), but there was also a corresponding significant decrease in whole plant hydraulic conductance as calculated from sap flow and water potential measurements, suggesting changes in plant hydraulics had a role in stomatal regulation (Domec et al. 2009). This study further observed in field measurements that whole plant conductivity was controlled by leaf conductance at higher soil moisture levels and root conductance at lower soil moisture (Domec et al. 2009).

3 Varietal drought response classification

3.1 Background

Plants regulate their water use efficiency in response to changes in water status brought about in response to drought conditions. This water use efficiency, and hence level of drought stress during the berry ripening period can be assessed using measurement of carbon isotope discrimination ($\delta^{13}C$) in berry juice sugars collected at maturity (Chaves et al., 2010; Costa et al., 2012; Gaudillère et al., 2002; Tomás et al., 2012; Bchir et al., 2016; Bota et al., 2016). By collecting $\delta^{13}C$ measurements across multiple years with different drought conditions, the drought stress response of a given variety may be assessed. If vines of different varieties are studied under the same conditions, then the relative drought stress response of the varieties can be compared.

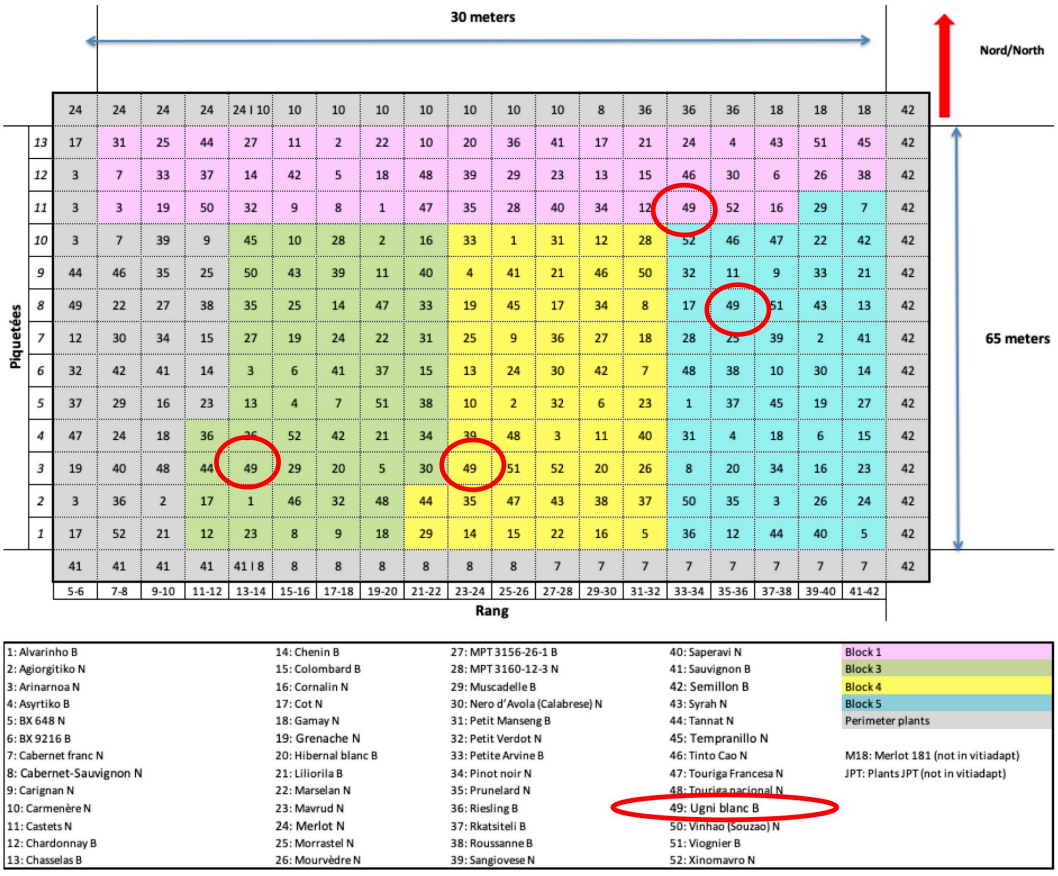

Figure 2. Schematic plan of the VitAdapt experimental vineyard, showing as an example, the location of four groups of ten vines each of Ugni blanc (red circles).

In the journal article presented in this chapter, entitled "*Using $\delta^{13}C$ and hydroscapes for discriminating cultivar specific drought responses*" (Plantevin et al., 2022), the drought stress responses of 48 different varieties are compared based on data collected over seven years from vines planted in four replicate plots in the VitAdapt experimental vineyard in Bordeaux. As depicted in Figure 2, with the location of Ugni blanc vines circled in red as an example, the common-garden replicate layout of the VitAdapt vineyards allows for the variability of soil conditions, which can exist even within the same vineyard, to be properly accounted for (Destrac-Irvine and van Leeuwen, 2017). With multiple years of data, the innate water use efficiency can be evaluated in years of less stressed conditions and the range of responses can be assessed across varying drought stress conditions. With corresponding measurement of the phenology in the vineyard, the effects of the timing of the post-véraison period in relationship to the progression of drought conditions over the season can also be accounted for. This data is then used to create a drought tolerance classification of these varieties using a hierarchical cluster analysis. The classification will help inform grower selection of plant material well adapted for their yield or berry composition objectives in current, or future growing conditions at a given location.

Midday and predawn leaf water potential (Ψ_L and Ψ_{PD}) are two other means of assessing vine water status, and if made during the berry ripening period can corroborate $\delta^{13}C$ measurements. They can also be used to create *hydroscapes*, which provide an indication of how strictly a variety manages its water status across a range of drought conditions (Martínez-Vilalta et al., 2014; Meinzer et al., 2016). In this study certain metrics from such hydroscapes were compared against $\delta^{13}C$ measurements to identify relationships between the different metrics.

3.2 Journal article

Using $\delta^{13}C$ and hydroscapes for discriminating cultivar specific drought responses

Marc Plantevin[1*], Mark Gowdy[1*], Agnès Destrac-Irvine[1], Elisa Marguerit[1], Gregory Gambetta[1], Cornelis van Leeuwen[1]

[1] EGFV, Univ. Bordeaux, Bordeaux Sciences Agro, INRAE, ISVV, F-33882 Villenave d'Ornon, France

[*] *Marc Plantevin and Mark Gowdy contributed equally to this article and should both be considered as first authors.*

Published in *Oeno One*, June 2022, Volume 56-2, Article 5434

OENO One
VINE AND WINE OPEN ACCESS JOURNAL
By IVES International Viticulture & Enology Society
2nd ClimWine Symposium terclim July 3 – 8, 2022 | Bordeaux, France XIVth International Terroir Congress

DOI:10.20870/oeno-one.2022.56.2.5434
OPEN ACCESS

ORIGINAL RESEARCH ARTICLE

Using $\delta^{13}C$ and hydroscapes for discriminating cultivar specific drought responses

Marc Plantevin[1*], Mark Gowdy[1], Agnès Destrac-Irvine[1], Elisa Marguerit[1], Gregory A. Gambetta[1] and Cornelis van Leeuwen[1]

[1] EGFV, Univ. Bordeaux, Bordeaux Sciences Agro, INRAE, ISVV, F-33882 Villenave d'Ornon, France
Marc Plantevin and Mark Gowdy contributed equally to this article and should both be considered as first authors.

This article is published in cooperation with Terclim 2022 (XIVth International Terroir Congress and 2nd ClimWine Symposium), 3-8 July 2022, Bordeaux, France.

*correspondence:
marc.plantevin@inrae.fr

Associate editor:
Cassandra Collins

Received:
27 February 2022

Accepted:
19 April 2022

Date of publication to be defined (June 2022)

ABSTRACT

Measurement of carbon isotope discrimination in berry juice at maturity ($\delta^{13}C$) provides an integrated assessment of vine water status and water use efficiency (WUE) during the period of berry ripening, and when collected over multiple seasons, can provide an indication of drought stress responses. Berry juice $\delta^{13}C$ measurements were carried out on 48 different varieties planted in a common garden experiment in Bordeaux, France from 2014 through 2020 and found important differences across this large panel of varieties. Cluster analysis showed that $\delta^{13}C$ values are likely affected by the differing phenology of each variety, resulting in berry ripening of different varieties taking place under different conditions of soil water availability within the same year. Accounting for these phenological differences, the cluster analysis created a classification of varieties that corresponds well to our current empirical understanding of their relative drought tolerance. In addition, using measurements of predawn and midday leaf water potential measurements collected over four seasons on a subset of six varieties, a hydroscape approach was used to develop a list of metrics indicative of the sensitivity of stomatal regulation to water stress (i.e. an/isohydric behaviour). Key hydroscape metrics were also found to be well correlated with some $\delta^{13}C$ metrics. A variety's water potential regulation as characterized by a minimum critical leaf water potential as determined from hydroscapes was strongly correlated to $\delta^{13}C$ values under well-watered conditions, suggesting that the latter may be a useful indicator of drought stress response.

KEYWORDS: water use efficiency, carbon isotopic discrimination, water potential, drought tolerance, VitAdapt, hydroscapes, grapevine, *Vitis vinifera*

INTRODUCTION

Vines are cultivated in a wide range of climates, from very dry (such as Cyprus or Aragon, Spain) to extremely wet (such as the Hunter Valley, Australia). The reason for the commercial success of vineyards across such a large range of environments can be explained by the winegrowers' ability to adapt through viticultural practices or by choosing plant material adapted to the local climatic conditions. These adaptations are increasingly important as local environmental conditions are changing under the effect of climate change (IPCC, 2021). Rainfall patterns are changing, with precipitation increasing, or decreasing depending on the region. An increase in temperature and thus evaporative demand will induce drier conditions in most winegrowing regions, even in those with unchanged precipitation regimes. As a result, adaptations are needed to maintain commercially viable viticulture in current winegrowing areas (Fraga *et al*., 2012; Ollat *et al*., 2016; van Leeuwen and Darriet, 2016).

Vines react to water deficits by closing their stomata (Winkel and Rambal, 1990; Williams and Araujo, 2002), which reduces carbon assimilation (Flexas *et al.,* 1998). Despite this reduction in photosynthesis, mild water deficit has positive effects in fine wine production: micro-climatic conditions are improved (better light penetration in the canopy due to lower vigour); more carbohydrates are available for berry ripening due to reduced competition with shoot growth; and berries become smaller with increased levels of anthocyanins in the produced wines (Roby *et al*., 2004; Keller, 2010; Carbonneau *et al*., 2015; Triolo *et al*., 2019). The positive impact of mild water deficit has also been shown on most aroma compounds in grapes and wines (van Leeuwen *et al*., 2020) as well as on the sensory properties of aged red Bordeaux wines (Le Menn *et al*., 2019).

However, water deficits can also lead to yield reductions that may negatively impact commercial viability (van Leeuwen *et al*., 2019a). Under severe water deficit, yield is highly impacted and grape ripening (e.g., sugar accumulation) can slow down or even stop in extreme conditions (van Leeuwen and Darriet, 2016). Although vines can survive under severe droughts and are unlikely to die (Charrier *et al*., 2018), commercially viable fine wine production may become more difficult under increased levels of water deficit.

Many options for adapting viticulture to a warmer and drier future are available, such as changes in canopy management practices, vineyard planting densities, or plant material selection (e.g., clones, rootstocks, and/or varieties) (Fraga *et al*., 2012; van Leeuwen *et al*., 2019a; van Leeuwen *et al*., 2019b). To inform future plant material selection, the drought responses of different varieties need to be better characterized. Assessing the regulation of vine water status is fundamental in making this characterization. Measurements of vine water potentials and the use of carbon isotope discrimination are two methods that have proven particularly useful in assessing water status, each with its own caveats (Choné *et al*., 2001; Gaudillère *et al*., 2002; Cifre *et al*., 2005; van Leeuwen *et al*., 2009; Santesteban *et al.,* 2012).

$\delta^{13}C$ provides an integrative measure of the water status of the plant over a given period of time and can be assessed in leaves and/or berry juice at the end of the season (Gaudillère *et al*., 2002; Santesteban *et al*., 2012). During the process of photosynthesis there is a discrimination against assimilation of CO_2 containing ^{13}C isotopes due to the higher reactivity of ^{12}C isotopes with the Rubisco enzyme in the photosynthesis reaction. In addition, the rate of diffusion of $^{13}CO_2$ through the stomata and leaf boundary layer is less than for $^{12}CO_2$. This results in lower $^{13}C/^{12}C$ isotope ratios in carbohydrates photosynthesized at that time when compared to atmospheric CO_2 (Farquhar 1989; Santesteban *et al*. 2012). As stomata close in response to drought stress, the $^{13}C/^{12}C$ ratio rises in the intercellular space and sugars formed and incorporated into various plant tissues at that time will contain a modified ratio of carbon isotopes (Bchir *et al*., 2016).

When assessed on berry juice at maturity, $\delta^{13}C$ is a useful measure of the level of water deficit that existed during the time sugars in the berry juice accumulate (van Leeuwen *et al*., 2009). $\delta^{13}C$ effectively provides a measure of the ratio between the rate of photosynthesis and the stomatal opening over a period of time (Farquhar, 1989). This is similar to the ratio representing water use efficiency (WUE), which at the leaf level is the amount of carbon assimilated by photosynthesis (A_n) per amount of water transpired (g_s), with a less negative $\delta^{13}C$ corresponding to less stomatal opening and higher WUE (Medrano *et al*., 2010, Souza *et al*., 2005, Bchir *et al*., 2016). A study of eight own-rooted *Vitis vinifera* varieties found a strong positive correlation between $\delta^{13}C$ and leaf-level WUE (Tomás *et al*., 2014).

Vine water status can also be assessed by different measures of leaf water potential. Midday leaf water potential (Ψ_L) is a measure of the immediate negative water potential (i.e., suction) in the leaf in response to many factors, such as vapour pressure deficit, stomatal closure, soil water status, and plant hydraulic conductivity (Choné *et al*., 2001). Predawn leaf water potential (Ψ_{PD}) is experienced at night when the vines have equilibrated with the soil water potential (Williams and Araujo, 2002) and can be considered as a proxy for soil water availability (Gaudin *et al*., 2017), or more precisely of the water availability in the most humid soil layer (Améglio *et al*., 1999).

The amount of stomatal regulation in response to changing Ψ_L varies among genotypes, a concept which has been referred to as (an)isohydristicity (Tardieu and Simonneau, 1998; Hochberg *et al*., 2018). An anisohydric species allows transpiration and photosynthesis at more negative Ψ_L while an isohydric species will regulate stomata at less negative Ψ_L, decreasing transpiration and eventually photosynthesis (Tardieu and Simonneau, 1998). Plant species do not adhere to strict (an)isohydric definitions, but instead vary across a continuum from anisohydric to isohydric (Chaves *et al*., 2010; Klein, 2014) and this is also true across *Vitis vinifera* varieties, for which differences across genotypes mainly occur at medium levels of water deficit (Levin *et al*., 2019). In addition, growth conditions (e.g., greenhouse *vs* field grown) and the climatic conditions which impact the range of

water potentials can influence isohydric versus anisohydric behaviour even within the same genotype (Chaves *et al*., 2010; Charrier *et al*., 2018, Hochberg *et al*., 2018).

Recently the "hydroscape" approach was proposed to visualize how plants regulate their water potential by means of stomatal regulation and to classify genotypes according to their behaviour under drought stress (Martínez-Vilalta *et al*., 2014). The area of the hydroscape plot defines the range over which a plant regulates its Ψ_L as a function of $\Psi_{PD,}$ with the larger the range, the less strict (i.e., more anisohydric) the genotype is at controlling its stomatal conductance under water deficit (Meinzer *et al*., 2016). Conversely, a small hydroscape indicates a genotype with more strict stomatal control (i.e., more isohydric). This methodology has shown to be effective in classifying drought-responses of different species (Li *et al*., 2019, Meinzer *et al*., 2016, Álvarez-Maldini *et al*., 2021). Hydroscapes, however, are time-consuming to produce, requiring multiple measurements of Ψ_{PD} and Ψ_L over a wide range of water deficits.

This study evaluates the drought stress responses of several grapevine varieties by means of $\delta^{13}C$ measurements in berry juice sugars and by hydroscapes. Some apparent relationships between the results obtained by both methods are also discussed.

MATERIALS AND METHODS

1. VitAdapt vineyard

Data for this study were obtained in the VitAdapt experimental vineyard located at the INRAE (Institut National de Recherche pour l'Agriculture et l'Alimentation) research center of Bordeaux, in France (44°47'23.8''N, 0°34'39.3"W) (Destrac-Irvine and van Leeuwen, 2017). The soil is composed mainly of gravel and sand, representative of the Pessac-Leognan AOP (Bordeaux, France). The vineyard was planted in 2009 with 52 different varieties, including 4 hybrids and 48 *Vitis vinifera* L. cultivars on a 0.7 ha parcel with 46 rows of 75 vines each on a density of 5,555 vines/ha (row spacing of 1.8 m and inter vine spacing of 1.0 m). The trunk height is 0.5 m and grapevines are pruned to a double guyot and topped during the growing season at 1.5 m. Each variety was planted on Selection Oppenheim 4 (SO4) rootstock, clone 761. Each variety was tested for major virus diseases and only clean material was planted. There is a mowed cover crop in between each vine row with mechanical tillage under the vine row. The vineyard is dry-farmed and fertilisation is adjusted based on petiole analyses carried out at mid-veraison. To account for soil variability, the VitAdapt experimental design was laid out in randomized blocks with each block containing two rows of five vines per variety. For this study, four blocks were sampled.

2. Carbon isotope discrimination ($\delta^{13}C$)

Measurements of $\delta^{13}C$ were taken from berry juice sugar collected each year at maturity from 10 vines of each variety in each of the four blocks. Measurements of grape sugars and acids were carried out weekly starting at mid-véraison and maturity was considered when sugars started to plateau-off and acidity was low. Sampling was started in 2014, five years after initial planting in 2009, and continued each year through 2020. Berries were harvested from the 10 vines in each block and juice was extracted and centrifuged at 13,500 rpm for 10 minutes (Sigma 13 6K15, SIGMA Laborzentrifugen GmbH, Osterode am Harz, Germany). The juice was then analyzed on a Vario Micro Cube elemental analyzer coupled in a continuous flow mode to an isotopic ratio mass spectrometer (IsoPrime, Elementar). Glutamic acid USGS40 and Caffeine IAEA-600 were used as international standards during the analyses. All results are expressed in delta notation ($\delta^{13}C$) and reported relative to the Vienna Pee Dee Belemnite (VPDB) international reference. Over the seven years a total of 17 to 28 $\delta^{13}C$ measurements were obtained for each variety.

From 2017 through 2020 $\delta^{13}C$ was also measured on eight individual vines of six varieties (Cabernet-Sauvignon, Merlot, Grenache, Tempranillo, Semillon, Ugni blanc), two of each from the four blocks, upon which water potential measurements were also taken periodically over the season. Of these individual vines, some started to lose too many leaves due to disease pressure or multiple water potential measurements, in which case water potential was taken on an adjacent vine, upon which $\delta^{13}C$ was also measured with the values being averaged.

3. Water Potential

Water potential measurements were taken periodically over the seasons 2017 through 2020 on two vines each in the four blocks of Cabernet-Sauvignon, Grenache, Merlot, Semillon, Tempranillo and Ugni blanc. These varieties are some of the most widely planted varieties worldwide (Anderson and Aryal, 2013). Merlot, Tempranillo and Semillon (Rogiers *et al*., 2009) are known for being sensitive to drought stress, while Cabernet-Sauvignon and Grenache are renown for being less sensitive (Santesteban *et al*., 2009). No data were obtained on Grenache in 2018 because of downy mildew damage and measurements on Ugni blanc did not start until 2018. Measurements were collected at seven timepoints in 2017 and 2018 and six timepoints in 2019 and 2020.

From each vine on each sampling date, three types of water potential were measured with leaf water potential (Ψ_L) and stem water potential (Ψ_S) measurements beginning at 2:00 p.m. on a given day and predawn water potential (Ψ_{PD}) started around 3 a.m. the morning after, with all measurements completed within two hours. For midday Ψ_S measurements the leaves were sealed in foil covered bags while on the plant one hour prior (Choné *et al*., 2001). Measurements were taken by the method of Scholander *et al.* (1965) using a pressure chamber with digital manometer (DG MECA, 33175 Gradignan, France).

4. Hydroscapes

The method for preparing hydroscapes was adapted from the concepts presented by Meinzer *et al*. (2016), Charrier *et al*. (2018), and Hochberg *et al*. (2018). First, following the procedure of Meinzer *et al*., (2016), a scatter plot is

made of Ψ_L on the vertical axis and corresponding Ψ_{PD} on the horizontal axis using only the minimum values of Ψ_{PD} and Ψ_L measured from replicate vines on each date. By using minimum Ψ_L values, data that was more influenced by non-limiting conditions for other variables, such as vapour pressure deficit, were removed. Then a 1:1 line is added representing the point at which $\Psi_{PD} = \Psi_L$, a theoretical condition when stomata are completely closed and the whole vine is in equilibrium with soil matric potential.

Then following the method of Charrier *et al.* (2018), bins of Ψ_{PD} for every 0.05 MPa were made and the average of all the minimum Ψ_L measurements within each bin was calculated. Then starting with the bin-averaged Ψ_L at zero Ψ_{PD} (the intercept), the bin averages for progressively more negative Ψ_{PD} are sequentially compiled into a linear regression using bin averages at all previous, less negative Ψ_{PD}. This is done iteratively until the coefficient of determination (r^2) starts to decrease, suggestive of a breakpoint (called critical leaf water potential, Ψ_{Lcrit}) in the linear relationship between Ψ_L and Ψ_{PD} (Hochberg *et al.*, 2018). From this point, the data suggests the bin-average Ψ_L at more negative Ψ_{PD} will have similar values that form a horizontal line of slope zero at Ψ_{Lcrit}. This represents the lowest Ψ_L against which the plant will regulate its stomatal conductance at increasingly negative Ψ_{PD}. In uncontrolled field conditions, the condition of $\Psi_{PD} = \Psi_L$ is rarely achieved, so the horizontal line at Ψ_{Lcrit} must be extended to meet the 1:1 line in order to complete the enclosure of the hydroscape. The area of the hydroscape is then bounded by the horizontal line at Ψ_{Lcrit} (a in Figure 1), the 1:1 line (b in Figure 1), the vertical line at $\Psi_{PD} = 0$ (c in Figure 1), and the regressed line between the

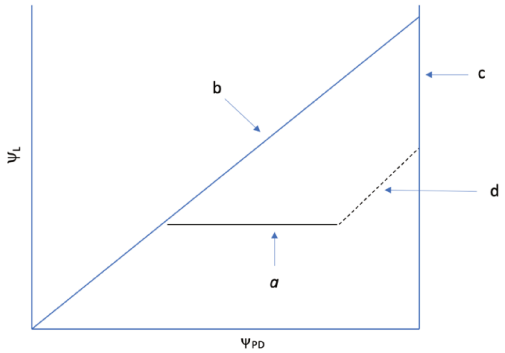

FIGURE 1. A conceptual hydroscape bordered by the line representing the Ψ_{Lcrit} (a), the 1:1 line (b), the vertical line at $\Psi_{PD} = 0$ (c) and the regressed line between the intercept at $\Psi_{PD} = 0$ and Ψ_{Lcrit} (d).

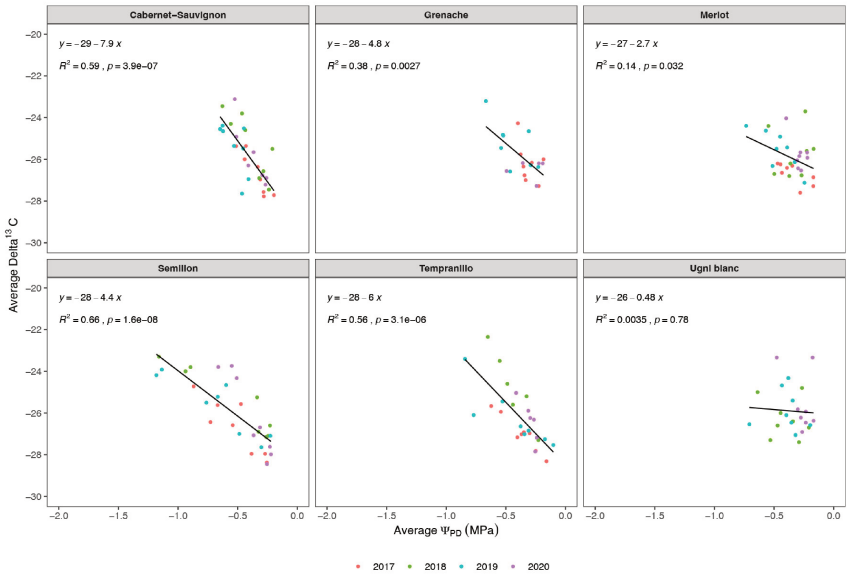

FIGURE 2. Individual vine $\delta^{13}C$ as a function of Ψ_{PD}, averaged over the data collected between 20 days before until 60 days after veraison, for six varieties in 2017 (except for Ugni blanc), 2018 (except for Grenache), 2019 and 2020 in Villenave d'Ornon, France.

intercept at Ψ_{PD} = 0 and Ψ_{Lcrit} (d in Figure 1). In theory, the greater the area enclosed by the hydroscape, the more anisohydric the variety (Meinzer *et al*., 2016).

Filtering, graphing, and linear regression analysis was performed in the *R* software environment using several functions from the *dplyr* package (Wickham *et al*., 2021a) and the *ggplot2* package (Wickham *et al*., 2021b) with hierarchical clustering analyses and dendrograms being done using the *cluster* package.

RESULTS AND DISCUSSION

1. Climate conditions

The two years with the greatest water deficits were 2016 followed by 2018. Some years showed particular climatic conditions. In 2015 (globally a dry year), August was very rainy (109.5 mm). In 2017, evaporative demand was low in May and rainfall was high in September (82 mm), which explains why water deficit was low in this year despite a dry July and August. 2020 was one of the earliest vintages ever in Bordeaux, with high rainfall in May and June, while July was very dry (2.5 mm) and rainfall in August was close to average (46.5 mm). More information regarding vine water status during these years is presented in Figures S1 and S2.

2. Carbon isotope discrimination ($\delta^{13}C$)

2.1 Relationship of berry juice $\delta^{13}C$ to leaf water status

Figure 2 presents plots of $\delta^{13}C$ on an individual vine basis for six varieties from 2017 through 2020 versus the corresponding average Ψ_{PD} measured during berry ripening (i.e., from 20 days before mid-veraison until 60 days after veraison). The $\delta^{13}C$ and average Ψ_{PD} were well correlated for Cabernet-Sauvignon, Grenache, Semillon and Tempranillo, while not as well correlated for Merlot and Ugni blanc (Note, only three years of data were collected for Ugni blanc and Grenache). Plots of $\delta^{13}C$ versus Ψ_S (not shown) showed similar relationships. These results are consistent with previous studies showing $\delta^{13}C$ as being well correlated to Ψ_{PD} (Gaudillère *et al*., 2002) and to midday Ψ_S (Santesteban *et al*., 2012) suggesting increased water use efficiency in response to increasing vine water deficit.

2.2 Varietal differences in $\delta^{13}C$

Figure 3 presents the range of $\delta^{13}C$ values for each of the 48 varieties across the seven years of measurement, with the thickness of the violin plot indicative of the distribution of values and the black dot representing the mean of all measurements. As discussed in the next section, the average $\delta^{13}C$ measured in the year with the most negative values is an important metric of drought responses for a given variety. The red dots on the violin plots represent this minimum mean value for each variety and are the values upon which the varieties are ordered along the vertical axis in Figure 3.

$\delta^{13}C$ is variety dependent, with Tinto Cão showing the most negative mean values across all years (black dots) and Colombard showing the least negative mean values. The difference in these mean $\delta^{13}C$ values across the 48 varieties is up to 2.8 ‰, representing a 44 % variation across the full range of varieties relative to Tinto Cão. Some varieties (e.g., Liliorila and Ugni blanc) appear to operate in a narrower range of $\delta^{13}C$ values across the years, while others (e.g., Touriga nacional and Saperavi) operate across a wider range of $\delta^{13}C$. As discussed in the next section, the range of $\delta^{13}C$ provides an indication of the plasticity of a variety to adapt its WUE to dry versus wet conditions.

An effect is also observed across the years with the lowest and highest mean $\delta^{13}C$ values for each variety. For years with the most negative $\delta^{13}C$ values, as associated with wetter conditions and lower WUE during ripening, a difference of up to 3.1 ‰, or a 50 % variation was observed across all varieties relative to the variety with the most negative corresponding $\delta^{13}C$ value (Saperavi). For years with the least negative $\delta^{13}C$ values, as associated with drier conditions and higher WUE during ripening, a difference of up to 4.0 ‰, or a 63 % variation was observed across all varieties relative to the variety with the least negative corresponding $\delta^{13}C$ values (Xynomavro)

In addition to apparent varietal differences, measured $\delta^{13}C$ may also be impacted by the different phenology of each variety, with later ripening varieties being more likely to experience water deficits during the sugar loading period than earlier varieties. Thus, in attempting to characterize genetically determined varietal differences in $\delta^{13}C$, differences in the phenology of the berry ripening period in relationship to the driest times of the season must also be considered.

2.3 Categorization based on key traits

Several combinations of key $\delta^{13}C$ and other physiological traits were used in a hierarchical clustering analysis (HCA) to identify groupings of varieties with similar characteristics. The most consistent groupings were obtained when HCA was applied using the following three traits: "veraison date", "minimum $\delta^{13}C$" (i.e., $\delta^{13}C$ in non-limiting conditions) and "range of $\delta^{13}C$" (i.e., the difference between $\delta^{13}C$ in a wet vintage compared to a dry vintage). The HCA in Figure 4 suggests a range and groupings of varieties based on the above three key traits. All varieties defined traditionally as drought-tolerant (blue arrows) and all varieties defined traditionally as non-drought-tolerant (green arrows) were separated between the two distinct groups. Moreover, varieties generally grown in dry climates were separated from varieties generally grown in more humid climates. While it is very complex to define drought tolerance quantitatively, a consensus could possibly be reached by considering the yield and quality data of the different varieties in the scientific literature and from the wine industry.

Interestingly, the classification based on HCA provided more consistent results with the minimum value of $\delta^{13}C$ (i.e., non-limiting conditions) compared to the maximum value of $\delta^{13}C$ (i.e., limiting conditions). Varieties with a more negative $\delta^{13}C$ in non-limiting conditions may have a greater stomatal conductance and thus greater transpiration and water use early in the season which could more quickly deplete available

soil water (Lebon *et al.*, 2003) and increase the likelihood of water deficits during berry ripening. This hypothesis is supported by the Ψ_{PD} data (Figure 2) where Tempranillo and Semillon, varieties with very relatively negative $\delta^{13}C$ in non-limiting conditions are the two varieties that reached the most negative Ψ_{PD}. The other metric of interest in this HCA classification is the difference between the minimum value of $\delta^{13}C$ (i.e., the $\delta^{13}C$ under non-limiting conditions) and the maximum value of $\delta^{13}C$ (i.e., the $\delta^{13}C$ under limiting conditions). This trait would characterize the plasticity of the variety to adapt to the drought conditions of the vintage.

One confounding factor in assessing the $\delta^{13}C$ characteristics of different varieties is the timing of phenological stages. Of particular concern with $\delta^{13}C$ in berry juice sugars is the vine water status during the period of sugar loading in the berries, roughly starting one week to ten days before

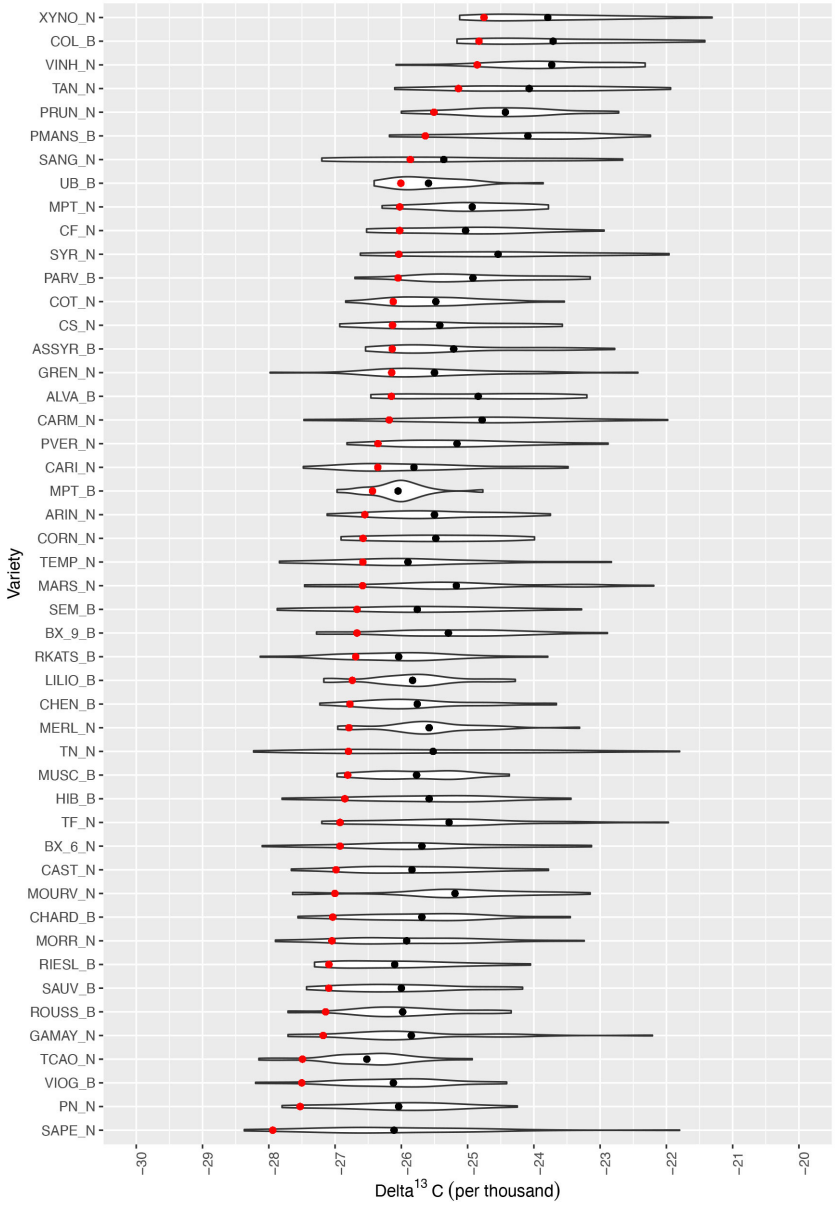

FIGURE 3. Violin plot of the $\delta^{13}C$ data for 48 varieties from 2014 to 2020 in Villenave d'Ornon, France. The black dots represent the average value of $\delta^{13}C$ and the red dots the average value of $\delta^{13}C$ in the wettest year (classified from the less negative to the most negative). The full names of the varieties are presented in Supplementary Materials, Table S1.

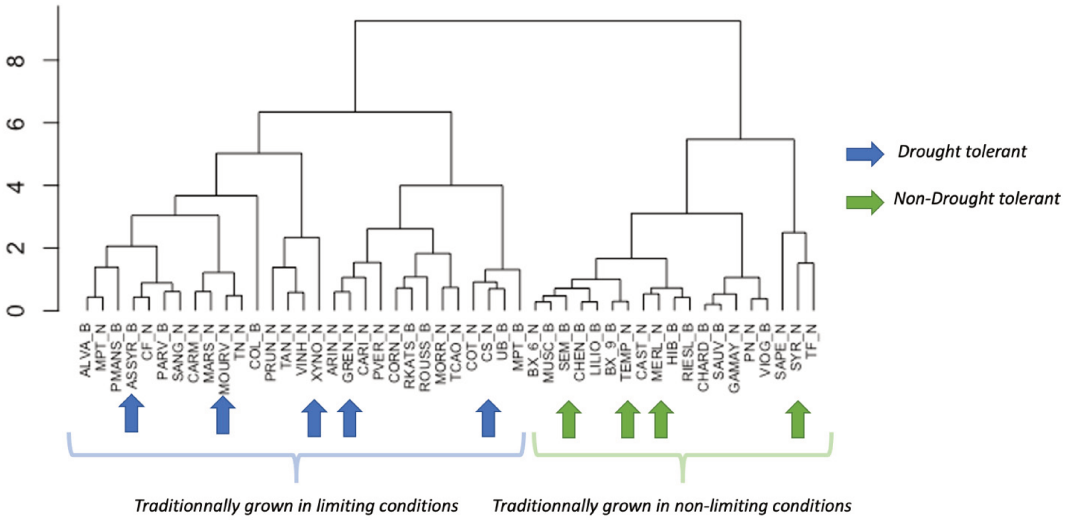

FIGURE 4. Hierarchical Clustering Analyses (HCA) performed with the Ward method of the 48 varieties as a function of "Average Veraison (DOY)", "Minimum $\delta^{13}C$" and "Range of $\delta^{13}C$".

mid-veraison and ending three or four weeks after mid-veraison (Suter *et al*., 2021). In most years, water deficit increases as the season progresses, which means that an early variety faces less water deficit during berry ripening compared to late varieties. Interestingly, adding average mid-veraison dates in the HCA classification improves the separation of drought sensitive versus drought tolerant varieties, as defined by hydroscapes in section 3 below. The relationship between the characteristics "late ripening" and "drought tolerant" may be due to the fact that late ripening varieties were selected to grow in warm climates, which are also most often dry climates. In the HCA presented in Figure 4, most varieties grown around Mediterranean basin are classified in the left panel, such as Assyrtiko, Sangiovese, Mourvèdre, Grenache, Carignan, and Rkatsiteli.

3. Hydroscapes

3.1. Constructed hydroscapes

Hydroscapes are presented in Figure 5 for the six varieties using individual vine data for which there was both $\delta^{13}C$ and corresponding water potential data. Grenache has the smallest hydroscape surface and is known for being very strict in its stomatal regulation (Schultz, 2003). Semillon, the variety with the largest hydroscape, is known for its anisohydric behaviour, due to its poor control over stomatal conductance, leading to substantial nighttime transpiration (Rogiers *et al*., 2009; Dayer *et al*., 2020; Dayer *et al*., 2021). In the same study of Rogiers *et al*., (2009), Cabernet-Sauvignon and Merlot were not significantly different in terms of stomatal conductance which corresponds with our finding of the two varieties having a similar hydroscape surface (10.7 MPa^2 and 10.9 MPa^2, respectively).

These results are also consistent with empirical knowledge gathered in production areas. In La Rioja (Spain), Grenache is planted in the driest parts of the production area around the town of Logroño, while Tempranillo dominates in the cooler locations at higher altitude, where drought- and heat-stress are less frequent. Semillon thrives in the Atlantic climate of Bordeaux (France) and is the major variety in the Hunter Valley (Australia), one of the wettest production areas in the world (Johnson, 2013). The drought responses of Ugni blanc (Trebbiano) is less well documented, but these results suggest that it may be well adapted to dry conditions. The hydroscape approach, however, only refers to stomatal behaviour of plants under various levels of water deficit. Drought responses involve other mechanisms like hydraulic conductance, osmotic adjustment, leaf versus root development, duration of the crop cycle, and timing of phenology to ensure development in the wettest part of the season (Tardieu *et al*., 2018).

3.2. The metrics of the hydroscapes

The areas of the hydroscapes presented in Figure 5 provide an insight into the stomatal behaviour of plants under drought conditions, but other metrics can also be extracted (see also Figure S3 in supplementary materials). For example, the intercept of the hydroscape represents the least negative Ψ_L observed under non-limiting water availability (least negative Ψ_{PD}). Interestingly, this intercept is very different for Grenache compared to Semillon (-0.96 MPa of Ψ_L and -1.4 MPa of Ψ_L, respectively). This may be explained by differences in stomatal conductance, which was observed as being higher in Semillon than Grenache (Rogiers *et al*., 2009). The slope of the hydroscape also differs among varieties, with Grenache having the steepest slope compared to the other varieties.

A distinct critical midday leaf water potential (Ψ_{Lcrit}) is more evident for Grenache, Ugni blanc, Cabernet-Sauvignon and Merlot, but less so for Tempranillo and Semillon.

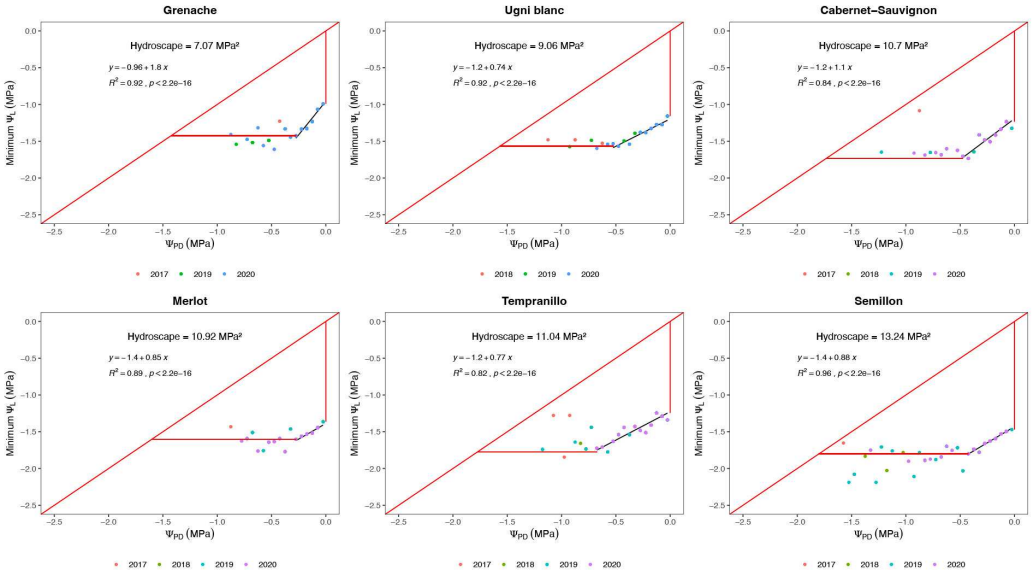

FIGURE 5. Modified hydroscape representation for field data, with their corresponding areas in MPa^2. Varieties are classified from the smallest to the largest hydroscape. The study was carried out in Villenave d'Ornon in 2017 (except for Ugni blanc), 2018 (except for Grenache), 2019 and 2020.

The variation observed for Tempranillo and Semillon could be due to a variety of factors, including differences in vapour pressure deficit during the precise time of measure, and/or measurement artifacts (e.g., severe levels of stress causing petiole embolisms, hydraulically disconnecting the measured leaf from the vine). There are also differences in the Ψ_{PD} at which Ψ_{Lcrit} is reached. For example, Merlot reaches Ψ_{Lcrit} at Ψ_{PD} = -0.3 MPa, while Tempranillo reaches Ψ_{Lcrit} at Ψ_{PD} = -0.7 MPa.

The Ψ_{Lcrit} is a very important metric related to the mortality thresholds of various plant species under drought (Choat *et al.*, 2018). Cultivars with high stomatal conductance in well-watered conditions will deplete soil water earlier in the season. Depending on the degree to which stomatal conductance is adjusted under decreasing Ψ_{PD}, these cultivars could face more severe water deficits. For example in this study, Tempranillo had one of the largest hydroscapes and most negative critical Ψ_L. It was also observed that among the 48 varieties, Tempranillo was one of the earliest varieties to show leaf wilting and leaf abscission.

Another metric of interest is the range of Ψ_{PD} at which a variety normally operates, representing its ability to extract water at low soil water potential. As discussed above, this can be linked to less stringent stomatal control (e.g., Grenache operates over a small range of Ψ_{PD} because of a very strict stomatal control). Some varieties appear able to extract water at very low Ψ_{PD} which may be due to the root architecture associated with the cultivar x rootstock combination. It is impossible, however, to assess the rooting zone of the vines in field conditions, which may vary from one vine to the other in the VitAdapt parcel due to soil heterogeneity. It is also possible that the variety influences the ability of the rootstock to explore the soil more or less profoundly (Tandonnet *et al.*, 2010). Vines having access to a greater volume of soil water due to a greater rooting depth are likely to experience less negative values of Ψ_{PD}.

The approach presented offers a possible way of classifying varieties according to their level of (an)isohydricity, an important criterion in drought tolerance (i.e., the larger the hydroscape, the more drought sensitive). Results are in line with the literature regarding stomatal behaviour, in particular for the well documented varieties Grenache and Semillon (Schultz, 2003; Rogiers *et al.*, 2009). Results were obtained on six varieties only and need to be confirmed on a wider range of cultivars. It would also be interesting to assess whether, for a given variety, the hydroscapes have a different shape when the data are collected on different soil types, or with different rootstocks. One of the limitations of the hydroscape approach is that it requires time-consuming water potential field data collected, ideally over multiple years.

4. Comparison of $\delta^{13}C$ and hydroscapes

Both $\delta^{13}C$ and hydroscapes are mainly driven by the stomatal behaviour of plants (Farquhar, 1989; Meinzer *et al.*, 2016). Hydroscapes were constructed as described above for six varieties for which there were also measurements of $\delta^{13}C$. Several metrics were extracted from the analysis performed using these two tools and are listed in Table 1 along with the associated values for each variety.

A correlation analysis of the metrics presented in Table 1 across the different varieties is presented in Figure 6. It is observed that the size of the hydroscapes is strongly

TABLE 1. Metrics of hydroscapes and $\delta^{13}C$ for six grapevine varieties. Varieties are classified from the lowest to the highest hydroscape area as representative of (an)isohydristicity. For each metric, values are classified with shades of green.

Variety	Intercept (MPa)	Slope (MPa)	Ψ_{Lcrit} (MPa)	Range of Ψ_{PD} (MPa)	Hydroscape (MPa^2)	Range of Ψ_L^* (MPa)	Range of $\delta^{13}C$ (‰)	Max $\delta^{13}C$ (‰)	Min $\delta^{13}C$ (‰)
Grenache	-0.96	1.80	-1.43	-0.89	7.07	0.47	4.08	-23.20	-27.28
Ugni blanc	-1.2	0.74	-1.57	-1.12	9.06	0.37	4.06	-23.34	-27.40
Cabernet-Sauvignon	-1.2	1.10	-1.73	-1.23	10.70	0.53	4.65	-23.11	-27.76
Merlot	-1.4	0.85	-1.60	-0.89	10.92	0.20	3.90	-23.70	-27.60
Tempranillo	-1.2	0.77	-1.78	-1.18	11.04	0.58	5.96	-22.35	-28.31
Semillon	-1.4	0.88	-1.80	-1.58	13.24	0.40	5.15	-23.30	-28.45

* Difference on the y-axis between the intercept of the hydroscape and the Ψ_{Lcrit}.

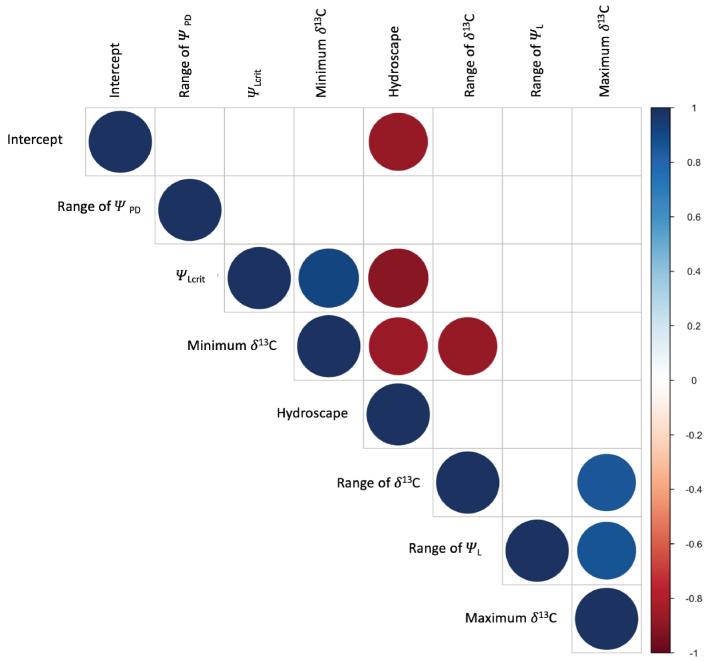

FIGURE 6. A correlation heatmap of the metrics extracted from the hydroscapes and from the $\delta^{13}C$ (as shown in Table 1). Only significant correlations at $P < 0.05$ are indicated.

dependent on two variables, the intercept and the Ψ_{Lcrit}. While the intercept becomes more negative the size of the hydroscape increases, suggesting a generally anisohydric behaviour even at low Ψ_{PD}. A similar dynamic exists with a more negative Ψ_{Lcrit} also being associated with a larger hydroscape.

The minimum $\delta^{13}C$, which is the most negative $\delta^{13}C$ obtained in non-limiting conditions, appears better correlated to hydraulic traits from the hydroscapes than does the maximum $\delta^{13}C$, which is the least negative $\delta^{13}C$ obtained in dry conditions. Minimum $\delta^{13}C$ is well correlated negatively with the area of the hydroscapes (Hydroscape) and positively with Ψ_{Lcrit}, suggesting the anisohydric behaviour of a larger hydroscape is somehow associated with a lower level of water use efficiency in well-watered conditions (Chaves *et al.*, 2010). Increased water use in non-limiting conditions, as suggested by more negative Ψ_L, may lead to greater water deficits later in the season and hence less negative $\delta^{13}C$.

By integrating the $\delta^{13}C$ metrics with the insights provided by the hydroscapes metrics, minimum $\delta^{13}C$ appears to be a relatively easily accessible metric to classify grapevine varieties according to their drought responses. It should be noted that, although these metrics are easy to collect in field conditions, they need to be measured over multiple years in homogeneous soil conditions, or with enough replicates to rule-out possible variability in soil water holding

capacity. These conditions were met in the VitAdapt setting (Destrac-Irvine and van Leeuwen, 2017).

CONCLUSION

The measured $\delta^{13}C$ in berry juice sugars provides an indication of vine water status during the period of sugar accumulation from veraison through maturity, as was confirmed by comparison against corresponding measurements of predawn water potential on six varieties over four seasons. Distinct differences in $\delta^{13}C$ measured in berry juice sugar collected in a vineyard setting over seven years of differing climatic conditions found significant differences across 48 varieties. The drought responses of these varieties were then ranked using a hierarchical cluster analysis based on: i) the mean $\delta^{13}C$ in years of relatively low water stress; ii) the range of $\delta^{13}C$ for a variety as measured in wet versus dry years; and iii) the day of year of mid-veraison. This ranking corresponded well with generally understood drought tolerance characteristics of the different varieties. Of particular importance were the highly variable mid-veraison dates for the different varieties affecting the water deficits experienced by each variety, and hence the corresponding measured $\delta^{13}C$ in a given year, independent of the genotype response.

The predawn measurements on the six varieties over four years, along with corresponding midday leaf water potential measurements were used to construct hydroscapes, which allowed insight into the stomatal behaviour of these varieties. Among several hydroscape metrics, minimum critical leaf water potential (Ψ_{Lcrit}), and the closely related total area of the hydroscape were considered to provide a good indication of drought stress sensitivity. Less negative values of Ψ_{Lcrit} and correspondingly smaller hydroscape areas suggest an isohydric variety, which regulates its stomata more strictly to maintain water potential. Conversely, more negative Ψ_{Lcrit} and larger hydroscapes are suggestive of a more anisohydric variety, which regulates its stomata less strictly, allowing for more negative water potentials.

Comparison of $\delta^{13}C$ and hydroscape metrics found minimum $\delta^{13}C$ (i.e., from years with less limiting conditions) to be correlated negatively with the area of the hydroscapes and positively correlated with Ψ_{Lcrit}, suggesting the anisohydric behaviour of a larger hydroscape is somehow associated with a lower level of water use efficiency. This may be due to increased water use in non-limiting conditions as suggested by more negative Ψ_{L}, resulting in greater water deficits and more stress later in the season and hence less negative $\delta^{13}C$. This also suggests that this minimum $\delta^{13}C$ could provide a relatively easy way to classify grapevine varieties according to their drought stress responses.

ACKNOWLEDGMENTS

This study was carried out with support from Jas. Hennessy & Co. (16100 Cognac, France). The VitAdapt Project is supported by the Conseil Interprofessionnel des Vins de Bordeaux (CIVB), the Conseil Régional d'Aquitaine and the Institut National de Recherche pour l'Agriculture, l'Alimentation et l'Environnement (INRAE). This study has been carried out with financial support from the French National Research Agency (ANR) in the frame of the Investments for the future Programme, within the Cluster of Excellence COTE (ANR-10-LABX-45). The authors would like to thank INRAE, UEVB, F-33882, Villenave d'Ornon, France, for its contribution to the maintenance of the VitAdapt experiment.

REFERENCES

Álvarez-Maldini, C., Acevedo, M., & Pinto, M. (2021). Hydroscapes: A useful metric for distinguishing iso-/anisohydric behaviour in almond cultivars. *Plants*, *10*(6), 1249. https://doi.org/10.3390/plants10061249

Améglio, T., Archer, P., Cohen, M., Valancogne, C., Daudet, F. A., Dayau, S., & Cruiziat, P. (1999). Significance and limits in the use of predawn leaf water potential for tree irrigation. *Plant and Soil*, *207*(2), 155-167. https://doi.org/10.1023/A:1026415302759

Anderson, K., & Aryal, N. R. (2013). *Which winegrape varieties are grown where? A global empirical picture* (p. 700). University of Adelaide Press. https://doi.org/10.20851/winegrapes

Bchir, A., Escalona, J., Galle, A., Hernández-Montes, E., Tortosa, I., Braham, M., & Medrano, H. (2016). Carbon isotope discrimination ($\delta^{13}C$) as an indicator of vine water status and water use efficiency (WUE): Looking for the most representative sample and sampling time. *Agricultural Water Management*, *167*, 11–20. https://doi.org/10.1016/j.agwat.2015.12.018

Carbonneau, A., Deloire, A., Torregrosa, L., Jaillard, B., Pellegrino, A., Metay, A., Ojeda, H., Lebon, E., & Abbal, P. (2015). *Traité de la vigne: Physiologie, terroir, culture.* (Issue 2ème ed., p. 592 p.). Dunod. https://hal.archives-ouvertes.fr/hal-02154373

Charrier, G., Delzon, S., Domec, J.-C., Zhang, L., Delmas, C. E. L., Merlin, I., Corso, D., King, A., Ojeda, H., Ollat, N., Prieto, J. A., Scholach, T., Skinner, P., van Leeuwen, C., & Gambetta, G. A. (2018). Drought will not leave your glass empty: Low risk of hydraulic failure revealed by long-term drought observations in world's top wine regions. *Science Advances*, *4*(1), eaao6969. https://doi.org/10.1126/sciadv.aao6969

Chaves, M. M., Zarrouk, O., Francisco, R., Costa, J. M., Santos, T., Regalado, A. P., Rodrigues, M. L., & Lopes, C. M. (2010). Grapevine under deficit irrigation: Hints from physiological and molecular data. *Annals of Botany*, *105*(5), 661–676. https://doi.org/10.1093/aob/mcq030

Cifre, J., Bota, J., Escalona, J. M., Medrano, H., & Flexas, J. (2005). Physiological tools for irrigation scheduling in grapevine (*Vitis vinifera* L.): An open gate to improve water-use efficiency?. *Agriculture, Ecosystems & Environment*, *106*(2-3), 159-170. https://doi.org/10.1016/j.agee.2004.10.005

Choat, B., Brodribb, T. J., Brodersen, C. R., Duursma, R. A., López, R., & Medlyn, B. E. (2018). Triggers of tree mortality under drought. *Nature*, *558* (7711), 531–539. https://doi.org/10.1038/s41586-018-0240-x

Choné, X., van Leeuwen, C., Dubourdieu, D., Gaudillère, J. P., (2001). Stem water potential is a sensitive indicator of grapevine water status. *Annals of Botany*, *87*(4), 477–483. https://doi.org/10.1006/anbo.2000.1361

Dayer, S., Herrera, J. C., Dai, Z., Burlett, R., Lamarque, L. J., Delzon, S., Bortolami, G., Cochard, H., & Gambetta, G. A. (2020).

The sequence and thresholds of leaf hydraulic traits underlying grapevine varietal differences in drought tolerance. *Journal of Experimental Botany*, *71*(14), 4333–4344. https://doi.org/10.1093/jxb/eraa186

Dayer, S., Herrera, J. C., Dai, Z., Burlett, R., Lamarque, L. J., Delzon, S., Bortolami, G., Cochard, H., & Gambetta, G. A. (2021). Nighttime transpiration represents a negligible part of water loss and does not increase the risk of water stress in grapevine. *Plant, Cell & Environment*, *44*(2), 387–398. https://doi.org/10.1111/pce.13923

Destrac-Irvine, A., & van Leeuwen, C. (2017). VitAdapt : an experimental program to study the behaviour of a wide range of *Vitis vinifera* varieties in a context of climate change in the Bordeaux vineyards. In: proceedings of Climwine, sustainable grape and wine production in the context of climate change, 11-13 April 2016, Bordeaux, p. 165-171.

Farquhar, G. (1989). Carbon isotope discrimination and photosynthesis. *Annual Review of Plant Physiology and Plant Molecular Biology*, *40*(1), 503–537. https://doi.org/10.1146/annurev.arplant.40.1.503

Flexas, J., Escalona, J. M., & Medrano, H. (1998). Down-regulation of photosynthesis by drought under field conditions in grapevine leaves. *Functional Plant Biology*, *25*(8), 893-900. https://doi.org/10.1071/PP98054

Fraga, H., Malheiro, A. C., Moutinho-Pereira, J., & Santos, J. A. (2012). An overview of climate change impacts on European viticulture. *Food and Energy Security*, *1*(2), 94–110. https://doi.org/10.1002/fes3.14

Gaudillère, J., van Leeuwen, C., & Ollat, N. (2002). Carbon isotope composition of sugars in grapevine, an integrated indicator of vineyard water status. *Journal of Experimental Botany*, *53*(369), 757–763. https://doi.org/10.1093/jexbot/53.369.757

Gaudin, R., Roux, S., & Tisseyre, B. (2017). Linking the transpirable soil water content of a vineyard to predawn leaf water potential measurements. *Agricultural Water Management*, *182*, 13-23. https://doi.org/10.1016/j.agwat.2016.12.006

Hochberg, U., Rockwell, F. E., Holbrook, N. M., & Cochard, H. (2018). Iso/Anisohydry: A Plant–Environment Interaction Rather Than a Simple Hydraulic Trait. *Trends in Plant Science*, *23*(2), 112–120. https://doi.org/10.1016/j.tplants.2017.11.002

Johnson, H.J. R. (2013). *The World Atlas of Wine, 7th Edition*. Mitchell Beazley.

Keller, M.. (2010). *The Science of Grapevines—1st Edition*. Elsevier Science Publishing Co Inc, Academic Press Inc.

Klein, T. (2014). The variability of stomatal sensitivity to leaf water potential across tree species indicates a continuum between isohydric and anisohydric behaviours. *Functional Ecology*, *28*(6), 1313–1320. https://doi.org/10.1111/1365-2435.12289

Lebon, E., Dumas, V., & Pieri, P. (2003). Modelling the seasonal dynamics of the soil water balance of vineyards. *Functional Plant Biology*, *30*, 12. https://doi.org/10.1071/FP02222

Le Menn, N., van Leeuwen, C., Picard, M., Riquier, L., Revel, G., & Marchand, S. (2019). Effect of Vine Water and Nitrogen Status, as Well as Temperature, on Some Aroma Compounds of Aged Red Bordeaux Wines. *Journal of Agricultural and Food Chemistry*, *67*. https://doi.org/10.1021/acs.jafc.9b00591

Levin, A. D., Williams, L. E., Matthews (2019). A continuum of stomatal responses to water deficits among 17 wine grape cultivars (*Vitis vinifera*). *Functional Plant Biology*, *47*(1), 11–25. https://doi.org/10.1071/FP19073

Li, X., Blackman, C. J., Peters, J. M. R., Choat, B., Rymer, P. D., Medlyn, B. E., & Tissue, D. T. (2019). More than iso/anisohydry: Hydroscapes integrate plant water use and drought tolerance traits in 10 eucalypt species from contrasting climates. *Functional Ecology*, *33*(6), 1035–1049. https://doi.org/10.1111/1365-2435.13320

Martínez-Vilalta, J., Poyatos, R., Aguadé, D., Retana, J., & Mencuccini, M. (2014). A new look at water transport regulation in plants. *New Phytologist*, *204*(1), 105–115. https://doi.org/10.1111/nph.12912

Medrano, H., Flexas, J., Ribas-Carbó, M., & Gulías, J. (2010). Measuring Water Use Efficiency in Grapevines. In S. Delrot, H. Medrano, E. Or, L. Bavaresco, & S. Grando (Eds.), *Methodologies and Results in Grapevine Research* (pp. 123–134). Springer Netherlands. https://doi.org/10.1007/978-90-481-9283-0_9

Meinzer, F. C., Woodruff, D. R., Marias, D. E., Smith, D. D., McCulloh, K. A., Howard, A. R., & Magedman, A. L. (2016). Mapping 'hydroscapes' along the iso- to anisohydric continuum of stomatal regulation of plant water status. *Ecology Letters*, *19*(11), 1343–1352. https://doi.org/10.1111/ele.12670

Ollat, N., Touzard, J.-M., & van Leeuwen, C. (2016). Climate Change Impacts and Adaptations: New Challenges for the Wine Industry. *Journal of Wine Economics*, *11*(01), 139–149. https://doi.org/10.1017/jwe.2016.3

Roby, G., Harbertson, J. F., Adams, D. A., & Matthews, M. A. (2004). Berry size and vine water deficits as factors in winegrape composition: Anthocyanins and tannins. *Australian Journal of Grape and Wine Research*, *10*(2), 100–107. https://doi.org/10.1111/j.1755-0238.2004.tb00012.x

Rogiers, S. Y., Greer, D. H., Hutton, R. J., & Landsberg, J. J. (2009). Does night-time transpiration contribute to anisohydric behaviour in a *Vitis vinifera* cultivar? *Journal of Experimental Botany*, *60*(13), 3751–3763. https://doi.org/10.1093/jxb/erp217

Santesteban, L. G., Miranda, C., & Royo, J. B. (2009). Effect of water deficit and rewatering on leaf gas exchange and transpiration decline of excised leaves of four grapevine (*Vitis vinifera* L.) cultivars. *Scientia Horticulturae*, *121*(4), 434–439. https://doi.org/10.1016/j.scienta.2009.03.008

Santesteban, L. G., Miranda, C., Urretavizcaya, I., & Royo, J. B. (2012). Carbon isotope ratio of whole berries as an estimator of plant water status in grapevine (*Vitis vinifera* L.) cv. 'Tempranillo.' *Scientia Horticulturae*, *146*, 7–13. https://doi.org/10.1016/j.scienta.2012.08.006

Scholander, P. F., Bradstreet, E. D., Hemmingsen, E. A., & Hammel, H. T. (1965). Sap Pressure in Vascular Plants. *Science*, *148*(3668), 339–346. https://doi.org/10.1126/science.148.3668.339

Schultz, H. R. (2003). Differences in hydraulic architecture account for near-isohydric and anisohydric behaviour of two field-grown *Vitis vinifera* L. cultivars during drought. *Plant, Cell & Environment*, *26*(8), 1393–1405. https://doi.org/10.1046/j.1365-3040.2003.01064.x

Souza, D., R, C., Maroco, J. P., Santos, D., P, T., Rodrigues, M. L., Lopes, C. M., Pereira, J. S., & Chaves, M. M. (2005). Impact of deficit irrigation on water use efficiency and carbon isotope composition ($\delta^{13}C$) of field-grown grapevines under Mediterranean climate. *Journal of Experimental Botany*, *56*(418), 2163–2172. https://doi.org/10.1093/jxb/eri216

Suter, B., Destrac-Irvine, A., Gowdy, M., Dai, Z., & van Leeuwen, C. (2021). Adapting Wine Grape Ripening to Global Change Requires a Multi-Trait Approach. *Frontiers in Plant Science*, *12*, 624867. https://doi.org/10.3389/fpls.2021.624867

Tandonnet, J.-P., Cookson, S., Vivin, P., & Ollat, N. (2010). Scion genotype biomass allocation and root development in grafted grapevine. *Australian Journal of Grape and Wine Research*, *16*, 290–300. https://doi.org/10.1111/j.1755-0238.2009.00090.x

Tardieu, F., & Simonneau, T. (1998). Variability among species of stomatal control under fluctuating soil water status and evaporative demand : modelling isohydric and anisohydric behaviours. *Journal of Experimental Botany*, *49*(Special), 419432. https://doi.org/10.1093/jxb/49.special_issue.419

Tardieu, F., Simonneau, T., & Muller, B. (2018). The physiological basis of drought tolerance in crop plants : a scenario-dependent probabilistic approach. *Annual Review of Plant Biology*, *69*(1), 733759. https://doi.org/10.1146/annurev-arplant-042817-040218

Tomás, M., Medrano, H., Brugnoli, E., Escalona, J. m., Martorell, S., Pou, A., Ribas-Carbó, M., & Flexas, J. (2014). Variability of mesophyll conductance in grapevine cultivars under water stress conditions in relation to leaf anatomy and water use efficiency. *Australian Journal of Grape and Wine Research*, *20*(2), 272–280. https://doi.org/10.1111/ajgw.12069

Triolo, R., Roby, J. P., Pisciotta, A., Di Lorenzo, R., & van Leeuwen, C. (2019). Impact of vine water status on berry mass and berry tissue development of Cabernet franc (*Vitis vinifera* L.), assessed at berry level. *Journal of the Science of Food and Agriculture*, *99*(13), 5711-5719. https://doi.org/10.1002/jsfa.9834

van Leeuwen, C., & Darriet, P. (2016). The Impact of Climate Change on Viticulture and Wine Quality. *Journal of Wine Economics*, *11*(01), 150–167. https://doi.org/10.1017/jwe.2015.21

van Leeuwen, C., Tregoat, O., Choné, X., Bois, B., Pernet, D., Gaudillère, J.-P., & others. (2009). Vine water status is a key factor in grape ripening and vintage quality for red Bordeaux wine. How can it be assessed for vineyard management purposes. *J. Int. Sci. Vigne Vin*, *43*(3), 121–134. https://doi.org/10.20870/oeno-one.2009.43.3.798

van Leeuwen, C., Pieri, P., Gowdy, M., Ollat, N., & Roby, J. P. (2019a). Reduced density is an environmental friendly and cost effective solution to increase resilience to drought in vineyards in a contexte of climate change. *OENO One*, *53*(2), 129-146. https://doi.org/10.20870/oeno-one.2019.53.2.2420

van Leeuwen, C., Destrac-Irvine, A., Dubernet, M., Duchêne, E., Gowdy, M., Marguerit, E., Pieri, P., Parker, A., de Rességuier, L., & Ollat, N. (2019b). An update on the impact of climate change in viticulture and potential adaptations. *Agronomy*, *9*(9), 514. https://doi.org/10.3390/agronomy9090514

van Leeuwen, C., Barbe, J. C., Darriet, P., Geffroy, O., Gomès, E., Guillaumie, S., Helwi, P., Laboyrie, J., Lytra, G., Le Menn, N., Marchand, S., Picard., M., Pons., A., Schüttler A. & Thibon, C. (2020). Recent advancements in understanding the terroir effect on aromas in grapes and wines: This article is published in cooperation with the XIIIth International Terroir Congress November 17-18 2020, Adelaide, Australia. Guest editors: Cassandra Collins and Roberta De Bei. *OENO One*, *54*(4), 985-1006. https://doi.org/10.20870/oeno-one.2020.54.4.3983

Wickham, H., François, R., Henry, L., Müller, K., & RStudio. (2021a). *Dplyr : A Grammar of Data Manipulation* (1.0.7) [Logiciel]. https://cran.r-project.org/web/packages/dplyr/index.html

Wickham, H., Chang, W., Henry, L., Pedersen, T. L., Takahashi, K., Wilke, C., Woo, K., Yutani, H., Dunnington, D., & RStudio. (2021b). *Ggplot2 : Create elegant data visualisations using the grammar of graphics* (3.3.5) [Logiciel]. https://cran.r-project.org/web/packages/ggplot2/index.html

Williams, L., & Araujo, F. J. (2002). Correlations among Predawn Leaf, Midday Leaf, and Midday Stem Water Potential and their Correlations with other Measures of Soil and Plant Water Status in *Vitis vinifera*. *Journal of the American Society for Horticultural Science*, *127*, 448–454. https://doi.org/10.21273/JASHS.127.3.448

Winkel, T., & Rambal, S. (1990). Stomatal conductance of some grapevines growing in the field under a Mediterranean environment. *Agricultural and Forest Meteorology*, *51*(2), 107-121. https://doi.org/10.1016/0168-1923(90)90010-4

SUPPLEMENTARY DATA
Plantevin, M., Gowdy, M., Destrac-Irvine, A., Marguerit, E., Gambetta, G. A., & van Leeuwen, C. (2022). Using $\delta^{13}C$ and hydroscapes for discriminating cultivar specific drought responses: This article is published in cooperation with Terclim 2022 (XIVth International Terroir Congress and 2nd ClimWine Symposium), 3-8 July 2022, Bordeaux, France. *OENO One*, *56*(2).
https://doi.org/10.20870/oeno-one.2022.56.2.5434

Supplemental Materials

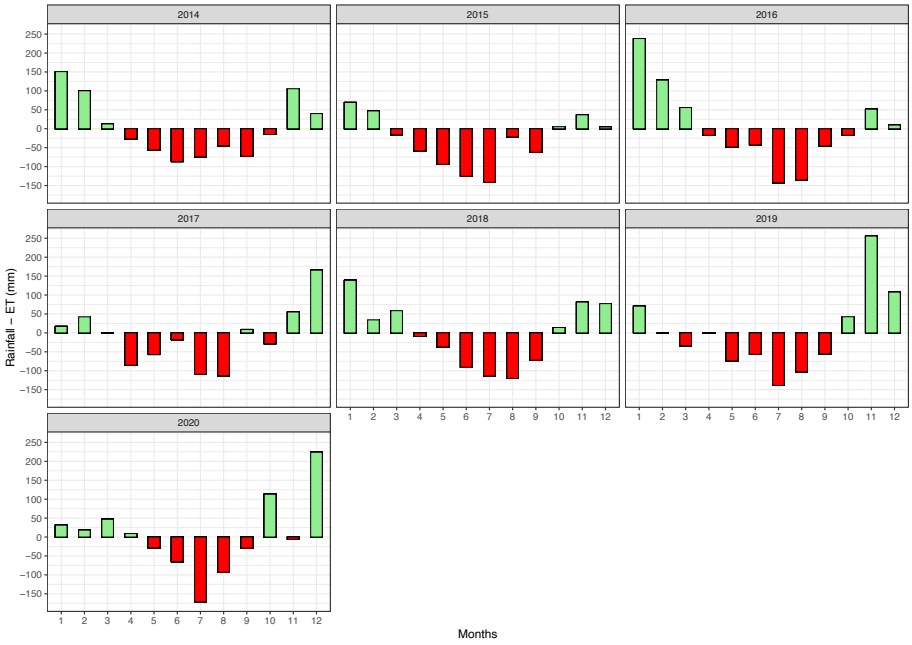

SUPPLEMENTARY FIGURE S1. Monthly evaporative demand (Rainfall – Evapotranspiration) for 2014 to 2020.

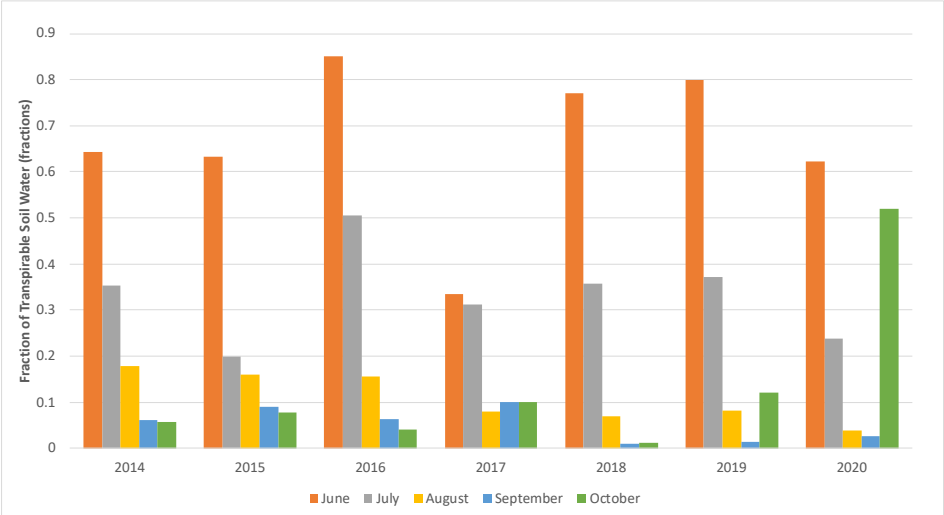

SUPPLEMENTARY FIGURE S2. Monthly fraction of transpirable soil water (FTSW) during the growing season for the years 2014 to 2020.

SUPPLEMENTARY DATA
Plantevin, M., Gowdy, M., Destrac-Irvine, A., Marguerit, E., Gambetta, G. A., & van Leeuwen, C. (2022). Using $\delta^{13}C$ and hydroscapes for discriminating cultivar specific drought responses: This article is published in cooperation with Terclim 2022 (XIVth International Terroir Congress and 2nd ClimWine Symposium), 3-8 July 2022, Bordeaux, France. *OENO One*, *56*(2).
https://doi.org/10.20870/oeno-one.2022.56.2.5434

Variety	Abbreviation	Variety	Abbreviation
Alvarinho	ALVA_B	MPT-3156-26-1	MPT_B
Arinarnoa	ARIN_N	MPT-3160-12-3	MPT_N
Asyrtiko	ASSYR_B	Muscadelle	MUSC_B
BX-648	BX_6_N	Petit Manseng	PMANS_B
BX-9216	BX_9_B	Petit Verdot	PVER_N
Cabernet Franc	CF_N	Petite Arvine	PARV_B
Cabernet Sauvignon	CS_N	Pinot Noir	PN_N
Carignan	CARI_N	Prunelard	PRUN_N
Carmenère	CARM_N	Riesling	RIESL_B
Castets	CAST_N	Rkatsiteli	RKATS_B
Chardonnay	CHARD_B	Roussanne	ROUSS_B
Chasselas	CHASS_B	Sangiovese	SANG_N
Chenin	CHEN_B	Saperavi	SAPE_N
Colombard	COL_B	Sauvignon	SAUV_B
Cornalin	CORN_N	Semillon	SEM_B
Cot	COT_N	Syrah	SYR_N
Gamay	GAMAY_N	Tannat	TAN_N
Grenache	GREN_N	Tempranillo	TEMP_N
Hibernal Blanc	HIB_B	Tinto Cao	TCAO_N
Liliorila	LILIO_B	Touriga Francesa	TF_N
Marselan	MARS_N	Touriga Nacional	TN_N
Mavrud	MAV_N	Ugni Blanc	UB_B
Merlot	MERL_N	Vinhao (Souzao)	VINH_N
Morrastel	MORR_N	Viognier	VIOG_B
Mourvèdre	MOURV_N	Xinomavro	XYNO_N

SUPPLEMENTARY Table S1. Full names of the varieties studied and their relative abbreviations.

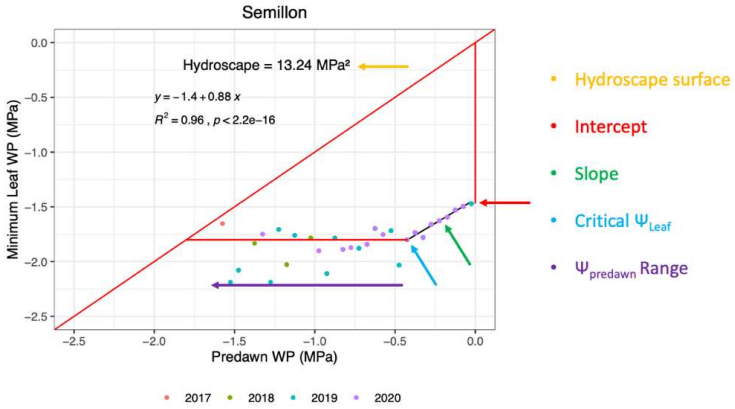

SUPPLEMENTARY Figure S4. The different metrics of the hydroscape.

3.3 Discussion

Measurement of carbon isotope discrimination in berry juice at maturity ($\delta^{13}C$) and corresponding water potential measurements during the berry ripening period over four seasons confirmed results from prior studies that suggested $\delta^{13}C$ provides an integrated assessment of vine water status during the period of berry ripening (Gaudillère et al., 2002; van Leeuwen et al., 2010; Bchir et al., 2016). But in order for such measurements to be useful for growers as an indication of the relative level of drought stress during berry ripening, $\delta^{13}C$ data over several seasons would be required to establish the range of drought response of a given variety into the level of stress in a given year can be judged.

Various $\delta^{13}C$ metrics and vine phenology measured on 48 different varieties in the same growing conditions over seven years were also used to create a classification of drought tolerance that matched well with prior understandings of the relative drought tolerance of different varieties, whether gained empirically based on grower observations in dry conditions, or in published articles in peer reviewed journals. The selected classification was performed using a hierarchical cluster analysis (HCA) based on the following observed traits for each variety: i) the day of year (DOY) of véraison; ii) the $\delta^{13}C$ in the wettest year; and iii) the range of $\delta^{13}C$ measurements between those in the driest and wettest years. As varieties with earlier véraison dates will tend to ripen in less stressed conditions that later varieties, this is important to account for this in any classification based on measurements of stress. $\delta^{13}C$ in the wettest year provides an idea of the water use efficiency in less water limited conditions, with less water efficient varieties potentially consuming available water more quickly early in the season and then experiencing greater stress levels later in the season. The range of $\delta^{13}C$ between wet and dry years indicates the reactivity, or sensitivity of the stress response of the varieties across extremes.

The HCA classification depicted in Figure 4 of Plantevin et al. (2022) is reproduced in Table 1 below, including for reference, the corresponding values of véraison date (DOY), $\delta^{13}C$ in the wettest year, and the range of $\delta^{13}C$ measurements. The HCA classification obtained in this way is unique and could be very useful for growers considering what plant material to select based on their potential stress responses to a set of anticipated growing conditions.

Table 1. Classification of 48 varieties resulting from the hierarchical cluster analysis based on véraison date (DOY), $\delta^{13}C$ in the wettest year, and the range of $\delta^{13}C$ measurements.

More drought tolerant

Rank	Variety	Veraison DOY	min year d13C	d13C range
1	Alvarinho	213	−26.2	2.2
2	MPT-3160-12-3	211	−26.0	2.2
3	Petit Manseng	215	−25.6	2.6
4	Asyrtiko	219	−26.1	2.3
5	Cabernet Franc	221	−26.0	2.2
6	Petite Arvine	216	−26.1	2.3
7	Sangiovese	218	−25.9	2.0
8	Carmenère	215	−26.2	2.6
9	Marselan	215	−26.6	2.7
10	Mourvèdre	216	−27.0	2.8
11	Touriga Nacional	217	−26.8	3.0
12	Colombard	210	−24.8	3.2
13	Prunelard	223	−25.5	1.8
14	Tannat	218	−25.1	2.0
15	Vinhao (Souzao)	220	−24.9	2.1
16	Xinomavro	227	−24.8	2.7
17	Arinarnoa	222	−26.6	1.9
18	Grenache	222	−26.1	1.8
19	Carignan	224	−26.4	1.4
20	Petit Verdot	228	−26.4	2.1
21	Cornalin	219	−26.6	2.0
22	Rkatsiteli	217	−26.7	1.7
23	Roussanne	218	−27.1	2.2
24	Morrastel	223	−27.0	2.1
25	Tinto Cao	223	−27.5	1.9
26	Cot	214	−26.1	1.7
27	Cabernet Sauvignon	218	−26.1	1.6
28	Ugni Blanc	216	−26.0	1.3
29	MPT-3156-26-1	215	−26.4	1.0

Less drought tolerant

Rank	Variety	Veraison DOY	min year d13C	d13C range
30	BX-648	211	−26.9	2.0
31	Muscadelle	210	−26.8	2.0
32	Semillon	209	−26.7	2.0
33	Chenin	212	−26.8	1.8
34	Liliorila	212	−26.7	2.0
35	BX-9216	210	−26.7	2.3
36	Tempranillo	211	−26.6	2.2
37	Castets	215	−27.0	2.1
38	Merlot	215	−26.8	2.4
39	Hibernal Blanc	213	−26.9	2.2
40	Riesling	212	−27.1	2.2
41	Chardonnay	208	−27.0	2.5
42	Sauvignon blanc	208	−27.1	2.6
43	Gamay	210	−27.2	2.7
44	Pinot Noir	209	−27.5	2.5
45	Viognier	210	−27.5	2.4
46	Saperavi	213	−27.9	3.5
47	Syrah	212	−26.0	3.5
48	Touriga Francesa	209	−26.9	3.8

Hydroscapes were also constructed from measurements of midday and predawn leaf water potential (Ψ_L and Ψ_{PD}) measurements using a method that was modified from previous methods developed by Meinzer *et al.* (2016) and Charrier *et al.* (2018). The sizes of the hydroscapes are indicative of range of Ψ_L over which the vine will operate with smaller hydroscapes associated with more isohydric varieties that more readily close their stomata in order to regulate their leaf water potential, compared to those with larger hydroscapes, indicative of anisohydric varieties that allow their leaf water potential to operate at more negative levels. It is observed that the size of the hydroscape for a variety is strongly dependent on two hydroscape metrics, the lowest level of Ψ_L under non-limiting conditions (i.e., intercept at $\Psi_{PD} = 0$) and the lowest level of Ψ_L at high levels of stress (i.e., Ψ_{Lcrit} at very negative Ψ_{PD}). These key hydroscape metrics were then found to be well correlated

with the $\delta^{13}C$ obtained in years of relatively non-limiting conditions. This suggests the anisohydric behavior of a larger hydroscape is associated with a lower level of water use efficiency in well-watered conditions. Increased water use in non-limiting conditions, as suggested by a larger hydroscape, may lead to accelerated soil water depletion and greater water deficits later in the season and hence increasing $\delta^{13}C$. The relationship between these hydroscape and $\delta^{13}C$ metrics lends some interpretation and validation to the significance of the minimum year $\delta^{13}C$ metric, with the latter being much easier to obtain in the vineyard over several seasons and a wide range of varieties.

4 Carbon isotope discrimination in must, wine, and spirit

4.1 Background

The pending journal article presented in this chapter, entitled "*Carbon isotope discrimination as an indicator of vine water status is comparable in grape must, wine, and distilled wine spirit*" investigates how $\delta^{13}C$ in wine spirit (*eau de vie*) is potentially affected by a double distillation process, such as that used in the production of Cognac. If the $\delta^{13}C$ signal in eau de vie is conserved when compared to that in the source wine and parent grape must, then the $\delta^{13}C$ in eau de vie could be used to estimate the vine water status that existed during the corresponding berry ripening period. In turn, this could be useful for exploring retrospectively how sensory attributes of eau de vie are linked to vine water status, such as has been done previously for wine (Picard et al., 2017).

Figure 3. Laboratory-scale Charentaise style still used for production of eau de vie (photo courtesy of Conservatoire du Vignoble Charentais).

Measurements of $\delta^{13}C$ were made in grape must, fermented wine, and corresponding distilled spirit from nine varieties of interest in the Cognac region over either one or two seasons. Of particular importance was the use of a laboratory-scale still made of the same material and proportions as a traditional 25 hl capacity still (Figure 3) and using the same Charentaise-style distillation procedures. No prior studies of the effect of this double distillation process on the $\delta^{13}C$ signal in eau de vie were found in the literature.

4.2 Journal article

Carbon isotope discrimination as an indicator of vine water status is comparable in grape must, wine, and distilled wine spirit

Mark Gowdy[1], Sébastien Juillard[2], Marina Frouin[2], Xavier Poitou[3], Agnès Destrac-Irvine[1] and Cornelis van Leeuwen[1*]

[1] EGFV, Univ. Bordeaux, Bordeaux Sciences Agro, INRAE, ISVV, 33882 Villenave d'Ornon

[2] Conservatoire du Vignoble Charentais, Institut de Formation de Richemont, 16370 Cherves Richemont

[3] Jas. Hennessy & Co., 16100 Cognac

Brief research report published in *Frontiers in Food Chemistry and Technology*, July 2022, Volume 2, Article 936745

frontiers | Frontiers in Food Science and Technology

BRIEF RESEARCH REPORT
published: 01 July 2022
doi: 10.3389/frfst.2022.936745

Carbon Isotope Discrimination as an Indicator of Vine Water Status is Comparable in Grape Must, Wine, and Distilled Wine Spirits

*Mark Gowdy[1], Sébastien Julliard[2], Marina Frouin[2], Xavier Poitou[3], Agnès Destrac Irvine[1] and Cornelis van Leeuwen[1]**

[1]EGFV, Univ. Bordeaux, Bordeaux Sciences Agro, INRAE, ISVV, Villenave d'Ornon, Bordeaux, France, [2]Conservatoire du Vignoble Charentais, Institut de Formation de Richemont, Cherves-Richemont, France, [3]Jas Hennessy & Co., Cognac, France

Measurement of carbon isotope discrimination ($\delta^{13}C$) in berry juice sugars provides an integrative indicator of grapevine water status during berry ripening. Characterizing vine water status during this critical period is useful because it has an important effect on the quality of grapes and the resulting wine. The $\delta^{13}C$ of the sugar in grapes is also strongly correlated to the $\delta^{13}C$ of the ethanol that results when they are fermented into wine. This then provides a means of estimating from a sample of wine the vine water status that existed during the corresponding berry ripening period, and can be used to establish relations between vine water status and specific sensory attributes of wine quality. The same would be possible for evaluating the sensory attributes of wine spirit (*eau de vie*) if it was understood how the $\delta^{13}C$ signal was affected by the distillation process. In this study, the $\delta^{13}C$ in eau de vie, produced by a double distillation process similar to that used in the Cognac region of France, was measured and compared to its source wine and parent grape must. A strong relationship was found between the $\delta^{13}C$ of grape must and subsequent wine and eau de vie, suggesting the latter can indeed be used to estimate the vine water status that existed during the corresponding berry ripening period. In this way, future studies of sensory attributes of eau de vie can be linked to vine water status during berry ripening, such as has been done previously for wine.

Keywords: carbon isotope discrimination, *Vitis vinifera*, drought stress, distillation, wine, grape must

OPEN ACCESS

Edited by:
José S. Câmara, Universidade da Madeira, Portugal

Reviewed by:
Meleksen Akin, Iğdır Üniversitesi, Turkey
Pieter Verboven, KU Leuven, Belgium
Bhaskar Bondada, Washington State University, United States

****Correspondence:***
Cornelis van Leeuwen
vanleeuwen@agro-bordeaux.fr

Specialty section:
This article was submitted to Food Characterization, a section of the journal Frontiers in Food Science and Technology

Received: *05 May 2022*
Accepted: *08 June 2022*
Published: *01 July 2022*

Citation:
Gowdy M, Julliard S, Frouin M, Poitou X, Destrac Irvine A and van Leeuwen C (2022) Carbon Isotope Discrimination as an Indicator of Vine Water Status is Comparable in Grape Must, Wine, and Distilled Wine Spirits. Front. Food. Sci. Technol. 2:936745. doi: 10.3389/frfst.2022.936745

INTRODUCTION

As part of the Calvin cycle in the photosynthetic process of C_3 plants such as grapevines, the Rubisco enzyme preferentially binds to the more reactive ^{12}C isotopes contained in atmospheric CO_2, causing the $^{13}C/^{12}C$ ratio of the carbon fixed by the plant to be less that of the atmosphere (Farquhar, 1989). Carbon isotope discrimination ($\delta^{13}C$), expressed in parts per thousand (‰), is a function of the $^{13}C/^{12}C$ ratio measured in the carbon fixed by the plant relative to the $^{13}C/^{12}C$ ratio measured in a standard representative of the atmosphere (Santesteban et al., 2015). Discrimination in favor of ^{12}C, however, is reduced as stomata close in response to drought stress, and the amount of available ^{12}C in the intercellular space of the leaves gradually decreases (Santesteban et al., 2015). This makes measurement of $\delta^{13}C$ in berry juice sugars a good integrative indicator of vine water status during the corresponding berry ripening period (Gaudillère et al., 2002; Guyon et al., 2015; Bchir et al., 2016).

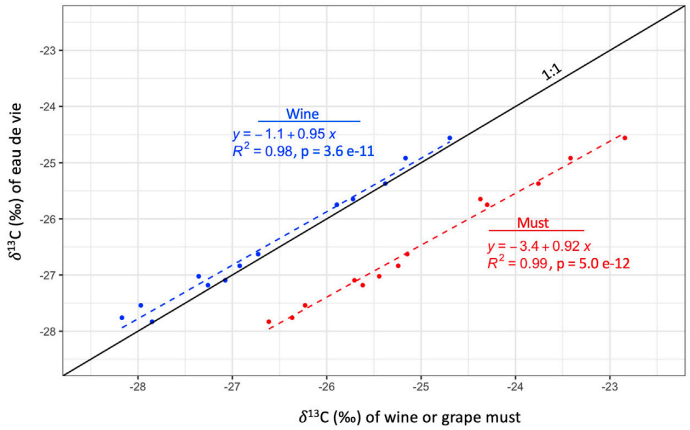

FIGURE 1 | Measured $\delta^{13}C$(‰) in eau-de-vie samples versus those measured in grape must samples (red line) and wine samples (blue line).

Being able to characterize wine water status, particularly during the berry ripening period, is useful because it has an important effect on canopy vigor, berry size and yield, and associated grape composition and development of phenolic and aroma compounds in finished wine (van Leeuwen et al., 2009). Measurement of $\delta^{13}C$ over multiple seasons under different levels of water stress can also provide an indication of varietal drought tolerance (Plantevin et al., 2022).

The $\delta^{13}C$ of the sugar in grape must has been found to be linearly related to the $\delta^{13}C$ of the ethanol that results from fermentation to wine, although shifted upwards in the range of 1.7‰ (Roßmann et al., 1996; Guyon et al., 2015). This connection between the $\delta^{13}C$ in grape must and wine provides a means of estimating from a sample of wine the vine water status that existed during the corresponding berry ripening period. This can be used then to establish relations between vine water status and specific sensory attributes of wine (Picard et al., 2017).

Cognac is a type of wine brandy produced in France, whereby wine fermented primarily from *Vitis vinfera* L. cv. Ugni blanc, Folle blanche, and Colombard is double distilled in copper pot stills to produce a wine spirit (*eau de vie*) that is then aged in oak barrels. The aim of this research is to characterize how $\delta^{13}C$ in the eau de vie produced by this process might be altered when compared to the source wine and parent grape must. If the $\delta^{13}C$ in the eau de vie is conserved in a quantifiable manner, this will allow for future studies to retrospectively estimate the vine water status that existed during the ripening of the grapes used to produce the eau de vie. This can then be used to study the relationships between vine water status and specific sensory attributes of eau de vie, as has been done before for wine.

MATERIALS AND METHODS

Carbon isotope discrimination ($\delta^{13}C$) was measured in grape must, fermented wine, and distilled spirit from varieties of interest in the Cognac region, including Ugni blanc, Ugni blanc lacinié, Monbadon, and Vidal 36 in both 2019 and 2020 and also on Colombard, Montils, Semillon, Folle blanche, and Folignan in 2020. The vines were planted as part of the ampelographic collection of the *Conservatoire du Vignoble Charentais* in Cherves-Richemont, France, just north of the city of Cognac (45°43′16.1″N 0°21′45.6″W) with an average age of about 20 years. The vineyard was planted on clay-limestone soil at a density of 5,000 vines/ha, with mowed grass cover crop and identical cultural practices. The vines are trained on a vertical shoot positioning trellis system with double Guyot pruning.

Each year for each variety, 10 kg of grapes were harvested and pressed in two stages at 3 bars of pressure, from which a sample was collected of the resulting grape must. A micro-vinification was then performed in the Charentaise style, without addition of sulphites or sugar, using a Cognac-specific LSA FC 9 yeast fermentation controlled at 21°C, no malolactic fermentation, and resulting in wine at about 10%–12% alcohol by volume. A sample was collected from the resulting wine, which was then stored at 4 °C prior to distillation. A traditional double distillation process was then performed on the wine (without lees) whereby the first cycle (*chauffe de vin*) had 0.5% of the *heads* removed with the *heart* taken over 8 hours, followed by a second cycle (*bonne chauffe*) that had 1.0% of the heads removed with the heart taken over five to 6 hours and no recycling of the *heads* or *tails*. These distillations were performed in a 1-L still made of the same material and proportions as a traditional 25 hL capacity Charentaise style still, including a traditional *tête de Maure* still head (Lavergne, 2020[1]).

Each grape must sample was mixed with an agitator-type vortex to ensure uniformity and centrifuged at 12,500 rpm for 10 min (Sigma 13 6K15, SIGMA Laborzentrifugen GmbH, Osterode am Harz, Germany). Afterwards, 5 µL were pipetted into a tin capsule

[1]Lavergne, J. (2020). Conservatoire du Vignoble Charentais, Cherves-Richemont, France. personal communication.

TABLE 1 | Measurements of $\delta^{13}C$ (‰) in grape must (Must), corresponding wine (Wine) and eau de vie (EDV) for nine varieties in 2019 and 2020 with differences between each and overall averages.

Variety	Year	Must	Wine	EDV	Must - Wine	Wine - EDV	Must - EDV
Vidal 36	2019	–22.84	–24.70	–24.56	1.86	–0.14	1.72
Vidal 36	2020	–23.76	–25.38	–25.37	1.62	–0.01	1.62
Monbadon	2019	–23.42	–25.17	–24.92	1.75	–0.25	1.50
Monbadon	2020	–24.37	–25.72	–25.65	1.35	–0.07	1.28
Ugni blanc lacinié	2019	–24.30	–25.89	–25.75	1.59	–0.14	1.45
Ugni blanc lacinié	2020	–25.15	–26.73	–26.63	1.58	–0.10	1.48
Ugni blanc	2019	–25.24	–26.92	–26.84	1.68	–0.08	1.59
Ugni blanc	2020	–25.62	–27.26	–27.18	1.64	–0.08	1.56
Folignan	2020	–25.44	–27.36	–27.02	1.91	–0.33	1.58
Folle blanche	2020	–25.71	–27.08	–27.10	1.37	0.02	1.39
Sémillon	2020	–26.23	–27.97	–27.54	1.74	–0.43	1.31
Montils	2020	–26.37	–28.17	–27.76	1.80	–0.41	1.39
Colombard	2020	–26.61	–27.85	–27.83	1.24	–0.02	1.22
				Average	1.63	–0.16	1.47

and oven dried at 60 °C. Random control samples were prepared from beet root juice with known $\delta^{13}C$ levels. Wine and eau de vie samples were analyzed directly without centrifuging or drying. All samples were analyzed at an external laboratory (UMR CNRS/ Plateforme GISMO UMR 6282 BIOGEOSCIENCES Université de Bourgogne, 21000 Dijon, France) where the carbon isotope content was measured using an Elementary Vario Analyzer (Elementar, Hanau) coupled for continuous flow to an isotopic mass spectrometer (Isoprime, Manchester). An analytical standard of Vienna Pee Dee Belemnite (VPDB) was used for reference, with $\delta^{13}C$ expressed in parts per thousand (‰).

Linear regression was used to characterize the relationship between measurements of $\delta^{13}C$ in eau de vie as the dependent variable versus $\delta^{13}C$ measured in grape must as the independent variable. The same was done for $\delta^{13}C$ in eau de vie versus $\delta^{13}C$ in source wine. The ordinary least square assumptions for each regression were then evaluated with: 1) quantile-quantile plots of standardized residuals to check for normal distribution and zero mean; 2) plots of standardized residuals versus fitted values to confirm absence of heteroscedasticity; and 3) plots of standardized residuals versus the independent variables to confirm the absence of endogeneity. Multiple linear regression analysis was performed in the *R* software environment using the *lm* function (R Core Team, 2021) and graphing was performed using the *ggplot2* package (Wickham et al., 2021).

RESULTS AND DISCUSSION

Based on linear regression analysis, a strong linear relationship was observed between $\delta^{13}C$ measured in eau de vie samples versus those measured in the corresponding wine samples (blue line in **Figure 1**) with a slope of 0.95, $r^2 = 0.98$ and p-value = 3.6×10^{-11}. Likewise, a strong linear relationship was observed between $\delta^{13}C$ measured in eau de vie samples versus those measured in the corresponding grape must (red line in **Figure 1**) with a slope of 0.92, $r^2 = 0.99$ and p-value = 5.0×10^{-12}. The residual plots for both regressions (not shown) demonstrated good normal distribution of residuals with zero mean and no heteroscedasticity, or endogeneity.

As shown in **Table 1**, for the range of measured values across all varieties and years, the average difference in $\delta^{13}C$ between wine and eau de vie samples was -0.16‰. This difference is not great despite the potential for the distillation process to separate compounds with lighter isotopes more easily than those with heavy isotopes. A possible explanation for this is the first fractions from the distillation (i.e., heads) enriched in light isotopes and the last fractions (i.e., tails) enriched in heavy isotopes are both discarded, and the remaining middle fraction (i.e., heart), which is conserved as eau de vie, has an average $\delta^{13}C$ close to that of the corresponding wine used in the distillation.

The average difference in $\delta^{13}C$ between grape must and wine measurements was 1.63‰ with a standard deviation of 0.20‰. This difference is close to the range of 1.7‰ observed by Roßmann et al. (1996) across multiple samples of Italian and German grape musts and wines over two different years. Then finally, the average difference between $\delta^{13}C$ in grape must and eau de vie samples was 1.47‰ with a standard deviation of 0.15‰. This value is very close to the sum of the must-to-wine and wine-to-eau de vie average differences.

CONCLUSION

The strong linear relationship observed between the $\delta^{13}C$ of grape must and eau de vie suggests the possibility of using the latter as a means of estimating the vine water status that existed during the corresponding berry ripening period. Based on this understanding, future studies can explore the relationships between sensory attributes of eau de vie and vine water status during ripening of the source grapes, as has been done before for wine. Also, to the

extent that eau de vie samples are segregated by vineyard location or region, the $\delta^{13}C$ of those samples could be used to explore associated differences in the vine water status across those locations. These findings could be further validated by measuring $\delta^{13}C$ in grape must, wine and eau de vie under conditions of full-scale production and with different amounts of heads and hearts being taken during the first and second distillation cycles as might be experienced during such production. These findings were based on eau de vie produced by a double distillation process as traditionally used in the Cognac region of France, and could be different for spirits produced by other distillation methods, such as with the continuous column still method used in the Armagnac region of France.

DATA AVAILABILITY STATEMENT

The original contributions presented in the study are included in the article/supplementary material, further inquiries can be directed to the corresponding author.

AUTHOR CONTRIBUTIONS

All authors listed have made a substantial, direct, and intellectual contribution to the work and approved it for publication.

FUNDING

This study has been carried out with financial support from Jas Hennessy & Co.

ACKNOWLEDGMENTS

In collaboration between the *Institut des Sciences de la Vigne et du Vin* and the *Conservatoire du Vignoble Charentais, Institut de Formation de Richemont.*

REFERENCES

Bchir, A., Escalona, J. M., Gallé, A., Hernández-Montes, E., Tortosa, I., Braham, M., et al. (2016). Carbon Isotope Discrimination ($\delta^{13}C$) as an Indicator of Vine Water Status and Water Use Efficiency (WUE): Looking for the Most Representative Sample and Sampling Time. *Agric. Water Manag.* 167, 11–20. doi:10.1016/j.agwat.2015.12.018

Farquhar, G. D., Ehleringer, J. R., and Hubick, K. T. (1989). Carbon Isotope Discrimination and Photosynthesis. *Annu. Rev. Plant. Physiol. Plant. Mol. Biol.* 40 (1), 503–537. doi:10.1146/annurev.pp.40.060189.002443

Gaudillère, J. P., van Leeuwen, C., and Ollat, N. (2002). Carbon Isotope Composition of Sugars in Grapevine, an Integrated Indicator of Vineyard Water Status. *J. Exp. Bot.* 53 (369), 757–763. doi:10.1093/jexbot/53.369.757

Guyon, F., van Leeuwen, C., Gaillard, L., Grand, M., Akoka, S., Remaud, G. S., et al. (2015). Comparative Study of ^{13}C Composition in Ethanol and Bulk Dry Wine Using Isotope Ratio Monitoring by Mass Spectrometry and by Nuclear Magnetic Resonance as an Indicator of Vine Water Status. *Anal. Bioanal. Chem.* 407 (30), 9053–9060. doi:10.1007/s00216-015-9072-9

Picard, M., van Leeuwen, C., Guyon, F., Gaillard, L., de Revel, G., and Marchand, S. (2017). Vine Water Deficit Impacts Aging Bouquet in Fine Red Bordeaux Wine. *Front. Chem.* 5, 56. doi:10.3389/fchem.2017.00056

Plantevin, M., Gowdy, M., Destrac-Irvine, A., Marguerit, E., Gambetta, G. A., and van Leeuwen, C. (2022). Using $\delta^{13}C$ and Hydroscapes for Discriminating Cultivar Specific Drought Responses. *OENO One.*

R Core Team (2021). *R: A Language and Environment for Statistical Computing. Version 4.1.1.* Vienna, Austria: R Foundation for Statistical Computing. Available at: https://www.R-project.org/ (Accessed September 20, 2021).

Roßmann, A., Schmidt, H.-L., Reniero, F., Versini, G., Moussa, I., and Merle, M. H. (1996). Stable Carbon Isotope Content in Ethanol of EC Data Bank Wines from Italy, France and Germany. *Z. Für Lebensm. Und Forsch.* 203 (3), 293–301. doi:10.1007/BF01192881

Santesteban, L. G., Miranda, C., Barbarin, I., and Royo, J. B. (2015). Application of the Measurement of the Natural Abundance of Stable Isotopes in Viticulture: A Review: Stable Isotopes in Viticulture: a Review. *Aust. J. Grape Wine Res.* 21 (2), 157–167. doi:10.1111/ajgw.12124

van Leeuwen, C., Trégoat, O., Choné, X., Bois, B., Pernet, D., and Gaudillère, J.-P. (2009). Vine Water Status Is a Key Factor in Grape Ripening and Vintage Quality for Red Bordeaux Wine. How Can it Be Assessed for Vineyard Management Purposes. *J. Int. Sci. Vigne Vin.* 43 (3), 121–134. doi:10.20870/oeno-one.2009.43.3.798

Wickham, H., Chang, W., Henry, L., Pedersen, T. L., Takahashi, K., Wilke, C., et al. (2021). ggplot2: Create Elegant Data Visualisations Using the Grammar of Graphics (3.3.5) [Computer Software]. Available at: https://CRAN.R-project.org/package=ggplot2 (Accessed January 18, 2022).

Conflict of Interest: XP was employed by Jas Hennessy & Co., Cognac, France.

The remaining authors declare that the research was conducted in the absence of any commercial or financial relationships that could be construed as a potential conflict of interest.

Publisher's Note: All claims expressed in this article are solely those of the authors and do not necessarily represent those of their affiliated organizations, or those of the publisher, the editors and the reviewers. Any product that may be evaluated in this article, or claim that may be made by its manufacturer, is not guaranteed or endorsed by the publisher.

4.3 Discussion

Measurements of $\delta^{13}C$ in *eau de vie* produced from a double distillation process, such as used in the Cognac AOC, was compared to $\delta^{13}C$ of the source wine and parent grape must. As confirmation, a strong linear relationship between $\delta^{13}C$ in grape must and associated wine was very similar to that found previously in the literature (Roßmann et al., 1996).

A nearly 1:1 linear relationship ($r^2 = 0.98$) was then found between the $\delta^{13}C$ of eau de vie and the associated source wine, suggesting the $\delta^{13}C$ of eau de vie could be used to estimate the vine water status that existed during the corresponding berry ripening period. This difference is negligible despite the potential for the distillation process to separate compounds with lighter isotopes more easily than those with heavy isotopes. A possible explanation for this is the first fractions from the distillation (i.e., heads) enriched in light isotopes and the last fractions (i.e., tails) enriched in heavy isotopes are both discarded, and the remaining middle fraction (i.e., heart), which is conserved as eau de vie, has an average $\delta^{13}C$ close to that of the corresponding wine used in the distillation.

An understanding of the effect of this process on $\delta^{13}C$ allows a retrospective estimation of the vine water status that existed during the ripening of the grapes used to produce the wine and subsequent eau de vie. As has been done for wine, this could then be used in future studies to establish relations between vine water status and specific sensory attributes of eau de vie quality. This could also be used to explore associated differences in the vine water status across different source vineyard locations.

5 Determining Bulk Stomatal Conductance (g_{bs})

5.1 Background

In response to changes in vine water status, grapevines regulate transpiration using various physiological mechanisms that alter conductance of water through the soil-plant-atmosphere continuum (McElrone et al., 2013). Expressed as *bulk stomatal conductance* (g_{bs}) at the canopy scale it is effectively the parallel combination of the stomatal conductance (g_s) of every leaf in the crop canopy (Kelliher et al., 1995) and varies diurnally in response to changes in vapor pressure deficit and net radiation, and over the season to changes in soil water deficits and the hydraulic conductivity of both the plant and the soil.

The journal article presented in this chapter, entitled "*Estimating Bulk Stomatal Conductance in Grapevine Canopies"* (Gowdy et al., 2022a) presents a simplified method for determination of g_{bs} in a vineyard setting. This approach is based on an established crop canopy energy flux model (Shuttleworth and Wallace, 1985) using measurements of individual vine sap flow, temperature and humidity within the vine canopy, and estimates of net radiation absorbed by the vine canopy. The methodology presented respects the particular energy flux dynamics of vineyards with open canopies, while avoiding problematic measurements of soil heat flux and boundary layer conductance needed by other methods, which can otherwise interfere with ongoing vineyard management practices. This method provides a more straightforward and robust means of calculating vine canopy conductance used in the next chapter of this thesis to evaluate the response of g_{bs} to changing atmospheric conditions and drought.

5.1.1 Big leaf vs. two-source energy flux models

At the leaf scale, *stomatal conductance* (g_s) is the ratio of water vapor, or carbon flux divided by the concentration gradient driving flux across the boundary layer at the leaf surface and can be estimated by using an inverted form of the Penman Monteith (PM) equation (Monteith and Unsworth 2013). As depicted schematically in Figure 4 below, at the field scale, transpiration from a crop canopy can be estimated by conceptually applying the PM equation as if the canopy were a *big leaf* that is horizontally uniform and entirely covers the soil below (Monteith and Unsworth 2013). This equation is based on an energy

balance assumption that has the sum of sensible heat flux (C) and latent heat flux (λE) being equal, but opposite to the net radiation absorbed by the canopy (R_g).

Applying the big leaf approach at the crop canopy scale, *canopy conductance* (g_c) can be calculated by rearranging the PM equation and inputting measured canopy transpiration (E), atmospheric vapor pressure deficits (VPD), net radiation absorbed by the canopy (R_g), and the bulk equivalent of boundary layer conductance (g_{bl}), with all fluxes and resistances expressed in terms of unit ground area below the canopy (Granier and Loustau, 1994; Granier et al., 2000; Lu et al., 2003). When applying the inverted PM equation in this manner, however, the big leaf approach requires the determination of net radiation absorbed by the canopy must account for heat flux from the ground below the canopy (G) and the aerodynamic boundary layer conductance (g_{bl}) above the vineyard (Monteith and Unsworth 2013). Such measurements can be cumbersome, error prone, and interfere with ongoing management practices in a production setting.

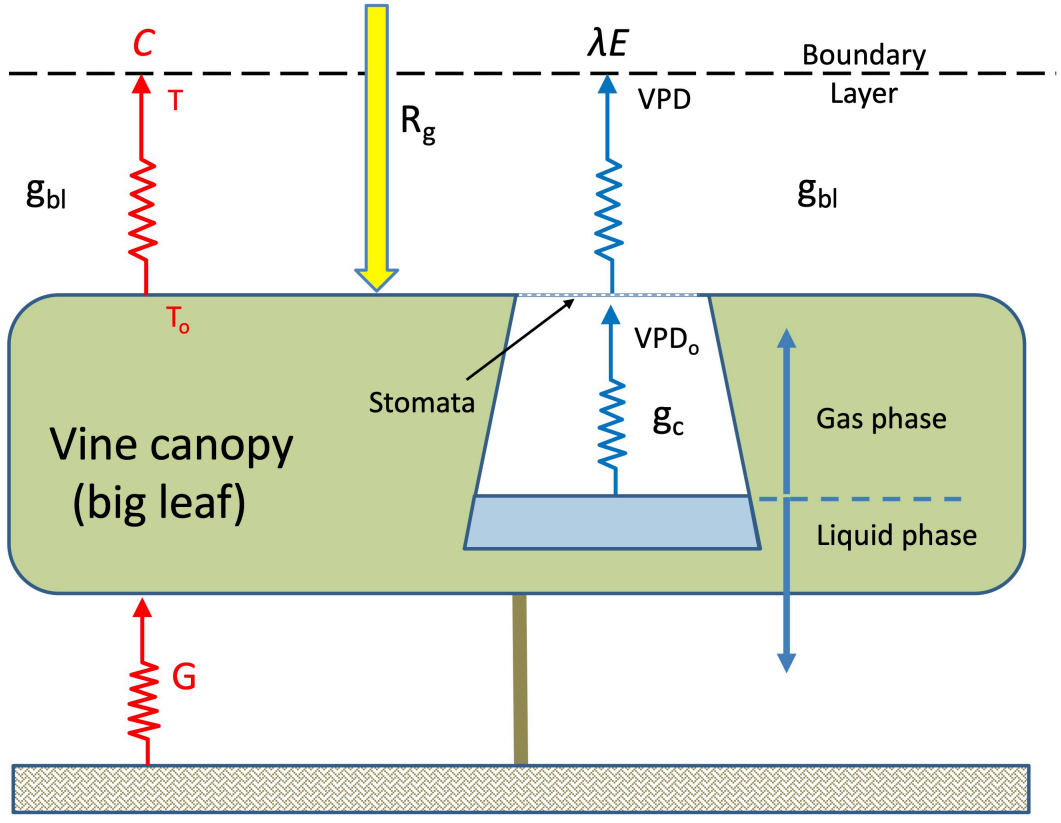

Figure 4. Schematic representation of the *big leaf* model based on the Penman Monteith equation (see text for variable descriptions.)

In modeling vineyards with open canopies (i.e., vines cultivated in rows and surrounded by exposed ground), however, the assumption of uniform distribution of sensible and latent heat flux from the canopy required for the big leaf approach is not met and can lead to anomalous determinations of g_c (Monteith and Unsworth 2013). In such cases, a modified two-source approach as developed by Shuttleworth and Wallace (1985) can be used to evaluate heat and water vapor flux from the crop canopy separately from the exposed ground surrounding the canopy.

As depicted schematically in Figure 5 below, this method only requires the determination of net radiation absorbed by the vine canopy (R_n), vapor pressure deficit in the vine canopy (D_c), transpiration flux (E), and an estimate of bulk boundary layer resistance to vapor flux (r_{bv}) and leads to a calculation of *bulk stomatal conductance* (g_{bs}), which is the inverse of bulk stomatal resistance (r_{bs}). Aside from being based on a more realistic representation of energy flux patterns of an open canopy, this approach does not require the measurement of soil heat flux or boundary layer conductance above the vineyard, greatly simplifying its determination.

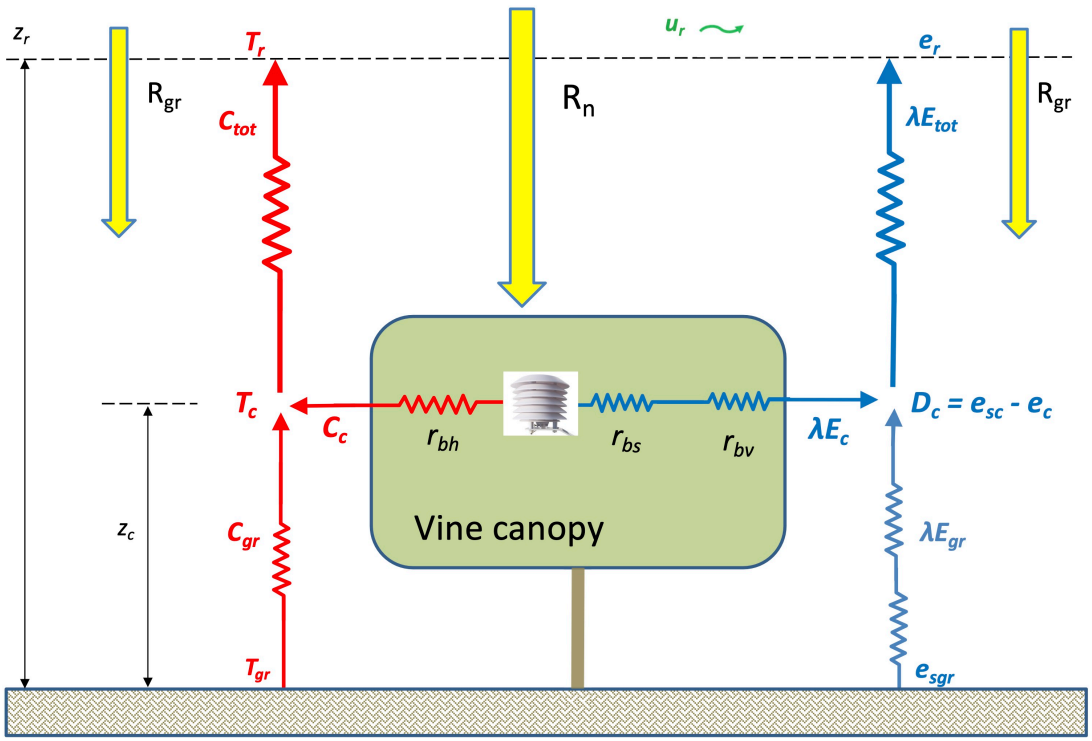

Figure 5. Schematic representation of the two-source energy fluxes of an open vineyard canopy.

5.1.2 Long wave radiation

Long wave (heat) radiation from the atmosphere, surrounding ground, and adjacent vine canopy rows are also a source of radiation for the vine canopies (Pieri, 2010) and it is recommended in FAO Irrigation and drainage paper No. 56 that it be accounted for in modeling of crop evapotranspiration (Allen et al., 1998). The proportion of radiation flux from the sky, ground, and adjacent vine rows incident on the vine canopy were calculated in this study using radiation view factors between these sources and the faces of the vine canopy adjusted to account for canopy porosity as described by Pieri (2010) and as depicted in Figure 6 through 8 below, including the equations for each. The canopies themselves were also assumed to radiate heat energy as a function of their temperature.

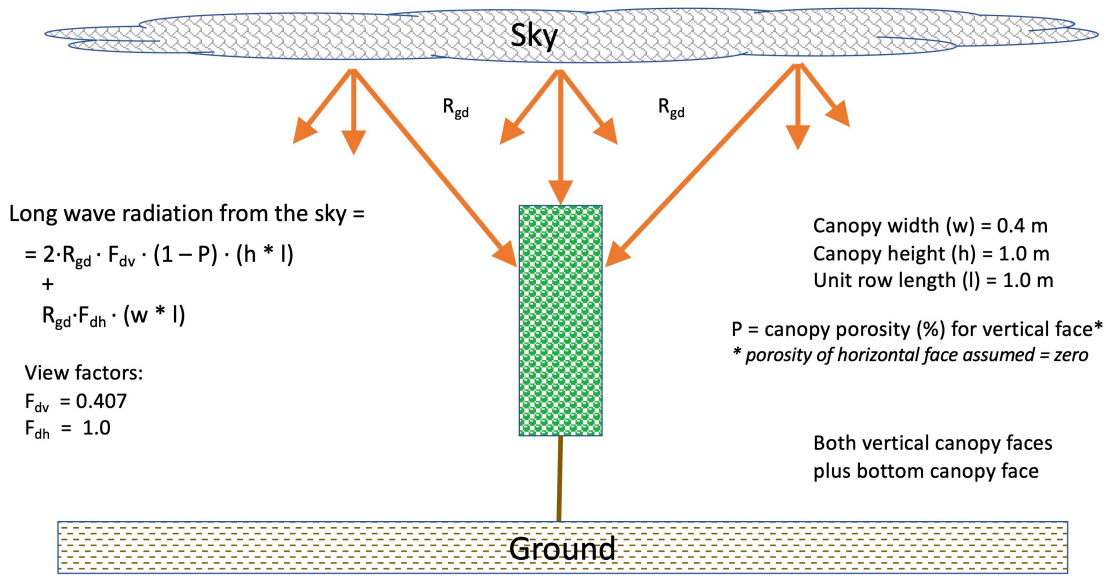

Figure 6. Calculation of long wave radiation absorbed from the sky by the vine canopy.

The net long wave radiation flux absorbed by the vine canopy (W m^{-2}) is then the sum of the amount absorbed from these three sources, minus the amount radiated from the canopy, expressed in terms of unit ground area attributable to each vine (i.e., row spacing x vine spacing).

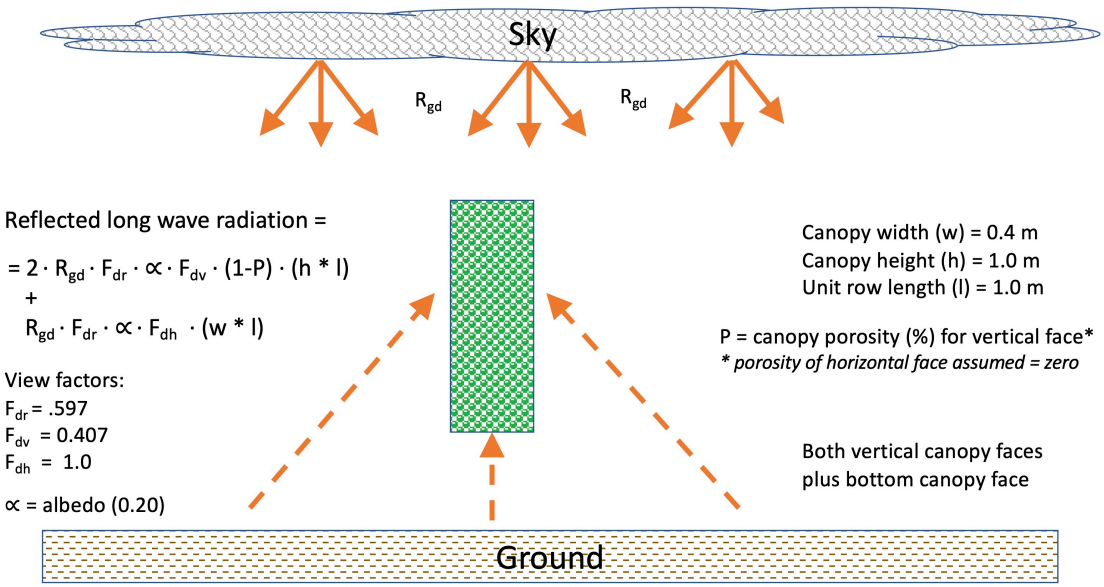

Figure 7. Calculation of long wave radiation reflected from the ground and absorbed by the vine canopy.

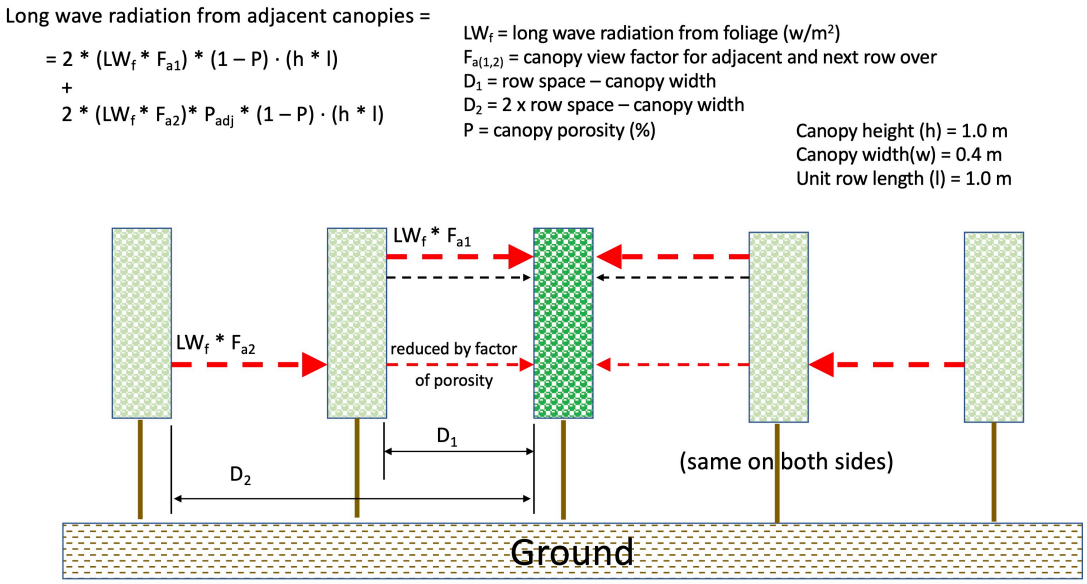

Figure 8. Calculation of long wave radiation absorbed by the vine canopy from adjacent vine canopies

5.1.3 Sap flow sensors

Key to the implementation of this method is the measurement of vine transpiration. For this purpose, we used heat balance sap flow sensors (Model SGEX, Dynamax Inc., Houston, TX, USA) that were installed on vine canes at a location where the flow of at least 30% of the whole vine would be measured (based on the relative number of shoots downstream of the sensor). Sap flow (g s^{-1}) was calculated from sensor signals collected every 15 minutes by a datalogger (Model SapIP, Dynamax Inc., Houston, TX, USA) and then scaled up for the whole vine based on the ratio of leaf area of the whole vine over the leaf area of shoots downstream the sap flow sensor (Lascano et al., 1992). Sap flow (g s^{-1}) was then divided by the area of vineyard ground attributable to each vine (i.e., row spacing x vine spacing) to give canopy transpiration flux (g s^{-1} m^{-2}).

Heat balance sap-flow sensors contain a series of thermocouples, a thermopile, and a heat source in a collar that is wrapped around a stem or trunk. The placement of thermocouples in the sensor collar are designed to measure radial and axial temperature gradients, which when combined with assumptions regarding thermal conductivity yield the flux of energy along the stem and radially outward. The flux of heat energy in the sap, which is related to the quantity of sap flow (mass/time) is then calculated by the difference between the axial and radial heat flux and the input of heat to the stem (Lascano et al., 2016). While other methods of measuring sap flow have been developed (Löf and Welander, 2009), the Dynamax collar design was preferred as it is relatively non-invasive, reducing the risk of long-term damage to the vines.

Figure 9 shows: a) SGEX sap flow sensor collar; and b) schematic of thermocouples and stem heater in the collar. For this study, sap flow signals were logged every 15 minutes, which produced sap flow signals such as those in Figure 10.

a)  b) 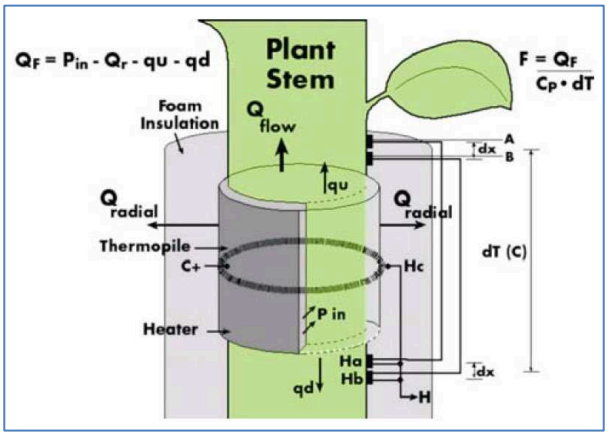

Figure 9. Photo of: a) Dynamax SGEX heat balance sap flow sensor collar; and b) schematic of thermocouples, thermopile and energy fluxes .(courtesy of Dynamax, Inc.)

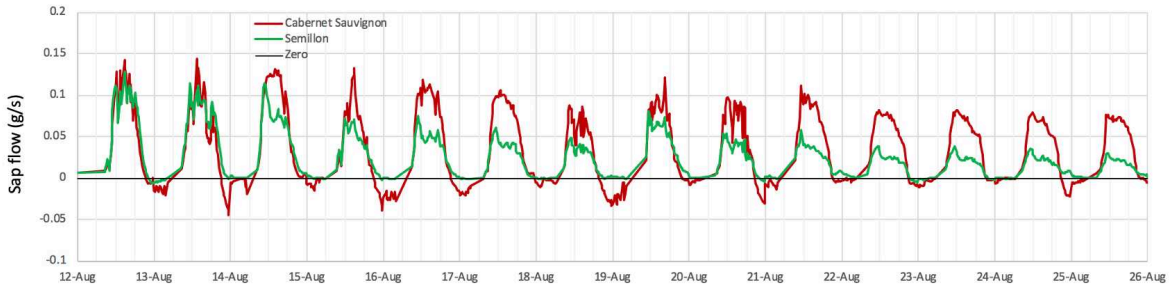

Figure 10. Example sap flow (g/s) from two different vines as calculated from thermocouple signals logged on 15-minute intervals.

5.2 Journal article

Estimating Bulk Stomatal Conductance in Grapevine Canopies

Mark Gowdy[1], Philippe Pieri[1], Bruno Suter[1], Elisa Marguerit[1], Agnès Destrac-Irvine[1], Gregory Gambetta[1], Cornelis van Leeuwen[1]

[1] EGFV, Bordeaux Sciences Agro, INRAE, Univ. Bordeaux, ISVV, F-33882 Villenave d'Ornon, France

Published in *Frontiers in Plant Science*, March 2022, Volume 13, Article 839378

frontiers in Plant Science

METHODS
published: 18 March 2022
doi: 10.3389/fpls.2022.839378

Estimating Bulk Stomatal Conductance in Grapevine Canopies

Mark Gowdy, Philippe Pieri, Bruno Suter, Elisa Marguerit, Agnès Destrac-Irvine, Gregory Gambetta and Cornelis van Leeuwen*

EGFV, Bordeaux Sciences Agro, INRAE, Université de Bordeaux, ISVV, Bordeaux, France

In response to changes in their environments, grapevines regulate transpiration using various physiological mechanisms that alter conductance of water through the soil-plant-atmosphere continuum. Expressed as *bulk stomatal conductance* at the canopy scale, it varies diurnally in response to changes in vapor pressure deficit and net radiation, and over the season to changes in soil water deficits and hydraulic conductivity of both the soil and plant. To help with future characterization of this dynamic response, a simplified method is presented for determining bulk stomatal conductance based on the crop canopy energy flux model by Shuttleworth and Wallace using measurements of individual vine sap flow, temperature and humidity within the vine canopy, and estimates of net radiation absorbed by the vine canopy. The methodology presented respects the energy flux dynamics of vineyards with open canopies, while avoiding problematic measurements of soil heat flux and boundary layer conductance needed by other methods, which might otherwise interfere with ongoing vineyard management practices. Based on this method and measurements taken on several vines in a non-irrigated vineyard in Bordeaux France, bulk stomatal conductance was estimated on 15-minute intervals from July to mid-September 2020 producing values similar to those presented for vineyards in the literature. Time-series plots of this conductance show significant diurnal variation and seasonal decreases in conductance associated with increased vine water stress as measured by predawn leaf water potential. Global sensitivity analysis using non-parametric regression found transpiration flux and vapor pressure deficit to be the most important input variables to the calculation of bulk stomatal conductance, with absorbed net radiation and bulk boundary layer conductance being much less important. Conversely, bulk stomatal conductance was one of the most important inputs when calculating vine transpiration, emphasizing the usefulness of characterizing its dynamic response for the purpose of estimating vine canopy transpiration in water use models.

Keywords: bulk boundary layer conductance, net radiation, transpiration, vineyard water-use models, vine water stress, vapor pressure deficit

OPEN ACCESS

Edited by:
Xinguang Zhu,
University of Chinese Academy of Sciences, China

Reviewed by:
Hailong Wang,
Sun Yat-sen University, China
Zidong Luo,
Institute of Subtropical Agriculture, (CAS), China

****Correspondence:***
Mark Gowdy
mark.gowdy@inrae.fr

Specialty section:
This article was submitted to Plant Physiology, a section of the journal Frontiers in Plant Science

Received: *19 December 2021*
Accepted: *21 February 2022*
Published: *18 March 2022*

Citation:
Gowdy M, Pieri P, Suter B, Marguerit E, Destrac-Irvine A, Gambetta G and van Leeuwen C (2022) Estimating Bulk Stomatal Conductance in Grapevine Canopies. Front. Plant Sci. 13:839378. doi: 10.3389/fpls.2022.839378

Abbreviations: Energy fluxes: C_c, sensible heat fluxes from the canopy; C_{gr}, at the ground; C_{tot}, total; λE_c, latent heat fluxes from the canopy; λE_{gr}, at the ground; λE_{tot}, total; R_c, net radiation absorbed by the canopy; R_{gr}, by the ground; Dimensions: h, height to top of canopy above the ground; d, zero plane displacement; z_o, roughness length; z_c, mean canopy height; z_r, reference height; Atmospheric parameters: T_c, temperature at mean canopy height; T_{gr}, at the ground; T_r, at reference height; e_{sc}, saturation vapor pressure at T_c; e_{sgr}, at T_{gr}; e_{sr}, at T_r; e_c, measured vapor pressure at z_c; e_r, at z_r; D_c, vapor pressure deficit ($e_{sc} - e_c$) at z_c; D_r, vapor pressure deficit ($e_{sr} - e_r$) at z_r; u_r, wind speed at z_r; Bulk canopy resistances: r_{bs}, bulk stomatal resistance; r_{bh}, bulk boundary layer resistance to heat flux; r_{bv}, bulk boundary layer resistance to water vapor flux; Water stress: Ψ_{PD}, pre-dawn leaf water potential.

INTRODUCTION

Grapevines regulate their water use (i.e., transpiration) in response to changing atmospheric demand and drought stress by regulating the conductance of water through the plant from the soil to the atmosphere (Oren et al., 1999; McElrone et al., 2013, Keller, 2015). This conductance is regulated by various physiologic mechanisms such as control of stomatal aperture and hydraulic conductivity of the vasculature (Lovisolo et al., 2010), with differences in response observed between varieties (Prieto et al., 2010; Costa et al., 2012). This stomata regulation is also affected by changes in plant water status through various physiological mechanisms (Oren et al., 1999; Roelfsema and Hedrich, 2005). Moreover, conductance varies diurnally (Lu et al., 2003; Zhang et al., 2012; Bai et al., 2015) and across the season (Herrera et al., 2021).

Vineyard water use modeling is often conducted using the FAO 56 approach of applying seasonally variable crop coefficients to estimates of evapotranspiration from a hypothetical reference crop (ET_o). Calculation of ET_o is based on an application of the Penman Monteith (PM) equation, including the assumption of a fixed conductance for the reference crop (Allen et al., 1998). As a result, this approach does not account for changes in conductance in response to changes in atmospheric demand or drought stress. One vineyard water use model adapted from the FAO approach applies a generic adjustment to transpiration as a function of diminishing soil water content (Lebon et al., 2003), but none include a dynamic representation of conductance response to changes in key environmental variables such as net radiation, vapor pressure deficit, or soil water availability. As a first step in developing such representations, a technically robust and implementable methodology for calculating vine canopy conductance in a vineyard setting is needed.

Developed conceptually at the leaf scale, the PM equation calculates latent heat (water vapor) flux from a leaf surface as a function of net radiation absorbed by the leaf, vapor pressure deficit gradients from within the leaf to the atmosphere, and boundary layer and stomatal resistances to this flux (Monteith and Unsworth, 2013). At the field scale, transpiration from a crop canopy can be estimated by conceptually applying the PM equation as if the canopy were a *big leaf* that is horizontally uniform and entirely covers the soil below (Monteith and Unsworth, 2013). At the leaf scale, *stomatal conductance* (g_s) is the ratio of water vapor, or carbon flux divided by the concentration gradient driving flux across the boundary layer at the leaf surface (Monteith and Unsworth, 2013) and is often measured by means of a porometer or gas exchange meter on individual leaves. Applying the big leaf approach at the crop canopy scale, *canopy conductance* (g_c) can be calculated by rearranging the PM equation and inputting measured canopy transpiration, atmospheric vapor pressure deficits, net radiation absorbed by the canopy, and the within-canopy (bulk) equivalent of boundary layer conductance, with all fluxes and resistances expressed in terms of unit ground area below the canopy (Granier and Loustau, 1994; Granier et al., 2000; Lu et al., 2003). The g_c resulting from this approach is effectively the parallel combination of the g_s of every leaf in the crop canopy (Kelliher et al., 1995).

The big leaf approach using the inverted PM equation has been applied to determining conductance of forest canopies based on sap flow measurement of transpiration from trees (Köstner et al., 1992; Granier et al., 2000; Ewers et al., 2005; Ghimire et al., 2014; Wang et al., 2014; Kučera et al., 2017), and has also been applied to determining g_c of vineyard canopies (Lu et al., 2003; Zhang et al., 2012; Bai et al., 2015). When applying the inverted PM equation in this manner, however, the determination of net radiation absorbed by the canopy must account for heat flux between the canopy and the ground below (Monteith and Unsworth, 2013). Estimating soil heat flux usually involves burying soil heat flux plates, determining soil thermal properties, measurement of temperature and moisture content in the soil profile, and will need to be implemented in multiple locations to account for spatial heterogeneity (Gao et al., 2017). Such instrumentation can be complicated and time consuming to implement properly, particularly in stony soils. The inverted PM equation approach to canopies also requires accounting for aerodynamic boundary layer conductance above the vineyard, involving measurement of wind speed and temperature profiles at multiple heights above the vineyard canopy (Monteith and Unsworth, 2013). Such measurement of soil heat flux and boundary layer conductance can be cumbersome and also interfere with ongoing management practices in a working vineyard. Alternatively, using the big leaf approach and an assumption of strong coupling between the crop canopy and the atmosphere allows for use of a simplified form of the inverted PM equation that does not require input of soil heat flux or aerodynamic boundary layer conductance (Phillips and Oren, 1998; Ewers and Oren, 2000) and has been applied to vineyards (Bai et al., 2015). The assumption of strong coupling between the vineyard canopy and the atmosphere, however, is based on the assumption that temperatures within the canopy (i.e., big leaf) and bulk air temperature above the canopy are similar (Ewers and Oren, 2000; Monteith and Unsworth, 2013), which may not be appropriate depending on meteorological conditions within and above the vineyard canopy.

In vineyards with open canopies, such as with vines cultivated in rows and surrounded by exposed ground, soil evaporation can account for over half of evapotranspiration (Lascano et al., 1992; Heilman et al., 1994). The big leaf model, however, is based on the assumption of uniform spatial distribution of sensible and latent heat flux from the canopy, and if applied to crops with open canopies may lead to anomalous determinations of g_c (Monteith and Unsworth, 2013). In such cases, a modified two-source approach as developed by Shuttleworth and Wallace (1985) can be used to evaluate heat and water vapor flux from the crop canopy separately from the exposed ground surrounding the canopy. This leads to a calculation of *bulk stomatal conductance* (g_{bs}) that does not require the measurement of soil heat flux or boundary layer conductance above the vineyard, greatly simplifying its determination. This g_{bs} is similar to g_c in that it represents the net effect of the g_s of all leaves in the portion of the vine canopy being considered. This two-source approach has been used to estimate evapotranspiration vineyards that

correlated well with eddy covariance measurements (Ortega-Farias et al., 2007, 2010; Ding et al., 2014).

Based on this two-source approach, a methodology is presented here for determination of g_{bs} for vineyards with open canopies using data from instrumentation having minimal interference with the operations of a working vineyard and avoiding problematic methodologies for measurement of parameters such as soil heat flux and atmospheric boundary layer.

METHODS

The heat and mass transfer theory behind the PM equation and the two-source energy flux model is presented in the literature using resistance to fluxes rather than conductance in order to facilitate the use of Ohms Law analogies (Monteith and Unsworth, 2013). The following presentation also uses resistances (s m^{-1}), with results being converted to conductance (m s^{-1}) by inversion, with the latter often used in plant physiology literature.

Heat Flux Model

For crops with open canopies, Shuttleworth and Wallace (1985) developed a one-dimensional model of sensible and latent heat fluxes separately from the crop canopy and the ground surrounding the canopy as part of a network of temperature and vapor pressure gradients and corresponding flux resistances. **Figure 1** presents a simplified schematic of this two-source representation applied to a vineyard with an open canopy.

An important assumption in this method is the *mean canopy height* (z_c), or the height at which constituents such as temperature and humidity are considered to be well mixed and uniformly distributed horizontally through the canopy (Shuttleworth and Wallace, 1985). It is the effective height from within the canopy where heat and vapor fluxes can be calculated using a PM type equation (Lhomme et al., 2012). This assumption relies on the open canopies being horizontally consistent across the field and with good aerodynamic mixing within the canopy (Shuttleworth and Wallace, 1985). While z_c is not needed in the calculation of g_{bs}, it was needed to determine the height at which the temperature and humidity sensors in the canopy were placed.

The mean canopy height is determined as the sum of the canopy *zero plane displacement* height (d, m) and the *roughness length* (z_o, m) (Shuttleworth and Wallace, 1985). Both are related to the apparent drag between the crop canopy and the wind moving over the canopy, with d being the height above the ground of the lower asymptote of the wind speed profile above the canopy, and z_o being the height above d where the wind speed theoretically goes to zero (Monteith and Unsworth, 2013; Alfieri et al., 2019). Studies have found values of d and z_o to be affected by canopy characteristics and differed as a function of wind direction (Chahine et al., 2014), but that flux estimates from a two-source energy balance model were relatively insensitive to such differences (Alfieri et al., 2019). Based on a study in a similarly configured vineyard, values of d ranged from 0.62 to 0.75h and z_o ranged from 0.08 to 0.14h, where h is the total height of the canopy above the ground (Chahine et al., 2014). With a vine canopy height at h = 1.5 m above the ground, d was estimated to be 1m above the ground and z_o at 0.15 m above that, with mean canopy height (z_c) being a total of 1.15 m above the ground.

Bulk Stomatal Conductance

Based on the two-source schematic as shown in **Figure 1** an adaptation of the PM equation is used to calculate latent heat flux from the vine canopy (λE_c) (Lhomme et al., 2012):

$$\lambda E_c = \frac{\triangle R_c + \rho C p\,(D_c)\,/r_{bh}}{\triangle + \gamma\left(n + \frac{r_{bs}}{r_{bh}}\right)}\,(Wm^{-2}) \quad (1)$$

where:

E_c = evaporative flux from canopy per unit ground area (g m^{-2} s^{-1})

λ = latent heat of vaporization for water = 2257 (J g^{-1})

D_c = vapor pressure deficit at mean canopy height (Pa)

R_c = net radiation absorbed by the vine canopy per unit ground area (W m^{-2})

r_{bs} = bulk stomatal resistance (s m^{-1})

r_{bh} = bulk boundary layer resistance to heat flux (s m^{-1})

n = 2 for grapevine leaves with stomata on one side only

γ = psychrometric constant at 1 atm and 20°C = 65.8 (Pa $C^{\circ -1}$)

Δ = rate of change in saturation vapor pressure versus temperature = 145 (Pa $C^{\circ -1}$)

ρC_p = heat content per unit volume of air at 20°C = 1212 (Pa $C^{\circ -1}$)

Equation 1 can then be rearranged to give bulk stomatal resistance:

$$r_{bs} = \frac{\triangle R_c r_{bh} + \rho C p(D_c)}{\lambda E_c \gamma} - r_{bh}\left(\frac{\triangle}{\gamma} - n\right)\,(sm^{-1}) \quad (2)$$

and bulk stomatal conductance is given by inversion:

$$g_{bs} = {r_{bs}}^{-1}(ms^{-1}) \quad (3)$$

The output units for the equations above result when input units shown in the text are used, with all conductance/resistance and fluxes expressed in terms of unit area of vineyard ground attributable to each vine (i.e., row spacing x vine spacing). Multiplying g_{bs} by the molar volume of air (41.04 mol/m^3 at 1 atm and 20°C) and converting units gives g_{bs} in terms of mmol m^{-2} s^{-1}, as often used in plant physiology literature.

Conceptually, r_{bs} is the parallel sum of the leaf level stomatal resistances (r_s, s m^{-1}) of all individual leaves in the canopy (Kelliher et al., 1995), and calculated as above provides an integrated measure of individual leaf resistances across the range of micro-meteorological conditions experienced by all the leaves in the canopy. A relationship between bulk and leaf-level stomatal conductance is given by the following equation based on leaf area index (LAI) and considering whether leaves have stomata on one or both sides (Lhomme et al., 2012):

$$r_{bs} = \frac{n^* r_s}{2^* LAI}\,(sm^{-1}) \quad (4)$$

where n = 2 for grapevine leaves with stomata on one side only.

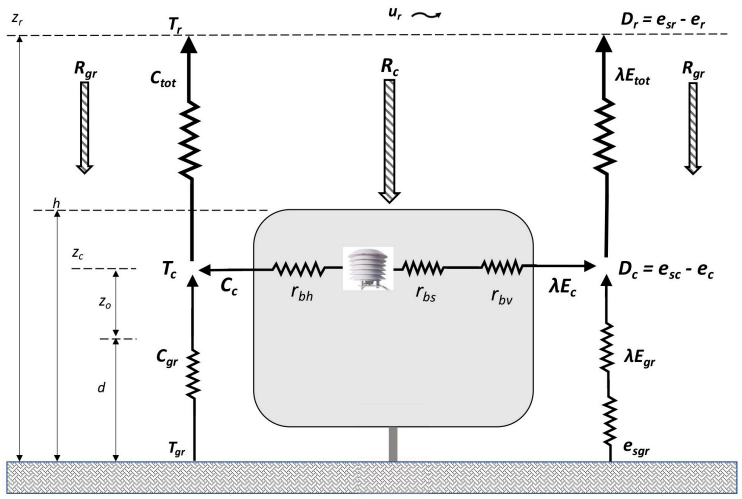

FIGURE 1 | Schematic of convective and radiative heat fluxes to and from the vine canopy and surrounding ground based on Shuttleworth and Wallace, 1985; Lhomme et al., 2012.

If the vine canopy covers more of the ground, however, such as with pergola style trellising or sprawling canopies, use of the big leaf model approach may be more appropriate with measurement of soil heat fluxes from beneath the canopy becoming more important.

Sensitivity Analysis

A global sensitivity analysis determines the relative importance of the input variables (predictors) to a mathematical model in determining the variation in the output of the model (response), across the range of input values (Iooss and Saltelli, 2017). Such analysis can also be used to characterize the effects of input variable interactions (Razavi and Gupta, 2015; Iooss and Saltelli, 2017). One approach to understanding the relative importance of input variables involves using the output of the model as the response variable in a regression analysis with the inputs to the model as the predictor variables (Saltelli et al., 2008; Razavi and Gupta, 2015).

Such a regression approach is the basis of a global sensitivity analysis of the PM equation using the input data collected for this study. The purpose is to understand the relative importance of the predictor variables in order to prioritize efforts in their determination. For example, the field measurement or estimation of a predictor variable with low importance might be simplified without significantly affecting model results.

A database of E_c, D_c, R_c, and r_{bh} data was first compiled from all vines in the study together with associated g_{bs} calculated using Eqs 2 and 3. This database was then used for the following two regression analyses:

- g_{bs} as the response variable with E_c, D_c, R_c, and r_{bh} as predictors, for the purpose of assessing the relative importance of the predictors in a regression model with the same form as the inverted PM equation used to calculate g_{bs} (Eqs 2 and 3).
- E_c as the response with g_{bs}, D_c, R_c, and r_{bh} as predictors, for the purpose of assessing the relative importance of the predictors in a regression model with the same form as the regular PM equation used to calculate transpiration (Eq. 1). Of particular interest is the relative importance of g_{bs} in the determination of E_c.

Preliminary review of the data suggested significant multicollinearity in the predictor variables (see correlation matrix in **Supplementary Figure S1**). Such multicollinearity is not surprising as transpiration (as regulated by changing conductance) is naturally related to vapor pressure deficit and net radiation (Jackson et al., 1981), and solar radiation is related to temperature (Hargreaves and Allen, 2003), and hence vapor pressure deficit.

This multicollinearity, however, can complicate global sensitivity analysis based on classical one-at-a-time, or linear regression methods (Razavi and Gupta, 2015). As an alternative, the random forest non-parametric regression method has been demonstrated as an effective way to perform global sensitivity analysis that is capable of handling interaction between predictors (Grömping, 2009; Antoniadis et al., 2021). A random forest methodology was therefore chosen for the two regression analyses described above.

The random forest methodology processes random selections of predictor variables through a large number of decision trees to find variable relationships that minimize mean square error in the response estimate when compared across many randomly generated test data sets (Breiman, 2001). Unlike parametric (i.e., linear or non-linear) regression methods, non-parametric methods such as random forest do not generate regression

coefficients that might otherwise be used to assess the relative importance of predictors. For this purpose, a *minimal depth* approach is used, which quantifies how quickly a predictor variable contributes to determining the response estimate across all the decision trees in the random forest model. The lower the depth number for a predictor, the more important the predictor, with the greatest possible importance having a depth of zero (Ishwaran et al., 2011).

The interactions between predictor variables were also evaluated from the random forest models using a *second order maximal subtree* approach by which *normalized relative minimal depths* of the different predictors are evaluated in a pairwise manner against each other (Ishwaran et al., 2011). The lower the difference in normalized minimal depths between predictors the more closely associated they are, with the interaction effect between variables of high importance having a greater effect on the response variable. For each pair of predictors, this approach generates a normalized index with 0 representing strong interaction and 1 representing none (Ishwaran et al., 2011).

Data analysis was performed using the R software environment (R Project for Statistical Computing, RRID:SCR_001905). Both random forest models were run using the *rfsrc* function of the *randomForestSRC* package for R (Ishwaran and Kogalur, 2021). The hyper parameters for both random forest models were first optimized using the *ranger* function of the *ranger* package for R (Wright et al., 2021). The relative importance of the predictor variables in the determining the response variables in both random forest models are evaluated using the *max.subtree* function of the *randomForestSRC* package for R (Ishwaran and Kogalur, 2021). The interactions between the predictor variables in both random forest models are evaluated using the *find.interactions* function of the *randomForestSRC* package for R (Ishwaran and Kogalur, 2021).

MATERIALS AND EQUIPMENT

The measurements for this study were taken on 10 individual grapevines in a vineyard, two each of *Vitis vinifera* L., cv. Cabernet-Sauvignon, Merlot, Tempranillo, Semillon, and Ugni blanc. Measurements of sap flow, temperature and humidity, and solar radiation were taken or interpolated to 15-minute intervals from June 30 to September 15, 2020 and canopy characteristics were measured periodically through the season.

Vineyard and Canopy Characteristics

The study was performed in a 0.6-hectare common garden experimental vineyard in Bordeaux, France (44° 47′ 0″ N, 0° 34′ 39″ W) with 52 varieties planted in a randomized block design. The vines are trained on a vertical shoot positioning trellis system with double Guyot pruning. The top and bottom of the vine canopy are 1.5 and 0.5 m above the ground, respectively, and 0.4 m wide, with canopy dimensions maintained by hedging twice during the growing season. Vine rows are orientated north-south with 1.8 m row spacing and 1.0 m vine spacing. The vines were planted on SO4 rootstock and the soils are clay-gravel typical for the Pessac-Léognan wine appellation (Destrac-Irvine and van Leeuwen, 2016). From 1991 through 2020 average annual total rainfall and reference evapotranspiration were 902 mm and 929 mm, respectively, with annual total solar radiation of 4,790 MJ m^{-2} and average maximum daily temperature from May through June of 25.5°C.

Leaf area was measured at three separate times during the season, in the first halves of July, August and September, respectively. Leaf area was determined by measuring the length and width of all the individual leaves on a subset (approximately 25%) of primary and secondary shoots of each vine. Leaf length and width dimensions were well correlated with individual leaf area as measured by a leaf area meter (Model LI-3100 LICOR Inc., Lincoln, NE, United States) before field measurements began. An average leaf size was calculated from all these individual leaf area measurements segregated based on primary or secondary shoots. These average leaf areas were then applied to a count of all leaves on the remaining primary and secondary shoots on each vine. Leaf area index (*LAI*, m^2 m^{-2}) is calculated as the total leaf area (m^2) for a vine divided by the area of vineyard ground attributable to each vine (i.e., row spacing × vine spacing). The porosity of each vine canopy was measured in the vineyard using a camera phone application (CANAPEO, Oklahoma State University Department of Plant and Soil Sciences, Stillwater, OK, United States) and interpolated linearly between measurements dates.

Transpiration Flux (E_c)

Heat balance sap flow sensors (Model SGEX, Dynamax Inc., Houston, TX, United States) were installed on one of the two canes of each vine, which were trained to the bottom trellis wire in a double Guyot manner at 50 cm above the ground. Based on manufacturer recommendations, the location of the sap flow sensor on a cane needed to be such that the flow of at least 30% of the vine's total shoots would be captured by the sensor. It was also found that the quality of the sensor readings benefited from emphasizing installation on straight and smooth cane internodes and by protecting sensors well against the rain.

Sap flow (g s^{-1}) was calculated from sensor signals collected by a datalogger (Model SapIP, Dynamax Inc., Houston, TX, United States) and then scaled up for the whole vine based on the ratio of leaf area of the whole vine to the leaf area of shoots downstream the sap flow sensor. Sap flow (g s^{-1}) was then divided by the area of vineyard ground attributable to each vine (i.e., row spacing x vine spacing) to give canopy evaporation (transpiration) flux, E_c (g s^{-1} m^{-2}).

Vapor Pressure Deficit (D_c)

Saturation vapor pressure, e_{sc} (Pa) at mean canopy height (z_c = 1.15 m above the ground) was calculated by Teten's equation using measured temperature T_c (°C) with the partial vapor pressure, e_c (Pa) calculated from e_{sc} using measured relative humidity. Temperature and humidity were measured using TinyTag Plus 2 probe/data loggers (Model TGP-4505 by Gemini Data Loggers, Chichester, West Sussex, England) with the temperature/relative humidity probes installed inside solar radiation shields (Model RS3 by Prosensor, Amanvillers,

France) and hung from a trellis wire in the vine canopy at the mean canopy height.

Net Radiation Flux Absorbed by the Vine Canopy (R_c)

The radiation flux (energy/time/unit area) incident on a crop canopy comes from sources of both shortwave solar radiation and long wave heat radiation in the environment. The net (intercepted minus reflected) radiation absorbed by the canopy is the sum of net shortwave radiation and net long wave radiation (Allen et al., 1998).

Shortwave Radiation

The method of Riou et al. (1989) was used for estimating the amount of such radiation absorbed by grapevine canopy. This radiation model was also used in the water balance model developed by Lebon et al. (2003). This method models the net shortwave radiation absorbed by a vine canopy as the sum of shortwave radiation from: (i) direct radiation from the sun; (ii) diffuse radiation scattered by the atmosphere or clouds; and (iii) both beam and diffuse radiation reflected from the soil in the space between vine rows minus that reflected again by the leaves of the canopy. The model outputs radiation flux (W m^{-2}) of shortwave radiation absorbed by the vine canopy expressed in terms of the unit area of vineyard ground attributable to each vine (i.e., row spacing × vine spacing) (Riou et al., 1989).

The method relies on inputs of canopy dimensions, row spacing, and vine spacing and accounts for an assumed, or measured porosity of the canopy. For the direct component of global radiation absorbed by the canopy, solar angles, such as the hour and height angles, were calculated for input to the model based on the latitude and longitude of the study site (Kalogirou, 2014; Widén and Munkhammar, 2019). Based on measurements of global (shortwave) radiation incident on the vineyard, and applying the approach described in Liu and Jordan (1960), the relative amounts of direct and diffuse shortwave radiation were calculated on 15-minute intervals over the season for input to the model. Global (shortwave) radiation flux was measured at a weather station next to the vineyard using a horizontally mounted pyranometer (Model No. CMP6 by Kipp & Zonen, Delft – Netherlands) on one-hour intervals, and then linearly interpolated to 15-minute intervals for the above calculations.

Long Wave Radiation

Long wave (heat) radiation from the atmosphere, surrounding ground, and adjacent vine canopy rows are also a source of radiation for the vine canopies (Pieri, 2010). The proportion of radiation flux from the sky, ground, and adjacent vine rows incident on the vine canopy were calculated using radiation view factors between these sources and the faces of the vine canopy. The amount of radiation flux intercepted by the canopy was then adjusted to account for canopy porosity. The canopies themselves were also assumed to radiate heat energy as a function of their temperature. The net long wave radiation absorbed by the vine canopy was then the sum of the amount absorbed from all sources, minus the amount radiated from the canopy, together expressed as long wave radiation flux (W m^{-2}) in terms of unit area of vineyard ground attributable to each vine (i.e., row spacing x vine spacing).

Long wave radiation flux from the sky (W m^{-2}) was measured on 15-minute intervals with an upward facing pyrgeometer (Model No. SL-510-SS, Apogee Instruments, Logan, UT, United States) on a mast 1.5 m above the vine canopy. Long wave radiation flux from the surrounding ground was determined by measurement of ground temperature using a rectangular field of view infrared radiometer (Model No. SI-1H1 IR, Apogee Instruments, Logan, UT, United States) and converted to long wave radiation flux (W m^{-2}) using the Stefan-Boltzmann equation with an assumed emissivity for dry grass of 0.98 (Rubio et al., 1997). The long wave energy radiated by the vine canopy and intercepted from adjacent vine canopies were calculated from the temperatures measured in the canopy and application of the Stefan-Boltzmann equation with an assumed emissivity for vine foliage of 0.98 (Jones et al., 2003; Pieri, 2010).

Bulk Boundary Layer Resistances to Heat and Vapor Flux (r_{bh} and r_{bv})

Development of Eq. 1 in the literature uses the bulk boundary layer conductance to heat flux (r_{bh}, s m^{-1}) as opposed to bulk boundary layer resistance to vapor flux (r_{bv}, s m^{-1}) based on the relationships in Eqs 5 and 6 below, in which n = 2 for grapevine leaves with stomata on one side only. Similar to bulk stomatal resistance, the bulk boundary layer resistances to heat and water vapor flux are canopy-level summations of the leaf-level boundary layer resistances across all leaves in the canopy stated in terms of unit ground area (Lhomme et al., 2012):

$$r_{bh} = \frac{r_{bl}}{2^{*}LAI}(sm^{-1}) \tag{5}$$

$$r_{bv} = n^{*}r_{bh} = \frac{2^{*}r_{bl}}{2^{*}LAI}\,(sm^{-1}) \tag{6}$$

where:

r_{bl} = is the one-sided leaf-level boundary layer resistance (s m^{-1}).

LAI = leaf area index.

One method of estimating r_{bl} requires the determination of wind speed at the top of the crop canopy (Choudhury and Monteith, 1988; Lhomme et al., 2012). This can be inferred from wind speed profiles measured at multiple heights above the crop canopy in the atmospheric boundary layer (Monteith and Unsworth, 2013). As an alternative, a basic assumption of r_{bl} = 25 s m^{-1} was proposed by Shuttleworth and Wallace (1985) and demonstrated to be adequate based on the relatively low importance of r_{bh} in the PM equation. The low importance of r_{bh} in the calculation of g_{bs} is also confirmed in the sensitivity analysis presented in the next section. This assumption of r_{bl} = 25 s m^{-1} has the additional benefit of avoiding the need for wind speed measurements as needed to determine the wind speed profile above the canopy. In climates with different prevailing temperature, vapor pressure deficit, or wind conditions, however, it may be found that r_{bh} is more important than presented here, in which case measurement of wind speeds may be beneficial.

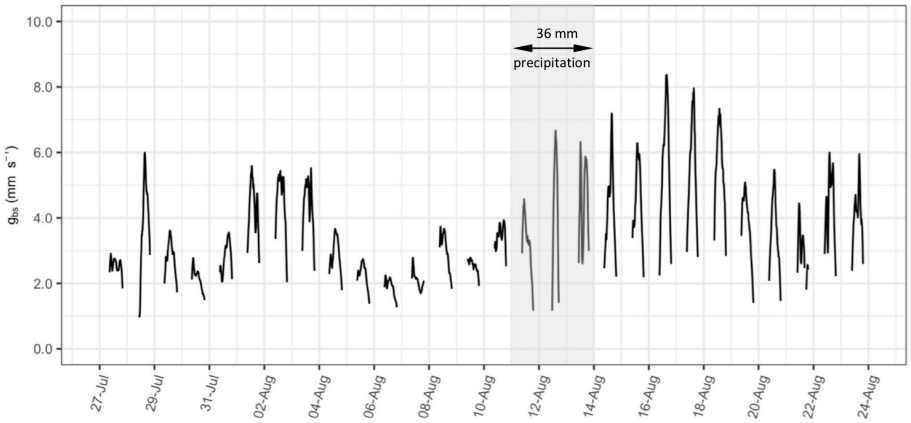

FIGURE 2 | Example timeseries of bulk stomatal conductance (g_{bs}, mm s^{-1}) calculated on 15-minute intervals from a selected vine (C6-2) between 27 July and 24 August, 2020. Shading indicates days over which there was 36 mm of precipitation.

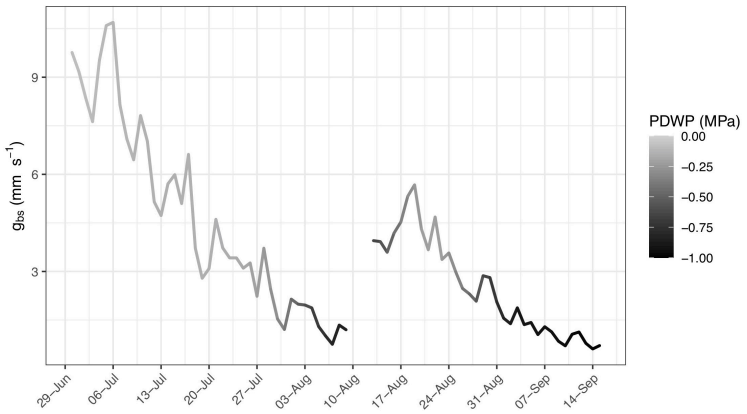

FIGURE 3 | Daily maximum hourly running average of 15-min estimates of the bulk stomatal conductance, g_{bs} (mm s^{-1}) from a selected vine (C5-2) between 30 June and 15 September, 2020 with shading of line representative of corresponding measured predawn leaf water potential varying from 0.0 MPa (light gray) to −1.0 MPa (black).

Predawn Leaf Water Potential

Predawn leaf water potential (Ψ_{PD}) measurements provide the water potential of the plant at night when the stomata are closed and the plant is in equilibrium with the root zone water potential (Choné et al., 2001) and is an accepted plant-based measurement of plant water stress (Sperry et al., 1996). Measurements of Ψ_{PD} were taken on each vine in the study at six times, roughly 10–14 days apart depending on weather, from early July through early September 2020. Leaf sampling and measurement were done early enough to ensure all was completed no later than 30 minutes prior to sunrise. Measurements were taken by the pressure chamber method of Scholander et al. (1965) using a pressure chamber with digital manometer (DG MECA, 33175 Gradignan, France).

RESULTS AND DISCUSSION

Bulk Stomatal Conductance

The time series of bulk stomatal conductance (g_{bs}, mm s^{-1}) calculated on 15-minute intervals is presented as an example in **Figure 2** for vine C6-2 between 27 July and 24 August 2020. Gaps in this 15-minute interval time series are caused by filtering of data when net radiation absorbed by vine canopy (R_c) is less than 50 W m^{-2} during the early morning and evening, or at night. The calculation of g_{bs} using Eqs 2 and 3 is prone to inaccuracy at low levels of R_c, and corresponding low levels of D_c and E_c. This approach of filtering low solar radiation data was also used in previous studies of conductance in vineyards (Lu et al., 2003; Zhang et al., 2012).

TABLE 1 | Predictor variable minimum depths and pairwise relative minimum depths between predictor variables for two regression models: **(A)** with g_{bs} as the response variable; and **(B)** with E_c as the response variable.

(A) With g_{bs} as response variable.

	Minimum	Pairwise relative minimum depths			
Variable	**Depth**	E_c	D_c	R_c	r_{bh}
E_c	0.00	—	0.05	0.29	0.31
D_c	1.00	0.05	—	0.26	0.29
R_c	6.20	0.11	0.11	—	0.12
r_{bh}	6.80	0.11	0.11	0.12	—

(B) With E_c as response variable.

	Minimum	Pairwise relative minimum depths			
Variable	**depth**	g_{bs}	D_c	R_c	r_{bh}
g_{bs}	0.00	—	0.07	0.14	0.25
D_c	1.62	0.05	—	0.18	0.20
R_c	3.00	0.07	0.07	—	0.11
r_{bh}	5.37	0.10	0.09	0.11	—

The diffusion rate of water vapor through stomata (i.e., stomatal conductance) is affected by: (i) solar radiation, which adds energy to the diffusion; (ii) vapor pressure deficit, which is the driving force for diffusion; and (iii) the effects of boundary layer resistance to diffusion at the leaf surface (Keller, 2015). At the canopy scale, diurnal fluctuations in R_c and D_c are likely responsible for the strong diurnal variation in 15-minute g_{bs} also observed in **Figure 2**, particularly on days with higher overall levels of conductance. The effect of boundary layer resistance, as accounted for in r_{bh}, however, will be largely a function of changes in leaf area over the course of the season.

Stomata regulation is also affected by changes in plant water status (Oren et al., 1999; Roelfsema and Hedrich, 2005), with predawn leaf water potential (Ψ_{PD}) providing a useful measure (Sperry et al., 1996; Choné et al., 2001). The effect of Ψ_{PD} on g_{bs} is observed in **Figure 3**, which presents the daily maximum hourly running average of 15-minute estimates of g_{bs} from a selected vine (C5-2) between 30 June and 15 September 2020, with shading of the line representing the corresponding measured Ψ_{PD}, varying from 0.0 MPa (light gray) to −1.0 MPa (black). The lowest levels of g_{bs} are observed when Ψ_{PD} is more negative. The shading associated with corresponding Ψ_{PD} measurements is also included in the plots of daily maximum hourly running average of 15-minute estimates of g_{bs} for all ten vines in **Supplementary Figure S2**.

Under heterogeneous moisture conditions, predawn water potential measurements have been found to equilibrate at less negative values with portions of the root zone having higher moisture content (Améglio et al., 1999), as may happen in a dry soil after a rainfall. Both **Figures 2**, **3** show a noticeable increase in overall levels of conductance for a few days after the only significant rainfall of the season (36 mm between 11–13 August). This may be the result of less negative Ψ_{PD} resulting from infiltration of rainfall into the upper part of the root zone. A similar increase in conductance after this rainfall was observed in the daily maximum hourly running average of g_{bs} for most of the ten vines as presented in **Supplementary Figure S2**.

The maximum observed g_{bs} over the season for each of the 10 vines in this study ranged from around 5 to 10 mm s^{-1} with occasional peaks from around 10 to 15 mm s^{-1}. This compares well with canopy conductance up to 7.0 mm s^{-1} determined on cv. Sultana (Lu et al., 2003), values up to 8.5 mm s^{-1} determined on cv. Merlot (Zhang et al., 2012), and upward of 16 mm s^{-1} in morning hours and 12 mm s^{-1} in the afternoon hours determined on cv. Thompson Seedless (Bai et al., 2015). The differences in maximum observed g_{bs} between individual vines at a given time may be due to a combination of factors, such as differences in individual vine root access to water and hence vine water status, and genetic differences between varieties in stomatal response to changes in R_c and D_c.

A multi variable analysis of the above factors and others is beyond the scope of this paper, although the methodology presented here provides a useful means of determining g_{bs} for such future analysis.

Sensitivity Analysis and Variable Interactions

Two optimized random forest regression models, one model with g_{bs} as the response variable and the other with E_c as the response variable were created using the combined data from all 10 vines in the study. The minimum depths and pairwise variable interactions for the predictors from both of these random forest models are presented in **Table 1**.

Based on the minimum depth methodology, a predictor with a minimum depth of 0 is the most important in determining the response of the model, with the other predictors being relatively less important as their corresponding minimum depths increase (Ishwaran et al., 2011). For the model with g_{bs} as the response variable, **Table 1(A)** indicates that E_c is the most important

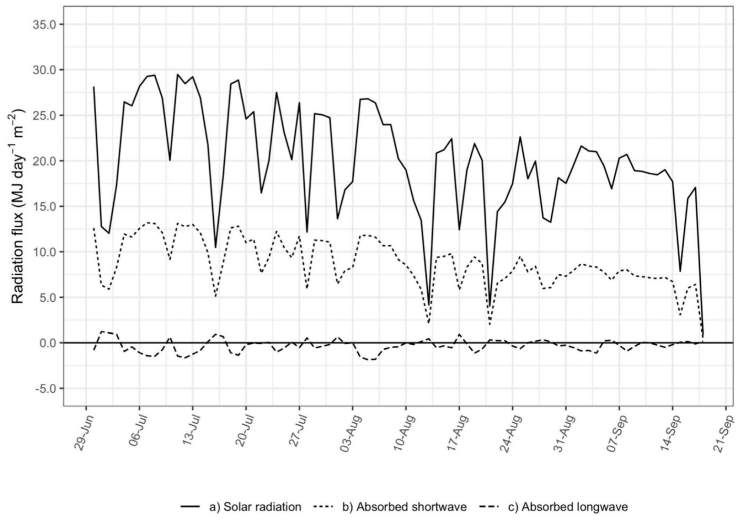

FIGURE 4 | Daily shortwave and long wave radiation flux (MJ day^{-1} m^{-2}) absorbed by the vine canopy (dashed lines) and solar radiation flux (MJ day^{-1} m^{-2}) incident on the vineyard (solid line).

predictor. Due to this importance, proper implementation of sap flow measurements to determine transpiration, and hence E_c should be emphasized. Conversely, in the model with E_c as the response variable, **Table 1(B)** indicates g_{bs} was the most important predictor, confirming the importance of properly characterizing g_{bs} when modeling the vine canopy component of transpiration in vineyard water balance models.

After E_c and g_{bs}, D_c is a significant predictor in both regressions, suggesting the quality of temperature and humidity measurements in the vine canopy and proper placement of instruments at the mean canopy height (z_c) should be emphasized. R_c was of relatively low importance in both regressions, and therefore a simplification in its method of estimation is proposed in the next section. The least important predictor in both regressions was r_{bh}, further justifying use of the simplified assumption of r_{bl} = 25 s m^{-1} as described earlier according to Shuttleworth and Wallace (1985) in Eqs 5 and 6, and eliminating the need for measurement of wind speed above the canopy.

The normalized pairwise relative minimum depths between predictor variables are also presented in **Tables 1(A,B)** for both regression models. The normalized depths (with 0 indicating strong interaction and 1 indicating no interaction) are shown for a given predictor variable in each row, with the strength of the interaction being greater for predictor variables of higher importance (Ishwaran and Kogalur, 2021). The interactions between E_c and D_c, the most important variables in the regression model for g_{bs}, are very strong at 0.05 in both pairings. Likewise, the interactions between g_{bs} and D_c, the most important variables in the regression model for E_c, are also strong at 0.05 and 0.07 for the two pairings. Interactions are observed between other variables, but they are less significant because of the lower importance of those variables. It should be noted, however, the results of the sensitivity analysis could vary with different ranges of D_c, R_c, wind speed, or *LAI* as might be experienced in different years, locations, or vineyards with different designs or subject to different management practices.

The finding of significant interactions between important variables confirms the preliminary observations in the correlation matrix in **Supplementary Figure S1** and supports the use of the random forest regression approach for the sensitivity analysis, which is capable of handling such variable interactions. Such strong interaction may also affect any additional regression analysis aimed at characterizing the relationship between g_{bs} and other environmental variables.

Net Radiation (R_c)

Figure 4 presents modeled net shortwave and net long wave radiation flux absorbed by the vine canopy and the measured global radiation flux incident on the whole vineyard, expressed in terms of the amount of energy absorbed by the vine canopy per day per unit vineyard ground area (MJ day^{-1} m^{-2}). Daily fluxes were tallied with values of 15-minute R_c greater than 50 W m^{-2} to match the filtering used in the calculation of g_{bs}.

The shortwave radiation absorbed by the canopy follows closely with global radiation incident on the vineyard and represents the majority of the total radiation absorbed by the vine canopy. Net long wave radiation averaged close to zero on most days, although it could represent up to 30% of total net radiation when shortwave radiation is low. This is associated with cloudy conditions when transpiration is already low and not contributing much to vineyard water use.

For that reason, and because of the relatively low importance of R_c in the regressions with either g_{bs} or E_c, net long wave radiation absorbed by the vine canopy was disregarded in the estimation of R_c used in the final calculations of g_{bs}. This has the benefit in the future of eliminating instrumentation in the vineyard for measurement of long wave radiation from the sky and surrounding ground. Similarly, other studies of conductance in vineyards did not account for long wave radiation in determining net radiation (Lu et al., 2003; Zhang et al., 2012; Bai et al., 2015). However, if R_c is found to be a more important variable in the determination of g_{bs} or E_c, then measurement of long wave radiation may be beneficial, perhaps as in cloudier climates.

CONCLUSION

Based on the two-source energy flux approach of Shuttleworth and Wallace (1985), a methodology is presented here for determination of g_{bs} for vineyards with open canopies, using measurements of: (i) vine transpiration measured by sap flow as needed to calculate transpiration flux from the canopy; (ii) measurements of temperature and relative humidity in the vine canopy as needed to calculate vapor pressure deficit; (iii) solar radiation measures as needed to estimate the net radiation absorbed by the vine canopy; and (iv) vine canopy dimensions, porosity, and leaf area as needed for the above. Diurnal variations in 15-minute estimates of g_{bs} were observed, with maximum daily levels comparing well with previously published values for grapevines the literature. Decreases in g_{bs} over the season were also observed in association with more negative Ψ_{PD}.

This methodology respects the energy flux dynamics of vineyards with open canopies, while avoiding involved and error-prone measurements that can also interfere with the operations of a working vineyard. It does not require measurement of soil heat flux, boundary layer conductance above the vineyard, nor long wave radiation, although consideration may need to be given to such measurements in other climates or vineyard configurations. It provides a practical means of quantifying conductance for further study of conductance response to changes in atmospheric demand and drought stress.

A global sensitivity analysis using data from the study found E_c and D_c are the most important variables in the determination of g_{bs}, therefore warranting attention in their field measurement. Conversely, g_{bs} was found to be the most important predictor of E_c, emphasizing the importance of having better representations of conductance response in vineyard water use models.

DATA AVAILABILITY STATEMENT

The raw data supporting the conclusions of this article will be made available by the authors, without undue reservation.

AUTHOR CONTRIBUTIONS

MG and AD-I coordinated and executed field measurements. PP advised on instrumentation and theoretical basis for analysis. MG compiled the dataset and worked with BS on statistical analysis. All authors were involved in design of the study, helped guide its execution, and participated in the writing and editing of the submitted manuscript.

FUNDING

This study has been carried out with financial support from Jas. Hennessy & Co. (16100 Cognac, France) and the French National Research Agency (ANR) in the frame of the Investments for the future Programme, within the Cluster of Excellence COTE (ANR-10-LABX-45). The VitAdapt vineyard is supported by the Conseil Interprofessionnel des Vins de Bordeaux (CIVB), the Conseil Régional d'Aquitaine, Bordeaux University through LabEx and the Institut National de Recherche pour l'Agriculture, l'Alimentation et l'Environnement (INRAE).

ACKNOWLEDGMENTS

We would like to thank Guillermo Gutiérrez, Eylul Kadaifci, and Alfonso Domínguez Zamudio for their tireless involvement in data collection, and to the INRAE, UEVB, F-33882, Villenave d'Ornon, France, for its management of the VitAdapt vineyard and assistance with implementing instrumentation.

SUPPLEMENTARY MATERIAL

The Supplementary Material for this article can be found online at: https://www.frontiersin.org/articles/10.3389/fpls.2022.839378/full#supplementary-material

REFERENCES

Alfieri, J. G., Kustas, W. P., Nieto, H., Prueger, J. H., Hipps, L. E., McKee, L. G., et al. (2019). Influence of wind direction on the surface roughness of vineyards. *Irrig. Sci.* 37, 359–373. doi: 10.1007/s00271-018-0610-z

Allen, R. G., Pereira, L. S., Raes, D., and Smith, M. (1998). *FAO Irrigation And Drainage Paper No. 56*. Rome: Food and Agriculture Organization of the United Nations, 97–156.

Améglio, T., Archer, P., Cohen, M., Valancogne, C., Daudet, F., Dayau, S., et al. (1999). Significance and limits in the use of predawn leaf water potential for tree irrigation. *Plant Soil* 207, 155–167. doi: 10.1023/A:1026415302759

Antoniadis, A., Lambert-Lacroix, S., and Poggi, J.-M. (2021). Random forests for global sensitivity analysis: a selective review. *Reliab. Eng. Syst. Saf.* 206:107312. doi: 10.1016/j.ress.2020.107312

Bai, Y., Zhu, G., Su, Y., Zhang, K., Han, T., Ma, J., et al. (2015). Hysteresis loops between canopy conductance of grapevines and meteorological variables in an oasis ecosystem. *Agric. For. Meteorol.* 214–215, 319–327.

Breiman, L. (2001). Random forests. *Mach. Learn.* 45, 5–32. doi: 10.1023/A:1010933404324

Chahine, A., Dupont, S., Sinfort, C., and Brunet, Y. (2014). Wind-flow dynamics over a vineyard. *Bound. Layer Meteorol.* 151, 557–577. doi: 10.1007/s10546-013-9900-4

Choné, X., van Leeuwen, C., Chéry, P., and Ribereau-Gayan, P. (2001). Terroir Influence on water status and nitrogen status of non-irrigated cabernet sauvignon (*Vitis vinifera*). Vegetative development, must and wine composition (Example of a medoc top estate vineyard, saint julien area, bordeaux, 1997). *South Afr. J. Vitic.* 22, 8–15. doi: 10.21548/22-1-2159

Choudhury, B. J., and Monteith, J. L. (1988). A four-layer model for the heat budget of homogeneous land surfaces. *Q. J. R. Meteorol. Soc.* 114, 373–398. doi: 10.1002/qj.49711448006

Costa, J. M., Ortuño, M. F., Lopes, C. M., Chaves, M. M., Costa, J. M., Ortuño, M. F., et al. (2012). Grapevine varieties exhibiting differences in stomatal response to water deficit. *Funct. Plant Biol.* 39, 179–189. doi: 10.1071/FP11156

Destrac-Irvine, A., and van Leeuwen, C. (2016). "The Vitadapt project: extensive phenotyping of a wide range of varieties in order to optimize the use of genetic diversity within the *Vitis vinifera* species as a tool for adaptation to a changing environment," in *Proceedings of the Climwine 2016 – Sustainable Grape And Wine Production In The Context Of Climate Change*, (Bordeaux), 165–171.

Ding, R., Kang, S., Du, T., Hao, X., and Zhang, Y. (2014). Scaling up stomatal conductance from leaf to canopy using a dual-leaf model for estimating crop evapotranspiration. *PLoS One* 9:e95584. doi: 10.1371/journal.pone.0095584

Ewers, B. E., and Oren, R. (2000). Analyses of assumptions and errors in the calculation of stomatal conductance from sap flux measurements. *Tree Physiol.* 20, 579–589. doi: 10.1093/treephys/20.9.579

Ewers, B. E., Gower, S. T., Bond-Lamberty, B., and Wang, C. K. (2005). Effects of stand age and tree species on canopy transpiration and average stomatal conductance of boreal forests. *Plant Cell Environ.* 28, 660–678. doi: 10.1111/j.1365-3040.2005.01312.x

Gao, Z., Russell, E. S., Missik, J. E. C., Huang, M., Chen, X., Strickland, C. E., et al. (2017). A novel approach to evaluate soil heat flux calculation: an analytical review of nine methods. *J. Geophys. Res. Atmospheres* 122, 6934–6949. doi: 10.1002/2017JD027160

Ghimire, C. P., Lubczynski, M. W., Bruijnzeel, L. A., and Chavarro-Rincón, D. (2014). Transpiration and canopy conductance of two contrasting forest types in the Lesser Himalaya of Central Nepal. *Agric. For. Meteorol.* 197, 76–90. doi: 10.1016/j.agrformet.2014.05.012

Granier, A., and Loustau, D. (1994). Measuring and modelling the transpiration of a maritime pine canopy from sap-flow data. *Agric. For. Meteorol.* 71, 61–81. doi: 10.1016/0168-1923(94)90100-7

Granier, A., Biron, P., and Lemoine, D. (2000). Water balance, transpiration and canopy conductance in two beech stands. *Agric. For. Meteorol.* 100, 291–308. doi: 10.1016/S0168-1923(99)00151-3

Grömping, U. (2009). Variable importance assessment in regression: linear regression versus random forest. *Am. Stat.* 63, 308–319. doi: 10.1198/tast.2009.08199

Hargreaves, G. H., and Allen, R. G. (2003). History and evaluation of hargreaves evapotranspiration equation. *J. Irrig. Drain. Eng.* 129, 53–63. doi: 10.1061/(ASCE)0733-94372003129:1(53)

Heilman, J. L., McInnes, K. J., Savage, M. J., Gesch, R. W., and Lascano, R. J. (1994). Soil and canopy energy balances in a west Texas vineyard. *Agric. For. Meteorol.* 71, 99–114. doi: 10.1016/0168-1923(94)90102-3

Herrera, J. C., Calderan, A., Gambetta, G. A., Peterlunger, E., Forneck, A., Sivilotti, P., et al. (2021). Stomatal responses in grapevine become increasingly more tolerant to low water potentials throughout the growing season. *Plant J. Cell Mol. Biol.* 109, 804–815. doi: 10.1111/tpj.15591

Iooss, B., and Saltelli, A. (2017). "Introduction to sensitivity analysis," in *Handbook of Uncertainty Quantification*, eds R. Ghanem, D. Higdon, and H. Owhadi (Cham: Springer International Publishing), 1103–1122. doi: 10.1007/978-3-319-12385-1_31

Ishwaran, H., and Kogalur, U. B. (2021). *randomForestSRC: Fast Unified Random Forests for Survival, Regression, and Classification (RF-SRC).* Available online at: https://CRAN.R-project.org/package=randomForestSRC (accessed November 13, 2021).

Ishwaran, H., Kogalur, U. B., Chen, X., and Minn, A. J. (2011). Random survival forests for high-dimensional data. *Stat. Anal. Data Min.* 4, 115–132. doi: 10.1002/sam.10103

Jackson, R. D., Idso, S. B., Reginato, R. J., and Pinter, P. J. (1981). Canopy temperature as a crop water stress indicator. *Water Resour. Res.* 17, 1133–1138. doi: 10.1029/WR017i004p01133

Jones, H. G., Archer, N., Rotenberg, E., and Casa, R. (2003). Radiation measurement for plant ecophysiology. *J. Exp. Bot.* 54, 879–889. doi: 10.1093/jxb/erg116

Kalogirou, S. (2014). *Solar Energy Engineering*. Amsterdam: Elsevier, doi: 10.1016/C2011-0-07038-2

Keller, M. (2015). *The Science of Grapevines: Anatomy and Physiology*, 2nd Edn. Boston, MA: Academic Press.

Kelliher, F. M., Leuning, R., Raupach, M. R., and Schulze, E.-D. (1995). Maximum conductances for evaporation from global vegetation types. *Agric. For. Meteorol.* 73, 1–16. doi: 10.1016/0168-1923(94)02178-M

Köstner, B. M. M., Schulze, E.-D., Kelliher, F. M., Hollinger, D. Y., Byers, J. N., Hunt, J. E., et al. (1992). Transpiration and canopy conductance in a pristine broad-leaved forest of Nothofagus: an analysis of xylem sap flow and eddy correlation measurements. *Oecologia* 91, 350–359. doi: 10.1007/BF00317623

Kučera, J., Brito, P., Jiménez, M. S., and Urban, J. (2017). Direct Penman–Monteith parameterization for estimating stomatal conductance and modeling sap flow. *Trees* 31, 873–885. doi: 10.1007/s00468-016-1513-3

Lascano, R. J., Baumhardt, R. L., and Lipe, W. N. (1992). Measurement of water flow in young grapevines using the stem heat balance method. *Am. J. Enol. Vitic.* 43, 159–165.

Lebon, E., Dumas, V., Pieri, P., and Schultz, H. R. (2003). Modelling the seasonal dynamics of the soil water balance of vineyards. *Funct. Plant Biol.* 30, 699–710. doi: 10.1071/FP02222

Lhomme, J. P., Montes, C., Jacob, F., and Prévot, L. (2012). Evaporation from heterogeneous and sparse canopies: on the formulations related to multi-source representations. *Bound. Layer Meteorol.* 144, 243–262. doi: 10.1007/s10546-012-9713-x

Liu, B. Y. H., and Jordan, R. C. (1960). The interrelationship and characteristic distribution of direct, diffuse and total solar radiation. *Sol. Energy* 4, 1–19. doi: 10.1016/0038-092X(60)90062-1

Lovisolo, C., Perrone, I., Carra, A., Ferrandino, A., Flexas, J., Medrano, H., et al. (2010). Drought-induced changes in development and function of grapevine (*Vitis* spp.) organs and in their hydraulic and non-hydraulic interactions at the whole-plant level: a physiological and molecular update. *Funct. Plant Biol.* 37:98. doi: 10.1071/FP09191

Lu, P., Yunusa, I. A. M., Walker, R. R., and Müller, W. J. (2003). Regulation of canopy conductance and transpiration and their modelling in irrigated grapevines. *Funct. Plant Biol.* 30, 689–698. doi: 10.1071/FP02181

McElrone, A. J., Choat, B., Gambetta, G. A., and Brodersen, C. R. (2013). *Water uptake and Transport In Vascular Plants. Nat. Educ. Knowl. 4*. Available online at: http://www.nature.com.zhongjivip.net/scitable/knowledge/library/water-uptake-and-transport-in-vascular-plants-103016037 (accessed June 4, 2016).

Monteith, J., and Unsworth, M. (2013). *Principles of Environmental Physics: Plants, Animals, and the Atmosphere*. Cambridge, MA: Academic Press.

Oren, R., Sperry, J. S., Katul, G. G., Pataki, D. E., Ewers, B. E., Phillips, N., et al. (1999). Survey and synthesis of intra- and interspecific variation in stomatal sensitivity to vapour pressure deficit. *Plant Cell Environ.* 22, 1515–1526. doi: 10.1046/j.1365-3040.1999.00513.x

Ortega-Farias, S., Carrasco, M., Olioso, A., Acevedo, C., and Poblete, C. (2007). Latent heat flux over cabernet sauvignon vineyard using the shuttleworth and wallace model. *Irrig. Sci.* 25, 161–170. doi: 10.1007/s00271-006-0047-7

Ortega-Farias, S., Poblete-Echeverría, C., and Brisson, N. (2010). Parameterization of a two-layer model for estimating vineyard evapotranspiration using meteorological measurements. *Agric. For. Meteorol.* 150, 276–286. doi: 10.1016/j.agrformet.2009.11.012

Phillips, N., and Oren, R. (1998). A comparison of daily representations of canopy conductance based on two conditional time-averaging methods and the dependence of daily conductance on environmental factors. *Ann. Sci. For.* 55, 217–235. doi: 10.1051/forest:19980113

Pieri, P. (2010). Modelling radiative balance in a row-crop canopy: row–soil surface net radiation partition. *Ecol. Model.* 221, 791–801. doi: 10.1016/j.ecolmodel.2009.11.019

Prieto, J. A., Lebon, É, and Ojeda, H. (2010). Stomatal behavior of different grapevine cultivars in response to soil water status and air water vapor pressure deficit. *OENO One* 44, 9–20. doi: 10.20870/oeno-one.2010.44.1.1459

Razavi, S., and Gupta, H. V. (2015). What do we mean by sensitivity analysis? The need for comprehensive characterization of "global" sensitivity in Earth and Environmental systems models. *Water Resour. Res.* 51, 3070–3092. doi: 10.1002/2014WR016527

Riou, C., Valancogne, C., and Pieri, P. (1989). Un modèle simple d'interception du rayonnement solaire par la vigne – vérification expérimentale. *Agronomie* 9, 441–450. doi: 10.1051/agro:19890502

Roelfsema, M. R. G., and Hedrich, R. (2005). In the light of stomatal opening: new insights into 'the Watergate': tansley review. *New Phytol.* 167, 665–691. doi: 10.1111/j.1469-8137.2005.01460.x

Rubio, E., Caselles, V., and Badenas, C. (1997). Emissivity measurements of several soils and vegetation types in the 8–14, μm Wave band: analysis of two field methods. *Remote Sens. Environ.* 59, 490–521.

Saltelli, A., Ratto, M., Andres, T., Campolongo, F., Cariboni, J., Gatelli, D., et al. (2008). *Global Sensitivity Analysis: The Primer*. Chichester: John Wiley & Sons, Ltd, doi: 10.1002/9780470725184.ch6

Scholander, P. F., Bradstreet, E. D., Hemmingsen, E. A., and Hammel, H. T. (1965). Sap pressure in vascular plants. *Science* 148, 339–346. doi: 10.1126/science.148.3668.339

Shuttleworth, W. J., and Wallace, J. S. (1985). Evaporation from sparse crops-an energy combination theory. *Q. J. R. Meteorol. Soc.* 111, 839–855. doi: 10.1002/qj.49711146910

Sperry, J. S., Saliendra, N. Z., Pockman, W. T., Cochard, H., Cruiziat, P., Davis, S. D., et al. (1996). New evidence for large negative xylem pressures and their measurement by the pressure chamber method. *Plant Cell Environ.* 19, 427–436. doi: 10.1111/j.1365-3040.1996.tb00334.x

Wang, H., Guan, H., Deng, Z., and Simmons, C. T. (2014). Optimization of canopy conductance models from concurrent measurements of sap flow and stem water potential on Drooping Sheoak in South Australia. *Water Resour. Res.* 50, 6154–6167. doi: 10.1002/2013WR014818

Widén, J., and Munkhammar, J. (2019). *Solar Radiation Theory. Uppsala University*. Available online at: http://urn.kb.se/resolve?urn=urn:nbn:se:uu:diva-381852 (accessed September 27, 2020).

Wright, M. N., Wager, S., and Probst, P. (2021). *ranger: A Fast Implementation of Random Forests*. Available online at: https://CRAN.R-project.org/package=ranger (accessed November 13, 2021).

Zhang, Y., Oren, R., and Kang, S. (2012). Spatiotemporal variation of crown-scale stomatal conductance in an arid *Vitis vinifera* L. cv. Merlot vineyard: direct effects of hydraulic properties and indirect effects of canopy leaf area. *Tree Physiol.* 32, 262–279. doi: 10.1093/treephys/tpr120

Conflict of Interest: The authors declare that the research was conducted in the absence of any commercial or financial relationships that could be construed as a potential conflict of interest.

Supplementary Figure 1. Correlation matrix of pairwise interactions between calculated bulk boundary layer conductance, g_{bs} (mm s^{-1}); latent heat flux, E_c (W m^{-2}); vapor pressure deficit, D_c (Pa); net radiation absorbed by the vine canopy, R_c (W m^{-2}), and bulk boundary layer resistance to heat flux, r_{bh} (s m^{-1}), including data density contours and moving regression (LOESS) line.

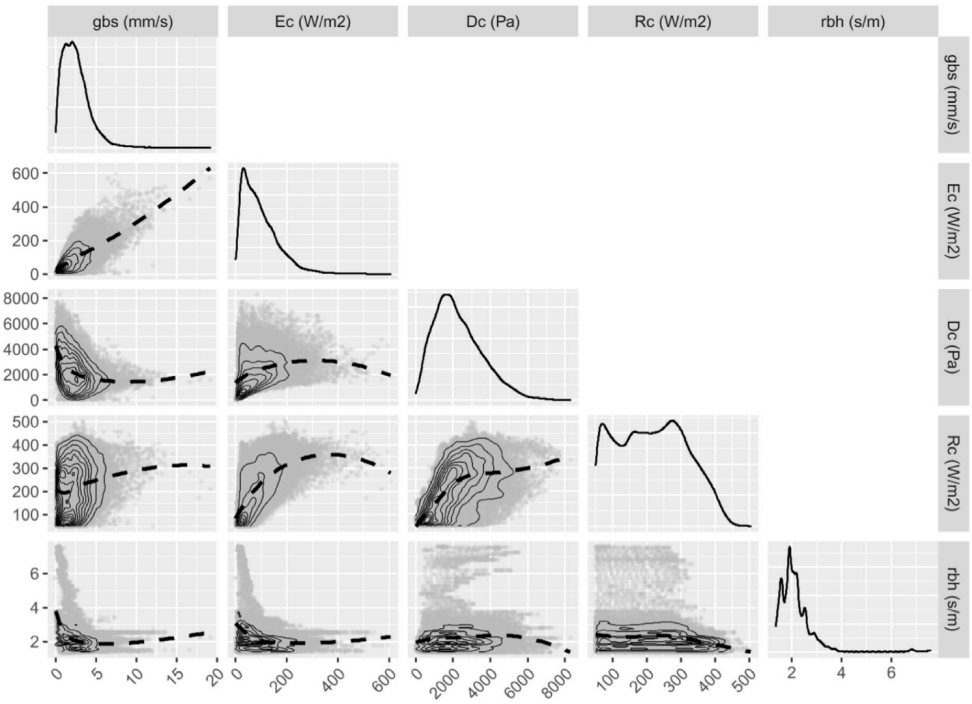

Supplementary Figure 2. Daily maximum hourly running average of 15-minute estimates of the bulk stomatal conductance, g_{bs} (mm s^{-2}) of 10 individual vines from 30 June to 15 September 2020 with shading of line representing corresponding measured predawn leaf water potential varying from zero (light grey) to -1.0 MPa (black).

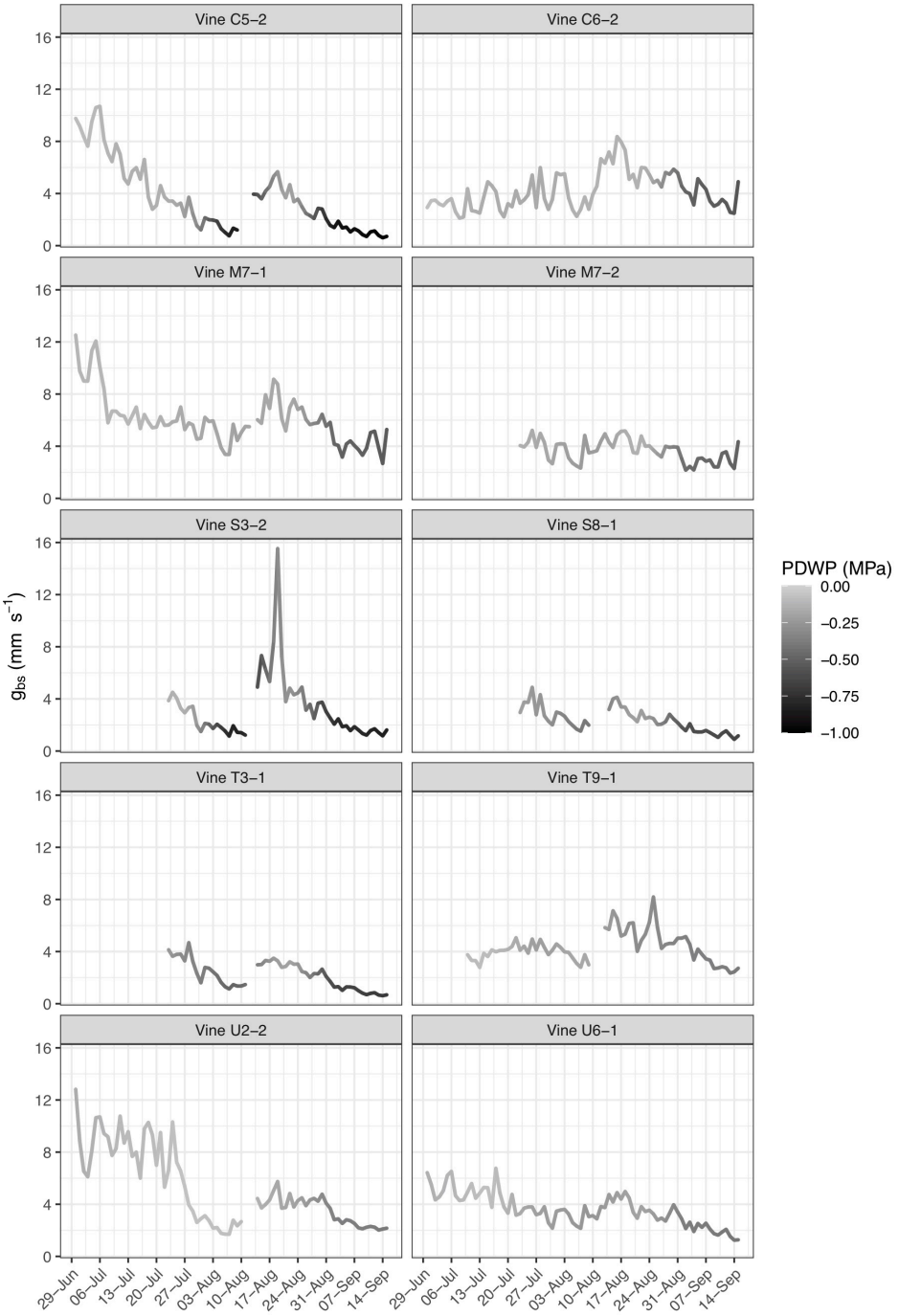

5.3 Discussion

Based on the two-source energy flux approach of Shuttleworth and Wallace (1985) and as described further by Lhomme (2012), a method is presented for a relatively straight-forward determination of g_{bs} for vineyards with open canopies, using measurements of: i) vine transpiration measured by sap flow as needed to calculate transpiration flux from the canopy; ii) measurements of temperature and relative humidity in the vine canopy as needed to calculate vapor pressure deficit; iii) solar radiation measures as needed to estimate the net radiation absorbed by the vine canopy; and iv) vine canopy dimensions, porosity, and leaf area. The method produced results that compared well with other estimates of vine canopy conductance in the literature and demonstrated the expected diurnal and seasonal trends.

This method considers separately the heat and vapor flux from the vine canopy and the ground surrounding the vine canopy in the interrow space, providing a more realistic representation of the actual energy fluxes from an open canopy than the big leaf application of the Penman Monteith (PM) equation, which is more appropriate for closed crop canopies (Monteith and Unsworth, 2013). It also does not involve time consuming and error-prone measurements of heat flux from the ground below the crop, nor the boundary layer conductance above the vineyard, which can also otherwise interfere with the operations of an operational vineyard. A more simplified field method increases the likelihood that more data can be collected across different varieties, climates, and growing conditions.

A global sensitivity analysis was performed using a random forest non-parametric regression analysis (Grömping, 2009; Antoniadis et al., 2021), which found E_c and D_c to be the most important variables in the determination of g_{bs}, therefore warranting attention in their field measurement. Conversely, g_{bs} was found to be the most important predictor of $E_{c,}$ emphasizing the importance of having better representations of conductance response in vineyard water use models.

Also, based on measurements of long wave radiation from both the ground and the sky, and temperature measurements within the canopy, the net long wave radiation absorbed by

the vine canopy was also calculated using a view factor method as described by Pieri (2010). From this, it was observed that estimates of net long wave radiation absorbed by the vine canopy were very low when compared to net absorbed shortwave radiation. Combined with the finding from the sensitivity analysis (i.e., that total net radiation absorbed by the vine canopy is of lesser significance), it is proposed that the measurement of long wave radiation can be eliminated from this methodology without a significant impact on the calculation of bulk stomatal conductance. The benefit of simplifying the method and making it easier to implement may outweigh this loss, although verification of this finding may be warranted in vineyards with different canopy sizes, row spacings, and orientations.

Important in applying this method is the determination of the mean canopy height for the placement of temperature and humidity sensors as needed to calculating D_c, which based on the sensitivity analysis is one of the more important variables in the calculation of g_{bs}. The mean canopy height is the height at which constituents such as temperature and humidity are considered to be well mixed and uniformly distributed within and above the canopy (Shuttleworth and Wallace, 1985). While methods for estimating mean canopy height in vineyards have been published (Chahine et al., 2014), it might be useful in future studies, and not that difficult, to perform temperature and humidity measurement both inside the vine canopy and in the interrow space at difference elevations above the ground to perhaps confirm the estimated mean canopy height.

6 Varietal conductance response to changing environment

6.1 Background

Plant transpiration can be affected by vine water status (Hsiao, 1973), vapor pressure deficits (Oren et al., 1999) and net radiation (Monteith and Unsworth, 2013). Transpiration is moderated as the plant regulates the conductance of water across the soil-plant-atmosphere continuum (McElrone et al., 2013) in response to such factors. This regulation of conductance is achieved by various physiological mechanisms such as control of stomatal aperture and hydraulic conductivity of the vasculature (Lovisolo et al., 2010). Determining a relationship between conductance, and hence transpiration with these factors could be useful for modeling transpiration under current or future climate conditions. And while other factors can affect vine conductance, these factors are of interest due to the potential for them to be affected by climate change.

The purpose of the journal article presented in this chapter, entitled "*Variety-specific response of bulk stomatal conductance of grapevine canopies to changes in net radiation, atmospheric demand, and drought stress.*" (Gowdy et al., 2022b) was to simultaneously measure bulk stomatal conductance (g_{bs}) as the response variable, and vine water status, vapor pressure deficit, and net radiation as the predictor variables to develop relationships between these variables for five different varieties using a readily interpretable multiple linear regression analysis. The regression coefficients for the predictors from this type of analysis will be comparable between themselves for a given variety and across the different varieties. Also, using these regression coefficients, simulations of transpiration can be generated for each variety and compared against the vine transpiration component of an existing vineyard balance model.

Current water balance models use an approach based on estimates of reference crop evapotranspiration to which a stress coefficient is applied to account for drought stress related decreases in transpiration (Allen et al., 1998; Lebon et al., 2003; Pieri and Bois, 2007). Such modeling approaches, however, are not parameterized to distinguish differences in conductance/transpiration regulation between different varieties. If this study discernable and significant differences in the conductance, and hence transpiration were

observed in response to changes in soil water deficits and atmospheric demand for the different varieties.

Prior studies have evaluated the canopy conductance of individual grapevine varieties at the vineyard scale (Lu et al., 2003; Rogiers et al., 2009; Zhang et al., 2012; Bai et al., 2015), however, this study provides a direct comparison between five varieties in the same growing conditions and using the same, relatively simple and robust methodology, producing readily interpretable coefficients from a multiple linear regression analysis. This could be useful for future development of variety specific vineyard water balance models, which could then be useful for evaluating adaptation strategies under future climate change scenarios.

6.1.1 Multiple linear regression analysis

The selection of an appropriate regression analysis was an important consideration in developing the relationships between vine canopy conductance as the independent variable, and the various predictor variables that were considered. A multiple linear regression analysis was chosen in order to obtain a readily interpretable model. While non-linear, or non-parametric regression analysis might provide a better fit with lower model residuals than multiple linear regression, the coefficients from such models become less readily interpretable (Shmueli, 2010). The predictor variable coefficients from multiple linear regression are readily interpretable as the mean change in the response variable for one standard deviation change in the associated predictor when based on standardized data, with their absolute values being directly comparable (Frost, 2020) for a given variety or across the different varieties.

The input data needed for this type of study naturally contains non-linearity and collinearity, so careful data filtering, transformation, and selection of variables was needed to create readily interpretable multiple linear regression model that satisfied ordinary least squares assumptions. For example, the equation for calculating g_{bs} was observed to give unrealistically high and erratic results when input values of radiation, vapor pressure deficit, and transpiration were low, particularly in the early morning and evening. Previous studies of vine conductance in vineyards made similar observations and took an approach of filtering low net radiation data to address such issues (Lu *et al.*, 2003; Zhang *et al.*,

2012). Also, biological and environmental data often demonstrate non-linear relationships and collinearity between variables (Dormann et al., 2013), so consideration of variable transformation were also required. In addition, interactions between the predictor variables can significantly inflate the variance of the residuals (Frost, 2020), and consideration may need to be given not using certain variables that create problems. All of these considerations will involve a trial-and-error process involving inspection of the various residual plots after each iteration.

6.1.2 Vineyard water balance modeling

Simulations of vine transpiration using the coefficients generated by the regressions were compared against those from an existing vineyard water balance model. In concept, crop water balance models add all the inputs of water to the crop root zone (e.g. precipitation, irrigation) and subtract all the extractions (e.g. transpiration, soil evaporation), with the difference either adding or subtracting to the root zone water balance (i.e., *FTSW*) within upper and lower limits. These models provide a daily estimate of soil water content and are useful alternatives to direct measures that may be too intensive or impractical due to site conditions (Pellegrino et al., 2006; van Leeuwen et al., 2010).

The calculations of the Pieri and Bois (2007) vineyard water balance model used for this study, which are based in large part on those outlined in Lebon et al. (2003), are broken into three components consisting of: i) a soil water reservoir with a volume equal to the total transpirable soil water (*TTSW*) from which inputs and extractions to the vine root zone are tabulated; ii) a geometric representation of the vine canopy used to partition incident solar radiation between separate calculations of vine transpiration and soil evaporation; and iii) a daily representation of atmospheric conditions based on local meteorological data for the purpose of calculating reference evapotranspiration and rainfall. The model outputs daily estimates of vine transpiration, soil evaporation, and fraction of total available transpirable soil water (*FTSW*, mm^3/mm^3) in the root zone.

The evapotranspiration component of both these models is divided into two parts: i) soil evaporation; and ii) vine canopy transpiration. The vine canopy transpiration component is calculated in two steps. First the potential vine transpiration (TV_p), or the vine transpiration assumed under well-watered, non-stressed conditions, is calculated as the portion of

reference evapotranspiration for the entire vineyard, calculated using the Penman formula (Penman, 1948), that is equal to the proportion of total solar radiation incident on the vineyard absorbed by the vine canopy, determined by the method of Riou et al. (1989). As the soil water content in the modeled soil water reservoir decreases to a threshold value, these models begin factoring in reductions to TV_p to account for the reduction in transpiration/conductance associated with drought stress.

Lebon et al. (2003) uses an empirically based reduction function that assumes no effect on vine transpiration until the fraction of transpirable soil water (*FTSW*) reached 0.4 with a linear reduction in transpiration as *FTSW* continues below that to zero. The method of Pieri and Bois (2007), however, uses a non-linear reduction function mechanistically based on the relationship between soil matric potential and *FTSW* as presented in Pieri and Gaudillère (2005). Neither of these approaches, however, account for the potential differences that may exist between varieties in how they regulate conductance, and hence transpiration, in response to changes in vine water status, atmospheric demand, and net radiation levels.

6.2 Journal article

Variety-specific response of bulk stomatal conductance of grapevine canopies to changes in net radiation, atmospheric demand, and drought stress.

Mark Gowdy[1*], Bruno Suter[1], Philippe Pieri[1], Elisa Marguerit[1], Agnès Destrac Irvine[1], Gregory A. Gambetta[1], Cornelis van Leeuwen[1*]

[1]EGFV, Bordeaux Sciences Agro, INRAE, Univ. Bordeaux, ISVV, F-33882 Villenave d'Ornon, France

Published in *Oeno One*, June 2022, Volume 56-2, Article 5435

OENO One
VINE AND WINE OPEN ACCESS JOURNAL
By IVES International Viticulture & Enology Society
2nd ClimWine Symposium terclim July 3 – 8, 2022 | Bordeaux, France XIVth International Terroir Congress

DOI:10.20870/oeno-one.2022.56.2.5435
OPEN ACCESS

ORIGINAL RESEARCH ARTICLE

Variety-specific response of bulk stomatal conductance of grapevine canopies to changes in net radiation, atmospheric demand, and drought stress

Mark Gowdy[1], Bruno Suter[1], Philippe Pieri[1], Elisa Marguerit[1], Agnès Destrac Irvine[1], Gregory A. Gambetta[1] and Cornelis van Leeuwen[1*]

[1] EGFV, Univ. Bordeaux, Bordeaux Sciences Agro, INRAE, ISVV, F-33882 Villenave d'Ornon, France

This article is published in cooperation with Terclim 2022 (XIVth International Terroir Congress and 2nd ClimWine Symposium), 3-8 July 2022, Bordeaux, France.

*correspondence:
vanleeuwen@agro-bordeaux.fr

Associate editor:
Hans Schultz

Received:
28 February 2022

Accepted:
14 April 2022

Published:
21 June 2022

ABSTRACT

In wine growing regions around the world, climate change has the potential to affect vine transpiration and overall vineyard water use due to related changes in daily atmospheric conditions and soil water deficits. Grapevines control their transpiration in response to such changes by regulating conductance of water through the soil-plant-atmosphere continuum. The response of bulk stomatal conductance, the vine canopy equivalent of stomatal conductance, to such changes were studied on Cabernet-Sauvignon, Merlot, Tempranillo, Ugni blanc, and Semillon vines in a non-irrigated vineyard in Bordeaux France. Whole-vine sap flow, temperature and humidity in the vine canopy, and net radiation absorbed by the vine canopy were measured on 15-minute intervals from early July through mid-September 2020, together with periodic measurements of leaf area, canopy porosity, and predawn leaf water potential. From these data, bulk stomatal conductance was calculated on 15-minute intervals, and multiple linear regression analysis was performed to identify key variables and their relative effect on conductance. For the regression analysis, attention was focused on addressing non-linearity and collinearity in the explanatory variables and developing a model that was readily interpretable.

Variability of vapour pressure deficit in the vine canopy over the day and predawn water potential over the season explained much of the variability in bulk stomatal conductance overall, with relative differences between varieties appearing to be driven in large part by differences in conductance response to predawn water potential between the varieties. Transpiration simulations based on the regression equations found similar differences between varieties in terms of daily and seasonal transpiration. These simulations also compared well with those from an accepted vineyard water balance model, although there appeared to be differences between the two approaches in the rate at which conductance, and hence transpiration is reduced as a function of decreasing soil water content (i.e., increasing water deficit stress). By better characterizing the response of bulk stomatal conductance, the dynamics of vine transpiration can be better parameterized in vineyard water use modeling of current and future climate scenarios.

KEYWORDS: grapevine, climate change, drought stress, vineyard water use models, *Vitis vinifera*, cultivar

INTRODUCTION

Grapevines regulate their water use in response to changing atmospheric demand and drought stress by regulating the conductance of water through the soil-plant-atmosphere continuum (McElrone *et al.*, 2013). This conductance is regulated by various physiological mechanisms such as control of stomatal aperture and hydraulic conductivity of the vasculature (Lovisolo *et al.*, 2010). The resistance to water vapour diffusion through open stomata is much greater than the resistance of water through the vasculature, with that through the stomata becoming the controlling factor in overall transpiration (Sack and Holbrook, 2006; Krounbi and Lazarovitch, 2011). Stomatal regulation of conductance varies diurnally (Bai *et al.*, 2015; Lu *et al.*, 2003; Zhang *et al.*, 2012), across the season (Herrera *et al.*, 2021), and with differences in response to changing environmental variables observed between varieties (Costa *et al.*, 2012; Prieto *et al.*, 2010).

Plant species that readily close their stomata to reduce transpiration and maintain constant leaf water potential when faced with increasing vapour pressure deficit, and/or decreasing soil water status are classified as *isohydric*, while those that keep their stomata open and allow for more negative leaf water potential are classified as *anisohydric* (Tardieu and Simonneau, 1998). This stomatal regulation, however, does not always fit neatly into these categories (Martínez-Vilalta *et al.*, 2014), with some species demonstrating responses that vary with water stress (Levin *et al.*, 2020), or a hybrid response such as *isohydrodynamic*, whereby stomata are regulated to maintain a roughly constant difference between leaf and soil water potential (Franks *et al.*, 2007; Domec and Johnson, 2012; Zhang *et al.*, 2012; Charrier *et al.,* 2018). Within the species *Vitis vinifera*, different varieties demonstrate a range of response dynamics, which are difficult to categorize, or they display inconsistent dynamics across numerous different studies (Chaves *et al.*, 2010; Lavoie-Lamoureux *et al.*, 2017). For example, Syrah has often been found in studies to demonstrate anisohydric response (Prieto *et al.*, 2010; Schultz, 2003), but in others has demonstrated near-isohydric response for this variety (Pou *et al.*, 2012), although such differences could be attributable to soil and climate differences (Hochberg *et al*., 2018).

The ability of the soil to deliver water through its pore spaces to the roots is also a key component in the soil-plant-atmosphere continuum. Depending on the texture of the soil, water potential decreases as the soil water content decreases, particularly once the fraction of transpirable soil water drops below about 0.4 (Schultz, 1996; Lebon *et al.*, 2003) as experienced during drought conditions. This leads to a corresponding reduction in the hydraulic conductivity within the soil matrix supplying water to the roots (Krounbi and Lazarovitch, 2011; Tramontini *et al.*, 2012) and therefore the overall conductance across the soil-plant-atmosphere continuum, and hence stomatal conductance.

Crop evapotranspiration (ET_c) is often modeled using the FAO 56 approach of applying seasonally variable crop coefficients (K_c) to estimates of reference crop evapotranspiration (ET_o), which are calculated using the Penman Monteith (PM) equation based on an assumption of well-watered conditions and an associated fixed crop canopy conductance (Allen *et al.*, 1998). To account for drought stress this approach then applies a stress coefficient (K_s) to ET_c to calculate adjusted crop evapotranspiration ($ET_{c\ adj}$). K_s is assumed to be 1.0 (i.e., no water stress) until the modeled balance of available soil water decreases below a threshold value, below which the Ks decreases linearly to zero where the soil water content reaches the wilting point. A vineyard water balance model adapted from this FAO approach was developed by Lebon *et al.* (2003), although it is not parameterized to distinguish differences in transpiration between varieties.

Being able to characterize variety-specific changes in conductance in response to changing atmospheric conditions and drought would help improve modeling of the vine canopy transpiration component in vineyard water balance models, particularly for evaluating different adaptation strategies under future climate change scenarios. Therefore, the main goal of this study is to quantify and differentiate the response of bulk stomatal conductance (g_{bs}) of different grapevine varieties to changes in key environmental variables potentially affected by climate change, and to simulate transpiration using these relationships for comparison against an existing vineyard water balance model. As described by Gowdy *et al.* (2022), g_{bs} can be calculated in vineyards with open canopies based on an inverted Penman-Monteith type transpiration equation and the assumptions of the two-source energy flux approach developed by Shuttleworth and Wallace (1985). The total conductance of the vine canopy (g_{bs}) is effectively the stomatal conductance of every leaf in the canopy acting together in a parallel circuit, which conceptually is the sum of the stomatal conductance of all those leaves (Kelliher *et al.*, 1995).

The diffusion of water vapour through stomata is affected by: i) solar radiation, which provides energy for evaporation and diffusion; ii) vapour pressure deficit, which is the driving force for diffusion; and iii) the effects of boundary layer resistance to diffusion at the leaf surface (Keller, 2015). The stomatal openings themselves can also be affect by changes in light levels (Shimazaki *et al.*, 2007) and vapour pressure deficit (Oren *et al.*, 1999). By analogy at the vine canopy scale, the amount of net radiation absorbed by the vine canopy (R_c) provides the energy for canopy transpiration (Monteith and Unsworth, 2013) and can be affected by changes in cloud cover associated with climate change (Mendoza *et al.*, 2021) and global dimming/brightening associated with human-induced pollution and its interaction with the climate (Wild, 2009). Canopy dimensions are also an important factor in determining R_c (Riou *et al.*, 1989; Pieri, 2010) and can be modified by growers as an adaptation to climate change (van Leeuwen *et al.*, 2019a). Similarly, vapour pressure deficit in the canopy (D_c) may be affected by climate change related impacts on air and canopy temperatures, and the tendency towards lower relative humidity in near-surface air over land as observed in

the last 20 years in the mid-latitudes and Mediterranean (Willett *et al.*, 2014). Another variable for consideration is the leaf area index (*LAI*), which in turn affects bulk boundary layer resistance (Shuttleworth and Wallace, 1985; Lhomme *et al.*, 2012). *LAI* can be affected by vine vigour, which can depend on the variety, the rootstock and the available resources, such as water and nutrients (Smart and Robinson, 1991). Then, later in the season it can be affected by leaf drop. Grapevines are known to drop leaves in response to increasingly intense drought conditions as a way of controlling their transpiration (Zufferey *et al.*, 2011).

Additionally, vine water deficit stress can have an important effect on vine transpiration and conductance. Physiological vine responses, such as changes in photosynthesis, stomatal closure, and shoot growth characteristics in response to water deficit stress, are often correlated well with water potential (Lebon *et al.*, 2003; Pellegrino *et al.*, 2006). Measurement of predawn leaf water potential (Ψ_{PD}) is an accepted plant-based measurement of plant water status (Sperry *et al.*, 1996), which gives the water potential of the plant at the end of the night when the stomata are closed and the plant is in equilibrium with the root zone water potential (Choné *et al.*, 2001). Climate change has the potential to affect vine water stress if there are changes in precipitation and/or vineyard evapotranspiration. As an adaptation, the planting density of new vineyards can be decreased, or irrigation can be used (van Leeuwen *et al.*, 2019a; van Leeuwen *et al.*, 2019b).

In this paper, a multiple linear regression approach was used in an iterative fashion to develop an explanatory statistical model of calculated g_{bs} as the response variable against: i) net radiation absorbed by the vine canopy; ii) vapour pressure deficit in the vine canopy; and iii) predawn leaf water potential as the three predictor variables. The emphasis is on developing a model that is readily interpretable for the purpose of characterizing the dynamics of this response.

MATERIALS AND EQUIPMENT

The measurements for this study were taken on 10 individual grapevines in a vineyard, two each of *Vitis vinifera* L., cv. Cabernet-Sauvignon, Merlot, Tempranillo, Semillon, and Ugni blanc. Measurements of sap flow, temperature and humidity, and solar radiation were taken or interpolated to 15-minute intervals from 30 June through 15 September 2020 and canopy characteristics were measured periodically through the season.

1. Vineyard and canopy characteristics

The study was performed in a 0.6-hectare common garden experimental vineyard in Bordeaux, France (44° 47' 0" N, 0° 34' 39" W) with 52 varieties planted in a randomized block design, in which the varieties were planted in 5 replicate blocks of 10 vines each. All measured vines were located in different blocks of the vineyard, with the exception of the two Merlot vines, which were in two different rows within the same block. The vines are trained on a vertical shoot positioning trellis system with double Guyot pruning. The top and bottom of the vine canopy are 1.5 m and 0.5 m above the ground respectively and 0.4 m wide, with canopy dimensions maintained by hedging twice during the growing season. Vine rows are orientated north-south with 1.8 m row spacing and 1.0 m vine spacing. There is a mowed cover crop in between each vine row with mechanical tillage under the vine row. The vines were planted on SO4 rootstock and the soils are sandy-clay-gravel typical for the Pessac-Léognan wine appellation (Destrac-Irvine and van Leeuwen, 2017). From 1991 through 2020 average annual total rainfall and reference evapotranspiration were 902 mm and 929 mm respectively with annual solar radiation of 4790 MJ m^{-2} and average maximum daily temperature from May through September of 25.5 C°.

Leaf area was measured three times during the season in the first halves of July, August and September respectively. Leaf area was determined on each vine by first measuring the length and width of all individual leaves on one primary shoot and all its secondary shoots, which averaged just over 100 leaves on each vine on each measurement date. Those dimensions were well correlated with individual leaf area as measured by a leaf area meter (Model LI-3100 LICOR Inc., Lincoln, NE, USA) before field measurements began. An average size of leaves on primary and secondary shoots were then calculated and applied to a count of all the leaves on the remaining primary and secondary shoots on each vine. Leaf area index (*LAI*, m^2 m^{-2}) is calculated as the total leaf area (m^2) for a vine divided by the area of vineyard ground attributable to each vine (i.e., row spacing x vine spacing). The porosity of each vine canopy was measured in the vineyard using a camera phone application (CANAPEO, Oklahoma State University Department of Plant and Soil Sciences, Stillwater, OK, USA) on the same dates as leaf area measurement with any missing measurements being filled in using a regression between measured leaf area and porosity.

2. Field measurements

Transpiration flux (E_c) was measured by heat balance sap flow sensors (Model SGEX, Dynamax Inc., Houston, TX, USA) that were installed on vine canes at a location where the flow of at least 30 % of the whole vine would be measured (based on the relative number of shoots downstream of the sensor). Sap flow (g s^{-1}) was calculated from sensor signals collected by a datalogger (Model SapIP, Dynamax Inc., Houston, TX, USA) and then scaled up for the whole vine based on the ratio of leaf area of the whole vine over the leaf area of shoots downstream the sap flow sensor. Sap flow (g s^{-1}) was then divided by the area of vineyard ground attributable to each vine (i.e., row spacing x vine spacing) to give canopy transpiration flux, E_c (g s^{-1} m^{-2}).

Vapour pressure deficit (D_c) was measured in the vine canopy at 1.15 m above the ground. This height was estimated to be that above which heat and vapour flux from both the vine canopy and ground surrounding the vine rows is well mixed (Shuttleworth and Wallace, 1985; Gowdy *et al.*, 2022). The mean canopy height was estimated using empirical relationships for vineyards based primarily on canopy height

(Chahine *et al.*, 2014). The saturation vapour pressure, e_{sc} (Pa) was calculated by Teten's equation using measured temperature T_c (C°) with the partial vapour pressure, e_c (Pa) calculated from e_{sc} using measured relative humidity. Temperature and humidity were measured using TinyTag Plus 2 probe/data loggers (Model TGP-4505 by Gemini Data Loggers, Chichester, West Sussex, England) with the temperature/relative humidity probes installed inside solar radiation shields (Model RS3 by Prosensor, Amanvillers, France) and hung from a trellis wire in the vine canopy at the mean canopy height.

Global (shortwave) radiation flux was measured at a weather station next to the vineyard using a horizontally mounted pyranometer (Model No. CMP6 by Kipp & Zonen, Delft - The Netherlands) on one-hour intervals, and then linearly interpolated to 15-minute intervals.

Measurements of Ψ_{PD} were taken on each vine in the study at six times during the season, roughly 10-14 days apart depending on weather, from early July through early September 2020. Sampling and measurement were done early enough to ensure all measurements were completed no later than 30 minutes prior to sunrise. Measurements were taken on one leaf per vine by the method of Scholander *et al.* (1965) using a pressure chamber with digital manometer (DG MECA, 33175 Gradignan, France).

METHODS

A multiple linear regression analysis was performed in an iterative fashion by: i) applying data filters and calculating bulk stomatal conductance; ii) making necessary data transformations; iii) selecting predictor variables to include in the final regression model; and iv) verifying that ordinary least squared assumptions are properly met in the final regression model. The intent of the above is to obtain a readily interpretable model with the best possible fit. While non-linear, or non-parametric regression analysis might provide a better fit with lower residuals, the coefficients from such models become less readily interpretable (Shmueli, 2010).

1. Data compilation and filtering

A database of R_c and D_c was compiled from measurements and estimates on 15-minute intervals from 30 June through 15 September 2020. Missing data were replaced by linear interpolation if there were no more than four missing 15-minute measurements between available data points, otherwise gaps in the data were maintained. Measurements of Ψ_{PD} and *LAI* were also included, but as they were obtained only periodically during the season, those data were interpolated to a daily time step using a local weighted regression (LOESS) curve between measurements. Over the study period there was only one significant rain event of 36 mm on 11 through 13 August 2020, with Ψ_{PD} taken just 4 days before and 7 days afterwards. During the remainder of the study period, no other daily rainfall total exceeded more than a few millimeters, which is well below an amount that would affect predawn water potential.

The equation for calculating g_{bs} (as described in the next section) was observed to give unrealistically high and erratic results when input values of R_c, D_c, or E_c were low, particularly in the early morning and evening. These low values also introduced irregularities in the residual plots for regressions that included them. The data, therefore, were filtered on a trial-and-error basis to eliminate these problems. Previous studies of conductance in vineyards took a similar approach of filtering low net radiation data to address such issues (Lu *et al.*, 2003; Zhang *et al.*, 2012).

The selected filters were applied separately to the data from individual vines when R_c < 90 W m^{-2} or D_c < 900 Pa or if E_c was less than the 30th percentile of all values for a given vine. The latter filter was applied on a percentile basis due to the differing ranges of E_c observed across the different vines measured. Otherwise, fixed filter thresholds might disproportionally remove more data from vines with generally lower E_c than other vines. The E_c data in general was strongly skewed towards lower values, so application of the filters removed data records at times when E_c was very low, resulting in only a 9 to 14 percent reduction, depending on the vine, in measured transpiration over the season. This reduction ranged slightly higher from 9 to 18 percent for transpiration during times when drought stress, as measured by predawn water potential was less than - 4.0 bars. The loss of these values was not considered significant for the purpose of regression analysis aimed at defining relationships at higher transpiration rates when the majority of vine water use actually takes place.

After the data from each vine was filtered, they were all combined into one database for regression analysis. Summary statistics for the combined database are presented in Supplementary Table S1. It is noted that due to sporadic instrument outages and differing start times, the number of 15-minute data points collected on the vines of each variety were different. Also, units for R_c and D_c in the final regressions were converted to kW/m^2 and kPa respectively to avoid problematically small coefficients that resulted when using the units specified for Equations 1 and 2.

Data compilation, filtering, and graphing were performed in the *R* software environment (R Core Team, 2021) using several functions from the *dplyr* package (Wickham *et al.*, 2021b) and the *ggplot2* package (Wickham *et al.*, 2021a).

2. Bulk stomatal conductance

As presented by Gowdy *et al.* (2022) bulk stomatal conductance (g_{bs}) is determined from the 2-layer energy flux model for sparse crop canopies, like those of vineyards, as developed by Shuttleworth and Wallace (1985) using a Penman-Monteith (PM) type equation for calculation of latent heat flux from the vine canopy as given by Equation 1 (Lhomme *et al.*, 2012).

▸ Equation 1: $\lambda E_c = \frac{\Delta R_c + \rho C p (D_c)/r_{bh}}{\Delta + \gamma\left(n + \frac{r_{bs}}{r_{bh}}\right)}$ (W m^{-2})

This equation is first rearranged to give the bulk stomatal resistance (r_{bs}) as given in Equation 2 and followed by g_{bs} from Equation 3.

▸ Equation 2:

$$r_{bs} = \frac{\Delta R_c * r_{bh} + \rho C p D_c}{\lambda E_c \gamma} - r_{bh}\left(\frac{\Delta}{\gamma} - n\right) \qquad (\text{s m}^{-1})$$

and bulk stomatal conductance is given by inversion:

▸ Equation 3: $g_{bs} = r_{bs}^{-1}$ (m s^{-1})

where:

E_c = transpiration flux from canopy per unit ground area (g m^{-2} s^{-1})

λ = latent heat of vaporization for water = 2257 (J g^{-1})

D_c = vapour pressure deficit at mean canopy height (Pa)

R_c = net radiation absorbed by the vine canopy per unit ground area (W m^{-2})

r_{bs} = bulk stomatal resistance (s m^{-1})

r_{bh} = bulk boundary layer resistance to heat flux (s m^{-1})

n = 2 for grapevine leaves with stomata on one side only

γ = psychrometric constant at 1 atm and 20°C = 65.8 (Pa C°$^{-1}$)

Δ = rate of change in saturation vapour pressure versus temperature = 145 (Pa C°$^{-1}$)

ρCp = heat content per unit volume of air at 20°C = 1212 (Pa C°$^{-1}$)

The output units for Equation 2 (s m^{-1}) and Equation 3 (m s^{-1}) result when the above input units are used, with all conductance/resistance and fluxes expressed in terms of unit area of vineyard ground attributable to each vine (i.e., row spacing x vine spacing).

The method of Riou *et al.* (1989) was used for estimating the amount of such radiation absorbed by grapevine canopy (R_c) as needed for input to Equations 1 or 2. Relying on inputs of canopy dimensions, row spacing, vine spacing, and canopy porosity, along with measured solar radiation and various solar angles, this model outputs radiation flux (W m^{-2}) of shortwave radiation absorbed by the vine canopy expressed in terms of the unit area of vineyard ground attributable to each vine (i.e., row spacing x vine spacing) (Riou *et al.,* 1989).

The canopy bulk boundary layer resistance to heat flux (r_{bh}) needed as input to Equations 1 and 2 is given by Equation 4 below and represents the canopy-level summation of the leaf-level boundary layer resistances across all leaves in the canopy stated in terms of unit ground area (Lhomme *et al.,* 2012):

▸ Equation 4: $r_{bh} = \frac{r_{bl}}{2 * LAI}$ (s m^{-1})

where:

r_{bl} = leaf-level boundary layer resistance (s m^{-1}) = 25 s m^{-1} per Shuttleworth and Wallace (1985).

LAI = leaf area index.

Using input data from the compiled and filtered database, g_{bs} was calculated using Equations 2 and 3 and r_{bh} was calculated using Equation 4, with the results of both appended back to the database.

3. Response variable transformation

Biological and environmental data often demonstrate non-linear relationships and collinearity between variables (Dormann *et al.*, 2013), which must be addressed in order to meet the required assumptions of ordinary least squared regression analysis.

Figure 1 presents bulk stomatal conductance (g_{bs}) plotted versus 15-minute canopy vapour pressure deficit (D_c), net radiation absorbed by the canopy (R_c), and interpolated predawn leaf water potential (Ψ_{PD}) for each variety separately. In previous studies of *Vitis vinifera* varieties, non-linear relationships between g_{bs} and D_c have been observed (Prieto *et al.*, 2010; Lu *et al.*, 2003). A similar non-linear relationship also existed between the g_{bs} and Ψ_{PD} data, while the relationship between g_{bs} and R_c did not demonstrate any non-linear characteristics.

To address the non-linearity in the relationship between g_{bs} and both D_c and Ψ_{PD}, a $\log_{10}$ transformation of g_{bs} was used as the response variable in subsequent regression analyses. For the data from all 10 vines combined, Figure 2 presents the $\log_{10}$ transformation of g_{bs} plotted against 15-minute D_c, R_c, and interpolated Ψ_{PD} data demonstrating roughly linear relationships for each relationship. The effect of the data filters can also be seen in the plot panels for R_c and D_c in both Figures 1 and 2.

4. Predictor variable selection

The process of selecting variables to consider for inclusion in the regression analysis began with Ψ_{PD} and the key input variables to Equations 2 and 3 for calculation of g_{bs}, including R_c, D_c, and r_{bh}.

Vine water status, as measured by Ψ_{PD}, is well understood to have an effect on conductance, and was found to have a statistically significant and strong effect on g_{bs} in the final regression analysis. But unlike the 15-minute interval measurements of R_c and D_c, the periodic measurements of Ψ_{PD} will miss some of the range and response of the varying water status experienced by the vines. This is unavoidable due to the nature of measuring leaf water potential. The final regression analysis also shows R_c and D_c as having statistically significant and strong effects on g_{bs} and were retained in the final model.

Regression model iterations including r_{bh} as a predictor generated statistically significant ($p < 0.05$) coefficients for that variable, but they explained only a small portion of variation in g_{bs}. This also concurs with findings from Gowdy *et al.* (2022) and from Shuttleworth and Wallace (1985) that found r_{bh} to be of much less importance than the other input variables in the determination of g_{bs}. Furthermore, there was strong collinearity between r_{bh} and Ψ_{PD}, which contributed to very high variance inflation factors for the two variables and their interactions.

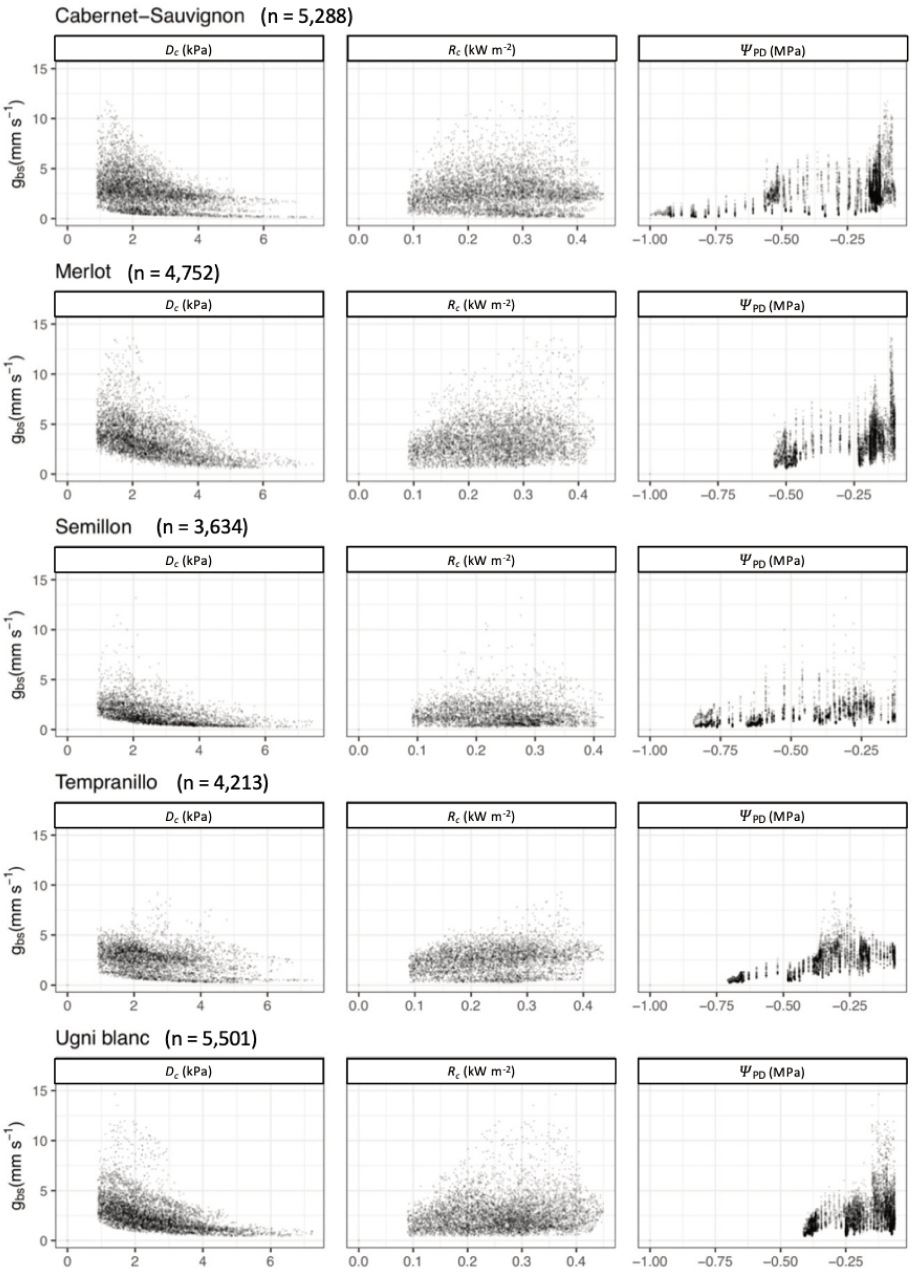

FIGURE 1. Bulk stomatal conductance (g_{bs}) plotted versus canopy vapour pressure deficit (D_c), net radiation absorbed by the canopy (R_c), and interpolated predawn leaf water potential (Ψ_{PD}) by variety.

This collinearity is associated with the leaf loss that coincides with the gradual increase in water stress over the season and the resulting more negative Ψ_{PD}.

As a result, r_{bh} was excluded from the final regression analysis. E_c is also an input to Equation 2, but was not considered in the regressions as regulation of g_{bs} is how plants control E_c, making the two strongly collinear and of minimal explanatory value.

In addition to the main effects of the predictor variables described above, interaction terms between these variables were also considered in a regression analysis based on standardized data (Supplementary Table S2). While nearly all interaction terms from this regression had coefficients that

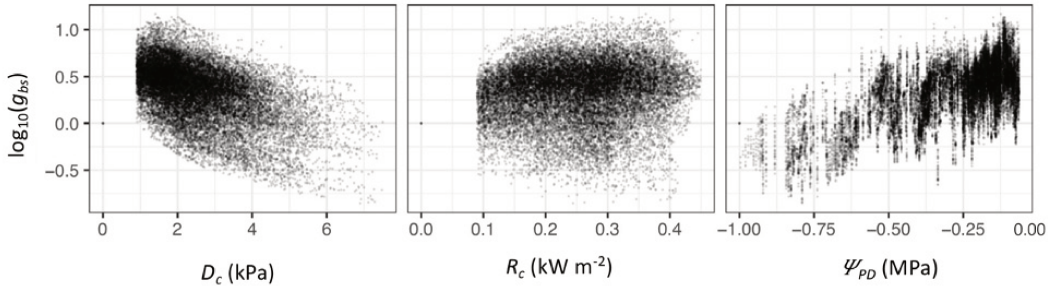

FIGURE 2. Log_{10} transformation of g_{bs} plotted versus canopy vapour pressure deficit (D_c), net radiation absorbed by the canopy (R_c), and interpolated predawn leaf water potential (Ψ_{PD}) with data from all 10 vines together (n = 23388).

were significant ($p < 0.05$), their importance was not great compared to those for the main effects and furthermore, added considerable complexity to the model and its interpretability. The regression analysis was run again on the standardized data with the interaction terms excluded, which resulted in a model fit that was only slightly diminished and much simpler to interpret (Supplementary Table S3). For reference, the same regression without interactions was run again with raw data (Supplementary Table S4). The predictor variables retained in the final multiple linear regression model, therefore, were R_c, D_c and Ψ_{PD}, with no interaction terms included.

5. Multiple linear regression and ad hoc analysis

The formula used for the regression analysis of $log_{10}(g_{bs})$ as the response variable with R_c, D_c, and Ψ_{PD} as continuous predictor variables and *variety* as a grouping factor variable is given by Equation 5:

▸ Equation 5: $log_{10}(g_{bs}) \sim (R_c + D_c + \Psi_{PD}) * variety$

Expressed in equation form, the multiple linear regression model resulting for each variety using the predictors selected above is given by Equation 6:

▸ Equation 6: $g_{bs} = \beta_0 + \beta_{Rc} * R_c + \beta_{Dc} * D_c + \beta_{\psi} * \Psi_{PD}$

where:

β_0 = y-axis intercept

$\beta_{Rc} = R_c$ regression coefficient

$\beta_{Dc} = D_c$ regression coefficient

$\beta_{\psi} = \Psi_{PD}$ regression coefficient.

The effect of each predictor is characterized by the associated coefficient (β), which when based on raw data represents the average change in the response variable for a given unit change in each of the predictor variables. The regression analysis was also performed using standardized response and predictor variable data, whereby each data point is both subtracted by the mean and divided by the standard deviation of all values for a given variable. In this way the data is both centered on zero and has the same scale in terms of standard deviations from the mean. When based on standardized data, the resulting coefficients for the predictors represent the mean change in the response variable for one standard deviation change in the associated predictor. This is useful because with all data on the same scale, the absolute value of the regression coefficients for the different predictors can be compared directly to understand their relative effect on the response variable (Frost, 2020).

Due to sporadic instrument outages and differing start times, the number of 15-minute data points collected on the vines of each variety were different. Also, even though it was minimized by the filtering and transformations, there was still a low level of collinearity between input variables as observed in the variance inflation factors (described further below). Such factors may complicate an ad hoc comparison of regression coefficients that might be obtained from regressions performed using the data from each variety separately.

As an alternative, the filtered and transformed data from all vines was pooled together and a factor variable representing the different varieties was added, which is then included as part of an interaction term with each of the predictors. From this regression, the coefficients for each predictor are calculated as *marginal mean slopes*, whereby the average effect of each predictor on the response variable is calculated separately for each variety, at the same time assuming the mean values of all the other predictor variables (Searle *et al.*, 1980; Lenth *et al.*, 2022). This approach is useful in that the p-value for each interaction term indicates the significance of the difference between the coefficients (Lenth *et al.*, 2022). The regression coefficients of the selected predictor variables were all significant ($p < 0.05$) and explained meaningful amounts of the variation in $log_{10}(g_{bs})$. For comparison purposes, separate variety specific regressions were performed (not presented) which gave identical regression coefficients and nearly identical intercept terms, suggesting that, in fact, the effect of the unbalanced data between varieties and the interactions were not that great.

After each iteration, variance inflation factors (VIFs) were evaluated for each predictor variable and its interactions, if included. VIFs identify the presence and strength of interactions between model terms. The goal is for the VIFs for each predictor variable and any interaction

term to be below a generally accepted value of 5.0, with 1.0 representing complete independence (Frost, 2020). The VIFs for predictors R_c, D_c, and Ψ_{PD} in the final regression model based on combined data, whether standardized, or raw were 1.2, 1.2, and 1.1 respectively, which are well below a standard threshold of 5.0. The low VIFs suggest the effects of interactions were either successfully avoided by variable selection, or removed by filtering and transformation. The coefficient of determination (r^2), or the fraction of $log_{10}(g_{bs})$ variance explained by the final model, whether based on raw or standardized data, was 0.701. Both the adjusted r^2 and predicted r^2 were also 0.701 in both cases, suggesting the model is not overfitted.

For multiple linear regression it is also important to check whether the underlying ordinary least square assumptions are satisfied. In Supplementary Figures S1 a) and b) the standardized model residuals are normally distributed with a mean of zero. Supplementary Figure S1 c) shows relatively constant variance in the standardized residuals plotted versus fitted values (i.e., no heteroscedasticity) and in Supplementary Figures S1 d) through f) there is relatively constant variance in the standardized residuals plotted versus the three predictor variable plots (i.e., no endogeneity). The residual plots for regressions based on standardized and raw data were identical, except for being on different scales.

Multiple linear regression analysis was performed in the *R* software environment (R Core Team, 2021) using the *lm* function; variance inflation factors were calculated using the *vif* function of the *car* package (Fox *et al.*, 2021); and calculation of estimated marginal means of linear slopes were done using the *emtrends* function from the *emmeans* package (Lenth *et al.*, 2022).

6. Transpiration simulations

The variety-specific predictor variable coefficients from the regression analysis based on raw data were used to simulate and compare vine canopy transpiration across varieties and to compare against simulations from an existing vineyard water balance model.

6.1 Water balance model simulations

A time series of daily vine canopy transpiration and associated soil water depletions were estimated using the vineyard water balance model developed by Pieri and Bois (2007), as based on the methodology described in Lebon *et al.* (2003). For the purpose of comparison with regression model-based simulations, actual data from the 2020 growing season was also used in the water balance model, consisting of measured daily maximum and minimum temperature, rainfall, and solar radiation. It also requires inputs of canopy configuration and porosity and assumptions regarding total transpirable soil water (*TTSW*). This model, however, is not parameterized to distinguish differences in transpiration response between varieties, so only one generic transpiration estimate is produced.

The vine canopy transpiration component of evapotranspiration in this model is determined by first calculating the fraction of total incident radiation to the vineyard that is captured by the canopy (minus that which is reflected) using the method of Riou *et al.* (1989). This fraction is then applied to the reference crop evapotranspiration (i.e., soil evaporation plus vine transpiration) as calculated by the Penman equation and adjusted early in the season to account for gradual development of the canopy starting at budbreak. Also accounting for soil evaporation and precipitation, the model then tracks the daily balance of water in the assumed volume of *TTSW* within the vineyard root zone.

As the fraction of remaining total available transpirable soil water (*FTSW*) in the root zone decreases, the model factors in reductions in transpiration to account for the reduced stomatal conductance associated with increasing drought stress. This reduction is achieved by a function relating the ratio of modeled vine transpiration to maximum vine transpiration (TV/TV_{max}) versus *FTSW* as presented in Pieri and Gaudillere (2005).

6.2 Regression model-based simulations

Using the final variety-specific regression equations, transpiration was simulated by first calculating a time series of $log_{10}(g_{bs})$ for each variety using a common 15-minute time series of predictor input data as measured during the 2020 growing season. For this purpose, the predictor coefficients determined based on raw data were used. A time series of g_{bs} was then calculated by taking the base 10 antilog of $log_{10}(g_{bs})$, which was then input to Equation 1 along with the corresponding R_c, D_c, and r_{bh} data to give an associated estimate of transpiration summed on a daily basis (mm day^{-1}). All data, including that which was filtered before the regression analysis, was included in the transpiration simulations.

For these simulations, a time series of 15-minute measurements of R_c, and D_c from the 2020 season was selected from a representative vine. The time series of R_c and D_c across all 10 vines measured in the study were very similar. This is understandable as the amount of radiation absorbed by the vine canopy (R_c) is strongly influenced by canopy dimensions and porosity (Riou *et al.*, 1989; Pieri, 2010), which were all very similar for each vine. And while vapour pressure deficit in the vine canopy (D_c) was affected by vine transpiration, it was more strongly driven by ambient vapour pressure deficits and hence fairly similar across vines. Therefore, for the purpose of a common input to the transpiration simulations, R_c and D_c data from the vine with the most complete time series over the season was used in the regression equations for each of the five varieties.

The regression model-based simulations also require an input of Ψ_{PD}. For this purpose, a daily time series of Ψ_{PD} was developed using the output of *FTSW* from the corresponding water balance model, which was converted to Ψ_{PD} by the *FTSW* to Ψ_{PD} relationships published in Figure 3 of Lebon *et al.,* 2003. Differing levels of *TTSW* were assumed in the water balance model in order to understand the effect of the differing levels of associated *FTSW* on the regression

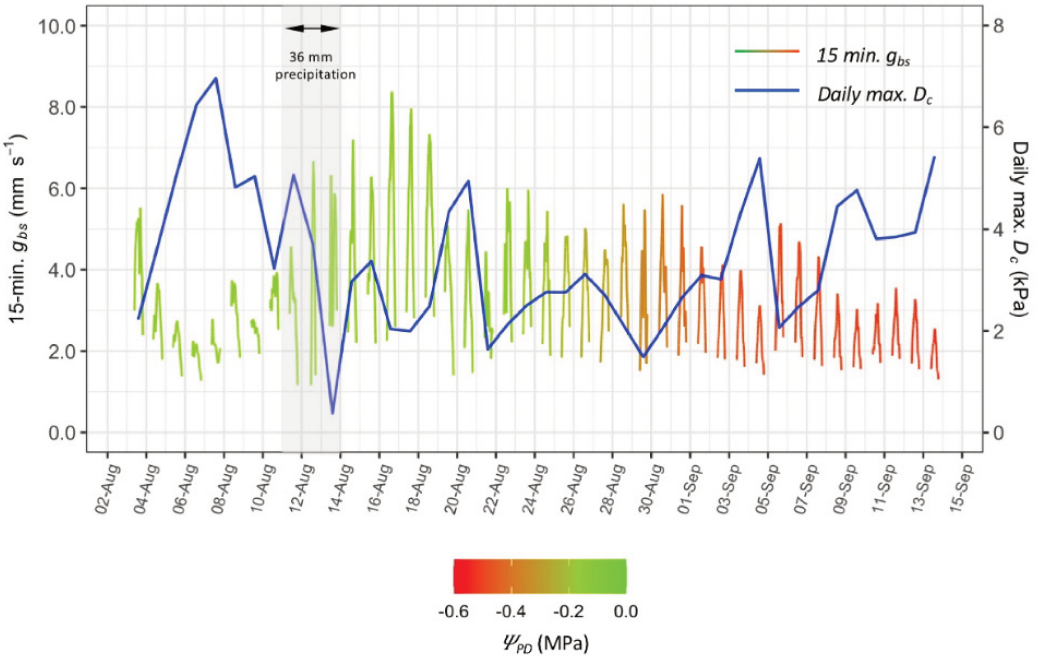

FIGURE 3. 15-minute time series of calculated bulk stomatal conductance (g_{bs}, mm s^{-1}) and daily maximum D_c (kPa) between 3 August through 13 September 2020 from one vine of Cabernet-Sauvignon, with colour gradient representing corresponding Ψ_{PD} (MPa).

model-based simulations. *TTSW* values of 240 mm and 200 mm were selected as described further below.

RESULTS

1. Bulk stomatal conductance (g_{bs})

Figure 3 presents the 15-minute time series of bulk stomatal conductance (g_{bs}, mm s^{-1}) calculated with Equations 2 and 3 using, as an example, data between 3 August through 13 September 2020 from one vine of Cabernet-Sauvignon. Gaps in this time series are due to filtering of data early in the morning and late in the evening that otherwise caused erratic determinations of g_{bs}. This line also has a colour gradient representing the corresponding interpolated Ψ_{PD}. Studies using somewhat similar approaches to estimate vine canopy conductance based on whole-plant transpiration measurements in vineyards found similar overall conductance levels and responses to changes in micrometeorological variables for c.v. Merlot (Zhang *et al.*, 2012), c.v. Sultana (Lu *et al.*, 2003), and cv. Thompson Seedless (Bai *et al.*, 2015), although the latter two studies did not evaluate the effect of decreasing soil water content over the season.

A noticeable increase in overall levels of conductance is observed after 36 mm of precipitation on 11 through 13 August, the only significant rainfall of the study period. Predawn water potential measurements have been found to equilibrate with portions of the root zone having the highest water content (Améglio *et al.*, 1999), such as may occur near the surface after a rainfall. A gradual decrease in both the overall level and diurnal amplitude of g_{bs} is also observed in conjunction with the gradual onset of more negative Ψ_{PD} (i.e., water deficit stress) and/or perhaps developmental changes over the season. It also appears that the g_{bs} timeseries is rather negatively correlated with the D_c timeseries (blue line in Figure 3) as might be expected from previous studies (Prieto *et al.*, 2010; Lu *et al.*, 2003).

The time series of g_{bs} calculated in this way for each vine, along with the corresponding predictor variable data time series were used in the subsequent multiple linear regressions.

2. Predictor variable coefficients

The multiple linear regression of $log_{10}(g_{bs})$ as the response variable with R_c, D_c, and Ψ_{PD} as continuous predictor variables was performed using *variety* as a grouping factor variable as described in Equation 5. From this, the regression coefficients (β) for the predictor variables as described in Equation 6 are presented separately for each variety in Tables 1a through 1c for R_c, D_c, and Ψ_{PD} respectively. As these coefficients were developed based on standardized data, the magnitudes of their absolute values are directly comparable across varieties.

There appears to be more of a differentiation between varieties in the Ψ_{PD} coefficients in Table 1c when compared to the predictors. And while the R_c coefficient covers a similar relative range, three of the varieties have very similar values in the mid-range as seen in Table 1a.

Table 2a presents the same predictor coefficients as in Tables 1a through 1c, instead listed in rows by variety, together with the y-axis intercepts. Based on standardized data,

TABLE 1. Predictor variable coefficients (β) from regressions using standardized $log_{10}(g_{bs})$ as the response and standardized predictors R_c (a), D_c (b), and Ψ_{PD} (c) as continuous predictor variables, by variety with upper and lower 95 % confidence limits (CL), p-values, and compact letter display of pairwise significance.

	Variety	β	Low CL	Upper CL	p-value	Pairwise
a) Standardized R_c coefficient	Cabernet-Sauvignon	0.161	0.145	0.177	~ 0	a
	Semillon	0.225	0.202	0.247	~ 0	b
	Tempranillo	0.255	0.235	0.275	~ 0	b
	Ugni blanc	0.256	0.241	0.272	~ 0	b
	Merlot	0.303	0.285	0.320	~ 0	c
b) Standardized D_c coefficient	Ugni blanc	-0.625	-0.641	-0.609	~ 0	a
	Semillon	-0.582	-0.601	-0.563	~ 0	b
	Cabernet-Sauvignon	-0.560	-0.577	-0.543	~ 0	b
	Merlot	-0.558	-0.575	-0.541	~ 0	b
	Tempranillo	-0.433	-0.452	-0.414	~ 0	c
c) Standardized Ψ_{PD} coefficient	Merlot	0.423	0.400	0.445	~ 0	a
	Semillon	0.458	0.441	0.474	~ 0	ab
	Ugni blanc	0.485	0.458	0.512	~ 0	bc
	Cabernet-Sauvignon	0.512	0.499	0.524	~ 0	c
	Tempranillo	0.773	0.752	0.794	~ 0	d

Pairwise comparisons with shared letters not significantly different ($p < 0.05$).

TABLE 2. Regression coefficients (β) from final regression analysis for y-axis intercepts and predictor variables R_c, D_c, and Ψ_{PD} with a) standardized data, and b) raw data.

	Variety	β_0	β_{Rc}	β_{Dc}	β_{Ψ}
a) with standardized data	Merlot	-0.036	0.303	-0.558	0.423
	Semillon	-0.036	0.225	-0.582	0.458
	Ugni blanc	-0.036	0.256	-0.625	0.485
	Cabernet-Sauvignon	-0.036	0.161	-0.560	0.512
	Tempranillo	-0.036	0.255	-0.433	0.773
b) with raw data	Merlot	0.788	1.110	-0.146	0.066
	Semillon	0.788	0.824	-0.153	0.072
	Ugni blanc	0.788	0.940	-0.164	0.076
	Cabernet-Sauvignon	0.788	0.589	-0.147	0.080
	Tempranillo	0.788	0.934	-0.114	0.121

the magnitude of the absolute value of these coefficients are now comparable across the three predictors for a given variety.

It is observed the absolute value of the D_c and Ψ_{PD} coefficients are comparable in magnitude, with both being about 1.5 to 3.5 times larger than the R_c coefficient, suggesting their greater importance in explaining the variation of g_{bs} observed in each corresponding variety. The relatively subdued response to R_c may be due to the relative consistent range of R_c measurements. As it is driven by solar radiation, whose daily fluctuations change only gradually over the season, R_c does not have the larger extremes seen in D_c and Ψ_{PD}, which then elicit greater responses from the vines.

For reference, Table 2b presents the same predictor coefficients based on raw data. When based on raw data, these coefficients can be used to calculate modeled bulk stomatal conductance ($\hat{g}_{bs}$) in its original units (mm s^{-1}) as needed for subsequent sensitivity analysis and transpiration simulations.

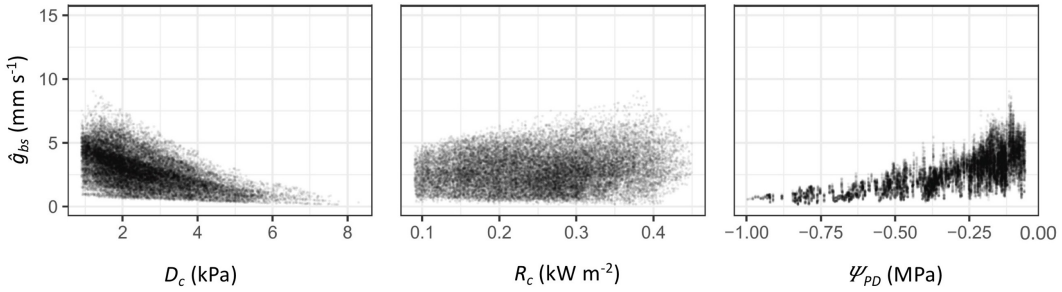

FIGURE 4. Back-transformed $\hat{g}_{bs}$ from modeled $log_{10}(g_{bs})$ plotted against D_c, R_c, and Ψ_{PD} data used for regressions from all 10 vines combined.

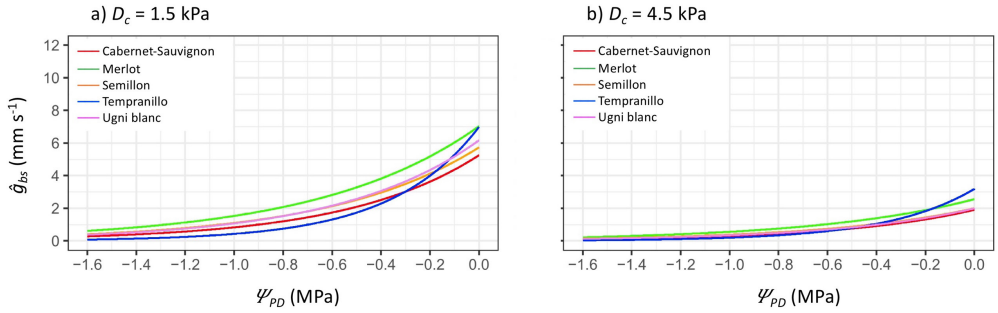

FIGURE 5. Modeled g_{bs} ($\hat{g}_{bs}$ mm s^{-1}) by variety plotted against a hypothetical range of Ψ_{PD} (MPa) with mean value of R_c = 0.263 kW m^{-2} and: a) D_c = 1.5 kPa; and b) D_c = 4.5 kPa.

The intercepts (β_0) in each of Tables 2a and 2b are the same across all varieties due to the regression model being performed on data from all varieties combined. If the regression is performed between $log_{10}(g_{bs})$ and R_c, D_c, and Ψ_{PD} without including the variety factor variable, the intercept of the regression is zero, as expected when using standardized data. Including the factor variable for variety, however, introduces a very small intercept term (-0.036) as seen in Table 2a.

3. Sensitivity analysis

The modeled bulk stomatal conductance ($\hat{g}_{bs}$), as back transformed from modeled $log_{10}(g_{bs})$, and then plotted against R_c, D_c, and Ψ_{PD} shows the non-linear relationships with D_c and Ψ_{PD} that remains after regression (Figure 4). The range of $\hat{g}_{bs}$ is somewhat diminished compared to the plots of raw calculated g_{bs} presented in Figure 1 due to the least squared fitting of the regression model.

Plots of $\hat{g}_{bs}$ across a range of hypothetical Ψ_{PD} values at fixed levels of D_c = 1.5 kPa and D_c = 4.5 kPa, and with a mean value of R_c = 0.263 kW m^{-2} (Figure 5) show higher overall $\hat{g}_{bs}$, and a greater spread in $\hat{g}_{bs}$ between varieties at lower D_c and more positive Ψ_{PD} levels. And in keeping with its larger Ψ_{PD} coefficient in Table 1c, $\hat{g}_{bs}$ for Tempranillo drops more quickly when compared to the other varieties as Ψ_{PD} becomes more negative. The general effect of increasing D_c can also be observed on the overall decrease in the $\hat{g}_{bs}$ response curve with respect to Ψ_{PD}.

In keeping with the lower absolute value of its D_c coefficient in Table 1b, the $\hat{g}_{bs}$ of Tempranillo drops off less quickly than the other varieties as D_c increases (Figure 6).

Again, with a mean value of R_c = 0.263 kW m^{-2}, the effect of more negative Ψ_{PD} = - 0.5 MPa versus Ψ_{PD} = - 0.1 MPa can also be observed in Figure 6, with an overall decrease in the levels of $\hat{g}_{bs}$ at the more negative Ψ_{PD}. The spread between varieties, however, remains fairly similar between the two levels of Ψ_{PD}, particularly at lower levels of D_c.

The biggest differences in $\hat{g}_{bs}$ between varieties were observed in the plot of $\hat{g}_{bs}$ versus R_c, particularly at the lower D_c = 1.5 kPa (Figure 7, panel a). The steeper nature of the $\hat{g}_{bs}$ versus R_c curve for Merlot is also particularly noticeable at D_c = 1.5 kPa, corresponding with its larger R_c coefficient when compared to other varieties as presented in Table 1a. Also, due to the smaller absolute value for its D_c coefficient observed above in Table 1b and Figure 6, the $\hat{g}_{bs}$ for Tempranillo does not decrease as much relative to the other varieties at higher D_c = 4.5 kPa (Figure 7, panel b). A fixed value of Ψ_{PD} = -0.1 MPa was assumed in both panels of Figure 7. However, the R_c coefficients are generally smaller than those for the other predictors, as can be seen in the relative flatness of the lines in Figure 7, and won't have as strong an influence on $\hat{g}_{bs}$.

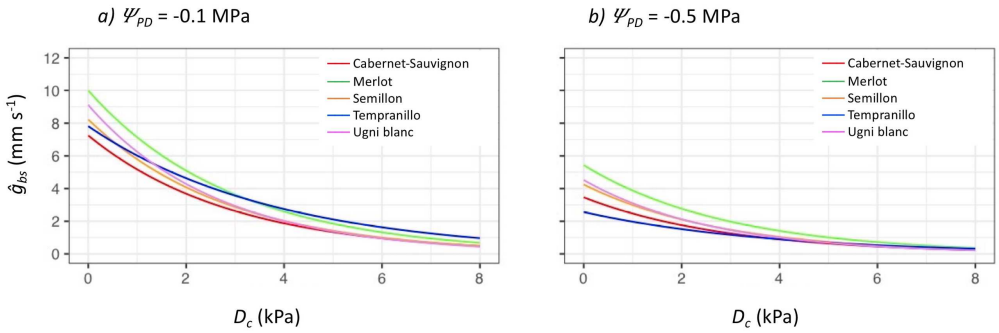

FIGURE 6. Modeled g_{bs} ($\hat{g}_{bs,}$ mm s^{-1}) by variety plotted against a hypothetical range of D_c (kPa) with mean value of R_c = 0.263 kW m^{-2} and: a) Ψ_{PD} = -0.1 MPa; and b) Ψ_{PD} = -0.5 MPa.

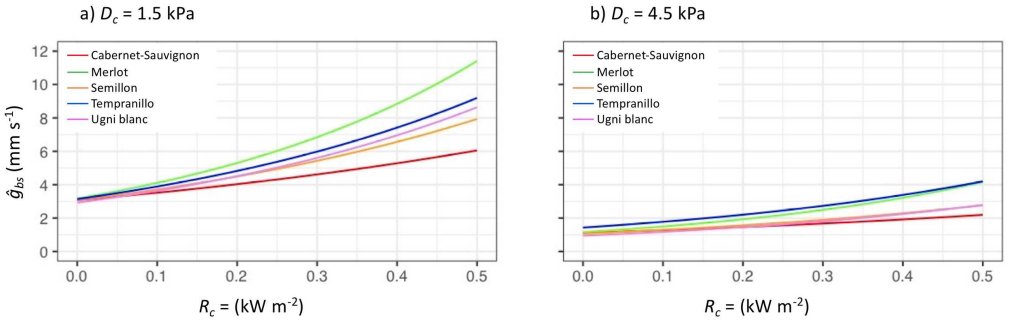

FIGURE 7. Modeled g_{bs} ($\hat{g}_{bs,}$ mm s^{-1}) by variety plotted against a hypothetical range of R_c (kW m^{-2}) with Ψ_{PD} = -0.1 MPa and : a) D_c = 1.5 kPa; and b) D_c = 4.5 kPa.

In general, across all the plots in Figures 5 through 7, Merlot has the highest $\hat{g}_{bs}$, while either Tempranillo, or Cabernet-Sauvignon had the lowest.

4. Simulations of canopy transpiration

Similar to the differences in $\hat{g}_{bs}$ observed in the sensitivity analysis above, the simulated transpiration for the five varieties calculated using their respective regression equations found Merlot to have the greatest daily and season total simulated transpiration, while Tempranillo or Cabernet-Sauvignon had the lowest, regardless of the *TTSW* assumption (coloured lines in Figure 8a for TTSW = 240 mm and Figure 8b for TTSW = 200). It is also observed that the ordering in the relative rates of simulated transpiration by variety in both figures follows the same ordering in magnitude of the Ψ_{PD} regression coefficients by variety in Table 1c. Although there are greater differences between varieties for the R_c coefficient as seen in Table 1a, the overall magnitude of the R_c coefficients relative to those for D_c and Ψ_{PD} were substantially smaller and hence have less effect on $\hat{g}_{bs}$.

These simulations were based on common R_c and D_c input data from the 2020 season, with the time series of Ψ_{PD} needed for the simulations generated by the water balance model using climate data for the same time period and assuming *TTSW* = 240 mm (Figure 8, panel a) and *TTSW* = 200 mm (Figure 8, panel b). An estimate of *TTSW* for the vineyard was not available, so these were considered two values within a reasonable range, which resulted in simulated transpiration rates similar to those measured during the study. The median daily transpiration rate from 30 June to 15 September 2020 period ranged, depending on the vine, between 1.0 to 2.7 mm per day, with the maximum ranging between 2.5 and 5.5 mm/day, depending on the vine. As they are all based on the same input data time series, these regression model-based simulations provide another form of sensitivity analysis across varieties, this time in terms of transpiration.

Comparison of the regression model-based simulation of vine transpiration (Figures 8a and 8b, coloured lines) against the water balance model simulation of vine transpiration excluding soil evaporation (Figures 8a and 8b, black line) finds generally good agreement. It appears, however, that the water balance model tends towards relatively higher transpiration, and therefore faster reductions in *FTSW* early in the season, leading to stronger transpiration reductions and underestimation of transpiration later in the season.

In the water balance model, transpiration is regulated as a function of *FTSW* using the relative transpiration (TV/TV_{max}) versus *FTSW* function from Pieri and Gaudillere (2005).

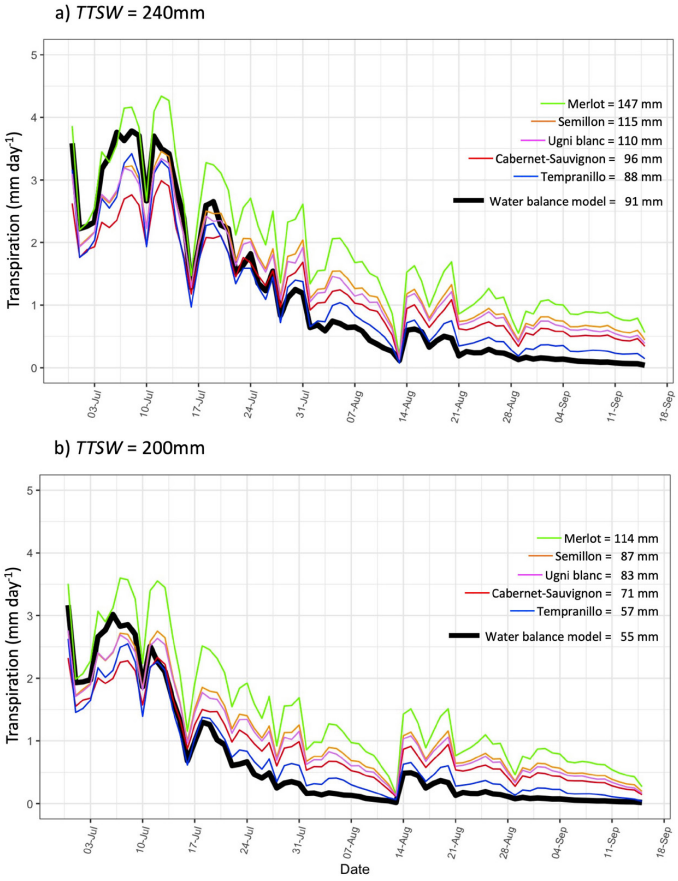

FIGURE 8. Daily total vine transpiration (mm/day) for five varieties simulated using regression coefficients (coloured lines) and the daily total vine transpiration (mm/day) component from the water balance (black line) in panel a) based on *TTSW* = 240mm and in panel b) based *TTSW* = 200mm, with legend including total simulated transpiration from 30 June to 15 September 2020.

Relative transpiration (TV/TV_{max}) is the ratio of simulated transpiration at a given moment over its maximum.

Figure 9 presents a plot of the (TV/TV_{max}) versus *FTSW* function used to regulate transpiration in the water balance model (black line) together with plots of the relative transpiration (TV/TV_{max}) versus *FTSW* resulting from the regression model-based simulations (coloured lines). From Figure 9 it appears that at higher *FTSW*, as experienced earlier in the season, the relative transpiration function of the water balance model allows for relatively higher transpiration compared to that resulting from the regression models. This may explain the relatively higher daily transpiration simulated by the water balance model as observed early in the season in Figure 8, leading to a more rapid reduction in *FTSW*, and hence reduced transpiration by way of the relative transpiration versus *FTSW* reduction function later in the season.

The ordering of the TV/TV_{max} versus *FTSW* curves resulting from the regression model-based simulations (coloured lines in Figure 9) are also the same as for the Ψ_{PD} coefficients in Table 1c. The variety most affected by *FTSW* in Figure 9 is also Tempranillo, as suggested by it having the largest Ψ_{PD} coefficient in Table 1c, remembering in all cases, that *FTSW* and Ψ_{PD} are assumed to follow the relationship published in Figure 3 of Lebon *et al.,* 2003.

As the *TTSW* assumption in water balance modeling decreases, for example from 240 mm to 200 mm as depicted in Figures 8 a) and b), the resulting overall *FTSW* also decreases. By way of the transpiration reduction functions in Figure 9 this leads to relatively lower rates of simulated daily transpiration seen in Figure 8 b) for *TTSW* = 200 mm, when compared to Figure 8 a) for *TTSW* = 240 mm. It should be noted, however, there is a great deal of uncertainty regarding the *TTSW* assumption in the water balance modeling due to soil conditions, planting density, and the rooting characteristics of different scion/rootstock combinations and even individual vines. Regardless, water balance model runs based on reasonable *TTSW* assumptions are still useful for comparison purposes.

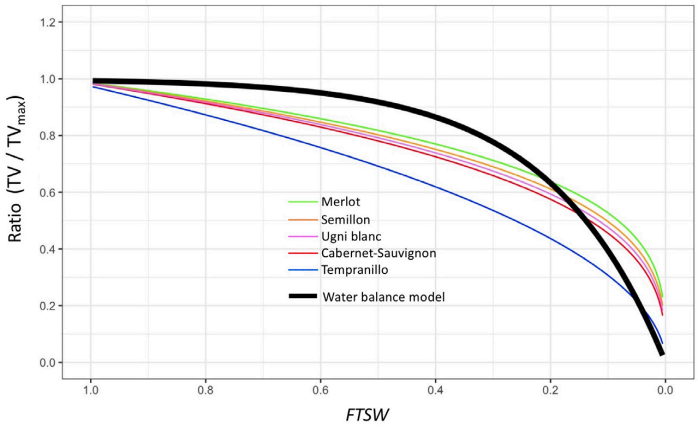

FIGURE 9. Relative transpiration (transpiration / maximum transpiration) as calculated using the regression models versus *FTSW* for each variety (coloured lines) and the transpiration reduction function used in the water balance model (black line).

Based on a constructed time series of input data, the simulation results above are not intended for direct comparisons to measured data, although there is general agreement with the latter falling in a similar range. In order to fully model transpiration using the variety specific regression equations, they would need to be part of a model that tracks soil water deficits or associated Ψ_{PD} over the course of the season in a feedback loop to the transpiration calculation. With differing transpiration rates for each variety, the resulting time series of *FTSW*, and hence Ψ_{PD} over the season, and its subsequent effect on transpiration would each be different.

DISCUSSION

In this study we developed estimates of whole-vine bulk stomatal conductance (g_{bs}) and quantified its response to changes in the environment. Vapour pressure deficit in the vine canopy (D_c) and available soil water, as measured by predawn leaf water potential (Ψ_{PD}) were the main drivers of changes in g_{bs}, with net radiation absorbed by the vine canopy (R_c) also being a factor. Although environmental drivers predominated, some significant differences in modeled g_{bs} ($\hat{g}_{bs}$) response, and hence simulated water use over the growing season were observed between varieties, however, further study may be needed to better distinguish those differences.

For both *TTSW* assumptions presented in Figures 8, Merlot had the highest seasonal total simulated transpiration, followed in order by Semillon, Ugni blanc, Cabernet-Sauvignon, and Tempranillo. As the inputs of R_c, D_c and Ψ_{PD} to the calculation of simulated transpiration are the same for all varieties, these differences are then explained by overall differences in $\hat{g}_{bs}$. Beginning after the week of 17 July the ordering of varieties in terms of daily transpiration are the same as for the seasonal totals. Prior to then, however, the ordering is somewhat different, particularly with regards to Tempranillo, which demonstrated a lesser decrease in $\hat{g}_{bs}$ in response to increasing D_c (Figure 6) and greater decrease in $\hat{g}_{bs}$ in response to decreasing Ψ_{PD} (Figure 7) when compared to the other four varieties. This suggests Tempranillo puts greater emphasis on responding to decreasing Ψ_{PD} than on increasing D_c when compared to the other varieties.

Field studies of Tempranillo found similar dynamics with regard to leaf-level stomatal conductance in response to predawn water potential (Medrano *et al.*, 2003; Yuste *et al.*, 2004; Intrigliolo and Castel, 2006), although they did not evaluate the effects of vapour pressure deficit on conductance, nor compare against any of the of the other varieties included in this study.

The change in the steepness of the slope in the relationship between $\hat{g}_{bs}$ versus R_c, D_c or Ψ_{PD} is observed in Figures 5, 6, and 7 respectively to be generally greater, whether positive or negative, for those varieties with higher $\hat{g}_{bs}$ at non-limited conditions. It is possible that varieties with higher overall g_{bs} under less limited conditions will transpire more, deplete soil water reserves more quickly, and experience greater levels of soil water stress (or require more irrigation) sooner in the season than those with overall lower g_{bs}. As Ψ_{PD} becomes more negative, then varieties with a greater β_ψ will begin to restrict their transpiration more quickly to adapt. The rooting depth and resulting *TTSW* for individual vines or varieties are also an important consideration in the onset of soil water depletion.

The different ways varieties regulate their conductance may result from varying interplay between the different physiological mechanisms controlling stomata. For example, studies on typically anisohydric varieties Merlot (Zhang *et al.* 2012) and Semillon (Rogiers *et al.*, 2012) observed anisohydric response at higher soil water status, but more isohydric response for both varieties at low soil water status. In both cases, the isohydric response followed a general tendency towards greater stomatal closure in response to increasing vapour pressure deficit, with this greater response

positively correlated with the reference gas exchange rate at non-limiting conditions, as expected from empirical and theoretical modeling (Oren *et al.*, 1999; Domec and Johnson, 2012). In the Merlot study, it was suggested the transition from anisohydric to isohydric response was due to a decrease in whole-plant conductance associated with decreased soil water status (Zhang *et al.* 2012). The Semillon study suggested the shift to isohydric behavior was attributable to increased abscisic acid (ABA) generated at lower soil water status, which further increases stomatal sensitivity to VPD (Rogiers *et al.* 2012). ABA produced in vine roots was also linked to changes in stomatal sensitivity in Cabernet-Sauvignon (Speirs *et al.*, 2013; Tramontini *et al.*, 2014). Changes in nature of the stomatal response for several varieties were also observed as a function of water deficit by Levin *et al.* (2020) with Tempranillo being slightly more sensitive to changes in Ψ_{PD} than Cabernet-Sauvignon.

Direct comparison of varietal responses from different studies is confounded by differences in measurement methodology, such as leaf-level measurement of conductance by gas exchange versus canopy conductance by sap flow. Future comparisons using the same, or similar methods would lead to more comparable results. And while all vines measured in this study were subjected to the same climate conditions, the g_{bs} response would be better characterized if using data from different years with different relative amounts of R_c, D_c and Ψ_{PD}. The results could also likely be different if performed in an overall different climate (*e.g.*, southern Europe, or northern France). Even being performed in the same vineyard, the soil conditions around the root zone of individual vines and its effect on rooting volume, access to water, etc., however, can still be quite heterogeneous (Smart *et al.*, 2006). Therefore, with only two vines per variety included in this study, the results could potentially be biased by the specific growing conditions experienced by those vines. Rootstocks and canopy management could also be influencing factor on vine conductance (Marguerit *et al.,* 2012; Picón-Toro *et al.*, 2012) and should be taken into consideration.

CONCLUSIONS

Based on data collected in a vineyard setting, a multiple linear regression analysis was able to quantify relationships across five different grapevine varieties between vine canopy bulk stomatal conductance (g_{bs}) and three key environmental variables: net radiation absorbed by the vine canopy (R_c); vapour pressure deficit in the vine canopy (D_c); and predawn lewaf water potential (Ψ_{PD}). Depending on the variety, D_c and Ψ_{PD} each had about 1.5 to 3.5 times greater effect on g_{bs} than R_c. Of these two more important predictors, the Ψ_{PD} regression coefficient was more differentiated across the five varieties than was the D_c coefficient. And while there was a significant range in R_c coefficients across varieties, their overall lower values mean they had less of an influence on the differences in g_{bs} response across varieties compared to the other predictors.

A comparison of transpiration simulated using the above regression results found a significant difference in the total growing season transpiration between varieties that appeared to be driven in large part by the difference across varieties in the effect of Ψ_{PD} on g_{bs}. There was a general tendency towards greater modeled g_{bs} ($\hat{g}_{bs}$) response, whether positive or negative, to changes in the predictor variables when $\hat{g}_{bs}$ at non-limiting conditions was greater. It was also observed that Tempranillo puts greater emphasis on reducing its g_{bs} in response to decreasing Ψ_{PD} than in response to increasing D_c when compared to the other varieties. These transpiration simulations were also compared against those from an accepted vineyard water balance model and found similar results, although there appeared to be differences between the two approaches in the rate at which conductance, and hence transpiration is reduced as a function of decreasing soil water content (i.e., increasing water deficit stress).

The input data needed for this type of study naturally contains non-linearity and collinearity, but careful selection of variables, transformations and filtering made for a readily interpretable multiple linear regression model that satisfied ordinary least squares assumptions. And aside from providing a method for quantifying the response of vine conductance to different environmental variables, the described approach may provide a basis for variety-specific modeling of the vine transpiration component in vineyard water balance models. Knowledge of such differences in g_{bs} response could help with selection of varieties that are better suited for future changes in certain growing conditions in a region, such as the prevailing atmospheric vapour pressure deficits, or amount of precipitation and expected soil water depletions.

ACKNOWLEDGEMENTS

The authors would like to thank Guillermo Gutiérrez, Eylul Kadaifci, and Alfonso Domínguez Zamudio for their very hard work in the vineyard, and to the INRAE, UEVB, F-33882, Villenave d'Ornon, France, for its management of the VitAdapt vineyard and assistance with implementing instrumentation.

This study has been carried out with financial support from Jas. Hennessy & Co. (16100 Cognac, France) and the French National Research Agency (ANR) in the frame of the Investments for the future Programme, within the Cluster of Excellence COTE (ANR-10-LABX-45). The VitAdapt vineyard is supported by the Conseil Interprofessionnel des Vins de Bordeaux (CIVB), the Conseil Régional d'Aquitaine, Bordeaux University through LabEx and the Institut National de Recherche pour l'Agriculture, l'Alimentation et l'Environnement (INRAE).

REFERENCES

Allen, R. G., Pereira, L. S., Raes, D., & Smith, M. (1998). FAO Irrigation and drainage paper No. 56. *Rome: Food and Agriculture Organization of the United Nations*, *56*, 97–156.

Améglio, T., Archer, P., Cohen, M., Valancogne, C., Daudet, F., Dayau, S., & Cruiziat, P. (1999). Significance and limits in the use of predawn leaf water potential for tree irrigation. *Plant and Soil*, *207*(2), 155–167. https://doi.org/10.1023/A:1026415302759

Bai, Y., Zhu, G., Su, Y., Zhang, K., Han, T., Ma, J., Wang, W., Ma, T., & Feng, L. (2015). Hysteresis loops between canopy conductance of grapevines and meteorological variables in an oasis ecosystem. *Agricultural and Forest Meteorology*, *214–215*, 319–327. https://doi.org/10.1016/j.agrformet.2015.08.267

Chahine, A., Dupont, S., Sinfort, C., & Brunet, Y. (2014). Wind-Flow Dynamics Over a Vineyard. *Boundary-Layer Meteorology*, *151*(3), 557–577. https://doi.org/10.1007/s10546-013-9900-4

Charrier, G., Delzon, S., Domec, J. C., Zhang, L., Delmas, C. E., Merlin, I., Corso, D., King, A., Ojeda, H., Ollat, N., Prieto, J., Scholash, T., Skinner, P., van Leeuwen, C., & Gambetta, G. A. (2018). Drought will not leave your glass empty: Low risk of hydraulic failure revealed by long-term drought observations in world's top wine regions. *Science Advances*, *4*(1), eaao6969. https://doi.org/10.1126/sciadv.aao6969

Chaves, M. M., Zarrouk, O., Francisco, R., Costa, J. M., Santos, T., Regalado, A. P., Rodrigues, M. L., & Lopes, C. M. (2010). Grapevine under deficit irrigation: Hints from physiological and molecular data. *Annals of Botany*, *105*(5), 661–676. https://doi.org/10.1093/aob/mcq030

Choné, X., van Leeuwen, C., Dubourdieu, D., & Gaudillère, J. P. (2001). Stem Water Potential is a Sensitive Indicator of Grapevine Water Status. *Annals of Botany*, *87*(4), 477–483. https://doi.org/10.1006/anbo.2000.1361

Costa, J. M., Ortuño, M. F., Lopes, C. M., Chaves, M. M., Costa, J. M., Ortuño, M. F., Lopes, C. M., & Chaves, M. M. (2012). Grapevine varieties exhibiting differences in stomatal response to water deficit. *Functional Plant Biology*, *39*(3), 179–189. https://doi.org/10.1071/FP11156

Destrac-Irvine, A., & van Leeuwen, C. (2017). The Vitadapt project: Extensive phenotyping of a wide range of varieties in order to optimize the use of genetic diversity within the *Vitis vinifera* species as a tool for adaptation to a changing environment. *Proceedings of Climwine 2016 - Sustainable Grape and Wine Production in the Context of Climate Change.*, 165–171.

Domec, J.-C., & Johnson, D. M. (2012). Does homeostasis or disturbance of homeostasis in minimum leaf water potential explain the isohydric versus anisohydric behavior of *Vitis vinifera* L. cultivars? *Tree Physiology*, *32*(3), 245–248. https://doi.org/10.1093/treephys/tps013

Dormann, C. F., Elith, J., Bacher, S., Buchmann, C., Carl, G., Carré, G., Marquéz, J. R. G., Gruber, B., Lafourcade, B., Leitão, P. J., Münkemüller, T., McClean, C., Osborne, P. E., Reineking, B., Schröder, B., Skidmore, A. K., Zurell, D., & Lautenbach, S. (2013). Collinearity: A review of methods to deal with it and a simulation study evaluating their performance. *Ecography*, *36*(1), 27–46. https://doi.org/10.1111/j.1600-0587.2012.07348.x

Fox, J., Weisberg, S., Price, B., Adler, D., Bates, D., Baud-Bovy, G., Bolker, B., Ellison, S., Firth, D., Friendly, M., Gorjanc, G., Graves, S., Heiberger, R., Krivitsky, P., Laboissiere, R., Maechler, M., Monette, G., Murdoch, D., Nilsson, H., … R-Core. (2021). *car: Companion to Applied Regression* (3.0-12) [Computer software]. https://CRAN.R-project.org/package=car

Franks, P. J., Drake, P. L., & Froend, R. H. (2007). Anisohydric but isohydrodynamic: Seasonally constant plant water potential gradient explained by a stomatal control mechanism incorporating variable plant hydraulic conductance. *Plant, Cell & Environment*, *30*(1), 19–30. https://doi.org/10.1111/j.1365-3040.2006.01600.x

Frost, J. (2020). *Regression Analysis: An Intuitive Guide for Using and Interpreting Linear Models*. Statistics By Jim Publishing.

Gowdy, M., Pieri, P., Suter, B., Marguerit, E., Destrac-Irvine, A., Gambetta, G., & van Leeuwen, C. (2022). Estimating Bulk Stomatal Conductance in Grapevine Canopies. *Frontiers in Plant Science*, *13*. https://www.frontiersin.org/article/10.3389/fpls.2022.839378

Herrera, J. C., Calderan, A., Gambetta, G. A., Peterlunger, E., Forneck, A., Sivilotti, P., Cochard, H., & Hochberg, U. (2021). Stomatal responses in grapevine become increasingly more tolerant to low water potentials throughout the growing season. *The Plant Journal: For Cell and Molecular Biology*. https://doi.org/10.1111/tpj.15591

Hochberg, U., Rockwell, F. E., Holbrook, N. M., & Cochard, H. (2018). Iso/Anisohydry: A Plant–Environment Interaction Rather Than a Simple Hydraulic Trait. *Trends in Plant Science*, *23*(2), 112–120. https://doi.org/10.1016/j.tplants.2017.11.002

Intrigliolo, D. S., & Castel, J. R. (2006). Vine and soil-based measures of water status in Tempranillo vineyard. *Vitis*, *45*(4), 157–163. https://doi.org/10.5073/vitis.2006.45.157-163

Keller, M. (2015). *The Science of Grapevines: Anatomy and Physiology* (2nd edition). Academic Press.

Kelliher, F. M., Leuning, R., Raupach, M. R., & Schulze, E.-D. (1995). Maximum conductances for evaporation from global vegetation types. *Agricultural and Forest Meteorology*, *73*(1), 1–16. https://doi.org/10.1016/0168-1923(94)02178-M

Krounbi, L., & Lazarovitch, N. (2011). Soil Hydraulic Properties Affecting Root Water Uptake. In J. Gliński, J. Horabik, and J. Lipiec (Eds.), *Encyclopedia of Agrophysics* (pp. 748–754). Springer Netherlands. https://doi.org/10.1007/978-90-481-3585-1_149

Lavoie-Lamoureux, A., Sacco, D., Risse, P.-A., & Lovisolo, C. (2017). Factors influencing stomatal conductance in response to water availability in grapevine: A meta-analysis. *Physiologia Plantarum*, *159*(4), 468–482. https://doi.org/10.1111/ppl.12530

Lebon, E., Dumas, V., Pieri, P., & Schultz, H. R. (2003). Modelling the seasonal dynamics of the soil water balance of vineyards. *Functional Plant Biology*, *30*(6), 699–710. https://doi.org/10.1071/FP02222

Lenth, R. V., Buerkner, P., Herve, M., Love, J., Miguez, F., Riebl, H., & Singmann, H. (2022). *emmeans: Estimated Marginal Means, aka Least-Squares Means* (1.7.2) [Computer software]. https://CRAN.R-project.org/package=emmeans

Levin, A. D., Williams, L. E., & Matthews, M. A. (2020). A continuum of stomatal responses to water deficits among 17 wine grape cultivars (*Vitis vinifera*). *Functional Plant Biology*, *47*(1), 11–25. https://doi.org/10.1071/FP19073

Lhomme, J. P., Montes, C., Jacob, F., & Prévot, L. (2012). Evaporation from Heterogeneous and Sparse Canopies: On the Formulations Related to Multi-Source Representations. *Boundary-Layer Meteorology*, *144*(2), 243–262. https://doi.org/10.1007/s10546-012-9713-x

Lovisolo, C., Perrone, I., Carra, A., Ferrandino, A., Flexas, J., Medrano, H., & Schubert, A. (2010). Drought-induced changes in development and function of grapevine (*Vitis* spp.) organs and in their hydraulic and non-hydraulic interactions at the whole-plant level: A physiological and molecular update. *Functional Plant Biology*, *37*(2), 98. https://doi.org/10.1071/FP09191

Lu, P., Yunusa, I. A. M., Walker, R. R., & Müller, W. J. (2003). Regulation of canopy conductance and transpiration and their modelling in irrigated grapevines. *Functional Plant Biology*, *30*(6), 689–698. https://doi.org/10.1071/FP02181

Marguerit, E., Brendel, O., Lebon, E., van Leeuwen, C., & Ollat, N. (2012). Rootstock control of scion transpiration and its acclimation to water deficit are controlled by different genes. *New Phytologist*, *194*(2), 416–429. https://doi.org/10.1111/j.1469-8137.2012.04059.x

Martínez-Vilalta, J., Poyatos, R., Aguadé, D., Retana, J., & Mencuccini, M. (2014). A new look at water transport regulation in plants. *New Phytologist*, *204*(1), 105–115. https://doi.org/10.1111/nph.12912

McElrone, A. J., Choat, B., Gambetta, G. A., & Brodersen, C. R. (2013). Water uptake and transport in vascular plants. *Nature Education Knowledge*, *4*(6). http://www.nature.com.zhongjivip.net/scitable/knowledge/library/water-uptake-and-transport-in-vascular-plants-103016037

Medrano, H., Escalona, J. M., Cifre, J., Bota, J., & Flexas, J. (2003). A ten-year study on the physiology of two Spanish grapevine cultivars under field conditions: Effects of water availability from leaf photosynthesis to grape yield and quality. *Functional Plant Biology*, *30*(6), 607–619. https://doi.org/10.1071/fp02110

Mendoza, V., Pazos, M., Garduño, R., & Mendoza, B. (2021). Thermodynamics of climate change between cloud cover, atmospheric temperature and humidity. *Scientific Reports*, *11*(1), 21244. https://doi.org/10.1038/s41598-021-00555-5

Monteith, J., & Unsworth, M. (2013). *Principles of Environmental Physics: Plants, Animals, and the Atmosphere*. Academic Press.

Oren, R., Sperry, J. S., Katul, G. G., Pataki, D. E., Ewers, B. E., Phillips, N., & Schäfer, K. V. R. (1999). Survey and synthesis of intra- and interspecific variation in stomatal sensitivity to vapour pressure deficit. *Plant, Cell & Environment*, *22*(12), 1515–1526. https://doi.org/10.1046/j.1365-3040.1999.00513.x

Pellegrino, A., Gozé, E., Lebon, E., & Wery, J. (2006). A model-based diagnosis tool to evaluate the water stress experienced by grapevine in field sites. *European Journal of Agronomy*, *25*(1), 49–59. https://doi.org/10.1016/j.eja.2006.03.003

Picón-Toro, J., González-Dugo, V., Uriarte, D., Mancha, L. A., & Testi, L. (2012). Effects of canopy size and water stress over the crop coefficient of a "Tempranillo" vineyard in south-western Spain. *Irrigation Science*, *30*(5), 419–432. https://doi.org/10.1007/s00271-012-0351-3

Pieri, P. (2010). Modelling radiative balance in a row-crop canopy: Row–soil surface net radiation partition. *Ecological Modelling*, *221*(5), 791–801. https://doi.org/10.1016/j.ecolmodel.2009.11.019

Pieri, P., & Bois, B. (2007). *Feuille de calcul excel du modèle de bilan hydrique de la vigne* (1 beta) [Computer software].

Pieri, P., & Gaudillere, J. P. (2005). Vines water stress derived from a soil water balance model—Sensitivity to soil and training system parameters. *XIV International GiESCO Viticulture Congress, Geisenheim, Germany, 23-27 August, 2005*, 457–463. https://www.cabdirect.org/cabdirect/abstract/20053214000

Prieto, J. A., Lebon, É., & Ojeda, H. (2010). Stomatal behavior of different grapevine cultivars in response to soil water status and air water vapour pressure deficit. *OENO One*, *44*(1), 9–20. https://doi.org/10.20870/oeno-one.2010.44.1.1459

Pou, A., Medrano, H., Tomàs, M., Martorell, S., Ribas-Carbó, M., & Flexas, J. (2012). Anisohydric behaviour in grapevines results in better performance under moderate water stress and recovery than isohydric behaviour. *Plant and Soil*, *359*(1), 335–349. https://doi.org/10.1007/s11104-012-1206-7

R Core Team. (2021). *R: A Language and Environment for Statistical Computing*. R Foundation for Statistical Computing. https://www.R-project.org/

Riou, C., Valancogne, C., & Pieri, P. (1989). Un modèle simple d'interception du rayonnement solaire par la vigne—Vérification expérimentale. *Agronomie*, *9*(5), 441–450. https://doi.org/10.1051/agro:19890502

Rogiers, S. Y., Greer, D. H., Hatfield, J. M., Hutton, R. J., Clarke, S. J., Hutchinson, P. A., & Somers, A. (2012). Stomatal response of an anisohydric grapevine cultivar to evaporative demand, available soil moisture and abscisic acid. *Tree Physiology*, *32*(3), 249–261. https://doi.org/10.1093/treephys/tpr131

Sack, L., & Holbrook, N. M. (2006). Leaf Hydraulics. *Annual Review of Plant Biology*, *57*(1), 361–381. https://doi.org/10.1146/annurev.arplant.56.032604.144141

Scholander, P. F., Bradstreet, E. D., Hemmingsen, E. A., & Hammel, H. T. (1965). Sap Pressure in Vascular Plants. *Science*. https://doi.org/10.1126/science.148.3668.339

Schultz, H. R. (1996). Water relations and photosynthetic responses of two grapevine cultivars of different geographical origin during water stress. *Acta Horticulturae*, *427*, 251–266. https://doi.org/10.17660/ActaHortic.1996.427.30

Schultz, H. R. (2003). Differences in hydraulic architecture account for near-isohydric and anisohydric behaviour of two field-grown *Vitis vinifera* L. cultivars during drought. *Plant, Cell & Environment*, *26*(8), 1393–1405. https://doi.org/10.1046/j.1365-3040.2003.01064.x

Searle, S. R., Speed, F. M., & Milliken, G. A. (1980). Population Marginal Means in the Linear Model: An Alternative to Least Squares Means. *The American Statistician*, *34*(4), 216–221. https://doi.org/10.1080/00031305.1980.10483031

Shimazaki, K., Doi, M., Assmann, S. M., & Kinoshita, T. (2007). Light Regulation of Stomatal Movement. *Annual Review of Plant Biology*, *58*(1), 219–247. https://doi.org/10.1146/annurev.arplant.57.032905.105434

Shmueli, G. (2010). *To Explain or To Predict?* (SSRN Scholarly Paper ID 1351252). Social Science Research Network. https://doi.org/10.2139/ssrn.1351252

Shuttleworth, W. J., & Wallace, J. S. (1985). Evaporation from sparse crops-an energy combination theory. *Quarterly Journal of the Royal Meteorological Society*, *111*(469), 839–855. https://doi.org/10.1002/qj.49711146910

Smart, D. R., Breazeale, A., & Zufferey, V. (2006). Physiological Changes in Plant Hydraulics Induced by Partial Root Removal of Irrigated Grapevine (*Vitis vinifera* cv. Syrah). *American Journal of Enology and Viticulture*, *57*(2), 201–209.

Smart, R., & Robinson, M. (1991). *Sunlight Into Wine*. WINETITLES.

Speirs, J., Binney, A., Collins, M., Edwards, E., & Loveys, B. (2013). Expression of ABA synthesis and metabolism genes under different irrigation strategies and atmospheric VPDs is associated with stomatal conductance in grapevine (*Vitis vinifera* L. cv Cabernet-Sauvignon). *Journal of Experimental Botany*, *64*(7), 1907–1916. https://doi.org/10.1093/jxb/ert052

Sperry, J. S., Saliendra, N. Z., Pockman, W. T., Cochard, H., Cruiziat, P., Davis, S. D., Ewers, F. W., & Tyree, M. T. (1996). New evidence for large negative xylem pressures and their measurement by the pressure chamber method. *Plant, Cell & Environment*, *19*(4), 427–436. https://doi.org/10.1111/j.1365-3040.1996.tb00334.x

Tardieu, F., & Simonneau, T. (1998). Variability among species of stomatal control under fluctuating soil water status and evaporative demand: Modelling isohydric and anisohydric behaviours. *Journal of Experimental Botany*, *49*(90001), 419–432. https://doi.org/10.1093/jexbot/49.suppl_1.419

Tramontini, S., van Leeuwen, C., Domec, J.-C., Destrac-Irvine, A., Basteau, C., Vitali, M., Mosbach-Schulz, O., & Lovisolo, C. (2012). Impact of soil texture and water availability on the hydraulic control of plant and grape-berry development. *Plant and Soil*, *368*(1–2), 215–230. https://doi.org/10.1007/s11104-012-1507-x

Tramontini, S., Döring, J., Vitali, M., Ferrandino, A., Stoll, M., & Lovisolo, C. (2014). Soil water-holding capacity mediates hydraulic and hormonal signals of near-isohydric and near-anisohydric Vitis cultivars in potted grapevines. *Functional Plant Biology*, *41*(11), 1119. https://doi.org/10.1071/FP13263

van Leeuwen, C., Destrac-Irvine, A., Dubernet, M., Duchêne, E., Gowdy, M., Marguerit, E., Pieri, P., Parker, A., de Rességuier, L.,

& Ollat, N. (2019a). An Update on the Impact of Climate Change in Viticulture and Potential Adaptations. *Agronomy*, *9*(9), 514. https://doi.org/10.3390/agronomy9090514

van Leeuwen, C., Pieri, P., Gowdy, M., Ollat, N., & Roby, J.-P. (2019b). Reduced density is an environmental friendly and cost effective solution to increase resilience to drought in vineyards in a context of climate change: *OENO One*, *53*(2), 129–146. https://doi.org/10.20870/oeno-one.2019.53.2.2420

Wickham, H., Chang, W., Henry, L., Pedersen, T. L., Takahashi, K., Wilke, C., Woo, K., Yutani, H., Dunnington, D., & RStudio. (2021a). *ggplot2: Create Elegant Data Visualisations Using the Grammar of Graphics* (3.3.5) [Computer software]. https://CRAN.R-project.org/package=ggplot2

Wickham, H., François, R., Henry, L., Müller, K., & RStudio. (2021b). *dplyr: A Grammar of Data Manipulation* (1.0.7) [Computer software]. https://CRAN.R-project.org/package=dplyr

Wild, M. (2009). Global dimming and brightening: A review. *Journal of Geophysical Research: Atmospheres*, *114*(D10). https://doi.org/10.1029/2008JD011470

Willett, K. M., Dunn, R. J. H., Thorne, P. W., Bell, S., de Podesta, M., Parker, D. E., Jones, P. D., & Williams Jr., C. N. (2014). HadISDH land surface multi-variable humidity and temperature record for climate monitoring. *Climate of the Past*, *10*(6), 1983–2006. https://doi.org/10.5194/cp-10-1983-2014

Yuste, J., Rubio, J. A., & Péez, A. (2004). Influence of Plant Density and Water Regime on Soil Water Use, Water Relations and Productivity of Trellis-Trained Tempranillo Grapevines. *Acta Horticulturae*, *646*, 187–193. https://doi.org/10.17660/ActaHortic.2004.646.24

Zhang, Y., Oren, R., & Kang, S. (2012). Spatiotemporal variation of crown-scale stomatal conductance in an arid *Vitis vinifera* L. cv. Merlot vineyard: Direct effects of hydraulic properties and indirect effects of canopy leaf area. *Tree Physiology*, *32*(3), 262–279. https://doi.org/10.1093/treephys/tpr120

Zufferey, V., Cochard, H., Ameglio, T., Spring, J.-L., & Viret, O. (2011). Diurnal cycles of embolism formation and repair in petioles of grapevine (*Vitis vinifera* cv. Chasselas). *Journal of Experimental Botany*, *62*(11), 3885–3894. https://doi.org/10.1093/jxb/err081.

SUPPLEMENTARY DATA
Gowdy, M., Suter, B., Pieri, P., Marguerit, E, Destrac Irvine, A., Gambetta, G., & van Leeuwen, C. (2022). Variety-specific response of bulk stomatal conductance of grapevine canopies to changes in net radiation, atmospheric demand, and drought stress. *OENO One*, *56*(2). Retrieved from https://oeno-one.eu/article/view/5435.

Supplementary data

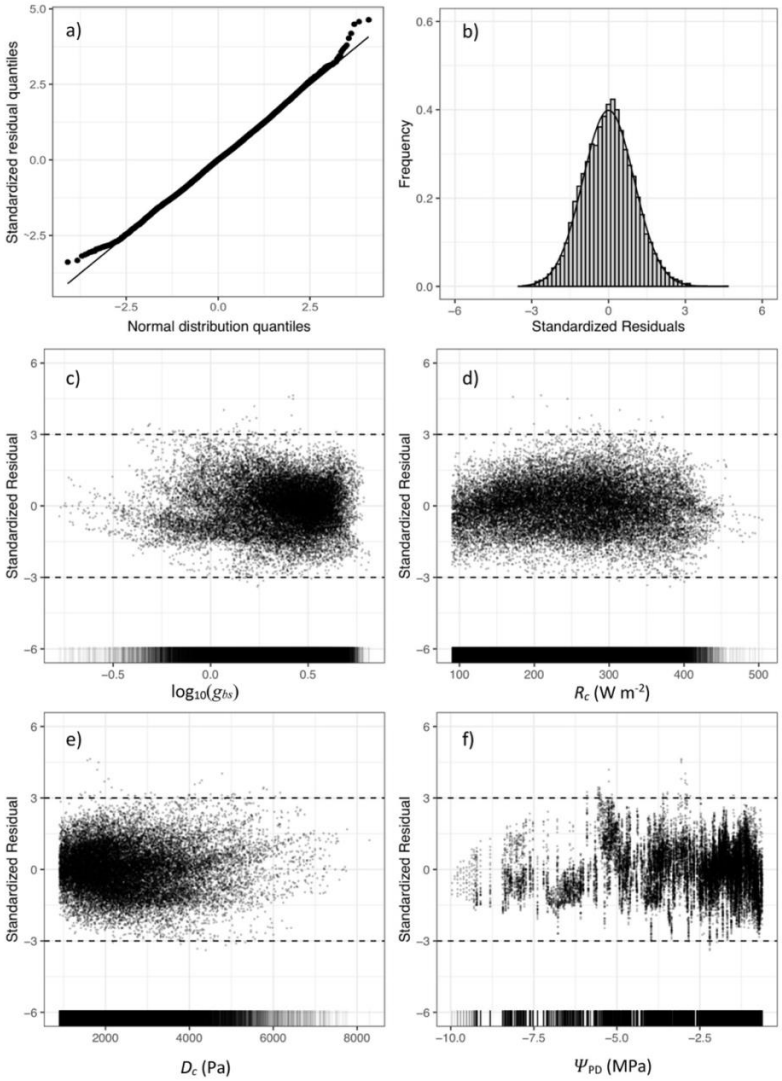

FIGURE S1. Residual plots for final multiple linear regression between log10(gbs) as the response variable and Rc, Dc, and ΨPD as the predictors without interactions and based on raw data, including a) quantile-quantile plot, b) histogram of standardized residuals, c) standardized residuals versus fitted value plot, and d-f) standardized residuals versus predictor variable plots for Rc, Dc, and ΨPD respectively.

SUPPLEMENTARY DATA
Gowdy, M., Suter, B., Pieri, P., Marguerit, E, Destrac Irvine, A., Gambetta, G., & van Leeuwen, C. (2022). Variety-specific response of bulk stomatal conductance of grapevine canopies to changes in net radiation, atmospheric demand, and drought stress. *OENO One*, *56*(2). Retrieved from https://oeno-one.eu/article/view/5435.

SUPPLEMENTARY TABLE S1. Summary statistics of raw input data to multiple linear regression analysis with $log_{10}(gbs)$ (gbsTrans) as the response variable, R_c (kRc), D_c (kDc), and Ψ_{PD} (PDWP) as predictors, and variety (Cepage) as a factor variable.

```
   Cepage        gbsTrans            kRc               kDc             PDWP
CS_N  :5288   Min.   :-0.8560   Min.   :0.09001   Min.   :0.900   Min.   :-9.9613
MERL_N:4752   1st Qu.: 0.1536   1st Qu.:0.18637   1st Qu.:1.679   1st Qu.:-3.8817
SEM_B :3634   Median : 0.3839   Median :0.25449   Median :2.335   Median :-2.2048
TEMP_N:4213   Mean   : 0.3359   Mean   :0.25284   Mean   :2.576   Mean   :-2.9126
UB_B  :5501   3rd Qu.: 0.5475   3rd Qu.:0.31422   3rd Qu.:3.253   3rd Qu.:-1.4139
              Max.   : 1.2831   Max.   :0.50441   Max.   :8.294   Max.   :-0.6295
```

SUPPLEMENTARY TABLE S2. Summary statistics of multiple linear regression based on standardized data with $log_{10}(gbs)$ (gbsTrans) as the response variable, R_c (kRc), D_c (kDc), and Ψ_{PD} (PDWP) as the predictor variables and their interactions, including variety (Cepage) as an interaction factor variable.

```
Call:
lm(formula = gbsTrans ~ ((kRc + kDc + PDWP)^2) * Cepage, data =
allregressdata)

Residuals:
     Min       1Q   Median       3Q      Max
-0.58582 -0.10944 -0.00651  0.10501  0.93325

Coefficients:
                          Estimate Std. Error t value Pr(>|t|)
(Intercept)              0.5383493  0.0187835  28.661  < 2e-16 ***
kRc                      1.6059744  0.0737306  21.782  < 2e-16 ***
kDc                     -0.0792256  0.0073451 -10.786  < 2e-16 ***
PDWP                     0.0483288  0.0032139  15.038  < 2e-16 ***
CepageMERL_N             0.0604980  0.0300394   2.014 0.044026 *
CepageSEM_B              0.1064914  0.0339030   3.141 0.001685 **
CepageTEMP_N             0.1426643  0.0326356   4.371 1.24e-05 ***
CepageUB_B               0.0557405  0.0299336   1.862 0.062596 .
kRc:kDc                 -0.2624314  0.0234677 -11.183  < 2e-16 ***
kRc:PDWP                 0.1580149  0.0149448  10.573  < 2e-16 ***
kDc:PDWP                -0.0028038  0.0009057  -3.096 0.001965 **
kRc:CepageMERL_N         0.0221705  0.1137785   0.195 0.845507
kRc:CepageSEM_B         -1.1624702  0.1399080  -8.309  < 2e-16 ***
kRc:CepageTEMP_N        -1.2814367  0.1293469  -9.907  < 2e-16 ***
kRc:CepageUB_B          -0.1064226  0.1093372  -0.973 0.330393
kDc:CepageMERL_N        -0.0428890  0.0113140  -3.791 0.000151 ***
kDc:CepageSEM_B         -0.0911997  0.0120338  -7.579 3.62e-14 ***
kDc:CepageTEMP_N         0.0519410  0.0119886   4.333 1.48e-05 ***
kDc:CepageUB_B          -0.0941343  0.0113203  -8.316  < 2e-16 ***
PDWP:CepageMERL_N       -0.0301985  0.0072680  -4.155 3.26e-05 ***
PDWP:CepageSEM_B        -0.0119276  0.0055795  -2.138 0.032546 *
PDWP:CepageTEMP_N        0.0304035  0.0066148   4.596 4.32e-06 ***
PDWP:CepageUB_B          0.0100201  0.0083787   1.196 0.231747
kRc:kDc:CepageMERL_N     0.1995373  0.0344661   5.789 7.16e-09 ***
kRc:kDc:CepageSEM_B      0.4787632  0.0366622  13.059  < 2e-16 ***
kRc:kDc:CepageTEMP_N     0.2975814  0.0359612   8.275  < 2e-16 ***
kRc:kDc:CepageUB_B       0.1938961  0.0337753   5.741 9.54e-09 ***
kRc:PDWP:CepageMERL_N    0.0126250  0.0290154   0.435 0.663484
kRc:PDWP:CepageSEM_B    -0.1050146  0.0243759  -4.308 1.65e-05 ***
kRc:PDWP:CepageTEMP_N   -0.3117412  0.0281336 -11.081  < 2e-16 ***
kRc:PDWP:CepageUB_B      0.0625507  0.0318471   1.964 0.049531 *
kDc:PDWP:CepageMERL_N    0.0059348  0.0018274   3.248 0.001165 **
kDc:PDWP:CepageSEM_B     0.0104445  0.0014805   7.055 1.78e-12 ***
kDc:PDWP:CepageTEMP_N    0.0310093  0.0018232  17.008  < 2e-16 ***
kDc:PDWP:CepageUB_B     -0.0104823  0.0021023  -4.986 6.21e-07 ***
---
Signif. codes:  0 ‘***’ 0.001 ‘**’ 0.01 ‘*’ 0.05 ‘.’ 0.1 ‘ ’ 1

Residual standard error: 0.1645 on 23353 degrees of freedom
Multiple R-squared:  0.7123,      Adjusted R-squared:  0.7119
F-statistic:  1701 on 34 and 23353 DF,  p-value: < 2.2e-16
```

SUPPLEMENTARY DATA
Gowdy, M., Suter, B., Pieri, P., Marguerit, E, Destrac Irvine, A., Gambetta, G., & van Leeuwen, C. (2022).
Variety-specific response of bulk stomatal conductance of grapevine canopies to changes in net radiation, atmospheric demand, and drought stress. *OENO One*, *56*(2). Retrieved from https://oeno-one.eu/article/view/5435.

SUPPLEMENTARY TABLE S3. Summary statistics of multiple linear regression based on standardized data with *log₁₀(gbs)* (gbsTrans) as the response variable, R_c (kRc), D_c (kDc), and Ψ_{PD} (PDWP) as continuous predictor variables and *variety* (Cepage) as a factor variable, without interaction terms.

```
Call:
lm(formula = gbsTrans ~ (kRc + kDc + PDWP) * Cepage, data =
allregressdata)

Residuals:
     Min       1Q   Median       3Q      Max
-1.88705 -0.37651 -0.02498  0.35470  2.99403

Coefficients:
                    Estimate Std. Error t value Pr(>|t|)
(Intercept)       -0.035583   0.007598  -4.683 2.84e-06 ***
kRc                0.160515   0.008168  19.652  < 2e-16 ***
kDc               -0.560282   0.008729 -64.185  < 2e-16 ***
PDWP               0.511652   0.006442  79.420  < 2e-16 ***
CepageMERL_N       0.424683   0.011267  37.692  < 2e-16 ***
CepageSEM_B       -0.185688   0.013955 -13.306  < 2e-16 ***
CepageTEMP_N       0.202323   0.011551  17.516  < 2e-16 ***
CepageUB_B        -0.221910   0.012455 -17.817  < 2e-16 ***
kRc:CepageMERL_N   0.142248   0.012070  11.785  < 2e-16 ***
kRc:CepageSEM_B    0.064162   0.014001   4.583 4.62e-06 ***
kRc:CepageTEMP_N   0.094227   0.012999   7.249 4.34e-13 ***
kRc:CepageUB_B     0.095883   0.011362   8.439  < 2e-16 ***
kDc:CepageMERL_N   0.002047   0.012254   0.167   0.8673
kDc:CepageSEM_B   -0.021394   0.013063  -1.638   0.1015
kDc:CepageTEMP_N   0.127153   0.012982   9.794  < 2e-16 ***
kDc:CepageUB_B    -0.064630   0.012004  -5.384 7.36e-08 ***
PDWP:CepageMERL_N -0.088986   0.013090  -6.798 1.09e-11 ***
PDWP:CepageSEM_B  -0.053947   0.010549  -5.114 3.18e-07 ***
PDWP:CepageTEMP_N  0.261454   0.012501  20.915  < 2e-16 ***
PDWP:CepageUB_B   -0.026584   0.015179  -1.751   0.0799 .
---
Signif. codes:  0 ‘***’ 0.001 ‘**’ 0.01 ‘*’ 0.05 ‘.’ 0.1 ‘ ’ 1

Residual standard error: 0.5468 on 23368 degrees of freedom
Multiple R-squared:  0.7012,      Adjusted R-squared:  0.701
F-statistic:  2887 on 19 and 23368 DF,  p-value: < 2.2e-16
```

SUPPLEMENTARY TABLE S4. Summary statistics of multiple linear regression based on raw data with *log₁₀(gbs)* (gbsTrans) as the response variable, R_c (kRc), D_c (kDc), and Ψ_{PD} (PDWP) as continuous predictor variables and *variety* (Cepage) as a factor variable, without interaction terms.

```
Call:
lm(formula = gbsTrans ~ (kRc + kDc + PDWP) * Cepage, data =
allregressdata)

Residuals:
     Min       1Q   Median       3Q      Max
-0.57840 -0.11540 -0.00766  0.10872  0.91770

Coefficients:
                     Estimate Std. Error t value Pr(>|t|)
(Intercept)         0.7880385  0.0082781  95.195  < 2e-16 ***
kRc                 0.5886853  0.0299549  19.652  < 2e-16 ***
kDc                -0.1469102  0.0022889 -64.185  < 2e-16 ***
PDWP                0.0801736  0.0010095  79.420  < 2e-16 ***
CepageMERL_N       -0.0437299  0.0128481  -3.404 0.000666 ***
CepageSEM_B        -0.1265844  0.0140383  -9.017  < 2e-16 ***
CepageTEMP_N        0.0080928  0.0135403   0.598 0.550057
CepageUB_B         -0.1254140  0.0126080  -9.947  < 2e-16 ***
kRc:CepageMERL_N    0.5216920  0.0442672  11.785  < 2e-16 ***
kRc:CepageSEM_B     0.2353142  0.0513494   4.583 4.62e-06 ***
kRc:CepageTEMP_N    0.3455768  0.0476744   7.249 4.34e-13 ***
kRc:CepageUB_B      0.3516471  0.0416687   8.439  < 2e-16 ***
kDc:CepageMERL_N    0.0005368  0.0032132   0.167 0.867311
kDc:CepageSEM_B    -0.0056097  0.0034251  -1.638 0.101477
kDc:CepageTEMP_N    0.0333406  0.0034041   9.794  < 2e-16 ***
kDc:CepageUB_B     -0.0169464  0.0031476  -5.384 7.36e-08 ***
PDWP:CepageMERL_N -0.0139437  0.0020511  -6.798 1.09e-11 ***
PDWP:CepageSEM_B  -0.0084532  0.0016529  -5.114 3.18e-07 ***
PDWP:CepageTEMP_N  0.0409686  0.0019588  20.915  < 2e-16 ***
PDWP:CepageUB_B   -0.0041656  0.0023784  -1.751 0.079882 .
---
Signif. codes:  0 ‘***’ 0.001 ‘**’ 0.01 ‘*’ 0.05 ‘.’ 0.1 ‘ ’ 1

Residual standard error: 0.1676 on 23368 degrees of freedom
Multiple R-squared:  0.7012,      Adjusted R-squared:  0.701
F-statistic:  2887 on 19 and 23368 DF,  p-value: < 2.2e-16
```

6.3 Discussion

6.3.1 Regression analysis results

The methodology presented in the previous chapter was used to estimate bulk stomatal conductance on 15-minute intervals from July to mid-September 2020 on several vines of Cabernet-Sauvignon, Merlot, Tempranillo, Ugni blanc, and Semillon, with its response being compared against measurements of vine water status, vapor pressure deficits, net radiation, leaf area index, and other parameters. After a process of trial-and-error to address non-linearity and collinearity in the data for the different variables, a multiple linear regression analysis found the variability of vapor pressure deficit in the vine canopy, and to a lesser extent the net radiation absorbed by the vine canopy over the course of the day, and predawn water potential over the season explained much of the variability in bulk stomatal conductance.

The intent of using a multiple linear analysis approach was to develop a model that was readily interpretable, with resulting regression coefficients for the different variables being physically meaningful and comparable between themselves and across the different varieties. This type of regression analysis, however, is not well suited for addressing non-linearity and collinearity in the explanatory variables, as is required to satisfy the underlying statistical assumptions. Non-linear, or non-parametric regression modeling approaches, such as used by Brillante et al. (2016), are less affected by collinearity in the input variables and may allow for a better modeling fit. But such models are less interpretable, in terms of characterizing and comparing the effect of different variables, and are more site-specific and less broadly applicable to vineyards with different soil, climate, and other conditions.

During the study there was an observed decrease in vine leaf area, and hence *LAI* for all vines after mid-August, which corresponded with a general decrease in vine water status (Ψ_{PD}) over the same period. As bulk boundary layer resistance (r_{bh}) is calculated based on *LAI*, this created relatively strong collinearity between r_{bh} and Ψ_{PD}, which resulted in high variable inflation factors and problems with the residual plots from the corresponding linear regressions. Based on this issue with collinearity, and the prior sensitivity analysis,

which found r_{bh} to be of relatively low significance in the determination of g_{bs} (Gowdy et al., 2022a), it was decided to eliminate r_{bh} from the final regression analysis. This can further simplify future application of this methodology by eliminating time consuming measurement of leaf area index needed for calculation of r_{bh}.

Depending on the variety, vapor pressure deficit (D_c) and vine water status (Ψ_{PD}) each had a generally greater effect on g_{bs} than R_c. Of these two predictors, the Ψ_{PD} regression coefficient was more differentiated across the five varieties than was the D_c coefficient. And while there was a significant range in R_c coefficients across varieties, their overall lower values mean they had less of an influence on the differences in g_{bs} response across varieties compared to the other predictors. Then using these coefficients along with a common input dataset, simulations of g_{bs} ($\hat{g}_{bs}$) showed a greater response to changes in each of the predictor variables when $\hat{g}_{bs}$ was overall greater under non-limiting conditions. With respect to D_c, this was as expected from empirical and theoretical modeling (Oren et al., 1999; Domec and Johnson, 2012). From these $\hat{g}_{bs}$ simulations (using common input data sets), it was also observed that Tempranillo appears to put greater emphasis on reducing its g_{bs} in response to decreasing Ψ_{PD} than in response to increasing D_c when compared to the other varieties.

6.3.2 Comparison with water balance model

Transpiration simulations based on the regression equations using input data from the 2020 season found similar differences between varieties in terms of daily and seasonal transpiration. These simulations also compared well with those from an accepted vineyard water balance model, although there appeared to be differences between the two approaches in the rate at which conductance, and hence transpiration is reduced as a function of decreasing soil water content (i.e., increasing water deficit stress). These differences in the transpiration reduction functions (see Figure 9 of Gowdy et al. 2022b) begin to provide a mechanistic explanation of the observed differences in simulated transpiration between the regression-based and water balance model simulations. The lower transpiration reduction early in the season associated with the curve used in the water balance model as based on Pieri and Gaudillere (2005), when compared to those from the regression-based models, allows for more transpiration early in the season and a

quicker depletion of soil water, and quicker decrease in transpiration, leading to a relative underestimate of transpiration later in the season.

For comparison purposes, in Figure 11 below, the regression model-based transpiration reduction functions are overlaid on a reproduction of the conductance reduction data presented in Figure 4 from Lebon *et al.* (2003), showing similar results.

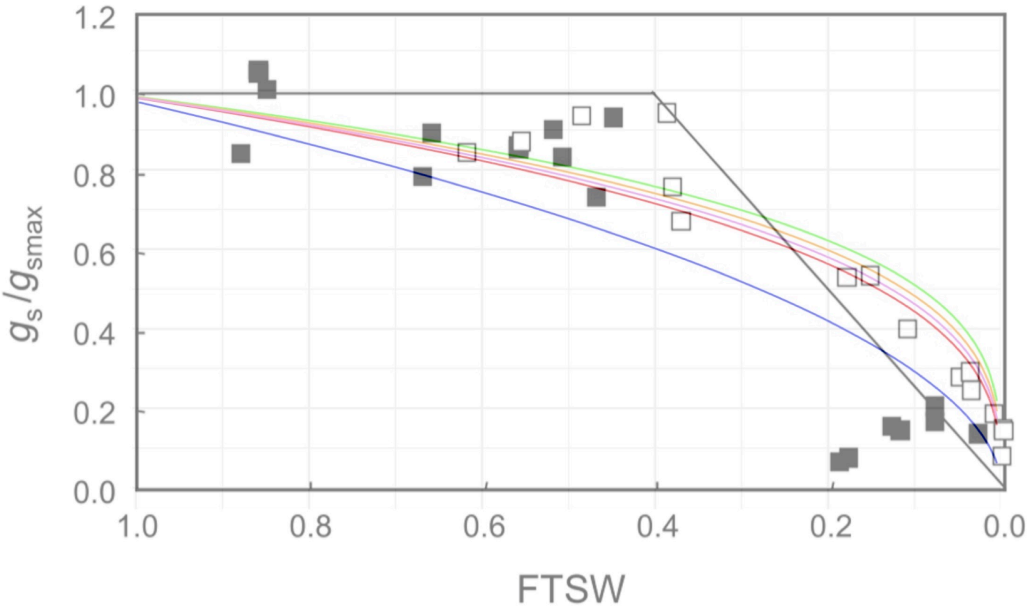

Figure 11. Reproduction of Figure 4 from Lebon *et al.* (2003) showing ratio of measured leaf level stomatal conductance (g_s) over the maximum g_s (g_{smax}) as a function of the fraction of transpirable soil water (*FTSW*) for Syrah from field measurements (open square) and a pot experiment (closed square), with transpiration (conductance) reduction curves from regression analysis for five varieties.

While current water balance modeling is an invaluable tool to help growers design and manage their vineyards, they are generic, without the ability to distinguish differences between varieties. While more data collected using the described approach is likely needed to make more definitive characterization of the behavior of the different varieties, it could provide the means of developing variety specific parameterization of the vine transpiration component of future water balance models. By better characterizing the response of bulk stomatal conductance, the dynamics of vine transpiration can be better parameterized in vineyard water use modeling of current and future climate scenarios. Physiological vine responses, such as changes in photosynthesis, stomatal closure, and shoot growth

characteristics in response to water deficits, are often correlated well with water potential (Pellegrino et al. 2006; Lebon et al. 2003) and could potentially be evaluated using the output from water balance models that output estimates of soil water content.

And while all vines measured in this study were subjected to the same climate conditions, the g_{bs} response would be better characterized if using data from different years with different relative amounts of R_c, D_c and Ψ_{PD}. The results could also likely be different if performed in an overall different climate (*e.g.*, southern Europe, or northern France). Even being performed in the same vineyard, the soil conditions around the root zone of individual vines and its effect on rooting volume, access to water, etc., however, can still be quite heterogeneous (Smart et al., 2006). Therefore, with only two vines per variety included in this study, the results could potentially be biased by the specific growing conditions experienced by those vines. Rootstocks and canopy management could also be influencing factor on vine conductance (Marguerit et al., 2012; Picón-Toro et al., 2012) and should be taken into consideration.

6.3.3 *TTSW* assumptions for water balance modeling

As part of developing the water balance modeling needed to create the time series of Ψ_{PD} for the regression-based transpiration simulations, and for comparison of the water balance model against those simulations, assumptions regarding the total transpirable soil water (*TTSW*) were required. It provides the beginning water balance for the water balance model, from which additions (from rainfall, or irrigation) or subtractions (from vine transpiration or soil evaporation) are made, and the daily fraction of transpirable soil water (*FTSW*) is calculated. It is effectively the amount of water available in the soil for the vines between field capacity and the wilting point, and is influenced by the soil texture, percent of course elements, and root depth and density (Pellegrino et al., 2004). Its determination is important, as results of water balance models are very sensitive to this assumption (van Leeuwen et al. 2010).

The minimum soil water level can be determined through field and laboratory measurement of *FTSW*, for example at a minimum soil water potential of -1.5 MPa (Pellegrino et al. 2004). Sometimes, however, direct field measurement of soil water content is not practical and *TTSW* can be estimating by applying *FTSW* to predawn water

potential relationships from other similar vineyards using a trial-and-error curve fitting technique (Pellegrino et al., 2006). It is also possible that theoretical relationships between soil matric potential and *FTSW* (Saxton et al., 1986; Pieri and Gaudillere, 2005) or soil matric potential and soil water content (van Genuchten, 1980) could be used to aid in such a curve fitting exercise, although the issue of estimating rooting depth may be difficult to resolve.

Measurements, or estimates of *TTSW* for the VitAdapt vineyard have not been made, and furthermore, could be highly variable on a vine-by-vine basis. Such measurements in the field can also be problematic in stony soils (van Leeuwen et al., 2010), such as those experienced in the vineyard used for this study. For this study it was decided, therefore to select two *TTSW* assumptions that generated a range of daily transpiration rates that were comparable to those measured using the sap flow sensors across all the vines.

7 Conclusions

The purpose of this thesis was to gain insight into how different grapevine varieties respond to drought stress by measuring changes in vine water use on different time scales. As the amount of soil water available to the plant decreases and/or its water loss increases due to increasing atmospheric demand, the water status of the vines will decrease and drought stress will increase. Different varieties are better able than others to maintain their water status and minimize drought stress in response.

Grapevines can have many different responses to drought stress, which may also differ depending on the timing of that stress during the growing season (Tardieu et al., 2018). Such stress responses generally include turgor loss, leaf loss, yield reduction, changes in berry ripening dynamics and composition, etc. The studies performed as part of this thesis were focused on how different grapevine varieties modify their water use as evaluated on different time scales, specifically: i) how water use efficiency is affected by drought stress during berry ripening period; and ii) how vine canopy conductance, and hence transpiration is affected over the season as a function of drought stress. In both cases, these responses are driven by how reactive the different varieties are in regulating stomatal closure, and hence water use in response to drought stress.

The study of drought stress response during the berry ripening period was based primarily on measurements of carbon isotope discrimination in berry juice sugar ($\delta^{13}C$) and pre-dawn and leaf water potential, allowing for a classification of differences in drought response across 48 varieties. Being performed in the VitAdapt common-garden vineyard, with randomly distributed replicate plantings, the effects of variable soil conditions, even within the same vineyard, could be properly accounted for. Then using an innovative method of measuring vine canopy conductance in a vineyard setting, the response of this conductance, and hence vine transpiration, were quantified against changes in soil water deficits and atmospheric conditions, highlighting different responses across five varieties.

The following is a summary of specific key conclusions from these studies and their implications. These studies were all performed in a working vineyard setting, with the intent of producing results more relevant to vineyard managers and producers of wine and wine-based spirits when compared to those coming from greenhouse studies.

7.1 Drought stress response during berry ripening

Measurement of carbon isotope discrimination in berry juice at maturity ($\delta^{13}C$) and corresponding water potential measurements during the berry ripening period over four seasons confirmed results from prior studies that suggest $\delta^{13}C$ provides an integrated assessment of vine water status during the period of berry ripening. Being able to characterize wine water status during this critical period is useful because it has an important effect on the quality potential of grapes and the resulting wine quality. This may be a useful tool for growers, purchasers of grapes (e.g., cooperative), or winemakers to retrospectively estimate the vine water status that existed in the vineyard for a particular growing season. For this purpose, however, the collection of $\delta^{13}C$ data over several seasons would be required to establish the range of drought response of a given variety against which the measured level of stress in a given year can be assessed.

To extend this use, measurements of $\delta^{13}C$ in *eau de vie* produced from a double distillation process, such as used in the Cognac AOC, was compared to the $\delta^{13}C$ of the source wine and parent grape must. A strong linear relationship was found between the $\delta^{13}C$ of grape must, wine and eau de vie, suggesting the latter could be used to estimate the vine water status that existed during the corresponding berry ripening period. This allows a retrospective estimation of the vine water status that existed during the ripening of the grapes used to produce the wine and subsequent eau de vie. As has been done for wine, this could then be used in future studies to establish relations between vine water status and specific sensory attributes of eau de vie quality.

Various $\delta^{13}C$ metrics and vine phenology measured on 48 different varieties in the same growing conditions over seven years were also used to create a classification of drought tolerance that matched well with prior understandings of the relative drought tolerance of different varieties. The selected classification was performed using a hierarchical cluster analysis (HCA) based on the following observed traits for each variety: the day of year (DOY) of véraison; the $\delta^{13}C$ in the wettest year; and the range of $\delta^{13}C$ measurements between those in the driest and wettest years. For each variety, these respectively account for the effect of the timing of berry ripening on experienced drought conditions, the innate water use efficiency, and the drought stress sensitivity across multiple seasons. The HCA

classification obtained in this way can be useful for grower selection of plant material based on the potential stress responses under future anticipated growing conditions.

Using measurements of predawn and midday leaf water potential (Ψ_{PD} and Ψ_L respectively) on a subset of six varieties, hydroscapes were created and a list of metrics indicative of the sensitivity of stomatal regulation of vine water status to water stress was produced. Such hydroscapes are indicative of range of Ψ_L over which the vine will operate, with smaller hydroscapes associated with more isohydric varieties and larger hydroscapes indicative of anisohydric varieties. It was observed that the size of the hydroscape for a variety is strongly dependent on the lowest level of Ψ_L under non-limiting conditions and the lowest level of Ψ_L at high levels of stress. These key hydroscape metrics were then found to be well correlated with the $\delta^{13}C$ obtained in years of relatively non-limiting conditions. This suggests the anisohydric behavior of a larger hydroscape is associated with a lower level of water use efficiency in well-watered conditions as indicated by more negative $\delta^{13}C$. Increased water use in non-limiting conditions, as suggested by a larger hydroscape, may lead to greater water deficits later in the season and hence increasing $\delta^{13}C$. The relationship between these hydroscape and $\delta^{13}C$ metrics lends some validation to the significance of the minimum year $\delta^{13}C$ metric, with the latter being much easier to obtain in the vineyard over several seasons and a wide range of varieties.

7.2 Vine canopy conductance response to drought stress

Climate change has the potential to affect vine transpiration and overall vineyard water use due to related changes in daily atmospheric conditions and soil water deficits. In response to such changes, grapevines regulate transpiration using various physiological mechanisms that alter conductance of water through the soil-plant-atmosphere continuum. As part of this thesis a simplified method for the determination of bulk stomatal conductance in a vineyard setting was developed and then used to study how that conductance was regulated by five different varieties in response to changes in vine water status, vapor pressure deficit, and net radiation.

The simplified method used in this study to determine bulk stomatal conductance is based a two-source crop canopy energy flux model, which considers separately the heat and vapor flux from the vine canopy and the ground surrounding the vine canopy in the

interrow space, using relatively straight-forward measurements of individual vine sap flow, temperature and humidity within the vine canopy, and estimates of net radiation absorbed by the vine canopy. In addition to providing a more realistic model of the actual energy fluxes in open vineyard canopies, this approach allows the determination of bulk stomatal conductance without the measurement of the flux of heat from the ground surrounding the vine canopy, nor the determination of the boundary layer resistance above the vineyard. The method produced results that compared well with other estimates of vine canopy conductance in the literature and demonstrated the expected diurnal and seasonal trends.

Sensitivity analysis using non-parametric regression analysis found transpiration flux and vapor pressure deficit to be the most important input variables to the calculation of bulk stomatal conductance, therefore warranting attention in their field measurement. On the other hand, absorbed net radiation and bulk boundary layer resistance were found to be much less important suggesting some opportunities for method simplification that would not significantly impact quality of the results. For example, it was observed that estimates of net long wave radiation absorbed by the vine canopy were very low when compared to net absorbed shortwave radiation, suggesting it could be eliminated from this methodology without a significant impact on the calculation of bulk stomatal conductance. The benefit of simplifying the method and making it easier to implement may outweigh this loss, although verification of this finding may be warranted in vineyards with different canopy sizes, row spacings, and orientations. A simplified field method increases the likelihood that more data can be collected across different varieties, climates, and growing conditions.

The above methodology was then used to estimate bulk stomatal conductance at 15-minute intervals on several vines of Cabernet-Sauvignon, Merlot, Tempranillo, Ugni blanc, and Semillon in a non-irrigated vineyard, with its response being compared against a number of biotic and abiotic parameters. After a process of trial-and-error to address collinearity and non-linearity in the data for the different variables, a multiple linear regression analysis was used to develop a readily interpretable model of bulk stomatal conductance as a function of vine water status, vapor pressure deficit, and net radiation, with regression coefficients for the different predictor variables being physically meaningful and comparable between themselves and across the different varieties. While other non-linear or non-parametric regression models can provide a better fit and handle some degree of

collinearity in the variables, they are less interpretable and more site-specific that the multiple linear regression approach used in this study.

Based on comparing the standardized coefficients generated by the regression modeling, the variability of vapor pressure deficit in the vine canopy over the day and predawn water potential over the season was observed to explain much of the variability in bulk stomatal conductance, with the variability of net radiation absorbed by the vine canopy explaining much less. The effect of vine water status on conductance was more differentiated across the five varieties than was the effect of vapor pressure deficit. And while there was a difference in the effect of net radiation across the varieties, its overall effect was much less when compared to vine water status and vapor pressure deficit.

It was also observed that the response of modeled conductance, as calculated using the regression model coefficients and input data from the same season, was of greater magnitude (whether positive or negative), to changes in the predictor variables when conductance at non-limiting conditions was also greater. Tempranillo was observed to put greater emphasis on reducing its conductance in response to decreasing vine water status than in response to increasing vapor pressure deficits when compared to the other varieties.

Transpiration simulations, also based on the regression model coefficients and input data from the same season, found similar differences between varieties in terms of daily and seasonal transpiration. These simulations also compared well with those from an accepted vineyard water balance model, although there appeared to be differences between the two approaches in the rate at which conductance, and hence transpiration is reduced as a function of decreasing soil water content (i.e., increasing water deficit stress).

The multiple linear regression approach used in this study, however, was not able to distinguish the effects of collinear variables, such as reduced leaf area index, which were strongly related to vine water status. As a result, bulk boundary layer resistance, which is based on leaf area index, and which was also found in the sensitivity analysis to be of less significance in the calculation of conductance, was eliminated from the final regression analysis. One benefit of this, however, it that it further simplifies this methodology by

eliminating the time-consuming measurement of leaf area index, while not having a significant negative effect on the explanatory power of the model.

While current water balance modeling is an invaluable tool to help growers design and manage their vineyards, they are generic, without the ability to distinguish differences between varieties. While more data collected using the described approach is likely needed to make more definitive characterization of the behavior of the different varieties, it could provide the means of developing variety specific parameterization of the vine transpiration component of future water balance models. By better characterizing the response of bulk stomatal conductance, the dynamics of vine transpiration could be better parameterized in vineyard water use modeling of current and future climate scenarios.

Another major challenge in water balance modeling of vineyards is the need to develop a realistic estimate of the total transpirable soil water (*TTSW*), which can have an important effect on results. *TTSW* can be highly variable on a vine-by-vine basis and problematic to measure, particularly in stony soils. For this study, measurements of *TTSW* were not available, and two *TTSW* assumptions were made such that the range of daily transpiration rates estimated by the water balance model were comparable to those measured using the sap flow sensors. Future studies could possibly use a curve fitting technique comparing measurements of predawn water potential to estimates, or measurements of soil water content to develop estimates of *TTSW*, although such approaches require some understanding of the nature of those relationship, which are challenging to obtain.

The topic of varietal responses to water deficits is complex, with many physiological responses and time frames to consider, and numerous means of measurement available. The studies presented in this thesis were able to characterize the drought stress response of several different varieties both in terms of changes in water use efficiency over the berry ripening period and changes in vine conductance both diurnally and seasonally, while using and comparing a number of different approaches to determining these responses. In the future, it may also be possible with data collected over multiple seasons to compare drought response characterizations produced by these two methods. For example, the response of canopy conductance to drought stress during the berry ripening period could be compared to measurements of $\delta^{13}C$.

References

Allen, R. G., Pereira, L. S., Raes, D., and Smith, M. (1998). FAO Irrigation and drainage paper No. 56. *Rome Food Agric. Organ. U. N.* 56, 97–156.

Améglio, T., Archer, P., Cohen, M., Valancogne, C., Daudet, F., Dayau, S., et al. (1999). Significance and limits in the use of predawn leaf water potential for tree irrigation. *Plant Soil* 207, 155–167. doi: 10.1023/A:1026415302759.

Antoniadis, A., Lambert-Lacroix, S., and Poggi, J.-M. (2021). Random forests for global sensitivity analysis: A selective review. *Reliab. Eng. Syst. Saf.* 206, 107312. doi: 10.1016/j.ress.2020.107312.

Bai, Y., Zhu, G., Su, Y., Zhang, K., Han, T., Ma, J., et al. (2015). Hysteresis loops between canopy conductance of grapevines and meteorological variables in an oasis ecosystem. *Agric. For. Meteorol.* 214–215, 319–327. doi: 10.1016/j.agrformet.2015.08.267.

Bartlett, M. K., Scoffoni, C., and Sack, L. (2012). The determinants of leaf turgor loss point and prediction of drought tolerance of species and biomes: a global meta-analysis. *Ecol. Lett.* 15, 393–405. doi: 10.1111/j.1461-0248.2012.01751.x.

Bchir, A., Escalona, J. M., Gallé, A., Hernández-Montes, E., Tortosa, I., Braham, M., et al. (2016). Carbon isotope discrimination (δ13C) as an indicator of vine water status and water use efficiency (WUE): Looking for the most representative sample and sampling time. *Agric. Water Manag.* 167, 11–20. doi: 10.1016/j.agwat.2015.12.018.

Bota, B. J., Flexas, J., and Medrano, H. (2001). Genetic variability of photosynthesis and water use in Balearic grapevine cultivars. *Ann. Appl. Biol.* 138, 353–361. doi: 10.1111/j.1744-7348.2001.tb00120.x.

Bota, J., Tomás, M., Flexas, J., Medrano, H., and Escalona, J. M. (2016). Differences among grapevine cultivars in their stomatal behavior and water use efficiency under progressive water stress. *Agric. Water Manag.* 164, 91–99. doi: 10.1016/j.agwat.2015.07.016.

Brillante, L., Mathieu, O., Lévêque, J., and Bois, B. (2016). Ecophysiological Modeling of Grapevine Water Stress in Burgundy Terroirs by a Machine-Learning Approach. *Front. Plant Sci.* 7. doi: 10.3389/fpls.2016.00796.

Brillante, L., Mathieu, O., Lévêque, J., van Leeuwen, C., and Bois, B. (2017). Water status and must composition in grapevine cv. Chardonnay with different soils and topography and a mini meta-analysis of the δ^{13}C/water potentials correlation. *J. Sci. Food Agric.* doi: 10.1002/jsfa.8516.

Buckley, T. N. (2005). The control of stomata by water balance. *New Phytol.* 168, 275–292. doi: 10.1111/j.1469-8137.2005.01543.x.

Buckley, T. N. (2016). Stomatal responses to humidity: has the "black box" finally been opened? *Plant Cell Environ.* 39, 482–484. doi: 10.1111/pce.12651.

Castellarin, S. D., Matthews, M. A., Di Gaspero, G., and Gambetta, G. A. (2007). Water deficits accelerate ripening and induce changes in gene expression regulating flavonoid biosynthesis in grape berries. *Planta* 227, 101–112. doi: 10.1007/s00425-007-0598-8.

Chahine, A., Dupont, S., Sinfort, C., and Brunet, Y. (2014). Wind-Flow Dynamics Over a Vineyard. *Bound.-Layer Meteorol.* 151, 557–577. doi: 10.1007/s10546-013-9900-4.

Charrier, G., Delzon, S., Domec, J.-C., Zhang, L., Delmas, C. E. L., Merlin, I., et al. (2018). Drought will not leave your glass empty: Low risk of hydraulic failure revealed by long-term drought observations in world's top wine regions. *Sci. Adv.* 4, eaao6969. doi: 10.1126/sciadv.aao6969.

Chaves, M. M., Zarrouk, O., Francisco, R., Costa, J. M., Santos, T., Regalado, A. P., et al. (2010). Grapevine under deficit irrigation: hints from physiological and molecular data. *Ann. Bot.* 105, 661–676. doi: 10.1093/aob/mcq030.

Choné, X., Van Leeuwen, C., Dubourdieu, D., and Gaudillère, J. P. (2001). Stem Water Potential is a Sensitive Indicator of Grapevine Water Status. *Ann. Bot.* 87, 477–483. doi: 10.1006/anbo.2000.1361.

Chouzouri, A., and Schultz, H. R. (2005). Hydraulic Anatomy, Cavitation Susceptibility and Gas-Exchange of Several Grapevine Cultivars of Different Geographic Origin. *Acta Hortic.*, 325–332. doi: 10.17660/ActaHortic.2005.689.38.

Collins, M. J., Fuentes, S., and Barlow, E. W. R. (2010). Partial rootzone drying and deficit irrigation increase stomatal sensitivity to vapour pressure deficit in anisohydric grapevines. *Funct. Plant Biol.* 37, 128–138. doi: 10.1071/FP09175.

Costa, J. M., Ortuño, M. F., Lopes, C. M., Chaves, M. M., Costa, J. M., Ortuño, M. F., et al. (2012). Grapevine varieties exhibiting differences in stomatal response to water deficit. *Funct. Plant Biol.* 39, 179–189. doi: 10.1071/FP11156.

Destrac-Irvine, A., and van Leeuwen, C. (2017). The Vitadapt project: extensive phenotyping of a wide range of varieties in order to optimize the use of genetic diversity within the Vitis vinifera species as a tool for adaptation to a changing environment. in *Proceedings of Climwine 2016 - Sustainable grape and wine production in the context of climate change.* (Bordeaux, France), 165–171.

Domec, J.-C., and Johnson, D. M. (2012). Does homeostasis or disturbance of homeostasis in minimum leaf water potential explain the isohydric versus anisohydric behavior of Vitis vinifera L. cultivars? *Tree Physiol.* 32, 245–248. doi: 10.1093/treephys/tps013.

Domec, J.-C., Noormets, A., King, J. S., Sun, G., Mcnulty, S. G., Gavazzi, M. J., et al. (2009). Decoupling the influence of leaf and root hydraulic conductances on stomatal conductance and its sensitivity to vapour pressure deficit as soil dries in a drained loblolly pine plantation. *Plant Cell Environ.* 32, 980–991. doi: 10.1111/j.1365-3040.2009.01981.x.

Dormann, C. F., Elith, J., Bacher, S., Buchmann, C., Carl, G., Carré, G., et al. (2013). Collinearity: a review of methods to deal with it and a simulation study evaluating their performance. *Ecography* 36, 27–46. doi: 10.1111/j.1600-0587.2012.07348.x.

Escalona, J. M., Fuentes, S., Tomás, M., Martorell, S., Flexas, J., and Medrano, H. (2013). Responses of leaf night transpiration to drought stress in Vitis vinifera L. *Agric. Water Manag.* 118, 50–58. doi: 10.1016/j.agwat.2012.11.018.

Farquhar, G. (1989). Carbon Isotope Discrimination And Photosynthesis. *Annu. Rev. Plant Physiol. Plant Mol. Biol.* 40, 503–537. doi: 10.1146/annurev.arplant.40.1.503.

Franks, P. J., Drake, P. L., and Froend, R. H. (2007). Anisohydric but isohydrodynamic: seasonally constant plant water potential gradient explained by a stomatal control mechanism incorporating variable plant hydraulic conductance. *Plant Cell Environ.* 30, 19–30. doi: 10.1111/j.1365-3040.2006.01600.x.

Frost, J. (2020). *Regression Analysis: An Intuitive Guide for Using and Interpreting Linear Models*. Statistics By Jim Publishing.

Gamon, J. A., and Pearcy, R. W. (1989). Leaf movement, stress avoidance and photosynthesis in Vitis californica. *Oecologia* 79, 475–481. doi: 10.1007/BF00378664.

Gaudillère, J.-P., Van Leeuwen, C., and Ollat, N. (2002). Carbon isotope composition of sugars in grapevine, an integrated indicator of vineyard water status. *J. Exp. Bot.* 53, 757–763. doi: 10.1093/jexbot/53.369.757.

Gowdy, M., Pieri, P., Suter, B., Marguerit, E., Destrac-Irvine, A., Gambetta, G., et al. (2022a). Estimating Bulk Stomatal Conductance in Grapevine Canopies. *Front. Plant Sci.* 13, 839378. doi: 10.3389/fpls.2022.839378.

Gowdy, M., Suter, B., Pieri, P., Marguerit, E., Destrac Irvine, A., Gambetta, G. A., et al. (2022b). Variety-specific response of bulk stomatal conductance of grapevine canopies to changes in net radiation, atmospheric demand, and drought stress. *OENO One* 56–3. doi: 10.20870/oeno-one.2022.56.2.5435.

Granier, A., and Loustau, D. (1994). Measuring and modelling the transpiration of a maritime pine canopy from sap-flow data. *Agric. For. Meteorol.* 71, 61–81. doi: 10.1016/0168-1923(94)90100-7.

Granier, A., Loustau, D., and Bréda, N. (2000). A generic model of forest canopy conductance dependent on climate, soil water availability and leaf area index. *Ann. For. Sci.* 57, 755–765. doi: 10.1051/forest:2000158.

Grömping, U. (2009). Variable Importance Assessment in Regression: Linear Regression versus Random Forest. *Am. Stat.* 63, 308–319. doi: 10.1198/tast.2009.08199.

Guyon, F., Leeuwen, C. van, Gaillard, L., Grand, M., Akoka, S., Remaud, G. S., et al. (2015). Comparative study of 13C composition in ethanol and bulk dry wine using isotope ratio monitoring by mass spectrometry and by nuclear magnetic resonance as an indicator of vine water status. *Anal. Bioanal. Chem.* 407, 9053–9060. doi: 10.1007/s00216-015-9072-9.

Herrera, J. C., Calderan, A., Gambetta, G. A., Peterlunger, E., Forneck, A., Sivilotti, P., et al. (2021). Stomatal responses in grapevine become increasingly more tolerant to low water potentials throughout the growing season. *Plant J. Cell Mol. Biol.* doi: 10.1111/tpj.15591.

Hochberg, U., Bonel, A. G., David-Schwartz, R., Degu, A., Fait, A., Cochard, H., et al. (2017a). Grapevine acclimation to water deficit: the adjustment of stomatal and hydraulic conductance differs from petiole embolism vulnerability. *Planta* 245, 1091–1104. doi: 10.1007/s00425-017-2662-3.

Hochberg, U., Windt, C. W., Ponomarenko, A., Zhang, Y.-J., Gersony, J., Rockwell, F. E., et al. (2017b). Stomatal Closure, Basal Leaf Embolism, and Shedding Protect the Hydraulic Integrity of Grape Stems. *Plant Physiol.* 174, 764–775. doi: 10.1104/pp.16.01816.

Hsiao, T. C. (1973). Plant Responses to Water Stress. *Annu. Rev. Plant Physiol.* 24, 519–570. doi: 10.1146/annurev.pp.24.060173.002511.

Hsiao, T. C., Acevedo, E., Fereres, E., Henderson, D. W., Monteith, J. L., and Weatherley, P. E. (1976). Water stress, growth and osmotic adjustment. *Philos. Trans. R. Soc. Lond. B Biol. Sci.* 273, 479–500. doi: 10.1098/rstb.1976.0026.

Keller, M. (2015). *The Science of Grapevines: Anatomy and Physiology*. 2nd edition. Amsterdam ; Boston: Academic Press.

Kelliher, F. M., Leuning, R., Raupach, M. R., and Schulze, E.-D. (1995). Maximum conductances for evaporation from global vegetation types. *Agric. For. Meteorol.* 73, 1–16. doi: 10.1016/0168-1923(94)02178-M.

Kirkham, M. B. (2005). *Principles of Soil and Plant Water Relations*. Elsevier Academic Press.

Koide, R. T., Robichaux, R. H., Morse, S. R., and Smith, C. M. (2000). "Plant water status, hydraulic resistance and capacitance - Ch. 9," in *Plant Physiological Ecology*, eds. R. W. Pearcy, J. R. Ehleringer, H. A. Mooney, and P. W. Rundel (Dordrecht: Springer Netherlands), 161–183. doi: 10.1007/978-94-010-9013-1_9.

Kramer, P. J., and Boyer, J. S. (1995). *Water relations of plants and soils*. Academic Press, Inc. Available at: http://udspace.udel.edu/handle/19716/2830 [Accessed May 10, 2020].

Krounbi, L., and Lazarovitch, N. (2011). "Soil Hydraulic Properties Affecting Root Water Uptake," in *Encyclopedia of Agrophysics*, eds. J. Gliński, J. Horabik, and J. Lipiec (Dordrecht: Springer Netherlands), 748–754. doi: 10.1007/978-90-481-3585-1_149.

Lascano, R. J., Baumhardt, R. L., and Lipe, W. N. (1992). Measurement of Water Flow in Young Grapevines Using the Stem Heat Balance Method. *Am. J. Enol. Vitic.* 43, 159–165.

Lascano, R. J., Goebel, T. S., Booker, J., Baker, J. T., and Iii, D. C. G. (2016). The Stem Heat Balance Method to Measure Transpiration: Evaluation of a New Sensor. *Agric. Sci.* 07, 604. doi: 10.4236/as.2016.79057.

Lavoie-Lamoureux, A., Sacco, D., Risse, P.-A., and Lovisolo, C. (2017). Factors influencing stomatal conductance in response to water availability in grapevine: a meta-analysis. *Physiol. Plant.* 159, 468–482. doi: 10.1111/ppl.12530.

Lebon, E., Dumas, V., Pieri, P., and Schultz, H. R. (2003). Modelling the seasonal dynamics of the soil water balance of vineyards. *Funct. Plant Biol.* 30, 699–710. doi: 10.1071/FP02222.

Levin, A. D., Williams, L. E., and Matthews, M. A. (2020). A continuum of stomatal responses to water deficits among 17 wine grape cultivars (Vitis vinifera). *Funct. Plant Biol.* 47, 11–25. doi: 10.1071/FP19073.

Lhomme, J. P., Montes, C., Jacob, F., and Prévot, L. (2012). Evaporation from Heterogeneous and Sparse Canopies: On the Formulations Related to Multi-Source Representations. *Bound.-Layer Meteorol.* 144, 243–262. doi: 10.1007/s10546-012-9713-x.

Löf, M., and Welander, N. T. (2009). Estimating sap flow from stem heat balances in Quercus robur L. seedlings in relation to light intensity: A comparison of two methods during the establishment phase. *Ann. For. Sci.* 66, 501–501. doi: 10.1051/forest/2009034.

Lovisolo, C., Perrone, I., Carra, A., Ferrandino, A., Flexas, J., Medrano, H., et al. (2010). Drought-induced changes in development and function of grapevine (*Vitis* spp.) organs and in their hydraulic and non-hydraulic interactions at the whole-plant level: a physiological and molecular update. *Funct. Plant Biol.* 37, 98. doi: 10.1071/FP09191.

Lovisolo, C., and Schubert, A. (1998). Effects of water stress on vessel size and xylem hydraulic conductivity in Vitis vinifera L. *J. Exp. Bot.* 49, 693–700. doi: 10.1093/jxb/49.321.693.

Lu, P., Yunusa, I. A. M., Walker, R. R., and Müller, W. J. (2003). Regulation of canopy conductance and transpiration and their modelling in irrigated grapevines. *Funct. Plant Biol.* 30, 689–698. doi: 10.1071/FP02181.

Marguerit, E., Brendel, O., Lebon, E., Van Leeuwen, C., and Ollat, N. (2012). Rootstock control of scion transpiration and its acclimation to water deficit are controlled by different genes. *New Phytol.* 194, 416–429. doi: 10.1111/j.1469-8137.2012.04059.x.

Martínez-Vilalta, J., Poyatos, R., Aguadé, D., Retana, J., and Mencuccini, M. (2014). A new look at water transport regulation in plants. *New Phytol.* 204, 105–115. doi: 10.1111/nph.12912.

McCutchan, H., and Shackel, K. A. (1992). Stem-water Potential as a Sensitive Indicator of Water Stress in Prune Trees (Prunus domestica L. cv. French). *J. Am. Soc. Hortic. Sci.* 117, 607–611.

McElrone, A. J., Choat, B., Gambetta, G. A., and Brodersen, C. R. (2013). Water uptake and transport in vascular plants. *Nat. Educ. Knowl.* 4. Available at: http://www.nature.com.zhongjivip.net/scitable/knowledge/library/water-uptake-and-transport-in-vascular-plants-103016037 [Accessed June 4, 2016].

Medrano, H., Tomás, M., Martorell, S., Escalona, J.-M., Pou, A., Fuentes, S., et al. (2015). Improving water use efficiency of vineyards in semi-arid regions. A review. *Agron. Sustain. Dev.* 35, 499–517. doi: 10.1007/s13593-014-0280-z.

Meinzer, F. C., Smith, D. D., Woodruff, D. R., Marias, D. E., McCulloh, K. A., Howard, A. R., et al. (2017). Stomatal kinetics and photosynthetic gas exchange along a continuum of isohydric to anisohydric regulation of plant water status. *Plant Cell Environ.* 40, 1618–1628. doi: 10.1111/pce.12970.

Meinzer, F. C., Woodruff, D. R., Marias, D. E., Mcculloh, K. A., and Sevanto, S. (2014). Dynamics of leaf water relations components in co-occurring iso- and anisohydric conifer species. *Plant Cell Environ.* 37, 2577–2586. doi: 10.1111/pce.12327.

Meinzer, F. C., Woodruff, D. R., Marias, D. E., Smith, D. D., McCulloh, K. A., Howard, A. R., et al. (2016). Mapping 'hydroscapes' along the iso- to anisohydric continuum of stomatal regulation of plant water status. *Ecol. Lett.* 19, 1343–1352. doi: 10.1111/ele.12670.

Mendoza, V., Pazos, M., Garduño, R., and Mendoza, B. (2021). Thermodynamics of climate change between cloud cover, atmospheric temperature and humidity. *Sci. Rep.* 11, 21244. doi: 10.1038/s41598-021-00555-5.

Monteith, J., and Unsworth, M. (2013). *Principles of Environmental Physics: Plants, Animals, and the Atmosphere*. Academic Press.

Montoro, A., and Sadras, V. (2014). Elevated temperature increased stomata size and leaf photosynthesis in shiraz grapevine. Available at: https://pubag.nal.usda.gov/catalog/813015 [Accessed May 29, 2022].

Naor, A., Gal, Y., and Bravdo, B. (1997). Crop load affects assimilation rate, stomatal conductance, stem water potential and water relations of field-grown Sauvignon blanc grapevines. *J. Exp. Bot.* 48, 1675–1680. doi: 10.1093/jxb/48.9.1675.

Naor, A., Klein, I., and Doron, I. (1995). Stem Water Potential and Apple Size. *J. Am. Soc. Hortic. Sci.* 120, 577–582.

Oren, R., Sperry, J. S., Katul, G. G., Pataki, D. E., Ewers, B. E., Phillips, N., et al. (1999). Survey and synthesis of intra- and interspecific variation in stomatal sensitivity to vapour pressure deficit. *Plant Cell Environ.* 22, 1515–1526. doi: 10.1046/j.1365-3040.1999.00513.x.

Pellegrino, A., Gozé, E., Lebon, E., and Wery, J. (2006). A model-based diagnosis tool to evaluate the water stress experienced by grapevine in field sites. *Eur. J. Agron.* 25, 49–59. doi: 10.1016/j.eja.2006.03.003.

Pellegrino, A., Lebon, E., Voltz, M., and Wery, J. (2004). Relationships between plant and soil water status in vine (Vitis vinifera L.). *Plant Soil* 266, 129–142. doi: 10.1007/s11104-005-0874-y.

Penman, H. L. (1948). Natural evaporation from open water, bare soil and grass. *Proc. R. Soc. Lond. Ser. Math. Phys. Sci.* 193, 120–145. doi: 10.1098/rspa.1948.0037.

Petrie, P. R., Trought, M. C. T., and Howell, G. S. (2000). Growth and dry matter partitioning of Pinot Noir (Vitis vinifera L.) in relation to leaf area and crop load. *Aust. J. Grape Wine Res.* 6, 40–45. doi: 10.1111/j.1755-0238.2000.tb00160.x.

Picard, M., van Leeuwen, C., Guyon, F., Gaillard, L., de Revel, G., and Marchand, S. (2017). Vine Water Deficit Impacts Aging Bouquet in Fine Red Bordeaux Wine. *Front. Chem.* 5. Available at: https://www.frontiersin.org/article/10.3389/fchem.2017.00056 [Accessed March 15, 2022].

Picón-Toro, J., González-Dugo, V., Uriarte, D., Mancha, L. A., and Testi, L. (2012). Effects of canopy size and water stress over the crop coefficient of a "Tempranillo" vineyard in south-western Spain. *Irrig. Sci.* 30, 419–432. doi: 10.1007/s00271-012-0351-3.

Pieri, P. (2010). Modelling radiative balance in a row-crop canopy: Row–soil surface net radiation partition. *Ecol. Model.* 221, 791–801. doi: 10.1016/j.ecolmodel.2009.11.019.

Pieri, P., and Bois, B. (2007). *Feuille de calcul excel du modèle de bilan hydrique de la vigne*.

Pieri, P., and Gaudillere, J. P. (2005). Vines water stress derived from a soil water balance model - sensitivity to soil and training system parameters. in *XIV International GESCO Viticulture Congress, Geisenheim, Germany, 23-27 August, 2005*, 457–463. Available at: https://www.cabdirect.org/cabdirect/abstract/20053214000 [Accessed February 6, 2020].

Plantevin, M., Gowdy, M., Destrac-Irvine, A., Marguerit, E., Gambetta, G. A., and van Leeuwen, C. (2022). Using δ13C and hydroscapes for discriminating cultivar specific drought responses. *OENO One* 56–3. doi: 10.20870/oeno-one.2022.56.2.5434.

Pou, A., Medrano, H., Tomàs, M., Martorell, S., Ribas-Carbó, M., and Flexas, J. (2012). Anisohydric behaviour in grapevines results in better performance under moderate water stress and recovery than isohydric behaviour. *Plant Soil* 359, 335–349. doi: 10.1007/s11104-012-1206-7.

Prieto, J. A., Lebon, É., and Ojeda, H. (2010). Stomatal behavior of different grapevine cultivars in response to soil water status and air water vapor pressure deficit. *OENO One* 44, 9–20. doi: 10.20870/oeno-one.2010.44.1.1459.

Riou, C., Valancogne, C., and Pieri, P. (1989). Un modèle simple d'interception du rayonnement solaire par la vigne - vérification expérimentale. *Agronomie* 9, 441–450. doi: 10.1051/agro:19890502.

Ritchie, G. A., and Hinckley, T. M. (1975). The Pressure Chamber as an Instrument for Ecological Research. *Adv. Ecol. Res.* 9, 165–254. doi: 10.1016/S0065-2504(08)60290-1.

Roelfsema, M. R. G., and Hedrich, R. (2005). In the light of stomatal opening: new insights into 'the Watergate': Tansley review. *New Phytol.* 167, 665–691. doi: 10.1111/j.1469-8137.2005.01460.x.

Rogiers, S. Y., Greer, D. H., Hatfield, J. M., Hutton, R. J., Clarke, S. J., Hutchinson, P. A., et al. (2012). Stomatal response of an anisohydric grapevine cultivar to evaporative demand, available soil moisture and abscisic acid. *Tree Physiol.* 32, 249–261. doi: 10.1093/treephys/tpr131.

Rogiers, S. Y., Greer, D. H., Hutton, R. J., and Landsberg, J. J. (2009). Does night-time transpiration contribute to anisohydric behaviour in a Vitis vinifera cultivar? *J. Exp. Bot.* 60, 3751–3763. doi: 10.1093/jxb/erp217.

Roßmann, A., Schmidt, H.-L., Reniero, F., Versini, G., Moussa, I., and Merle, M. H. (1996). Stable carbon isotope content in ethanol of EC data bank wines from Italy, France and Germany. *Z. Für Lebensm.-Unters. Forsch.* 203, 293–301. doi: 10.1007/BF01192881.

Sack, L., and Holbrook, N. M. (2006). Leaf Hydraulics. *Annu. Rev. Plant Biol.* 57, 361–381. doi: 10.1146/annurev.arplant.56.032604.144141.

Santesteban, L. G., Miranda, C., Barbarin, I., and Royo, J. B. (2015). Application of the measurement of the natural abundance of stable isotopes in viticulture: a review: Stable isotopes in viticulture: a review. *Aust. J. Grape Wine Res.* 21, 157–167. doi: 10.1111/ajgw.12124.

Saxton, K. E., Rawls, W. J., Romberger, J. S., and Papendick, R. I. (1986). Estimating Generalized Soil-water Characteristics from Texture. *Soil Sci. Soc. Am. J.* 50, 1031–1036. doi: 10.2136/sssaj1986.03615995005000040039x.

Scholander, P. F., Bradstreet, E. D., Hemmingsen, E. A., and Hammel, H. T. (1965). Sap Pressure in Vascular Plants. *Science*. doi: 10.1126/science.148.3668.339.

Schultz, H. R. (2003). Differences in hydraulic architecture account for near-isohydric and anisohydric behaviour of two field-grown Vitis vinifera L. cultivars during drought. *Plant Cell Environ.* 26, 1393–1405. doi: 10.1046/j.1365-3040.2003.01064.x.

Schultz, H. R. (2016). Global Climate Change, Sustainability, and Some Challenges for Grape and Wine Production. *J. Wine Econ.* 11, 181–200. doi: 10.1017/jwe.2015.31.

Schultz, H. R., and Matthews, M. A. (1993). Xylem development and hydraulic conductance in sun and shade shoots of grapevine (Vitis vinifera L.): evidence that low light uncouples water transport capacity from leaf area. *Planta* 190, 393–406. doi: 10.1007/BF00196969.

Shimazaki, K., Doi, M., Assmann, S. M., and Kinoshita, T. (2007). Light Regulation of Stomatal Movement. *Annu. Rev. Plant Biol.* 58, 219–247. doi: 10.1146/annurev.arplant.57.032905.105434.

Shmueli, G. (2010). To Explain or To Predict? Rochester, NY: Social Science Research Network doi: 10.2139/ssrn.1351252.

Shuttleworth, W. J., and Wallace, J. S. (1985). Evaporation from sparse crops-an energy combination theory. *Q. J. R. Meteorol. Soc.* 111, 839–855. doi: 10.1002/qj.49711146910.

Smart, D. R., Breazeale, A., and Zufferey, V. (2006). Physiological Changes in Plant Hydraulics Induced by Partial Root Removal of Irrigated Grapevine (Vitis vinifera cv. Syrah). *Am. J. Enol. Vitic.* 57, 201–209.

Smart, R. E. (1974). Photosynthesis by Grapevine Canopies. *J. Appl. Ecol.* 11, 997–1006. doi: 10.2307/2401759.

Smart, R., and Robinson, M. (1991). *Sunlight Into Wine*. WINETITLES.

Souza, D., R, C., Maroco, J. P., Santos, D., P, T., Rodrigues, M. L., et al. (2005). Impact of deficit irrigation on water use efficiency and carbon isotope composition (δ13C) of field-grown grapevines under Mediterranean climate. *J. Exp. Bot.* 56, 2163–2172. doi: 10.1093/jxb/eri216.

Sperry, J. S., Hacke, U. G., Oren, R., and Comstock, J. P. (2002). Water deficits and hydraulic limits to leaf water supply. *Plant Cell Environ.* 25, 251–263. doi: 10.1046/j.0016-8025.2001.00799.x.

Sperry, J. S., Stiller, V., and Hacke, U. G. (2003). Xylem hydraulics and the soil–plant–atmosphere continuum. *Agron. J.* 95, 1362–1370.

Steppe, K., and Lemeur, R. (2004). An experimental system for analysis of the dynamic sap-flow characteristics in young trees: results of a beech tree. *Funct. Plant Biol.* 31, 83–92. doi: 10.1071/fp03150.

Stoll, M., Loveys, B., and Dry, P. (2000). Hormonal changes induced by partial rootzone drying of irrigated grapevine. *J. Exp. Bot.* 51, 1627–1634. doi: 10.1093/jexbot/51.350.1627.

Taiz, L., and Zeiger, E. (2002). *Plant Physiology 3rd ed*. 3rd Revised edition edition. Sunderland, Mass: Oxford University Press Inc.

Tardieu, F., and Simonneau, T. (1998). Variability among species of stomatal control under fluctuating soil water status and evaporative demand: modelling isohydric and anisohydric behaviours. *J. Exp. Bot.* 49, 419–432. doi: 10.1093/jexbot/49.suppl_1.419.

Tardieu, F., Simonneau, T., and Muller, B. (2018). The Physiological Basis of Drought Tolerance in Crop Plants: A Scenario-Dependent Probabilistic Approach. *Annu. Rev. Plant Biol.* 69, 733–759. doi: 10.1146/annurev-arplant-042817-040218.

Tomás, M., Medrano, H., Pou, A., Escalona, J. m., Martorell, S., Ribas-Carbó, M., et al. (2012). Water-use efficiency in grapevine cultivars grown under controlled conditions: effects of water stress at the leaf and whole-plant level. *Aust. J. Grape Wine Res.* 18, 164–172. doi: 10.1111/j.1755-0238.2012.00184.x.

Turner, N. C. (1981). Techniques and experimental approaches for the measurement of plant water status. *Plant Soil* 58, 339–366. doi: 10.1007/BF02180062.

Tyree, M. T., and Ewers, F. W. (1991). The hydraulic architecture of trees and other woody plants. *New Phytol.* 119, 345–360. doi: 10.1111/j.1469-8137.1991.tb00035.x.

van Genuchten, M. Th. (1980). A closed-form equation for predicting the hydraulic conductivity of unsaturated soils. *Soil Sci. Soc. Am. J.* 44, 892–898.

van Leeuwen, C., Pieri, P., and Vivin, P. (2010). "Comparison of Three Operational Tools for the Assessment of Vine Water Status: Stem Water Potential, Carbon Isotope Discrimination Measured on Grape Sugar and Water Balance - Ch. 7," in *Methodologies and Results in Grapevine Research*, eds. S. Delrot, H. Medrano, E. Or, L. Bavaresco, and S. Grando (Dordrecht: Springer Netherlands), 87–106. doi: 10.1007/978-90-481-9283-0_7.

van Leeuwen, C., Tregoat, O., Choné, X., Bois, B., Pernet, D., Gaudillère, J.-P., et al. (2009). Vine water status is a key factor in grape ripening and vintage quality for red Bordeaux wine. How can it be assessed for vineyard management purposes. *J Int Sci Vigne Vin* 43, 121–134.

Wild, M. (2009). Global dimming and brightening: A review. *J. Geophys. Res. Atmospheres* 114. doi: 10.1029/2008JD011470.

Willett, K. M., Dunn, R. J. H., Thorne, P. W., Bell, S., de Podesta, M., Parker, D. E., et al. (2014). HadISDH land surface multi-variable humidity and temperature record for climate monitoring. *Clim. Past* 10, 1983–2006. doi: 10.5194/cp-10-1983-2014.

Williams, L. E., and Araujo, F. J. (2002). Correlations among Predawn Leaf, Midday Leaf, and Midday Stem Water Potential and their Correlations with other Measures of Soil and Plant Water Status in Vitis vinifera. *J. Am. Soc. Hortic. Sci.* 127, 448–454.

Williams, L. E., and Trout, T. J. (2005). Relationships among Vine- and Soil-Based Measures of Water Status in a Thompson Seedless Vineyard in Response to High-Frequency Drip Irrigation. *Am. J. Enol. Vitic.* 56, 357–366.

Zhang, Y., Oren, R., and Kang, S. (2012). Spatiotemporal variation of crown-scale stomatal conductance in an arid Vitis vinifera L. cv. Merlot vineyard: direct effects of hydraulic properties and indirect effects of canopy leaf area. *Tree Physiol.* 32, 262–279. doi: 10.1093/treephys/tpr120.